Additional Papers on Actinide Monitoring - Physics Aspects from JRC-Ispra
31st NEACRP Meeting (Copies available from NEACRP Secretariat)

Models for a Three-Parameter Analysis of Neutron Signal Correlation Measurements for Fissile Material Assay

D. M. Cifarelli, W. Hage

Correlation Analysis with Neutrol Count Distributions in Randomly or Segnal Triggered Time Intervals for Assay of Special Fissile Materials

W. Hage, D. M. Cifarelli

On the Factorial Monents of the Neutron Nultiplicity Distribution of Fission Cascades

W. Hage, D. M. Cifarelli

Correlation Analysis with Neutron Count Distributions in Randomly or Signal Triggered Time Intervals for Assay of Special Fissile Materials

W. Hage, D. M. Cifarelli

Verification of the Interpretation Models of the Neutron Auto-Correlator With Monte Carlo Calculations

F. Bevacqua, F. V. Frazzoli, W. Hage

Multiplication and Absorption Correction of Auto Correlator Measurement Data

W. Hage, A. Prosdocimi, V. Vocino

A Computer Controlled Shift Register System for The Automatiδ Assay of Plutonium Oxide by Passive Neutron Interrogation

R. Benoit, R. Haas*, W. Hage, A. Prosdocimi, B. L. Thaurel**, V. Vocino

A Transportable Instrument for Determination of Uranium Content in Powders or Pellents by Delayed Neutron Technique: DUCA

R. Adam, P. Agostini, L. Caldon, G. Cordani, M. Cuypers, N. Faress, R. Haas*, V. Vocino

A Photoneutron Active Interrogation Device: Physical Design, Calibration and Operational Experience

A. Prosdocimi, P. Dell'Oro

Performances and Operation of A Photoneutron Active Interrogation System for Non-Destructive Assay of U-235

A. Prosdocimi, P. Dell'Oro

Progress in PERLA

S. Guardini

Characterization of The Pu-Bearing Perla Standard

C. Bigliocca, S. Guardini, G. Guzzi, L. Haemers, F. Mousty, E. Kuhn, N. Doubek, R. Fiedler, A. Zoigner, S. Baumann, K. H. Nelges, G. Hesbacher P. De Regge, L. Vandevelde, R. Boden, D. Huys

Latest Development and Implementations of Instruments for Uranium Assay by Delayed Neutron Techniques

R. Adam, P. Agostini, L. Becker, M. Bernede, L. Caldon, G. Cordani, F. Farese, R. Haas, V. Vocino.

NORTH-HOLLAND
PHYSICS
PUBLISHING

MODELS FOR A THREE-PARAMETER ANALYSIS OF NEUTRON SIGNAL CORRELATION MEASUREMENTS FOR FISSILE MATERIAL ASSAY

D.M. CIFARELLI

Università L. Bocconi, Istituto di Metodi Quantitativi, 20136 Milano, Italy

W. HAGE

Commission of the European Communities, Joint Research Centre – Ispra Establishment, 21020 Ispra (Va), Italy

Received 19 December 1985 and in revised form 14 May 1986

For the nondestructive assay of Pu-containing fuel, interpretation models are derived to obtain its spontaneous fission rate or its Pu-mass equivalent. The factorial moments of the frequency distribution of neutron signal multiplets in signal and randomly triggered time intervals are used as measurement results.

Reprinted from NUCLEAR INSTRUMENTS AND METHODS
IN PHYSICS RESEARCH A

Nuclear Instruments and Methods in Physics Research A251 (1986) 550–563
North-Holland, Amsterdam

MODELS FOR A THREE-PARAMETER ANALYSIS OF NEUTRON SIGNAL CORRELATION MEASUREMENTS FOR FISSILE MATERIAL ASSAY

D.M. CIFARELLI

Università L. Bocconi, Istituto di Metodi Quantitativi, 20136 Milano, Italy

W. HAGE

Commission of the European Communities, Joint Research Centre – Ispra Establishment, 21020 Ispra (Va), Italy

Received 19 December 1985 and in revised form 14 May 1986

For the nondestructive assay of Pu-containing fuel, interpretation models are derived to obtain its spontaneous fission rate or its Pu-mass equivalent. The factorial moments of the frequency distribution of neutron signal multiplets in signal and randomly triggered time intervals are used as measurement results.

1. Introduction

The fissile mass of special fissile materials is determined via the measurement of the spontaneous fission rate knowing the isotopic composition of the fuel. Corrections are required for the neutron emission rate due to (α, n) reactions and neutron multiplication caused by primary neutrons. The neutron signal correlation technique permits the determination of the number of fissions generating a signal pulse train containing signals from (α, n) reactions. This distinction is possible because fission neutrons are emitted in groups per fission event, whereas (α, n) reactions produce mainly single neutrons. With this technique, neutrons emitted by a test item are slowed down in a moderator, diffuse there as thermal neutrons and are partially absorbed by neutron detectors incorporated in the moderator. Absorbed neutrons inside these detectors are transformed into electrical signals leading to a signal pulse train. Several methods [1–5] have been developed to analyze this pulse train giving two independent measurement results: the total counts and a quantity related to correlated signal pairs. In many practical applications, a two-parameter analysis is not sufficient if neutron multiplication corrections are required with an unknown (α, n) neutron emission rate, or if neutron multiplication is insignificant, but the test item modifies the neutron detection probability. The first case occurs with Pu-containing fuel with unknown age or contamination with light nuclei, the second when monitoring small test items with internal moderation (small waste packages or solutions). A three-parameter analysis can be performed [6], analyzing the pulse train such that the number of signal events inside fixed observation intervals is registered during a measurement time T_M.

The use of moments [7] of the respective probability distributions leads to simple interpretation models, especially with the factorial moments [8,9]. For the determination of three unknown parameters characterizing a test item, the factorial moments [9] and the model for fast fission [10,11] are applied.

2. Theory

Consider a signal correlator device which registers the number of signals existing inside fixed time intervals τ. These intervals are triggered either randomly or by each neutron signal [6,12]. The quantities

0168-9002/86/$03.50

obtained experimentally are the background multiplets $B_x(\tau)$ and the trigger multiplets $N_x(\tau)$ ($x = 0, 1, 2, 3, \cdots$), defined by [8,9], respectively,

$B_x(\tau)$ = number of events with x signals inside K randomly triggered inspection intervals;

$N_x(\tau)$ = number of events with x signals inside inspection intervals τ obtained during an observation time T_M. Each signal triggers an inspection interval τ.

This leads to the frequencies

$$b_x^+(\tau) = B_x(\tau)/K, \tag{1}$$

and

$$n_x^+(\tau) = N_x(\tau)/N_T, \tag{2}$$

where N_T is the number of total counts collected during the measurement time T_M. $b_x(\tau)$ and $n_x(\tau)$ are the probability counterparts to the frequencies $b_x^+(\tau)$ and $n_x^+(\tau)$. The factorial moments

$$m_{b(\mu)} = \sum_{x=\mu}^{\infty} \binom{x}{\mu} b_x(\tau) \cong \sum_{x=\mu}^{\infty} \binom{x}{\mu} b_x^+(\tau), \tag{3}$$

$$m_{n(\mu)} = \sum_{x=\mu}^{\infty} \binom{x}{\mu} n_x(\tau) \cong \sum_{x=\mu}^{\infty} \binom{x}{\mu} n_x^+(\tau), \tag{4}$$

as defined in eqs. (3) and (4) are the effective numbers of signal multiplets with μ signal events inside the observation intervals τ. These effective numbers are generated by $x \geqq \mu$ signal events inside randomly and signal-triggered intervals, and are referred to as randomly and signal-triggered factorial moments of order μ, respectively.

In ref. [9] recurrence formulas for the factorial moments $M_{b(\mu)}$ and $M_{n(\mu)}$ were derived. Both moments are not normalized on $\mu!$ in contrast to $m_{b(\mu)}$ and $m_{n(\mu)}$ of eqs. (3) and (4), respectively. With the identity

$$m_{b(\mu)} = \frac{M_{b(\mu)}}{\mu!} \text{ and } m_{n(\mu)} = \frac{M_{n(\mu)}}{\mu!},$$

the equivalent recurrence formulae of ref. [9] for the normalized factorial moments become

$$m_{b(\mu)} = \sum_{r=0}^{\mu-1} \frac{\mu - r}{\mu} m_{b(r)} m^*_{b(\mu-r)}, \tag{5}$$

and

$$m_{n(\mu)} = \sum_{q=0}^{\mu} m^*_{n(q)} m_{b(\mu-q)}, \tag{6}$$

with

$$m_{b(0)} = 1 \text{ and } m_{n(0)} = m^*_{n(0)} = 1.$$

The quantities $m^*_{b(m)}$ and $m^*_{n(m)}$ are analytical expressions and depend on the characteristics of the test sample, the moderator–detector assembly and the operational conditions of the multiplet analyzer. The following assumptions are introduced:

1) the test sample has point geometry,
2) fast neutron multiplication only takes place in the test sample,
3) no neutrons return from the detector head to the test sample,
4) induced fissions occur at the same time as the primary neutron emissions,
5) the time response function of the moderator detector assembly is a pure exponential function with decay constant λ,

6) the primary neutron energy has no influence on the thermal neutron detection probability ϵ,
7) the start of each observation interval τ of the trigger multiplets is delayed by the time T for each trigger signal,
8) no dead time losses of signals occur.

With these conditions the following holds:

$$m^*_{b(\mu)} = w(\mu)\epsilon^{\mu}\tau\left[S_\alpha\left\{(1-p)\delta_{1\mu} + \overline{\nu_{\alpha(\mu)}(p)}p\right\} + F_s\overline{\nu_{s(\mu)}(p)}\right], \tag{7}$$

and

$$m^*_{n(\mu)} = f^{\mu}\frac{\epsilon^{\mu+1}\tau}{m_{b(1)}}\left[S_\alpha\left\{(1-p)\delta_{0\mu} + \overline{\nu_{\alpha(\mu+1)}(p)}p\right\} + F_s\overline{\nu_{s(\mu+1)}(p)}\right], \tag{8}$$

with

$$w(\mu) = \sum_{K=0}^{\mu-1}\binom{\mu-1}{K}(-1)^K\frac{1-\mathrm{e}^{-\lambda\tau K}}{\lambda\tau K},$$

and

$$f = \mathrm{e}^{-\lambda T}(1-\mathrm{e}^{-\lambda\tau}). \tag{9}$$

For convenience the following quantity is introduced

$$R_{(\mu)} = \epsilon^{\mu}T_{\mathrm{M}}\left[S_\alpha\left\{(1-p)\delta_{1\mu} + \overline{\nu_{\alpha(\mu)}(p)}p\right\} + F_s\overline{\nu_{s(\mu)}(p)}\right]. \tag{10}$$

From eqs. (7) and (8) it then follows

$$R_{(\mu)} = \frac{m^*_{b(\mu)}}{w(\mu)}\frac{T_{\mathrm{M}}}{\tau} = \frac{m^*_{n(\mu-1)}}{f^{\mu-1}}N_{\mathrm{T}} \quad \text{for } \mu \geqq 1. \tag{11}$$

The symbols used are:

S_α = (α,n) neutron emission rate of test item,
F_s = spontaneous fission rate of test item,
p = probability that a neutron generates an induced fission event,
ϵ = probability for detection of a neutron,
τ = observation interval,
T = delay between trigger signal and start of observation interval τ,
λ = fundamental mode decay constant of moderator–detector assembly,
$P_{j\nu}(p)$ = probability for the emission of ν fast neutrons per prompt fission caused by a primary neutron generated by reaction j ($j=\alpha$ or I then (α,n) reaction or induced fission; $j=\mathrm{s}$ for spontaneous fission),
$\overline{\nu_{j(\mu)}(p)}$ = μth factorial moment of the $P_{j\nu}(p)$ distribution

$$\overline{\nu_{j(\mu)}(p)} = \sum_{\nu=\mu}^{\infty}\binom{\nu}{\mu}P_{j\nu}(p), \quad \delta_{n,\mu} = \begin{cases} 1 & \text{for } n=\mu, \\ 0 & \text{for } n\neq\mu. \end{cases} \tag{12}$$

Eqs. (5)–(12) permit a determination of the spontaneous fission rate F_s in the presence of (α,n) reactions and neutron multiplication. Analytical expressions [8] for $P_{j\nu}(p)$ lead to rather complex expressions even with the fast fission approximation. Moreover, recently analytical expressions were given in two independent publications [10,11] for the factorial moments $\overline{\nu_{j(\mu)}(p)}$ of this probability distribution. Using these relations and the fission escape multiplication M where

$$M = \frac{1-p}{1-p\overline{\nu}_{\mathrm{I}(1)}}, \tag{13}$$

the following expression for $\overline{\nu_{j(\mu)}(p)}$ is obtained from ref. [10] or [11] after some algebraic operations:

$$\overline{\nu_{j(\mu)}(p)} = M^{\mu} \sum_{k=1}^{\mu} a_{j\mu K} M^{k-1}, \tag{14}$$

with

$$a_{j11} = \bar{\nu}_{j(1)},$$

$$a_{j21} = \bar{\nu}_{j(2)} - \frac{\bar{\nu}_{j(1)}\bar{\nu}_{\mathrm{I}(2)}}{\bar{\nu}_{\mathrm{I}(1)} - 1},$$

$$a_{j31} = \bar{\nu}_{j(3)} - \frac{\bar{\nu}_{j(1)}\bar{\nu}_{\mathrm{I}(3)}}{\bar{\nu}_{\mathrm{I}(1)} - 1} - 2\frac{\bar{\nu}_{j(2)}\bar{\nu}_{\mathrm{I}(2)}}{\bar{\nu}_{\mathrm{I}(1)} - 1} + 2\frac{\bar{\nu}_{j(1)}\bar{\nu}^2_{\mathrm{I}(2)}}{\left(\bar{\nu}_{\mathrm{I}(1)} - 1\right)^2},$$

$$a_{j22} = \frac{\bar{\nu}_{j(1)}\bar{\nu}_{\mathrm{I}(2)}}{\bar{\nu}_{\mathrm{I}(1)} - 1},$$

$$a_{j32} = \frac{\bar{\nu}_{j(1)}\bar{\nu}_{\mathrm{I}(3)}}{\left(\bar{\nu}_{\mathrm{I}(1)} - 1\right)} + 2\frac{\bar{\nu}_{j(2)}\bar{\nu}_{\mathrm{I}(2)}}{\left(\bar{\nu}_{\mathrm{I}(1)} - 1\right)} - 4\frac{\bar{\nu}_{j(1)}\bar{\nu}^2_{\mathrm{I}(2)}}{\left(\bar{\nu}_{\mathrm{I}(1)} - 1\right)^2},$$

$$a_{j33} = 2\frac{\bar{\nu}_{j(1)}\bar{\nu}^2_{\mathrm{I}(2)}}{\left(\bar{\nu}_{\mathrm{I}(1)} - 1\right)^2}. \tag{15}$$

$\bar{\nu}_{\mathrm{I}(\mu)}$ is the factorial moment of order μ of the $P_{\mathrm{I}\nu}$ distribution for induced fission caused by primary fission neutrons. For $j = \mathrm{s}$, $\bar{\nu}_{j(\mu)}$ is the factorial moment of order μ of the $P_{\mathrm{s}\nu}$ distribution for spontaneous fission of the test sample. Within the uncertainty of the existing data for the P_ν distribution by fast neutron fission, it can be assumed that

$$\bar{\nu}_{\mathrm{I}(\mu)} = \bar{\nu}_{\alpha(\mu)}. \tag{16}$$

With eqs. (14) and (15) the interpretation of the neutron correlation technique requires as nuclear data only the moments of the $P_{j\nu}$ distribution of the isotopes present in the sample for spontaneous ($j = \mathrm{s}$) and induced fission ($j = \alpha = \mathrm{I}$) processes.

2.1. The factorial moments of the P_ν distribution

For spontaneous fission reactions there exists a large number of publications from which the $P_{\mathrm{s}\nu}$ distributions for the various spontaneous fission isotopes can be taken. A recent data evaluation has been performed in ref. [13]. For induced fission events mainly data for thermal neutron induced fissions [13–15] exist for the various fissile isotopes present in fuel. There is one exception: Fréhaut et al. have measured the $P_\nu(E)$ distribution of ^{239}Pu at various fission neutron energies E between 1 and 10 MeV. These data are at present evaluated at BNL [16]. In the analysis of the neutron signals the $\bar{\nu}_{\mathrm{I}(\mu)}$ values for an average fission neutron spectrum are required.

The average value of

$$\bar{\nu}_{\mathrm{I}(1)} = \sum_{\nu=1}^{\infty} \nu P_{\mathrm{I}\nu}$$

increases with neutron energy for the fissile isotopes leading to an even more pronounced increase of the moments with higher order μ. The procedure adopted to overcome this difficulty was to plot $\bar{\nu}_{\mathrm{I}(2)}$ as a function of $\bar{\nu}_{\mathrm{I}(1)}$ and $\bar{\nu}_{\mathrm{I}(3)}$ as a function of $\bar{\nu}_{\mathrm{I}(2)}$ for the isotopes with measured $P_{\mathrm{I}\nu}$ distributions from thermal fission. This resulted [13–16] in a parabolic dependence of $\bar{\nu}_{\mathrm{I}(2)}$ and $\bar{\nu}_{\mathrm{I}(3)}$ on $\bar{\nu}_{\mathrm{I}(1)}$ and $\bar{\nu}_{\mathrm{I}(2)}$,

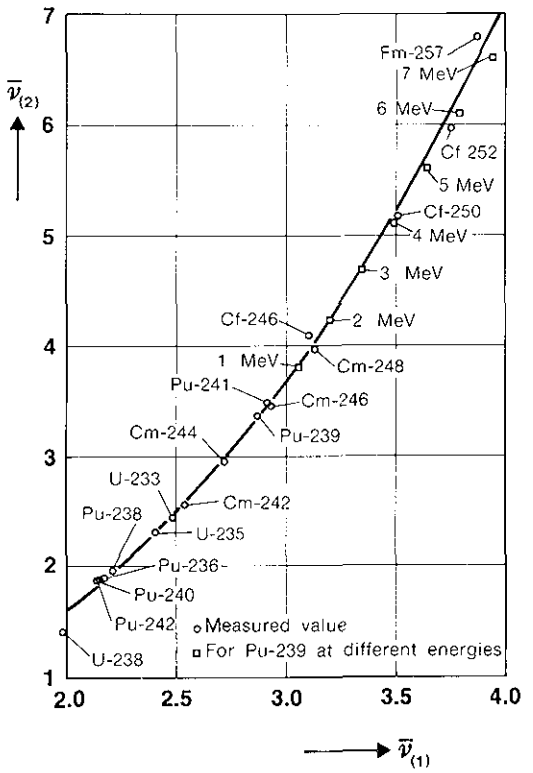

Fig. 1. $\bar{\nu}_{(2)}$ as a function of $\bar{\nu}_{(1)}$.

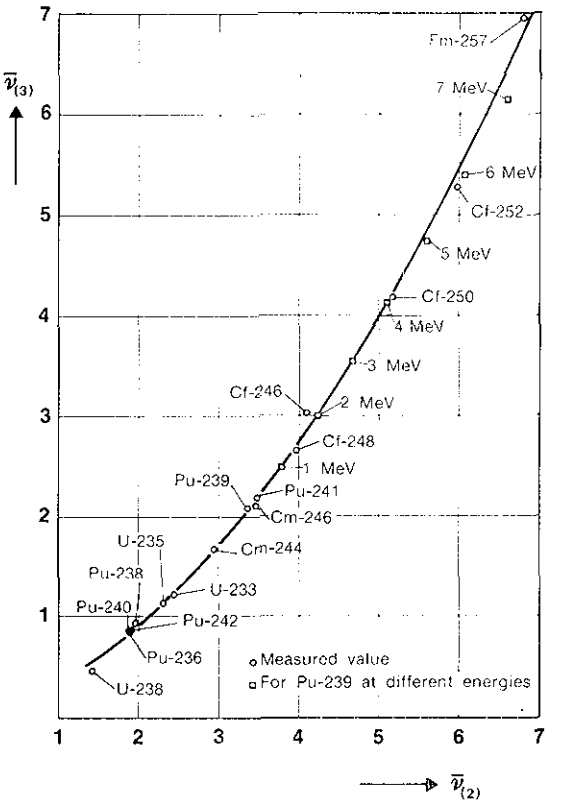

Fig. 2. $\bar{\nu}_{(3)}$ as a function of $\bar{\nu}_{(2)}$.

respectively (figs. 1 and 2). Determining with a Watt fission spectrum $f(E)$ [17] and the fission cross section $\sigma_f(E)$, the value of $\overline{\nu_{I(1)}(E_f)}$ [18] for a fission spectrum is obtained for each fast fissioning isotope:

$$\overline{\nu_{I(1)}(E_f)} = \frac{\int_0^\infty f(E)\bar{\nu}_{I(1)}(E)\sigma_f(E)\,\mathrm{d}E}{\int_0^\infty f(E)\sigma_f(E)\,\mathrm{d}E}. \tag{17}$$

Inserting the value of $\overline{\nu_{I(1)}(E_f)}$ into fig. 1 gives $\overline{\nu_{I(2)}(E_f)}$ and using this value in fig. 2, $\overline{\nu_{I(3)}(E_f)}$ is obtained as an approximation to a fission spectrum average.

In many cases $\overline{\nu_{I(1)}(E)}$ can be determined as the average value of the test sample with nuclear codes. From figs. 1 and 2 then follow the corresponding values for the higher factorial moments. The application of this procedure is valid as long as the neutron slowing down time inside the test item is much smaller than $1/\lambda$.

3. Formulae for typical cases

In the following, models for an interpretation of correlation measurements with three unknown parameters are derived. The cases considered are:

1) Absolute determination of spontaneous fission rate F_s with unknown (α, n) neutron source S_α and unknown neutron multiplication factor M with known instrumental parameters ϵ, λ, τ and T.
2) Relative determination of F_s with unknown S_α and M, using a reference sample.
3) Absolute determination of F_s with unknown S_α and ϵ and known M, λ, τ and T.

4) Absolute determination of F_s, ϵ and M with known α, λ, τ and T, α being the ratio $S_\alpha/\bar{\nu}_{s(1)}F_s$.
5) Determination of M for fissile material with negligible spontaneous fission rate ($F_s = 0$), unknown S_α and ϵ.

For all these methods the quantities R_1, R_2 and R_3 are determined from the randomly triggered multiplets applying eqs. (5) and (11):

$$R_1 = \frac{T_M}{\tau w(1)} m_{b(1)} = N_T, \tag{18}$$

$$R_2 = \frac{T_M}{\tau w(2)} \left[m_{b(2)} - \tfrac{1}{2} m_{b(1)}^2 \right], \tag{19}$$

$$R_3 = \frac{T_M}{\tau w(3)} \left[m_{b(3)} - m_{b(2)} m_{b(1)} + \tfrac{1}{3} m_{b(1)}^3 \right], \tag{20}$$

$$w(1) = 1, \quad w(2) = 1 - \frac{1}{\lambda\tau}(1 - e^{-\lambda\tau}),$$

$$w(3) = 1 - \frac{1}{2\lambda\tau}(3 - 4\, e^{-\lambda\tau} + e^{-2\lambda\tau}), \tag{21}$$

or from signal triggered multiplets with eqs. (6) and (11):

$$R_1 = m_{n(0)} N_T = N_T, \tag{22}$$

$$R_2 = \frac{N_T}{f} [m_{n(1)} - m_{b(1)}], \tag{23}$$

$$R_3 = \frac{N_T}{f^2} \left[m_{n(2)} - m_{b(1)} \{ m_{n(1)} - m_{b(1)} \} \left\{ 1 + \frac{w(2)}{f} \right\} - \tfrac{1}{2} m_{b(1)}^2 \right], \tag{24}$$

or by combining both types of multiplets [8].

The R_μ ($1 \leqq \mu \leqq 3$) obtained from the measured data can be expressed by the instrumental data of the detection head and the physical and nuclear data of the test item using eqs. (10), (14) and (15). They are:

$$R_1 = \epsilon [b_{11} F_s + b_{12} S_\alpha], \tag{25}$$

$$R_2 = \epsilon^2 [b_{21} F_s + b_{22} S_\alpha], \tag{26}$$

$$R_3 = \epsilon^3 [b_{31} F_s + b_{32} S_\alpha], \tag{27}$$

with

$$b_{11} = T_M M \bar{\nu}_{s(1)},$$

$$b_{21} = T_M M^2 \left[\bar{\nu}_{s(2)} + \frac{M-1}{\bar{\nu}_{I(1)} - 1} \bar{\nu}_{s(1)} \bar{\nu}_{I(2)} \right],$$

$$b_{31} = T_M M^3 \left[\bar{\nu}_{s(3)} + \frac{M-1}{\bar{\nu}_{I(1)} - 1} \{ \bar{\nu}_{s(1)} \bar{\nu}_{I(3)} + 2 \bar{\nu}_{s(2)} \bar{\nu}_{I(2)} \} + 2 \left(\frac{M-1}{\bar{\nu}_{I(1)} - 1} \right)^2 \bar{\nu}_{s(1)} \bar{\nu}_{I(2)}^2 \right],$$

$$b_{12} = T_M M,$$

$$b_{22} = T_M M^2 \frac{M-1}{\bar{\nu}_{I(1)^{-1}}} \bar{\nu}_{I(2)},$$

$$b_{32} = T_M M^3 \frac{M-1}{\bar{\nu}_{I(1)} - 1} \left[\bar{\nu}_{I(3)} + 2 \left(\frac{M-1}{\bar{\nu}_{I(1)} - 1} \right) \bar{\nu}_{I(2)}^2 \right]. \tag{28}$$

Eqs. (18)–(28) are used in order to derive the interpretation models for the abovementioned five cases. In eq. (28) $\bar{\nu}_{I(1)}$ is the spectrum average value of $\overline{\nu_{I(1)}(E_f)}$ defined in eq. (17). With known $\bar{\nu}_{I(1)}$ the numerical values of $\bar{\nu}_{I(2)}$ and $\bar{\nu}_{I(3)}$ are obtained from figs. 1 and 2, respectively.

Case 1: absolute determination of F_s, S_α and M.

For the absolute determination of F_s with an unknown (α, n) reaction rate S_α and neutron multiplication factor M, the instrumental data ϵ, λ, and nuclear data $\bar{\nu}_{s(\mu)}$ and $\bar{\nu}_{I(\mu)}$ of the test sample have to be known with sufficient precision. Eliminating in eqs. (25), (26) and (27) F_s and S_α and using the coefficients of eq. (28), an algebraic equation of order 3 in M is obtained [19]:

$$\alpha_0 + \alpha_1 M + \alpha_2 M^2 + \alpha_3 M^3 = 0, \tag{29}$$

with

$$\alpha_0 = -\frac{R_3}{\epsilon^3},$$

$$\alpha_1 = \frac{R_2}{\epsilon^2}\left[\frac{\bar{\nu}_{s(3)}}{\bar{\nu}_{s(2)}} - 2\frac{\bar{\nu}_{I(2)}}{\bar{\nu}_{I(1)}-1}\right],$$

$$\alpha_2 = \frac{R_1}{\epsilon}\frac{1}{\bar{\nu}_{I(1)}-1}\left[\frac{\bar{\nu}_{I(2)}\bar{\nu}_{s(3)}}{\bar{\nu}_{s(2)}} - \bar{\nu}_{I(3)}\right] + \frac{R_2}{\epsilon^2}\frac{2\bar{\nu}_{I(2)}}{\bar{\nu}_{I(1)}-1},$$

$$\alpha_3 = \frac{R_2 2\bar{\nu}_{I(2)}}{\epsilon^2(\bar{\nu}_{I(1)}-1)} - \alpha_2. \tag{30}$$

The neutron multiplication factor M is determined from eq. (29) by taking the solution with the smallest possible value of $M > 1$.

With the known multiplication M a solution of eqs. (25) and (26) with respect to the two unknowns F_s and S_α gives:

$$F_s = \frac{1}{T_M}\left[\frac{R_2}{\epsilon^2 M^2 \bar{\nu}_{s(2)}} - \frac{R_1\bar{\nu}_{I(2)}(M-1)}{\epsilon M\bar{\nu}_{s(2)}(\bar{\nu}_{I(1)}-1)}\right], \tag{31}$$

and

$$S_\alpha = \frac{1}{T_M}\left[\frac{R_1}{\epsilon M}\left[1 + \frac{\bar{\nu}_{s(1)}\bar{\nu}_{I(2)}(M-1)}{\bar{\nu}_{s(2)}(\bar{\nu}_{I(1)}-1)}\right] - \frac{R_2}{\epsilon^2 M^2}\frac{\bar{\nu}_{s(1)}}{\bar{\nu}_{s(2)}}\right]. \tag{32}$$

The spontaneous fission neutron emission rate is mainly determined by R_2, i.e. the measured signal doublets. As long as the (α, n) reaction rate is not the dominating contribution to R_1, the influence of the singlets is less important due to the M-1 weighting. Larger errors will occur in S_α because the first and second term of eq. (32) are of the same order of magnitude.

Case 2: relative determination of F_s.

For the relative determination of the spontaneous fission rate in the presence of (α, n) reactions and neutron multiplication, at least one well characterized reference sample must be available. Determining the R_μ values of the test sample and those of the reference sample $R_\mu(0)$ $(1 \leqq \mu \leqq 3)$ the instrumental parameters ϵ, λ and τ and T are eliminated completely if the factorial moments of randomly triggered intervals τ are used (see eqs. (18), (19) and (20)). This is also true when combining the randomly and signal triggered factorial moments [8]. It is no longer true when using the signal triggered factorial moments.

Applying eqs. (25), (26) and (27) for the test and reference samples, the following system of equations is obtained:

$$r_\mu = \frac{R_\mu}{R_\mu(0)}\left[F_s(0)b_{\mu 1}(0) + S_\alpha(0)b_{\mu 2}(0)\right] = F_s b_{\mu 1} + S_\alpha b_{\mu 2} \quad 1 \leqq \mu \leqq 3. \tag{33}$$

$b_{\mu 1}(0)$ and $b_{\mu 2}(0)$ are the known coefficients of eq. (28) of the reference sample with the known multiplication factor $M(0)$, the known nuclear data $\bar{\nu}_{s(\mu)}(0)$ and $\bar{\nu}_{I(\mu)}(0)$ and measurement time T_M. The coefficients $b_{\mu 1}$ and $b_{\mu 2}$ of the unknown test sample contain the unknown multiplication factor M and the known nuclear data $\bar{\nu}_{s(\mu)}$ and $\bar{\nu}_{I(\mu)}$. Eliminating by means of eqs. (31) and (32) F_s and S_α, an equation of order 3 for the determination of the multiplication factor M is again obtained:

$$\alpha_0^* + \alpha_1^* M + \alpha_2^* M^2 + \alpha_3^* M^3 = 0. \tag{34}$$

The coefficients α_i^* now depend on r_μ, which is proportional to the ratio $R_\mu/R_\mu(0)$ and to $F_s(0)$ and $S_\alpha(0)$ of the reference sample. They are:

$$\alpha_0^* = -r_3,$$

$$\alpha_1^* = r_2\left[\frac{\bar{\nu}_{s(3)}}{\bar{\nu}_{s(2)}} - 2\frac{\bar{\nu}_{I(2)}}{\bar{\nu}_{I(1)}-1}\right],$$

$$\alpha_2^* = r_1\frac{1}{(\bar{\nu}_{I(1)}-1)}\left[\frac{\bar{\nu}_{s(3)}\bar{\nu}_{I(2)}}{\bar{\nu}_{s(2)}} - \bar{\nu}_{I(3)}\right] + r_2\frac{2\bar{\nu}_{I(2)}}{\bar{\nu}_{I(1)}-1},$$

$$\alpha_3^* = r_2\frac{2\bar{\nu}_{I(2)}}{\bar{\nu}_{I(1)}-1} - \alpha_2^*, \tag{35}$$

with

$$r_1 = \frac{R_1}{R_1(0)}F_s(0)\bar{\nu}_{s(1)}C_1(0), \tag{36}$$

$$C_1(0) = M(0)[1+\alpha(0)], \tag{37}$$

$$r_2 = \frac{R_2}{R_2(0)}F_s(0)\bar{\nu}_{s(2)}C_2(0), \tag{38}$$

$$C_2(0) = M^2(0)\left[1 + (M(0)-1)(1+\alpha(0))\frac{\bar{\nu}_{s(1)}\bar{\nu}_{I(2)}}{\bar{\nu}_{I(1)}-1}\right], \tag{39}$$

$$r_3 = \frac{R_3}{R_3(0)}F_s(0)\bar{\nu}_{s(3)}C_3(0), \tag{40}$$

$$C_3(0) = M^3(0)\left[1 + 2(M(0)-1)\frac{\bar{\nu}_{s(2)}\bar{\nu}_{I(2)}}{\bar{\nu}_{s(3)}(\bar{\nu}_{I(1)}-1)} + (M(0)-1)(1+\alpha(0))\left\{[M(0)-1]\frac{\bar{\nu}_{s(1)}\bar{\nu}_{I(2)}^2}{\bar{\nu}_{s(3)}(\bar{\nu}_{I(1)}-1)^2} + \frac{\bar{\nu}_{s(1)}\bar{\nu}_{I(3)}}{\bar{\nu}_{s(3)}(\bar{\nu}_{I(1)}-1)}\right\}\right]. \tag{41}$$

With known multiplication factor M, the spontaneous fission and (α,n) reaction rates F_s and S_α, respectively, are given by:

$$F_s = \frac{r_2}{T_M M^2 \bar{\nu}_{s(2)}} - \frac{r_1(M-1)}{T_M M}\frac{\bar{\nu}_{I(2)}}{\bar{\nu}_{s(2)}(\bar{\nu}_{I(1)}-1)}, \tag{42}$$

$$S_\alpha = \frac{r_1}{T_M M}\left[1 + \frac{\bar{\nu}_{I(2)}\bar{\nu}_{s(1)}}{\bar{\nu}_{s(2)}(\bar{\nu}_{I(1)}-1)}(M-1)\right] - \frac{r_2}{T_M M^2}\frac{\bar{\nu}_{s(1)}}{\bar{\nu}_{s(2)}}. \tag{43}$$

In the case that there are several reference or test samples with known F_s, S_α and known multiplication factor M, the constant C_μ of eqs. (37), (39) and (41) serve to correct the R_μ values ($1 \leqq \mu \leqq 3$) for these two contributions.

The α and M corrected value of R_μ is:

$$R_{\mu c} = \epsilon^\mu F_s \bar{\nu}_{s(\mu)} T_M = R_\mu / C_\mu . \tag{44}$$

$R_{\mu c}$ has to lie within the error margins on a straight line with the given spontaneous fission rate F_{sD} (or the ^{240}Pu-mass equivalents) as abscissa, provided that the limitations of the model are valid and the nuclear data correctly chosen.

Case 3: absolute determination of F_s with unknown S_α and ϵ.

A spontaneous fission and (α, n) neutron emitter surrounded by moderating material influences the neutron detection probability of the detector head. A part of the source neutrons is slowed down in this moderator and is absorbed in the thermal neutron filters of the detector head. Such conditions exist when monitoring small waste packages with moderating material like polythene, paper, rubber, etc. In this case a determination of F_s, S_α and ϵ is required assuming that the neutron multiplication is either negligible or known.

First the neutron emission rate ratio

$$\alpha = \frac{S_\alpha}{\bar{\nu}_{s(1)} F_s} \tag{45}$$

is determined forming the ratio

$$\beta = \frac{R_2^2}{R_1 R_3} . \tag{46}$$

This ratio becomes independent of ϵ for a point source and independent of F_s by using eq. (45). Replacing R_1, R_2 and R_3 in eq. (46) by eqs. (25), (26) and (27), the following solution of a quadratic equation in α is found:

$$\alpha = \frac{\sqrt{B^2 + 4AC} - B}{2A} , \tag{47}$$

with

$$\begin{aligned} A &= \beta b_{11} b_{31} - b_{22}^2 \bar{\nu}_{s(1)}^2 , \\ B &= \beta b_{11} \left(b_{31} + b_{32} \bar{\nu}_{s(1)} \right) - 2 b_{21} b_{22} \bar{\nu}_{s(1)} , \\ C &= b_{21}^2 - \beta b_{11} b_{31} . \end{aligned} \tag{48}$$

The coefficients b_{ij} ($1 \leqq i \leqq 3$ and $1 \leqq j \leqq 2$) are defined in eq. (28). The ratio

$$\gamma = R_1^2 / R_2 \tag{49}$$

is independent of ϵ. It is used knowing the α-ratio for the determination of the spontaneous fission rate F_s:

$$F_s = \frac{\gamma \left(b_{21} + \alpha b_{22} \bar{\nu}_{s(1)} \right)}{T_M b_{11}^2 (1 + \alpha)^2} . \tag{50}$$

With known α and F_s the neutron detection probability ϵ follows from eq. (25). It is:

$$\epsilon = \frac{R_1}{F_s \bar{\nu}_{s(1)} M T_M (1 + \alpha)} . \tag{51}$$

Where there is no neutron multiplication, the following relations are valid:

$$M = 1,$$

$$\alpha = \frac{\bar{\nu}_{s(2)}^2}{\beta \bar{\nu}_{s(1)} \bar{\nu}_{s(3)}} - 1,$$

$$F_s = \gamma \frac{\bar{\nu}_{s(2)}}{\bar{\nu}_{s(1)}^2 (1+\alpha)^2 T_M},$$

and

$$\epsilon = \frac{R_1}{F_s \bar{\nu}_{s(1)} (1+\alpha) T_M}. \tag{52}$$

Case 4: absolute determination of F_s, ϵ and M with known α-ratio.

In some cases the α-ratio of waste items with internal moderation is better known than the neutron multiplication factor M. This occurs especially when measuring fuel fabrication waste of known isotopic composition and no or a known contamination with isotopes having a large (α, n) reaction cross section.

First a relation for the unknown neutron multiplication factor is obtained using eqs. (25), (26), (27) and (28), forming the ratio:

$$\beta = \frac{R_2^2}{R_1 R_3}. \tag{53}$$

After some algebraic operations, a quadratic equation for M is found with the solution:

$$M = \frac{Q + \sqrt{Q^2 - 4PR}}{2P}, \tag{54}$$

where

$$\begin{aligned} P &= \beta a_1 c_3 - b_2^2, \\ Q &= 2 a_2 b_2 - \beta a_1 b_3, \\ R &= \beta a_1 a_3 - a_2^2, \end{aligned} \tag{55}$$

and

$$\begin{aligned} a_1 &= \bar{\nu}_{s(1)} (1+\alpha), \\ a_2 &= \bar{\nu}_{s(2)} - \frac{\bar{\nu}_{s(1)} \bar{\nu}_{I(2)}}{\bar{\nu}_{I(1)} - 1} (1+\alpha), \\ b_2 &= \bar{\nu}_{s(2)} - a_2, \\ a_3 &= \bar{\nu}_{s(3)} - \frac{1}{\bar{\nu}_{I(1)} - 1} \left[2 \bar{\nu}_{s(2)} \bar{\nu}_{I(2)} + (1+\alpha) \bar{\nu}_{s(1)} \bar{\nu}_{I(3)} \right] + c_3, \\ b_3 &= \bar{\nu}_{s(3)} - a_3 - c_3, \\ c_3 &= 2(1+\alpha) \frac{\bar{\nu}_{s(1)} \bar{\nu}_{I(2)}^2}{\left(\bar{\nu}_{I(1)} - 1 \right)^2}. \end{aligned} \tag{56}$$

Having determined M, F_s follows directly from eq. (50).

Case 5: no spontaneous fission primary neutrons.

In some practical applications, fuel has no spontaneously fissioning isotopes but (α, n) primary neutrons. In these conditions the neutron multiplication M, the (α, n) reaction rate S_α and the detection

probability ϵ can be determined. This leads to the simple case that $b_{11} = b_{21} = b_{31} = 0$. From the ratio β an expression for M is obtained:

$$M = \frac{\beta}{1-\beta} \frac{\bar{\nu}_{I(3)}(\bar{\nu}_{I(1)} - 1)}{\bar{\nu}^2_{I(2)}} + 1. \tag{57}$$

The ratios β and γ serve to derive an equation for the determination of S_α:

$$S_\alpha = \frac{\gamma}{T_M} \frac{\beta}{1-\beta} \frac{\bar{\nu}_{I(3)}}{\bar{\nu}_{I(2)}}. \tag{58}$$

With known S_α and M, the detection probability ϵ follows simply from eq. (25).

4. Test of theory by experimental data

4.1. ϵ not modified by sample

Part of the derived analytical expressions was tested with experimental data using a 8.45 g metallic Pu sample exposed in a hollow cylindrical detector head of 1 m height and 32 ^{3}He proportional counters. By means of a computerized registration system [20], the factorial moments of the frequencies to have x signals inside, randomly and signal triggered observation intervals τ were measured. Table 1 gives the average values and the standard deviations of these moments obtained in eight different runs, each with a measurement time of 8 min. The predelay T for the three observation intervals $\tau_1 = 25.6$ μs, $\tau_2 = 51.2$ μs and $\tau_3 = 102.4$ μs was 6.4 μs in each case. The decay time of the detector head was 51.3 μs and its neutron detection probability $\epsilon = 0.27$. The latter quantity [20] was determined in a separate experiment from an unknown ^{252}Cf spontaneous fission neutron source, using the nuclear data for $\bar{\nu}_{s(1)}$ and $\bar{\nu}_{s(2)}$ and R_1 and

Table 1
Moments of randomly and signal-triggered observation intervals

ORDER OF MOMENT m	Moments $m_{b(m)}$ of Randomly Triggered Observation Intervals τ		
	$\tau =$ 25.6 μs	$\tau =$ 51.2 μs	$\tau =$ 102.4 μs
0	1.0000 ± 3.9 10^{-5}	0.99999 ± 7.99 10^{-5}	1.0000 ± 1.47 10^{-4}
1	6.61483 10^{-3} ± 2.25 10^{-5}	1.32301 10^{-2} ± 6.97 10^{-5}	2.64591 10^{-2} ± 1.36 10^{-4}
2	3.74852 10^{-4} ± 4.85 10^{-6}	1.31250 10^{-3} ± 2.52 10^{-5}	4.12235 10^{-3} ± 6.10 10^{-5}
3	1.67851 10^{-5} ± 1.35 10^{-6}	1.02862 10^{-4} ± 7.96 10^{-6}	4.88466 10^{-4} ± 2.54 10^{-5}
4	5.2053 10^{-7} ± 1.5 10^{-7}	6.80980 10^{-6} ± 1.79 10^{-6}	4.84310 10^{-5} ± 6.60 10^{-6}
	Moments $m_{n(m)}$ of Signal Triggered Observation Intervals τ		
0	1.00004 ± 2.10 10^{-3}	1.00003 ± 2.27 10^{-3}	9.99779 10^{-1} ± 2.32 10^{-3}
1	9.52149 10^{-2} ± 1.59 10^{-3}	1.54135 10^{-1} ± 1.84 10^{-3}	2.17687 10^{-1} ± 3.50 10^{-3}
2	5.85962 10^{-3} ± 4.47 10^{-4}	1.53349 10^{-2} ± 7.01 10^{-4}	3.09289 10^{-2} ± 2.77 10^{-3}
3	4.27510 10^{-4} ± 9.06 10^{-5}	1.25952 10^{-3} ± 1.63 10^{-4}	3.48763 10^{-3} ± 1.04 10^{-3}

$N'_T = 258.4\ s^{-1}$ $N'_B = 2.5\ s^{-1}$ (count rate with and without sample).

Table 2
Determined $M-1$, $\bar{\nu}_{s(1)}F_s$ and S_α

	RANDOMLY TRIGGERED INTERVALS		
	$\tau_1 = 25.6\ \mu s$	$\tau_2 = 51.2\ \mu s$	$\tau_3 = 102.4\ \mu s$
M-1	0.0183 ± 0.0036	0.0219 ± 0.0028	0.0206 ± 0.0026
$\bar{\nu}_{s(1)}F_s$ [1/s]	930 ± 6	920 ± 6	924 ± 6
S_α[1/s]	0.5	6.6 ± 13	5.1
	SIGNAL TRIGGERED INTERVALS		
M-1	0.0256 ± 0.0043	0.0223 ± 0.0015	0.0180 ± 0.0021
$\bar{\nu}_{s(1)}F_s$ [1/s]	920 ± 10	923 ± 4	930 ± 5
S_α[1/s]	4.3	4.7 ± 9	0.4
	SAMPLE DATA		REMARK
M-1	0.0240		TIMOC
$\bar{\nu}_{s(1)}F_s$ [1/s]	918 ± 24		
S_α[1/s]	0		

R_2 values derived from signal and randomly triggered observation intervals. In order to obtain the neutron multiplication M, the spontaneous fission rate F_s and the (α, n) neutron emission rate S_α, the formulae of case 1 are used, in connection with the factorial moments $m_{b(j)}$ $(j = 1, 2, 3)$ of table 1. First are determined the quantities R_j using eqs. (18), (19) and (20), calculating $w(j)$ $(j = 1, 2, 3)$ according to eq. (21). With known R_j, ϵ, $\bar{\nu}_{I(j)}$ and $\bar{\nu}_{s(j)}$, the coefficients α_i $(i = 0, 1, 2, 3)$ of an equation of third degree in M are obtained. For each gate length the neutron multiplication factor M is determined from the root of eq. (29) for $M > 1$. With known M, the spontaneous fission rate F_s, and the (α, n) neutron emission rate S_α follow from eqs. (31) and (32), respectively.

A similar procedure was applied using as measured data the factorial moments $m_{n(\mu)}$ $(\mu = 0, 1, 2)$ of the three signal triggered observation intervals τ.

Table 2 gives the results for $M-1$, $\bar{\nu}_{s(1)}$, F_s and S_α for both measurement methods and the three observation intervals. The uncertainties quoted are the standard deviations of the eight runs each analyzed individually. The results for the spontaneous fission neutron emission rates agree very well with the values known from the test sample [21]. The uncertainty in $\bar{\nu}_{s(1)}F_s$ of the test sample is mainly due to the uncertainty of the spontaneous fission neutron half-life of ^{240}Pu [22].

The determined quantities are within their error limits independent of the duration of the observation intervals and independent of the type of trigger interval used. The smallest statistical error appears to be for observation intervals τ close to the decay time of the detector head.

R_2 and R_3 can be obtained by combining the factorial moments of both signal and randomly triggered observation intervals. In this case the measured $m_{b(1)}$ and $m_{b(2)}$ [8] are taken to calculate R_2 and R_3. The values obtained for M, $\bar{\nu}_{s(1)}F_s$ and S_α lead to almost the same numerical values as found with the signal triggered factorial moments.

4.2. ϵ *modified by test sample*

Monitoring small waste packages of material containing hydrogen, the Pu mass is frequently so small that the neutron multiplication factor M becomes close to 1. In this case the spontaneous fission rate F_s, the (α, n) reaction rate S_α and the detection probability ϵ can be determined according to the formulas derived for case 3 by putting $M = 1$. However, if the Pu content is of the order of grams, then the determination of the spontaneous fission neutron emission rate $\bar{\nu}_{s(1)}F_s$ depends strongly on the neutron multiplication factor M.

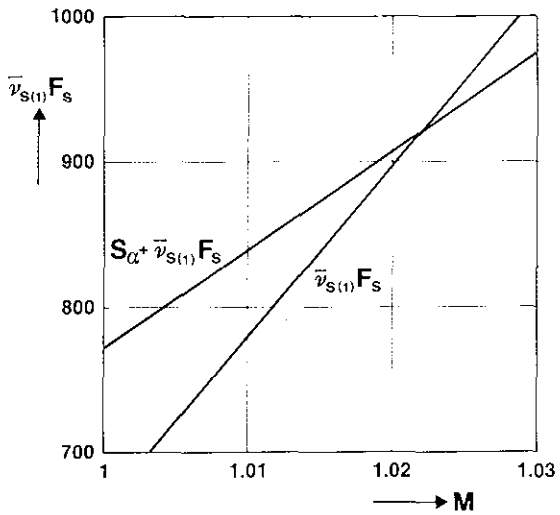

Fig. 3. Neutron emission rate as a function of M.

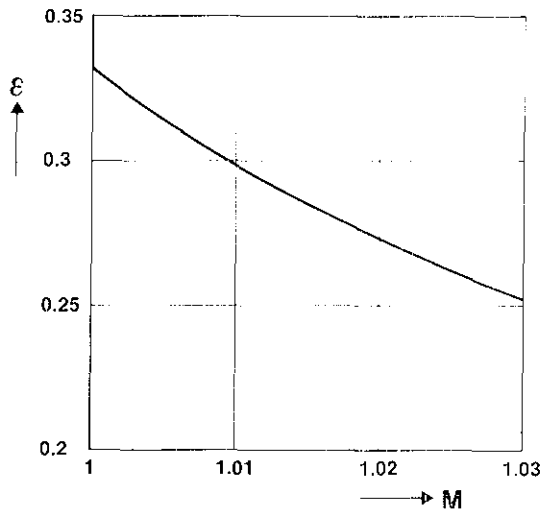

Fig. 4. Detection probability ϵ as a function of M.

Such conditions are presented in fig. 3 for the 8.45 g metallic Pu sample. This figure is based on the experimental data obtained from randomly triggered factorial moments with an observation interval $\tau = 51.2$ μs. Not knowing the characteristics of the sample, it is only possible to state that the multiplication factor is below 1.0219 since otherwise S_α would become negative. Knowing the isotopic composition of the fuel it is recommendable to determine an approximate value of the α-ratio, and to calculate with the formulas of case 4, F_s, M and ϵ. By this type of analysis the uncertainty in the determination of $\bar{\nu}_{s(1)}F_s$ can often be kept within smaller limits. Fig. 4 gives the neutron detection probability as a function of M for the same conditions as in fig. 3. The same tendency of $\bar{\nu}_{s(1)}F_s$ and ϵ as a function of M has been found in ref. [23] when analyzing the frequency distribution of a signal pulse train for randomly and signal triggered observation intervals.

5. Conclusions

The interpretation model has been tested successfully with a small Pu-metal sample. In the near future, tests will be carried out on the validity of the point model and the model for neutron multiplication with smaller and larger PuO_2 samples. Dead time corrections of the factorial moments are still a problem for further theoretical studies.

Acknowledgements

Many thanks are due to Mr. L. Bondar for providing some measured data. Much appreciated were discussions with Mr. N. Barrett, Mr. L. Bondar, Mr. R. Dierckx and Mr. A. Prosdocimi. Gratefully acknowledged is the assistance of Mrs. K. Caruso for performing the calculations and preparing the figures, and to Mrs. G. Tenti and Mrs. M. Van Andel for typing the manuscript.

References

[1] G. Birkhoff, L. Bondar, J. Ley, R. Berg, R. Swennen and G. Busca, EUR 5158e, Commission of the European Communities, Joint Research Centre, Ispra (1974).

[2] K. Böhnel, KfK-2203, Kernforschungszentrum Karlsruhe (1975).
[3] N. Ensslin, M.L. Evans, H.O. Menlove and J.E. Swansen, Nucl. Mater. Man. 7 (1978) 43.
[4] E.J. Dowdy, C.N. Henry, A.A. Robba and J.R. Pratt, Proc. Int. Symp. on Nuclear Material Safeguards, Vienna, SM-231/69 (IAEA, Vienna, 1978).
[5] M.O. Deighton, Nucl. Instr. and Meth. 165 (1979).
[6] L. Bondar, Proc. Int. Meeting on Monitoring of Plutonium Contaminated Waste, Ispra, Commission of the European Communities, Ispra (1979).
[7] N. Shenhav, Y. Segal and A. Notea, Nucl. Sci. Eng. 80 (1982) 61.
[8] R. Dierckx and W. Hage, Nucl. Sci. Eng. 85 (1983) 325.
[9] W. Hage and D.M. Cifarelli, Nucl. Sci. Eng. 89 (1985) 159.
[10] K. Böhnel, Nucl. Sci. Eng. 90 (1985) 75.
[11] W. Hage and D.M. Cifarelli, Nucl. Instr. and Meth. A236 (1985) 165.
[12] M.S. Krick and J.E. Swansen, Nucl. Instr. and Meth. 219 (1984) 385.
[13] M.S. Zucker and N.E. Holden, 6th ESARDA Symp. on Safeguards and Nuclear Material Management, Venice, Italy (1984).
[14] J.W. Boldeman and M.G. Hines, Nucl. Sci. Eng. 91 (1985) 114.
[15] N.E. Holden and M.S. Zucker, 7th ESARDA Symp. on Safeguards and Nuclear Material Management, Liège, Belgium (1985).
[16] M.S. Zucker (BNL), private communication (1985).
[17] Proc. Consultants, Meeting on Prompt Fission Neutron Spectra, IAEA, Vienna (1971).
[18] F. Manero and V.A. Konshin, At. En. Rev. 10 (1972) 637.
[19] W. Hage and D.M. Cifarelli, Proc. 26th INMM Ann. Meeting Albuquerque (1985).
[20] L. Bondar, Joint Research Centre, Ispra, private communication (1982).
[21] J.F. Gueugnon and K. Richter, European Institute for Transuranium Elements, Karlsruhe, Fabrication report K0282049 (1982).
[22] C. Budtz-Jørgensen and H.H. Knitter, Nucl. Sci. Eng. 79 (1981) 380.
[23] L. Bondar et al., ESARDA Proc., Venice, Italy (1984).

NUCLEAR SCIENCE AND ENGINEERING: 89, 159-176 (1985)

Correlation Analysis with Neutron Count Distributions in Randomly or Signal Triggered Time Intervals for Assay of Special Fissile Materials

W. Hage

Commission of the European Communities, Joint Research Centre
I-21020 Ispra (Varese), Italy

and

D. M. Cifarelli

Università L. Bocconi, Istituto di Metodi Quantitativi
I-20136 Milano, Italy

Received April 9, 1984
Accepted September 12, 1984

NUCLEAR SCIENCE AND ENGINEERING: 89, 159-176 (1985)

Correlation Analysis with Neutron Count Distributions in Randomly or Signal Triggered Time Intervals for Assay of Special Fissile Materials

W. Hage

Commission of the European Communities, Joint Research Centre
I-21020 Ispra (Varese), Italy

and

D. M. Cifarelli

Università L. Bocconi, Istituto di Metodi Quantitativi
I-20136 Milano, Italy

Received April 9, 1984
Accepted September 12, 1984

Abstract—*A mathematical model is derived for the probability distribution of neutron signal multiplets inside randomly and signal triggered time intervals for a generalized time response function of the neutron detector assembly. The theory is applied to assemblies with an exponential time decay of its neutron population. The probability distributions, their factorial moments, and moments are expressed as a function of the spontaneous fission rate, (α-n) reaction rate, neutron detection probability, probability that a neutron generates a fast fission, and nuclear data. Measurements with a plutonium sample are analyzed to check the derived algorithms for the factorial moments of the two probability distributions.*

Analyse de corrélation des distributions de comptes de neutrons dans des intervals de temps aléatoires ou déclenchés par les signaux pour l'essai des matériaux fissiles spéciaux

Résumé—*Un modèle mathématique est dérivé pour la distribution de probabilité des groupes de signaux neutroniques à l'intérieur d'intervals de temps. Ces intervals peuvent être déclenchés par des signaux neutroniques eux-mêmes ou par des signaux aléatoires. Le modèle est établi pour une réponse temporelle généralisée du détecteur neutronique. La théorie est appliquée pour des ensembles, pour lesquels la population neutronique décroit exponentiellement. Les distributions de probabilité, leurs moments factoriels et leurs moments dépendent du taux des fissions spontanées, du taux de la réaction (α-n), de la probabilité de détection neutronique, de la probabilité qu'un neutron donne lieu à une fission rapide et de données nucléaires. Des mesures faites sur un échantillon de Pu sont analysées pour tester les algorithmes dérivés pour les moments factoriels des distributions de probabilité.*

Korrelationsanalyse von Neutronenzählverteilungen in zufälligen oder signalgesteuerten Zeitintervallen für die Untersuchung von spaltbarem Material

Zusammenfassung—*Für eine allgemeine zeitliche Ausgleichsfunktion einer Neutronenzählanlage wurde ein mathematisches Modell für die Wahrscheinlichkeitsverteilung von Neutronensignalen innerhalb von zufälligen und signalgesteuerten Zeitintervallen hergeleitet. Die Theorie fand Anwendung für Zählanlagen mit einem exponentiellen Zerfallsgesetz der Neutronenbevölkerung. Die Wahrscheinlichkeitsverteilungen, ihre faktoriellen Momente, und ihre Momente erscheinen als Funktion der Spontanspaltrate, der (α-n)-Reaktionsrate, der Wahrscheinlichkeit für die Registrierung eines Neutrons, der Wahrscheinlichkeit daß ein Neutron eine Schnellspaltung erzeugt und kernphysikalischen Daten. Zur Überprüfung ihrer Gültigkeit wurden die abgeleiteten Gleichungen zur Interpretation von Messergebnissen mit einer Pu-Probe herangezogen.*

I. INTRODUCTION

The nondestructive assay of fissile material is a necessary tool to follow the flow of fissile material in a nuclear fuel cycle. In this paper, an analysis method for a passive neutron assay technique is elaborated. It is based on the determination of the spontaneous fission neutron emission rate of plutonium isotopes with even mass numbers (^{238}Pu, ^{240}Pu, ^{242}Pu) as an indicator for the fissile mass. This mass determination requires knowledge of the isotopic composition of the fuel, and needs a treatment of the neutrons generated by (α-n) reactions on light target nuclei (present in PuO_2) due to the strong alpha activity of most plutonium isotopes. A separation of the measured neutron signals generated by spontaneous fission from those of (α-n) reactions is achieved with time correlation analysis of these signals.

In this technique the neutrons emitted by a test item are slowed down in a moderator, diffuse there as thermal neutrons, and are partially absorbed by neutron detectors incorporated in the moderator assembly. The neutrons absorbed in the detectors are transformed in real time into electric signals and amplified, shaped, and converted into a signal pulse train. Two methods are in use for the analysis of this pulse train—the shift register[1,2] and the variable dead-time counter.[3-5] Both instruments deliver two experimental quantities—the total count and the correlated count. This permits the determination of the spontaneous fission rate F_s and either the (α-n) reaction rate S_α or the probability p that a primary source neutron generates an induced fission. For the assay of bulky fuel material containing plutonium, three experimental data are desired for a pure experimental determination of F_s, S_α, and p. In alpha-contaminated waste, neutron multiplication is less important; however, neutron absorption in the waste material modifies the neutron detection probability ϵ of the moderator detector assembly. In such measurement conditions a three-parameter analysis is suitable for a determination of F_s, S_α, and ϵ. Such a three-parameter analysis is performed in Refs. 6, 7, and 8.

In this technique the neutron signal pulse train is fed via a derandomizer[9] into a computer and analyzed to give the number of events with the same number of signals inside an analysis time interval τ. Two types of such intervals are used. One is triggered by each signal giving trigger multiplets; the other is triggered randomly to obtain the background multiplets.

In Refs. 6, 7, and 8, each of the two probability distributions is used to obtain F_s, S_α, p, or ϵ from their respective frequency distributions. One disadvantage of this treatment is that the probability distributions of both types of multiplets are complex expressions of these unknowns.

This disadvantage is avoided in Ref. 10 where the probability distributions of both the trigger and background multiplets are used together to obtain the factorial moments of the probability distribution of the correlated multiplets. This treatment leads to simple expressions for F_s, S_α, p, and ϵ. This method, however, requires the measurement of both the respective frequency distributions.

We avoid this by deriving both the moments and the factorial moments of the corresponding probability distributions. These lead to simple analytical expressions for F_s, S_α, p, and ϵ, which are then applied to the interpretation of the frequency distribution of the measured trigger and background multiplets.

II. THEORY

Section II gives a detailed derivation of a theory for the determination of the probability $b_x(t-\tau, t, T_1, T_2)$ to have x signals inside a randomly triggered time interval $t-\tau, t$. The fission events have an inhomogeneous Poisson distribution over the time interval T_1, T_2 where $0 \le T_1 \le T_2 \le t$. Furthermore, differential equations are derived giving the factorial moments and the moments of the $b_x(t-\tau, t, T_1, T_2)$ distribution.

II.A. Probability $b_x(t-\tau, t, T_1, T_2)$

To obtain an analytical expression for $b_x(t-\tau, t, T_1, T_2)$, it is assumed that the fission bursts occurring in the time interval $T_1, T_2 (T_1 < T_2 < t)$ have an inhomogeneous Poisson distribution and are generated by a spontaneous fission point source, whose fission rate $F_s(s)$ varies with time s.

During a single fission burst, ν spontaneous fission neutrons are emitted with the probability $P_{s\nu}$. These ν neutrons are slowed down in a moderator detector assembly, referred to as the detection head, and diffuse there as thermal neutrons. Of these ν-emitted neutrons, n ($\nu \ge n$) are absorbed inside the neutron detectors and transformed into electric signals with the probability $\epsilon^n(1-\epsilon)^{\nu-n}$ in $\binom{\nu}{n}$ distinct orderings; ϵ is then the probability for the detection of a neutron originating from a fission event.

Of these n-detected neutrons originating from the fission event at time ξ (Fig. 1), j fall into the interval $t-\tau, t$ with the probability $c(t, j, n, \xi)$. With these definitions the probability generating function $G_\xi(z)$ for the number of neutrons from a single burst of fission neutrons at time ξ with probability $P_{s\nu}$, that ν neutrons are emitted of which n are detected and j fall into the interval $t-\tau, t$ where $\nu \ge n \ge j \ge 0$, is

$$G_\xi(z) = \sum_{\nu=0}^{\infty} \sum_{n=0}^{\nu} \sum_{j=0}^{n} z^j P_{s\nu} \binom{\nu}{n} \epsilon^n (1-\epsilon)^{\nu-n} c(t, j, n, \xi) \ . \quad (1)$$

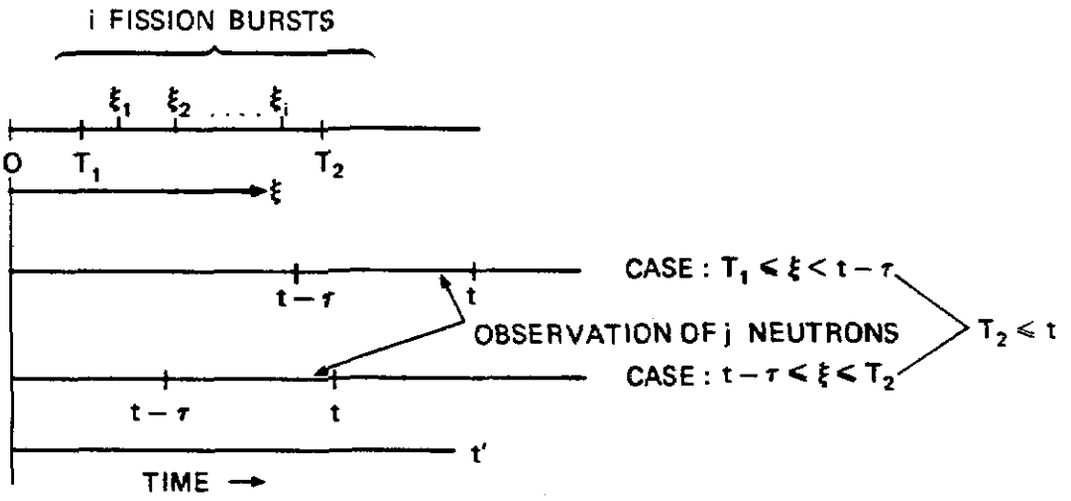

Fig. 1. Time diagram of fission bursts in $T_1 \le \xi \le T_2$ and observation of detected neutrons in $t-\tau \le t' \le t$.

If the neutron population originating from a single neutron burst decays in time according to the fundamental mode decay constant $1/\lambda$ of the detection head, then $c(t,j,n,\xi)$ is given by

$$c(t,j,n,\xi) = \binom{n}{j}\left\{\int_{max(\xi,t-\tau)}^{t} \exp[-\lambda(t'-\xi)]\lambda\,dt'\right\}^{j} \times\left\{1-\int_{max(\xi,t-\tau)}^{t} \exp[-\lambda(t'-\xi)]\lambda\,dt'\right\}^{n-j} . \tag{2}$$

The probability for detection of n neutrons from ν-emitted ones is

$$e_s(n) = \epsilon^n \sum_{\nu=n}^{\infty} P_{s\nu}\binom{\nu}{n}(1-\epsilon)^{\nu-n} . \tag{3}$$

The probability generating function $G_\xi(z)$ can then be written as

$$G_\xi(z) = \sum_{n=0}^{\infty}\sum_{j=0}^{n} z^j e_s(n)c(t,j,n,\xi) = \sum_{j=0}^{\infty} z^j \sum_{n=j}^{\infty} e_s(n)c(t,j,n,\xi) . \tag{4}$$

For $z=0$

$$G_\xi(0) = \sum_{n=0}^{\infty} e_s(n)c(t,o,n,\xi) , \tag{5}$$

which is the probability that from n-detected neutrons from a fission burst at ξ, none fall into the interval $t-\tau,t$.

The probability generating function $\pi[z|\xi_1,\xi_2,\ldots,\xi_i,N(T_1,T_2)=i]$ to register j signals in the interval $t-\tau,t$ produced by i fission bursts at i different times $\xi_1,\xi_2,\ldots,\xi_i$ inside the interval T_1,T_2 is formed by the product of the individual generating functions because the fissions occur independently one from the other. It is

$$\pi[z|\xi_1,\xi_2,\ldots,\xi_i,N(T_1,T_2)=i] = G_{\xi_1}(z)G_{\xi_2}(z)G_{\xi_3}(z)\ldots G_{\xi_i}(z) \tag{6}$$

and

$$\pi[z|\xi_1,\xi_2,\ldots,\xi_i,N(T_1,T_2)=i] = \sum_{n_1=0}^{\infty} e_s(n_1)\sum_{j_1=0}^{n_1} c(t,j_1,n_1,\xi_1)z^{j_1} \times \sum_{n_2=0}^{\infty} e_s(n_2)\sum_{j_2=0}^{n_2} c(t,j_2,n_2,\xi_2)z^{j_2} \ldots \sum_{n_i=0}^{\infty} e_s(n_i)\sum_{j_i=0}^{n_i} c(t,j_i,n_i,\xi_i)z^{j_i} , \tag{7}$$

with $T_1 \le \xi_1 \le \xi_2,\ldots, \le \xi_i \le T_2$ and $i=1,2,3,\ldots$.

Let us consider the time $\xi_1,\xi_2,\xi_3,\ldots,\xi_i$ to be subordinated by the i fissions in the interval T_1,T_2, $N(T_1,T_2)=i$. It is known that these random variables are distributed according to the density[11]

$$\varphi_i(\xi_1,\xi_2,\ldots,\xi_i) = i!\,\frac{F_s(\xi_1)F_s(\xi_2),\ldots,F_s(\xi_i)}{\left[\int_{T_1}^{T_2} F_s(s)\,ds\right]^i} \qquad T_1 \le \xi_1 \le \xi_2 \ldots \le \xi_i \le T_2 . \tag{8}$$

The probability generating function of i fission bursts $\pi[z|\xi_1,\xi_2,\ldots,\xi_i,N(T_1,T_2)=i]$ is now multiplied with its density function $\varphi_i(\xi_1,\xi_2,\ldots,\xi_i)$ and

integrated over the respective time intervals: $T_1 \le \xi_1 \le \xi_2 \le \xi_3 \ldots \le \xi_{i-1} \le \xi_i \le T_2$. It is given by

$$\pi_i(z, T_1) = \pi[z|N(T_1, T_2) = i] \tag{9}$$

$$= \int_{T_1}^{T_2} d\xi_1 \int_{\xi_1}^{T_2} d\xi_2 \ldots \int_{\xi_{i-1}}^{T_2} d\xi_i \pi[z|\xi_1, \xi_2, \ldots, \xi_i, N(T_1, T_2) = i] \varphi_i(\xi_1, \xi_2, \ldots, \xi_i) \ . \tag{10}$$

With Eqs. (7) and (8), Eq. (10) becomes

$$\pi_i(z, T_1) = \frac{i!}{\left[\int_{T_1}^{T_2} F_s(s)\, ds\right]^i} \left[\sum_{n_1=0}^{\infty} e_s(n_1) \sum_{j_1=0}^{n_1} z^{j_1} \int_{T_1}^{T_2} F_s(\xi_1) c(t, j_1, n_1, \xi_1)\, d\xi_1 \right.$$
$$\times \sum_{n_2=0}^{\infty} e_s(n_2) \sum_{j_2=0}^{n_2} z^{j_2} \int_{\xi_1}^{T_2} F_s(\xi_2) c(t, j_2, n_2, \xi_2)\, d\xi_2$$
$$\vdots$$
$$\left. \times \sum_{n_i=0}^{\infty} e_s(n_i) \sum_{j_i=0}^{n_i} z^{j_i} \int_{\xi_{i-1}}^{T_2} F_s(\xi_i) c(t, j_i, n_i, \xi_i)\, d\xi_i \right] \ . \tag{11}$$

This can be rearranged as follows:

$$\pi_i(z, T_1) = \frac{i}{\left[\int_{T_1}^{T_2} F_s(s)\, ds\right]^i} \sum_{n_1=0}^{\infty} e_s(n_1) \sum_{j_1=0}^{n_1} z^{j_1} \int_{T_1}^{T_2} F_s(\xi_1) c(t, j_1, n_1, \xi_1)\, d\xi_1 \left[\int_{\xi_1}^{T_2} F_s(s)\, ds\right]^{i-1}$$

$$\times \left\{ \frac{(i-1)!}{\left[\int_{\xi_1}^{T_2} F_s(s)\, ds\right]^{i-1}} \left[\sum_{n_2=0}^{\infty} e_s(n_2) \sum_{j_2=0}^{n_2} z^{j_2} \int_{\xi_1}^{T_2} F_s(\xi_2) c(t, j_2, n_2, \xi_2)\, d\xi_2 \right.\right.$$
$$\vdots$$
$$\left.\left. \times \sum_{n_i=0}^{\infty} e_s(n_i) \sum_{j_i=0}^{n_i} z^{j_i} \int_{\xi_{i-1}}^{T_2} F_s(\xi_i) c(t, j_i, n_i, \xi_i)\, d\xi_i \right] \right\} \ . \tag{12}$$

The last part of Eq. (12) is $\pi_{i-1}(z, \xi_1)$; hence,

$$\pi_i(z, T_1) = \frac{i}{\left[\int_{T_1}^{T_2} F_s(s)\, ds\right]^i} \sum_{n_1=0}^{\infty} e_s(n_1) \sum_{j_1=0}^{n_1} z^{j_1} \int_{T_1}^{T_2} F_s(\xi_1) c(t, j_1, n_1, \xi_1) \left[\int_{\xi_1}^{T_2} F_s(s)\, ds\right]^{i-1} \pi_{i-1}(z, \xi_1)\, d\xi_1 \ , \tag{13}$$

with $\pi_0(z, T_1) = 1$.

The probability generating function $\pi_i(z, T_1)$ is now multiplied by the probability of i fissions inside T_1, T_2 and summed over $0 \le i \le \infty$. It is

$$\pi(z, T_1) = \sum_{i=1}^{\infty} \pi_i(z, T_1) \frac{\left[\int_{T_1}^{T_2} F_s(s)\, ds\right]^i}{i!} \exp\left[-\int_{T_1}^{T_2} F_s(s)\, ds\right] + \pi_0(z, T_1) \exp\left[-\int_{T_1}^{T_2} F_s(s)\, ds\right] \ . \tag{14}$$

With Eq. (13) this becomes

$$\pi(z, T_1) = \sum_{i=1}^{\infty} \exp\left[-\int_{T_1}^{T_2} F_s(s)\, ds\right] \sum_{n_1=0}^{\infty} e_s(n_1) \sum_{j_1=0}^{n_1} z^{j_1} \int_{T_1}^{T_2} \left\{ F_s(\xi_1) c(t, j_1, n_1, \xi_1) \right.$$
$$\left. \times \frac{\left[\int_{\xi_1}^{T_2} F_s(s)\, ds\right]^{i-1}}{(i-1)!} \pi_{i-1}(z, \xi_1) \right\} d\xi_1 + \pi_0(z, T_1) \exp\left[-\int_{T_1}^{T_2} F_s(s)\, ds\right] \ . \tag{15}$$

Expression (15) simplifies after summation over i to the following integral equation (putting $n_1 = n$; $j_1 = j$; $\xi_1 = \xi$):

$$\pi(z,T_1) = \exp\left[-\int_{T_1}^{T_2} F_s(s)\,ds\right] \sum_{n=0}^{\infty} e_s(n) \times \sum_{j=0}^{n} z^j \int_{T_1}^{T_2} F_s(\xi) c(t,j,n,\xi) \pi(z,\xi) \times \exp\left[\int_{\xi}^{T_2} F_s(s)\,ds\right] d\xi + \pi_0(z,T_1) \exp\left[-\int_{T_1}^{T_2} F_s(s)\,ds\right] . \quad (16)$$

Equation (16) is transformed into a differential equation after partial differentiation with respect to T_1:

$$\frac{\partial \pi(z,T_1)}{\partial T_1} = \pi(z,T_1)\left[1 - \sum_{n=0}^{\infty} e_s(n) \times \sum_{j=0}^{n} z^j c(t,j,n,T_1)\right] F_s(T_1) . \quad (17)$$

The term inside the brackets of Eq. (17) is simplified as follows:

$$\sum_{n=0}^{\infty} e_s(n) \sum_{j=0}^{n} z^j c(t,j,n,T_1) = e_s(0) c(t,0,0,T_1) + \sum_{n=1}^{\infty} e_s(n) \sum_{j=0}^{n} z^j c(t,j,n,T_1) . \quad (18)$$

Thus, with $c(t,0,0,T_1) = 1$,

$$e_s(0) = 1 - \sum_{n=1}^{\infty} e_s(n) ,$$

and using Eq. (18), Eq. (17) reduces to the following expression:

$$\frac{d\pi(z,T_1)}{dT_1} = \pi(z,T_1) F_s(T_1) \sum_{j=1}^{\infty} (1 - z^j) \times \sum_{n=j}^{\infty} e_s(n) c(t,j,n,T_1) . \quad (19)$$

The solution of the differential equation for $0 \le T_1 \le T_2$ is given by

$$\pi(z,T_1) = \exp\left[\sum_{j=1}^{\infty} (z^j - 1) \Lambda_j(t-\tau,t,T_1,T_2)\right] , \quad (20)$$

with

$$\Lambda_j(t-\tau,t,T_1,T_2) = \sum_{n=j}^{\infty} e_s(n) \int_{T_1}^{T_2} F_s(s) c(t,j,n,s)\,ds . \quad (21)$$

Here, $\pi(z,T_1)$ is the probability generating function of a generalized Poisson distribution with the parameters $\Lambda_1(t-\tau,t,T_1,T_2)$, $\Lambda_2(t-\tau,t,T_1,T_2)\ldots$. It is identical with the expression presented in Ref. 1 for the case where $T_1 = 0$ and $T_2 = t$ and a time-independent spontaneous fission source. This starts directly with a difference equation similar to Eq. (17) without using explicitly the properties of the Poisson distribution of the spontaneous fission events.

Using

$$b_x(t-\tau,t,T_1,T_2) = \frac{1}{x!}\left[\frac{d^x \pi(z,T_1)}{dz^x}\right]_{z=0} , \quad (22)$$

the probability distribution $b_x(t-\tau,t,T_1,T_2)$ is obtained via Eqs. (20) and (21); $\pi(z,T_1)$ corresponds to the random variable X defined by

$$X = X_1 + 2X_2 + 3X_3 + \ldots , \quad (23)$$

where the X_j $(j = 1,2,3,\ldots)$ are mutually independent random variables distributed according to Poisson statistics with parameter $\Lambda_j(t-\tau,t,T_1,T_2)$.

If

$$e_s(n) = 0 \quad \text{for } n \ge N+1 ,$$

then the exponent of Eq. (20) becomes a sum limited by N.

The corresponding probability distribution then satisfies (as demonstrated in Appendix A)

$$x b_x = \Lambda_1 b_{x-1} + 2\Lambda_2 b_{x-2} + \ldots N\Lambda_N b_{x-N} , \quad (24)$$

with the abbreviations

$$b_x = b_x(t-\tau,t,T_1,T_2)$$

and

$$\Lambda_j = \Lambda_j(t-\tau,t,T_1,T_2)$$

for $x \ge N$.

The initial conditions are

$$b_0 = \exp\left(-\sum_{j=1}^{N} \Lambda_j\right)$$

$$1b_1 = \Lambda_1 b_0$$

$$2b_2 = \Lambda_1 b_1 + 2\Lambda_2 b_0$$

$$3b_3 = \Lambda_1 b_2 + 2\Lambda_2 b_1 + 3\Lambda_3 b_0$$

$$\vdots$$

$$(N-1)b_{N-1} = \sum_{j=1}^{N-1} j\Lambda_j b_{N-1-j} . \quad (25)$$

Equation (24) was presented in Ref. 1 to describe spontaneous fissions as a homogeneous Poisson process.

If $\Lambda_j \ne 0$ for each $j \ge 1$, then it follows from Eqs. (20), (21), and (22) that

$$xb_x = \sum_{j=1}^{x} j\Lambda_j b_{x-j} \tag{26}$$

for $x \geq 1$ and

$$b_0 = \exp\left(-\sum_{j=1}^{\infty} \Lambda_j\right) . \tag{27}$$

The explicit solution for b_x for $1 \leq j \leq N$ is

$$b_x = b_0 \sum_{\substack{1i_1+2i_2+\ldots Ni_N=x \\ 0 \leq i_j < \infty}} \frac{\Lambda_1^{i_1}\Lambda_2^{i_2}\ldots\Lambda_N^{i_N}}{i_1!i_2!\ldots i_N!} . \tag{28}$$

In Ref. 12, expressions are given for b_x for $T_1 = 0$, $T_2 = t$, $t \to \infty$ with $\Lambda_1 \neq 0$, $\Lambda_2 \neq 0$, $\Lambda_j = 0$ for $j > 2$ and a homogeneous Poisson process. This special case is covered by Eq. (28).

The figures i_j and the corresponding index j of the Λ_j $(1 \leq j \leq N)$ in Eq. (28) have a specific physical meaning. The value i_j is the number of fission events that contributes j signals to the x signals present in the interval $t-\tau, t$. For example, with $x = 4$ we have

$$\begin{aligned}
i_1 &= 4 \quad \text{and} \quad i_2 = i_3 = i_4 = 0 \\
2i_2 &= 4 , \quad i_2 = 2 , \quad \text{and} \quad i_1 = i_3 = i_4 = 0 \\
i_1 + 2i_2 &= 4 , \quad i_1 = 2 , \quad i_2 = 1 , \quad \text{and} \quad i_3 = i_4 = 0 \\
i_1 + 3i_3 &= 4 , \quad i_1 = 1 , \quad i_3 = 1 , \quad \text{and} \quad i_2 = i_4 = 0 \\
4i_4 &= 4 , \quad i_4 = 1 , \quad \text{and} \quad i_1 = i_2 = i_3 = 0 .
\end{aligned}$$

This leads to

$$b_4 = b_0\left(\frac{\Lambda_1^4}{4!} + \frac{\Lambda_2^2}{2!} + \frac{\Lambda_2^1\Lambda_1^2}{1!2!} + \frac{\Lambda_1^1\Lambda_3^1}{1!1!} + \frac{\Lambda_4^1}{1!}\right) . \tag{29}$$

When there are only single neutrons $j = 1$, Eq. (28) is then the well-known Poisson distribution for a time-dependent source emitting one neutron per burst.

Equations (24), (27), and (28) give the probability for x neutron signals inside the interval $t-\tau, t$ generated by fission bursts distributed according to an inhomogeneous Poisson distribution in the interval T_1, T_2. The derivation of the expressions shows that the neutron signals can appear in a different time sequence than the respective fissions generating the neutrons; i.e., overlapping of fission neutron signals can occur.

II.B. Moments of the $b_x(t-\tau, t, T_1, T_2)$ Distribution

To simplify Eqs. (27) and (28), we use their moments. The factorial moment of order m of the $b_x(t-\tau, t, T_1, T_2)$ distribution is defined by

$$M_{b(m)} = \sum_{x=m}^{\infty} x(x-1)\ldots(x-m+1)b_x , \qquad m \geq 0 , \tag{30}$$

using the abbreviations

$$M_{b(m)} = M_{b(m)}(t-\tau, t, T_1, T_2)$$

and

$$b_x = b_x(t-\tau, t, T_1, T_2) .$$

To get an analytical expression for $M_{b(m)}$, a differential equation for b_x is derived first using Eqs. (19) and (22). This leads to the following system of differential equations:

$$\frac{\partial b_x}{\partial T_1} = b_x F_s(T_1) \sum_{j=1}^{\infty}\sum_{n=j}^{\infty} e_s(n)c(tj,n,T_1) - \sum_{j=1}^{x} b_{x-j}F_s(T_1)\sum_{n=j}^{\infty} e_s(n)c(t,j,n,T_1) . \tag{31}$$

Equation (31) is transformed into a system of differential equations for $M_{b(m)}$ by multiplying both sides with the polynomial

$$x_{(m)} = x(x-1)(x-2)\ldots(x-m+1) \tag{32}$$

and summing over x starting with $x = m$. It is then

$$\frac{\partial M_{b(m)}}{\partial T_1} = M_{b(m)}F_s(T_1)\sum_{j=1}^{\infty}\sum_{n=j}^{\infty} e_s(n)c(t,j,n,T_1) - \sum_{x=m}^{\infty}\sum_{j=1}^{x} x_{(m)}b_{x-j}F_s(T_1) \times \sum_{n=j}^{\infty} e_s(n)c(t,j,n,T_1) . \tag{33}$$

The order of summation of the second expression on the right side of Eq. (33) is now interchanged. First, it is summed over the index j and then over $q = x - j$.

$$\frac{\partial M_{b(m)}}{\partial T_1} = M_{b(m)}F_s(T_1)\sum_{j=1}^{\infty}\sum_{n=j}^{\infty} e_s(n)c(t,j,n,T_1) - \sum_{j=m}^{\infty}\sum_{q=0}^{\infty}(j+q)_{(m)}b_q F_s(T_1)\sum_{n=j}^{\infty} e_s(n)c(t,j,n,T_1) - \sum_{j=1}^{m-1}\sum_{q=m-j}^{\infty}(j+q)_{(m)}b_q F_s(T_1)\sum_{n=j}^{\infty} e_s(n)c(t,j,n,T_1) . \tag{34}$$

The polynomial $(j+q)_{(m)}$ in Eq. (34) is replaced by

$$(j+q)_{(m)} = \sum_{r=0}^{m}\binom{m}{r} j_{(m-r)}q_{(r)} . \tag{35}$$

Furthermore, the following relation is used:

$$\frac{\partial \Lambda_j}{\partial T_1} = -F_s(T_1)\sum_{n=j}^{\infty} e_s(n)c(t,j,n,T_1) . \tag{36}$$

Inserting Eqs. (35) and (36) in Eq. (34) yields the following differential equation:

$$\frac{\partial M_{b(m)}}{\partial T_1} = \sum_{r=0}^{m-1}\sum_{j=m-r}^{\infty}\binom{m}{r} j_{(m-r)}M_{b(r)}\frac{\partial \Lambda_j}{\partial T_1} . \tag{37}$$

The integration is performed directly in the limits $T_1^* \le T_1 \le T_2$.

For the solution of Eq. (37) an abbreviation is first introduced for a factorial moment $M^*_{b(k)}$ of order k defined by

$$M^*_{b(k)} = \sum_{j=k}^{\infty} j_{(k)} \int_{T_1^*}^{T_2} F_s(T_1) \sum_{n=j}^{\infty} e_s(n) c(t,j,n,T_1)\, dT_1 = \sum_{j=k}^{\infty} j_{(k)} \Lambda_j \tag{38}$$

for $k \ge 1$, and using the abbreviation $\Lambda_j = \Lambda_j(t-\tau, t, T_1^*, T_2)$. Equation (38) is uniquely defined by the characteristics of the source, the detector assembly, and the time intervals of fission and neutron detection.

With this factorial moment of the physical properties, Eq. (37) becomes after integration

$$M_{b(m)} = \sum_{r=0}^{m-1} \binom{m}{r} \int_{T_1^*}^{T_2} M_{b(r)} \frac{\partial M^*_{b(m-r)}}{\partial T_1}\, dT_1 \tag{39}$$

for $m \ge 1$ and $M_{b(0)} = 1$.

From Eq. (39) the following solutions are obtained:

$$M_{b(1)} = M^*_{b(1)}$$

and

$$M_{b(2)} = M^*_{b(2)} + M^*_{b(1)} M_{b(1)}\ , \tag{40}$$

or in general

$$M_{b(m)} = \sum_{r=0}^{m-1} \binom{m-1}{r} M^*_{b(m-r)} M_{b(r)} \tag{41}$$

for $m \ge 1$.

A system of equations for the moments of the b_x distribution of order m is found following the same procedure as indicated for the factorial moments. It is

$$\mu_{bm}(t-\tau, t, T_1, T_2) = \sum_{x=1}^{\infty} x^m b_x(t-\tau, t, T_1, T_2)\ . \tag{42}$$

The corresponding differential equation is

$$\frac{\partial \mu_{bm}}{\partial T_1} = \sum_{j=1}^{\infty} \sum_{r=0}^{m-1} \binom{m}{r} j^{m-r} \mu_{br} \frac{\partial \Lambda_j}{\partial T_1}\ , \tag{43}$$

using $\mu_{bm} = \mu_{bm}(t-\tau, t, T_1, T_2)$ and $\Lambda_j = \Lambda_j(t-\tau, t, T_1, T_2)$.

Defining again a moment $\mu^*_{bk}(t-\tau, t, T_1, T_2)$ of order k characterizing the source and the neutron detection process,

$$\mu^*_{bk} = \sum_{j=1}^{\infty} j^k \int_{T_1^*}^{T_2} F_s(T_1) \sum_{n=j}^{\infty} e_s(n) c(t,j,n,T_1)\, dT_1 = \sum_{j=1}^{\infty} j^k \Lambda_j\ , \tag{44}$$

using the abbreviation $\mu^*_{bk} = \mu^*_{bk}(t-\tau, t, T_1, T_2)$, for $k \ge 1$, the following general expression for μ_{bm} is found:

$$\mu_{bm} = \sum_{r=0}^{m-1} \binom{m-1}{r} \mu^*_{b,m-r} \mu_{br} \tag{45}$$

for $m \ge 1$.

The great advantage in using the factorial moments or the moments of the b_x distribution [Eqs. (41) and (45)] for the interpretation of the measured moments $M_{b(m)}$ or μ_{bm} is that the source term $F_s(s)$ occurs as a linear term in $M^*_{b(k)}$ and μ^*_{bk}. This is not the case if the analytical expressions for b_x are directly used for the interpretation of the measured distribution.

III. APPLICATION OF THE THEORY TO SIGNAL MULTIPLETS WITH TIME CONSTANT SOURCES

In this section, the general theory is applied to specific cases in order to arrive at algorithms suitable for the interpretation of specific neutron correlator devices. Considered are correlator devices based on the measurement of the number of signals existing inside fixed time intervals τ. The intervals are triggered either randomly or by each neutron signal.[1,2,6-10] The quantities obtained experimentally are the background multiplets $B_x(\tau)$ and the trigger multiplets $N_x(\tau)$ $(x = 1,2,3,\dots)$, respectively, defined by[10]

$B_x(\tau)$ = number of events with x signals inside k randomly triggered inspection intervals τ

$N_x(\tau)$ = number of events with x signals inside the inspection intervals of duration τ obtained during an observation time T_M. Each neutron signal triggers an inspection time interval $\tau (T_M \gg \tau)$.

The frequency counterpart $b_x^+(\tau)$ to the probability $b_x(\tau)$ has x measured signals inside randomly triggered inspection intervals of duration τ and is

$$b_x^+(\tau) = \frac{B_x(\tau)}{k}\ . \tag{46}$$

Correspondingly, the frequency counterpart $n_x^+(\tau)$ to the probability $n_x(\tau)$, $n_x^+(\tau)$ has x signals inside signal triggered intervals of duration τ

$$n_x^+(\tau) = \frac{N_x(\tau)}{N_T}\ , \tag{47}$$

where N_T is the number of counts collected during the measurement time T_M, referred to as gross counts, and where

$$b_x(\tau) = b_x(t-\tau, t, T_1, T_2) \tag{48}$$

and

$$n_x(\tau) = n_x(t-\tau, t, T_1, T_2) \ , \tag{49}$$

for $T_1 = 0$, $T_2 = t$, $t \to \infty$.

The value of $n_x(\tau)$ is decomposed[10] into the probability $b_{x-y}(\tau)$ and the probability $r_y(\tau)$; $r_y(\tau)$ is the probability of having inside a triggered interval of duration τ, y other correlated signals, i.e., signals originating from the same fission event. Thus,[10]

$$n_x(\tau) = \sum_{y=0}^{x} r_y(\tau) b_{x-y}(\tau) \ , \tag{50}$$

with

$$\sum_{y=0}^{\infty} r_y(\tau) = 1 \ .$$

Reference 10 gives analytical expressions for $R_y(\tau) = r_y(\tau) N_T$ with neutron multiplication and $(\alpha$-$n)$ neutrons in the sample. The objective is therefore now limited to find, using the derived theory, analytical expressions for $b_x(\tau)$. Algorithms for $n_x(\tau)$ and the moments of $b_x(\tau)$ and $n_x(\tau)$ are then easily found.

III.A. Probability $b_x(\tau)$

The probability $b_x(\tau)$ is derived from the probability $b_x(t-\tau, t, T_1, T_2)$ for homogeneous Poisson distributed fission bursts in the interval $T_1 = 0$, $T_2 = t$ with neutron signals of these fissions registered in the interval $t-\tau, t$ with $t \to \infty$. Furthermore, it is assumed that the neutron population in the detection head generated by a neutron burst decays in time with its fundamental mode decay time $1/\lambda$. It then follows from Eqs. (2) and (21) for a time constant spontaneous fission rate F_s that for fission bursts in the interval $0 = T_1 \le \xi \le t-\tau$

$$\Lambda_j(t-\tau, t, 0, t-\tau) = F_s \sum_{n=j}^{\infty} e_s(n) \binom{n}{j} \sum_{k=0}^{n-j} \binom{n-j}{k} (-1)^k (e^{\lambda\tau} - 1)^{j+k} \times \frac{\exp[-\lambda\tau(j+k)] - \exp[-\lambda t(j+k)]}{\lambda(j+k)} \ , \tag{51}$$

and for fission bursts in the interval $t-\tau \le \xi \le t$

$$\Lambda_j(t-\tau, t, t-\tau, t) = F_s \sum_{n=j}^{\infty} e_s(n) \binom{n}{j} \sum_{k=0}^{j} \binom{j}{k} (-1)^k \times \frac{1 - \exp[-\lambda\tau(n+k-j)]}{\lambda(n+k-j)} \ . \tag{52}$$

With $t \to \infty$ the following expression for $\Lambda_j(\tau)$ is found:

$$\Lambda_j(\tau) = F_s \sum_{n=j}^{\infty} e_s(n) \binom{n}{j} \times \left(\sum_{k=0}^{n-j} \binom{n-j}{k} (-1)^k \left[\frac{1 - \exp(\lambda\tau)}{\lambda(j+k)} \right]^{j+k} + \sum_{k=0}^{j} \binom{j}{k} (-1)^k \times \frac{\{1 - \exp[-\lambda\tau(n+k-j)]\}}{\lambda(n+k-j)} \right) \ . \tag{53}$$

This leads, after rearranging the sums over k, to

$$\Lambda_j(\tau) = F_s \tau \sum_{n=j}^{\infty} e_s(n) w(n, j, \tau) \ , \tag{54}$$

with

$$w(n, j, \tau) = \binom{n}{j} \sum_{k=0}^{j-1} \binom{j-1}{k} (-1)^k \times \frac{\{1 - \exp[-\lambda\tau(n+k-j)]\}}{\lambda\tau(n+k-j)} \ . \tag{55}$$

Some expressions of $w(n, j, \tau)$ are listed in Appendix B.

The value of $\Lambda_j(\tau)$ is easily generalized for the case that the neutron source emits, in addition to the spontaneous fission neutrons, single neutrons generated by $(\alpha$-$n)$ reactions. If S_α is the time constant $(\alpha$-$n)$ neutron emission rate and ϵ_α the detection probability for neutrons from this process, then Eq. (54) for $\Lambda_j(\tau)$ reads

$$\Lambda_j(\tau) = S_\alpha \tau \epsilon_\alpha \delta_{1j} + F_s \tau \sum_{n=j}^{\infty} e_s(n) w(n, j, \tau) \ , \tag{56}$$

with $j \ge 1$, and

$$\delta_{1j} = \begin{cases} 1 & \text{for } j = 1 \\ 0 & \text{for } j \ne 1 \end{cases} \ ,$$

where δ_{1j} is the Kronecker symbol.

The effect of neutron multiplication inside the fissile source can be taken into account in Eq. (56) with the simplifications of Ref. 10. In this approximation each primary source neutron of a homogeneous Poisson distributed spontaneous fission burst triggers with a certain probability p [or p_α for $(\alpha$-$n)$ neutrons] a fission cascade of short duration compared to the decay time $1/\lambda$ of the neutron detection system. All neutrons escaping from this fission cascade enter into the detection head and give in this approximation a contribution to a new $P_\nu(p)$ distribution. This distribution is a complex function of the probability p that a fission neutron generates an induced fission and of the probabilities $P_{s\nu}$ and P_ν for the emission of ν neutrons due to spontaneous and induced fissions, respectively. With this model a term appears in Eq. (56) as

$$A = S_\alpha \tau (1 - p_\alpha) \epsilon_\alpha \delta_{1j} \ , \tag{57}$$

i.e., the number of neutrons from (α-n) reactions escaping with the probability $(1 - p_\alpha)$ an induced fission and being detected with the probability ϵ_α. The part $p_\alpha S_\alpha \tau$ triggers a fission cascade of which n neutrons are detected and j fall inside the interval τ. This contribution is

$$B = p_\alpha S_\alpha \tau \sum_{n=j}^{\infty} e_\alpha(n,p) w(n,j,\tau) \ , \tag{58}$$

with

$$e_\alpha(n,p) = \epsilon^n \sum_{\nu=n}^{\infty} \binom{\nu}{n} P_{\alpha\nu}(p) (1-\epsilon)^{\nu-n} \tag{59}$$

and

$$\sum_{\nu=0}^{\infty} P_{\alpha\nu}(p) = 1 \ ,$$

where $P_{\alpha\nu}(p)$ is the probability for the emission of ν neutrons per primary (α-n) source neutron, $(0 \le \nu < \infty)$ allowing fast neutron multiplication.[10]

The detection probability $e_\alpha(n,p)$ becomes a function of p via the $P_{\alpha\nu}(p)$ distribution of the fission cascade escape neutrons. For a fission cascade triggered by spontaneous fission events with a $P_{s\nu}$ distribution of the primary neutrons, a detection probability similar to Eq. (59) is found:

$$e_s(n,p) = \epsilon^n \sum_{\nu=n}^{\infty} \binom{\nu}{n} P_{s\nu}(p) (1-\epsilon)^{\nu-n} \tag{60}$$

and

$$\sum_{\nu=0}^{\infty} P_{s\nu}(p) = 1 \ ,$$

where $P_{s\nu}(p)$ is the probability for the emission of ν neutrons per spontaneous fission event with fast neutron multiplication. With fast neutron multiplication of the primary source neutrons, Eq. (56) then reads

$$\Lambda_j(\tau,p) = \tau \Big[S_\alpha (1 - p_\alpha) \epsilon_\alpha \delta_{1j} + p_\alpha S_\alpha \sum_{n=j}^{\infty} e_\alpha(n,p) w(n,j,\tau) + F_s \sum_{n=j}^{\infty} e_s(n,p) w(n,j,\tau) \Big] \tag{61}$$

for $j \ge 1$.

The probability $b_x(\tau)$ is according to Eqs. (28) and (61), respectively, proportional to $b_0(\tau)$ and to a polynomial of the order x in F_s and S_α with coefficients depending on powers in ϵ and $\exp(-\lambda\tau)$. In extreme cases of $\lambda\tau$, the equation system is considerably simplified.

Consider first a detection head with a very long decay time $1/\lambda$ and a relatively short observation interval $\tau(\lambda\tau \ll 1)$. With these conditions, $\Lambda_1(\lambda\tau \ll 1)$ is identical to the average number of counts collected during τ. The $\Lambda_j(\lambda\tau \ll 1)$ values for $j > 1$ are zero. Thus, $b_x(\tau)$ follows with Eq. (28) in the limit $\lambda\tau \to 0$, a pure homogeneous Poisson distribution.

In the other extreme case $(\lambda\tau \gg 1)$, the decay time of the detection head $1/\lambda$ is very short with respect to τ. In the limit $\lambda\tau \to \infty$, it follows that

$$\Lambda_j(\lambda\tau \to \infty) = \tau [S_\alpha (1 - p_\alpha) \epsilon_\alpha \delta_{1j} + p_\alpha S_\alpha e_\alpha(j,p) + F_s e_s(j,p)] \ .$$

These $\Lambda_j(\tau)$ values lead to a $b_x(\tau)$ distribution, which is still a generalized Poisson distribution.

III.B. Factorial Moments $M_{b(m)}(\tau)$ and $M^*_{b(m)}(\tau)$

Factorial moments $M_{b(m)}(\tau)$ and $M^*_{b(m)}(\tau)$ are derived from moments $M_{b(m)}(t-\tau, t, T_1, T_2)$ and $M^*_{b(m)}(t-\tau, t, T_1, T_2)$ for homogeneous Poisson distributed fission bursts in the interval $T_1 = 0$ and $T_2 = t$. Signal detection occurs in the interval $t-\tau, t$ with $t \to \infty$. With these conditions and time-independent spontaneous fission and (α-n) reaction rates F_s and S_α, Eq. (38) reads

$$M^*_{b(m)}(\tau) = \sum_{j=m}^{\infty} j_{(m)} \Lambda_j(\tau) \tag{62}$$

for $m \ge 1$.

The value of $\Lambda_j(\tau)$ is defined in Eq. (54) leading to the following expression for a pure spontaneous fission neutron source with a spontaneous fission rate F_s:

$$M^*_{b(m)}(\tau) = F_s \tau \sum_{j=m}^{\infty} j_{(m)} \sum_{n=j}^{\infty} e_s(n) w(n,j,\tau) \tag{63}$$

for $m \ge 1$.

With neutron multiplication and (α-n) reactions inside the sample, the expression for $\Lambda_j(\tau,p)$ of Eq. (61) must be used in Eq. (62). It is then

$$M^*_{b(m)}(\tau) = \tau \Big[S_\alpha (1 - p_\alpha) \epsilon_\alpha \delta_{1m} + p_\alpha S_\alpha \sum_{j=m}^{\infty} j_{(m)} \sum_{n=j}^{\infty} e_\alpha(n,p) w(n,j,\tau) + F_s \sum_{j=m}^{\infty} j_{(m)} \sum_{n=j}^{\infty} e_s(n,p) w(n,j,\tau) \Big] \tag{64}$$

for $m \ge 1$.

With the relation (see Appendix B)

$$\sum_{j=m}^{\infty} j_{(m)} w(n,j,\tau) = n_{(m)} w(m,m,\tau) \ , \qquad (65)$$

Eq. (64) reads

$$M^*_{b(m)}(\tau) = \tau \Big[S_\alpha (1-p_\alpha)\epsilon_\alpha \delta_{1m} + p_\alpha S_\alpha \sum_{n=m}^{\infty} e_\alpha(n,p) n_{(m)} w(m,m,\tau) + F_s \sum_{n=m}^{\infty} e_s(n,p) n_{(m)} w(m,m,\tau) \Big] \ . \qquad (66)$$

It is

$$\sum_{n=m}^{\infty} e_\alpha(n,p) n_{(m)} = \sum_{n=m}^{\infty} \sum_{\nu=n}^{\infty} P_{\alpha\nu}(p) \binom{\nu}{n} \epsilon^n (1-\epsilon)^{\nu-n} n_{(m)} = \epsilon^m \sum_{\nu=m}^{\infty} \nu_{(m)} P_{\alpha\nu}(p) = \epsilon^m \overline{\nu_{\alpha(m)}(p)} \ . \qquad (67)$$

In Eq. (67), $\overline{\nu_{\alpha(m)}(p)}$ is the effective factorial moment of the $P_{\alpha\nu}(p)$ distribution. Similarly, it follows that

$$\sum_{n=m}^{\infty} e_s(n,p) n_{(m)} = \epsilon^m \overline{\nu_{s(m)}(p)} \ , \qquad (68)$$

where $\overline{\nu_{s(m)}(p)}$ is the effective factorial moment of the $P_{s\nu}(p)$ distribution. Using Eqs. (67) and (68), Eq. (66) becomes

$$M^*_{b(m)}(\tau) = \tau \{ S_\alpha (1-p_\alpha)\epsilon_\alpha \delta_{1m} + [p_\alpha S_\alpha \overline{\nu_{\alpha(m)}(p)} + F_s \overline{\nu_{s(m)}(p)}] \epsilon^m w(m,m,\tau) \} \qquad (69)$$

for $m \geq 1$.

For $\overline{\nu_{\alpha(1)}(p)}$ and $\overline{\nu_{s(1)}(p)}$ exist the explicit expressions[10]

$$\overline{\nu_{\alpha(1)}(p)} = \frac{\bar{\nu}_{I\alpha}(1-p)}{1-p\bar{\nu}_I} = \sum_{\nu=1}^{\infty} P_{\alpha\nu}(p)\nu \qquad (70)$$

and

$$\overline{\nu_{s(1)}(p)} = \frac{\bar{\nu}_s(1-p)}{1-p\bar{\nu}_I} = \sum_{\nu=1}^{\infty} P_{\alpha\nu}(p)\nu \ , \qquad (71)$$

where

$\bar{\nu}_I$ = average number of emitted neutrons per induced fission event caused by neutrons with a fission neutron spectrum

$\bar{\nu}_{I\alpha}$ = average number of emitted neutrons per induced fission event caused by neutrons with an (α-n) neutron spectrum

$\bar{\nu}_s$ = average number of emitted neutrons per spontaneous fission event.

The factorial moment $M_{b(m)}(\tau)$ of order m of the measured distribution is obtained from Eq. (41) with fission bursts in the interval $0 = T_1 \leq \xi \leq T_2 = t$ and with $t \to \infty$. It is

$$M_{b(m)}(\tau) = \sum_{r=0}^{m-1} \binom{m-1}{r} M^*_{b(m-r)}(\tau) M_{b(r)}(\tau) \qquad (72)$$

for $m \geq 1$.

The analytical expressions for the moments of the $b_x(\tau)$ distribution are obtained as well directly from

$$M_{b(m)}(\tau) = \sum_{x=m}^{\infty} x_{(m)} b_x(\tau) \ , \qquad (73)$$

using Eq. (24) or (26) and Eq. (61).

The factorial moment $M^*_{b(1)}(\tau)$ gives with Eq. (69) the obvious expression for the gross counts collected during the interval τ. The factorial moment $M_{b(2)}(\tau)$ depends on $M^*_{b(2)}(\tau)$, $M^*_{b(1)}(\tau)$, and $M_{b(1)}(\tau)$. The measurement of this moment is known as the enhanced variance method[12] or the reduced variance method.[13] Reference 13 gives an analytical expression for this analysis method including an approximation for a fixed counter dead time. Without this approximation Ref. 13 gives the same results as Eqs. (69) and (72).

The moments $\mu^*_{bm}(\tau)$ and $\mu_{bm}(\tau)$ are obtained from Eqs. (44) and (45), respectively, for fission bursts in the interval $0 \leq T_1 \leq \xi \leq T_2 = t$ with $\lim t \to \infty$.

For a source with neutron multiplication and primary neutrons due to the spontaneous fission and (α-n) reactions, $\mu_{bm}(\tau)$ is given by

$$\mu^*_{bm}(\tau) = \sum_{j=1}^{\infty} j^m \Lambda_j(\tau) = \tau \Big[S_\alpha (1-p_\alpha)\epsilon_\alpha \delta_{1m} + p_\alpha S_\alpha \sum_{n=1}^{\infty} \sum_{n=j}^{\infty} j^m e_\alpha(n,p) w(n,j,\tau) + F_s \sum_{n=1}^{\infty} \sum_{n=j}^{\infty} j^m e_s(n,p) w(n,j,\tau) \Big] \qquad (74)$$

for $m \geq 1$.

After some algebraic operations it follows with Eqs. (55), (59), and (60) that

$$\mu^*_{bm}(\tau) = \tau\Bigg[S_\alpha(1-p_\alpha)\epsilon_\alpha\delta_{1m} + p_\alpha S_\alpha \sum_{q=1}^{m} \epsilon^q \frac{\overline{\nu_{\alpha q}(p)}}{q!} w(q,q,\tau) \times \sum_{n=1}^{q} \binom{q}{n} (-1)^{q-n} n^m + F_s \sum_{q=1}^{m} \epsilon^q \frac{\overline{\nu_{sq}(p)}}{q!} w(q,q,\tau) \times \sum_{n=1}^{q} \binom{q}{n} (-1)^{q-n} n^m \Bigg] \quad (75)$$

for $m \geq 1$.

The determination of $\mu_{bm}(\tau)$ is analogous to that of $M_{b(m)}(\tau)$.

Equation (75) is much more complicated than Eq. (69); therefore, an interpretation of the experimental data in the form of the moments $\mu_{bm}(\tau)$ is less advisable.

The analytical expressions found for the probability distribution $b_x(\tau)$ to have x signal events inside randomly triggered time intervals are rather complex expressions of S_α, F_s, ϵ, and p. A determination of these parameters from a measured distribution leads to rather extensive numerical efforts.[6-8] This is avoided by forming factorial moments of the $b_x(\tau)$ distribution. These lead to the simplest expressions for a practical data reduction. The $P_\nu(p)$ distribution does not appear explicitly, but its factorial moments do. These are calculated with the PENU code[14] for up to seven fission events. Recently, analytical expressions for these factorial moments have been derived[15,16] in a fast fission approximation.

III.C. Probability $n_x(\tau)$

The probability to find x signals inside a signal-triggered interval of duration τ is $n_x(\tau)$. According to Eq. (50), it is expressed as a product of $b_{x-y}(\tau)$ to have $(x-y)$ uncorrelated neutron signals inside randomly triggered time intervals and the probability $r_y(\tau)$ to have y correlated signals inside τ; i.e., these y signals are generated by the same fission burst. This latter quantity is taken from Ref. 10 and is reported without derivation. It is

$$r_y(\tau) = \frac{T_M}{N_T}\Bigg\{S_\alpha(1-p_\alpha)\epsilon_\alpha\delta_{0\alpha} + f^y(T,\tau)\sum_{n=y+1}^{\infty}[p_\alpha S_\alpha e_\alpha(n,p) + F_s e_s(n,p)] \times \sum_{k=1}^{n-y}\binom{n-k}{y}[1-f(T,\tau)]^{n-y-k}\Bigg\}, \quad (76)$$

with

$$N_T = M_{b(1)}(\tau)\frac{T_M}{\tau}$$

$$\delta_{0y} = \begin{cases} 1 & \text{for } y=0 \\ 0 & \text{for } y\neq 0 \end{cases}$$

$$f(T,\tau) = \exp(-\lambda T)[1-\exp(-\lambda\tau)] \quad \text{for } y \geq 0\ , \quad (77)$$

and where

T = delay time between signal trigger and initiation of inspection interval

T_M = total measurement time.

Equation (76) is valid for a point source with (α-n) and spontaneous fission primary neutrons, and fast neutron multiplication generating the neutron signal pulse train. It is considered that the first arriving signal triggers with a delay T the inspection interval τ. The number of signals y arriving in the inspection interval τ, being correlated with the trigger signal, determines the order of the multiplet $R_y(\tau)$ or the probability for its occurrence $r_y(\tau)$.

The probability $n_x(\tau)$ is defined by Eq. (50) and the expressions for $b_x(\tau)$ [Eq. (28)] and $r_y(\tau)$ [Eq. (76)]. As $\lambda\tau \to 0$, the distribution of the probability $n_x(\tau)$ approaches a homogeneous Poisson distribution. It is

$$r_0(\lambda\tau\to 0) = \frac{T_M}{N_T}[S_\alpha(1-p_\alpha)\epsilon_\alpha + p_\alpha S_\alpha\overline{\nu_{\alpha(1)}(p)} + F_s\overline{\nu_{s(1)}(p)}] \quad (78)$$

$$r_y(\lambda\tau\to 0) = 0 \quad \text{for } y>0$$

and

$$n_x(\lambda\tau\to 0) = r_0(\lambda\tau\to 0)b_x(\lambda\tau\to 0)\ . \quad (79)$$

A direct interpretation of the measured $n_x(\tau)$ distribution requires extensive computations, due to the complex expressions for $b_x(\tau)$ [Eq. (28)] and $r_y(\tau)$ [Eq. (76)].

III.D. Factorial Moments $M_{n(m)}(\tau)$ and $M^*_{n(m)}(\tau)$

The factorial moment of the $n_x(\tau)$ distribution of order m is defined by

$$M_{n(m)}(\tau) = \sum_{x=m}^{\infty} x(x-1)\ldots(x-m+1)n_x(\tau) = \sum_{x=m}^{\infty} x_{(m)}n_x(\tau) \quad (80)$$

for $m \geq 1$.

Replacing $n_x(\tau)$ in Eq. (80) with Eq. (50), the following general expression for the factorial moment of order m is found:

$$M_{n(m)}(\tau) = \sum_{q=0}^{m} \binom{m}{q} M^*_{n(q)}(\tau) M_{b(m-q)}(\tau) \ , \quad (81)$$

with

$$M^*_{n(q)}(\tau) = \sum_{x=q}^{\infty} x_{(q)} r_x(\tau) \quad (82)$$

$$M^*_{n(0)}(\tau) = 1$$

and $m \geq 1$.

The factorial moment $M^*_{n(q)}(\tau)$ is expressed as a function of the characteristics of the source, the neutron detection head, and the signal recording system.

With Eq. (76) it follows from Eq. (82), after some algebraic operations, that

$$M^*_{n(q)}(\tau) = \frac{\tau}{M_{b(1)}(\tau)} \left\{ S_\alpha (1 - p_\alpha) \epsilon_\alpha \delta_{0q} + \frac{\epsilon^{q+1}}{q+1} f^q(T,\tau) \times [p_\alpha S_\alpha \overline{\nu_{\alpha(q+1)}(p)} + F_s \overline{\nu_{s(q+1)}(p)}] \right\} \quad (83)$$

for $q \geq 0$. With Eq. (83) and the factorial moments $M^*_{b(m)}(\tau)$ and $M_{b(m-q)}(\tau)$ of the $b_{(m-q)}(\tau)$ distribution given in Eqs. (69) and (72), respectively, the factorial moment of the $n_x(\tau)$ distribution is completely defined.

It is not necessary that the moments $M_{b(m-q)}(\tau)$ are known by measurement. They can be expressed by combinations of factorial moments of the probability for trigger and background multiplets of lower order. Using Eq. (72) for $m = 2$, an expression for $M_{b(2)}(\tau)$ as a function of $M^*_{b(2)}(\tau)$ and $M_{b(1)}(\tau)$ is obtained. Replacing in this expression $M^*_{b(2)}(\tau)$ using Eq. (69) for $m = 2$ and Eq. (83) with $q = 1$, the following expression is found:

$$M_{b(2)}(\tau) = 2M_{b(1)}(\tau) M^*_{n(1)}(\tau) \frac{w(2,2,\tau)}{f(T,\tau)} + M^2_{b(1)}(\tau) \ . \quad (84)$$

In a similar way follows that

$$M_{b(3)}(\tau) = 3M_{b(1)}(\tau) M^*_{n(2)}(\tau) \frac{w(3,3,\tau)}{f^2(T,\tau)} + M^3_{b(1)}(\tau) + 3M^2_{b(1)}(\tau) 2M^*_{n(1)}(\tau) \frac{w(2,2,\tau)}{f(T,\tau)} \ . \quad (85)$$

The equations for the trigger multiplets and their factorial moments are derived for inspection intervals, being triggered by the first arriving signal of the part of the pulse train under investigation. The signals forming the multiplets normally arrive later than the trigger signal (Fig. 2). This, however, is not always the case. In some multiplet analyzers[17] the signal trigger of the inspection interval occurs with a delay T after the signal has left the inspection interval. In this case signals that have arrived earlier than the trigger signal but are still inside τ form the multiplet.

IV. VERIFICATION OF THE THEORY BY AN EXPERIMENT

The theory derived for the factorial moments of the probabilities $b_x(\tau)$ and $n_x(\tau)$ was tested with a metallic plutonium reference sample of 8.45 g. This permitted a test of the theory for a time-independent spontaneous fission rate in the absence of (α,n) reactions. This sample was measured inside a hollow cylindrical detection head with a polyethylene moderator and thirty-two 100-cm-long ^{3}He proportional counters. Four counters were connected to an amplifier discriminator chain to reduce dead-time losses. The

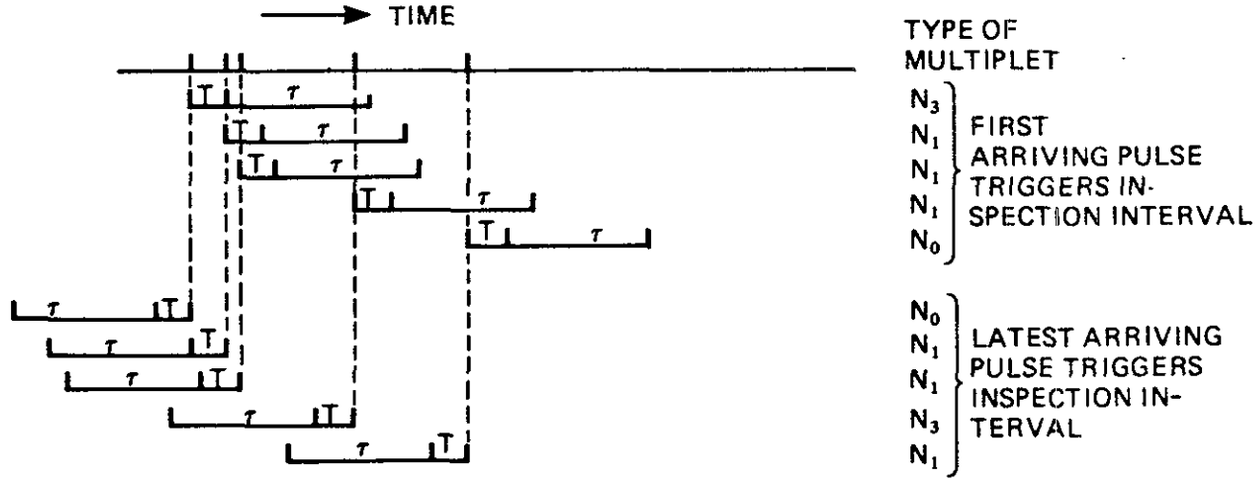

Fig. 2. Trigger multiplet types.

resulting pulse train of the eight channels was fed into a computer programmed to measure trigger and background multiplets.[6-8] Each signal from the amplifier chain triggered with a predelay of 6.4-μs three time channels ($\tau_1 = 25.6$ μs, $\tau_2 = 51.2$ μs, $\tau_3 = 102.4$ μs) to obtain three trigger multiplets for each order x. The background multiplets were obtained from periodically triggered not overlapping inspection intervals τ_1, τ_2, and τ_3. The obtained frequencies $b_x^+(\tau)$ and $n_x^+(\tau)$ and their respective standard deviations from the mean obtained during eight runs each with a measurement time of 8 min are given in Tables I and II (Ref. 18), respectively, for $x \leq 5$.

IV.A. Factorial Moments of the Probabilities $b_x(\tau)$

The factorial moments of the $b_x(\tau)$ distribution are then used to obtain an expression for $M^*_{b(2)}(\tau)$ and $M^*_{b(3)}(\tau)$ as a function of the measured quantities $M_{b(m)}(\tau)$ $(m = 1,2,3)$. It is

$$M^*_{b(2)}(\tau) = M_{b(2)}(\tau) - M^2_{b(1)}(\tau) \tag{86}$$

and

$$M^*_{b(3)}(\tau) = M_{b(3)}(\tau) - 2M^*_{b(2)}(\tau)M_{b(1)}(\tau) - M^*_{b(1)}(\tau)M_{b(2)}(\tau) \ . \tag{87}$$

The value of $M^*_{b(m)}(\tau)$ is from Eq. (69), a function of the source, detector, and signal register data. Using Eq. (69), for $m = 1$, 2, 3 and assuming for the measured plutonium sample $S_\alpha = 0$, the following ratio $\beta(p)$ is obtained[10]:

$$\beta(p) = \frac{3\overline{\nu_{s(2)}(p)}^2}{2\overline{\nu_{s(1)}(p)}\,\overline{\nu_{s(3)}(p)}} \approx \frac{3[M^*_{b(2)}(\tau)]^2 w(3,3,\tau)}{2M^*_{b(1)}(\tau)M^*_{b(3)}(\tau)w^2(2,2,\tau)} \ . \tag{88}$$

This ratio is a function of the probability p that a neutron generates an induced fission and of nuclear data. The value p is found by interpolation using the tabulated values of $\overline{\nu_{s(m)}(p)}$ given in Ref. 10 and the numerical values of $M^*_{b(m)}(\tau)$ defined by the factorial moments of the $b_x^+(\tau)$ distribution. These tables for $\overline{\nu_{s(m)}(p)}$ are obtained from the PENU code,[14] which

TABLE I

Frequency Distribution of Signals $b_x^+(\tau)$ Inside Randomly Triggered Intervals (Mean Values of Eight Runs)

	Interval Length					
	$\tau = 25.6$ μs		$\tau = 51.2$ μs		$\tau = 102.4$ μs	
x	$b_x^+(\tau)$	$\sigma[b_x^+(\tau)]$	$b_x^+(\tau)$	$\sigma[b_x^+(\tau)]$	$b_x^+(\tau)$	$\sigma[b_x^+(\tau)]$
0	9.9374×10^{-1}	2.0×10^{-5}	9.8798×10^{-1}	2.9×10^{-5}	9.7722×10^{-1}	5.3×10^{-5}
1	5.9134×10^{-3}	1.63×10^{-5}	1.0888×10^{-2}	3.7×10^{-5}	1.9503×10^{-2}	6.7×10^{-5}
2	3.2762×10^{-4}	1.7×10^{-6}	1.0417×10^{-3}	1.0×10^{-5}	2.9136×10^{-3}	1.7×10^{-5}
3	1.4703×10^{-5}	7.5×10^{-7}	7.8695×10^{-5}	2.9×10^{-6}	3.2868×10^{-4}	6.4×10^{-6}
4	5.2053×10^{-7}	1.5×10^{-7}	5.2736×10^{-6}	7.4×10^{-7}	3.1462×10^{-5}	2.9×10^{-6}
5	---	---	3.0724×10^{-7}	2.1×10^{-7}	3.3938×10^{-6}	7.4×10^{-7}

TABLE II

Frequency Distribution of Signals $n_x^+(\tau)$ Inside Signal Triggered Intervals (Mean Values of Eight Runs)

	Interval Length					
	$\tau = 25.6$ μs		$\tau = 51.2$ μs		$\tau = 102.4$ μs	
x	$n_x^+(\tau)$	$\sigma[n_x^+(\tau)]$	$n_x^+(\tau)$	$\sigma[n_x^+(\tau)]$	$n_x^+(\tau)$	$\sigma[n_x^+(\tau)]$
0	9.1033×10^{-1}	8.7×10^{-4}	8.6005×10^{-1}	9.9×10^{-4}	8.0983×10^{-1}	6.9×10^{-4}
1	8.4492×10^{-2}	9.4×10^{-4}	1.2693×10^{-1}	8.5×10^{-4}	1.6512×10^{-1}	5.3×10^{-4}
2	4.9677×10^{-3}	2.2×10^{-4}	1.2007×10^{-2}	3.2×10^{-4}	2.2186×10^{-2}	4.5×10^{-4}
3	2.1866×10^{-4}	6.1×10^{-5}	9.8487×10^{-4}	9.1×10^{-5}	2.3925×10^{-3}	5.4×10^{-4}
4	1.3545×10^{-5}	7.4×10^{-6}	4.9340×10^{-5}	1.8×10^{-5}	2.3511×10^{-4}	1.0×10^{-4}
5	1.5467×10^{-5}	---	7.7293×10^{-6}	5.9×10^{-9}	1.5469×10^{-5}	9.8×10^{-6}

calculates for specified p values the $P_\nu(p)$ distribution and the respective factorial moments. This code requires as input the P_ν distribution of the primary source neutrons and the P_ν distribution of the neutrons generated by induced fission events. From the ratio of $M^*_{b(2)}(\tau)$ and $M^*_{b(1)}(\tau)$, it follows that the probability for the detection of a neutron in the detection head is

$$\epsilon \simeq \frac{M^*_{b(2)}(\tau)}{M^*_{b(1)}(\tau)} \frac{\overline{\nu_{s(1)}(p)}}{\overline{\nu_{s(2)}(p)}\, w(2,2,\tau)} \quad . \tag{89}$$

The spontaneous fission neutron emission rate $\bar{\nu}_s F_s$ is finally derived from the gross counts $M_{b(1)}(\tau) = M^*_{b(1)}(\tau)$:

$$\bar{\nu}_s F_s \simeq \bar{\nu}_s \frac{M^*_{b(1)}(\tau)}{\epsilon \overline{\nu_{s(1)}(p)} \tau} \quad . \tag{90}$$

Table III summarizes the mean values of p, ϵ, and $\bar{\nu}_s F_s$ and the respective standard deviations of the mean. The obtained results agree with the reference data of the plutonium foil using a ^{240}Pu spontaneous fission half-life of 1.15×10^{11} yr given in Ref. 19. For the analysis of the measured data, the same $P_\nu(p)$ distribution as in Ref. 10 was used leading to a $\bar{\nu}_I$ for induced fission of 3.07.

It appears that the method tends to overestimate p and to underestimate ϵ leading to a slight overestimation of $\bar{\nu}_s F_s$. Calculating [using TIMOC (Ref. 20)] the fission probabilities for each individual isotope present in the plutonium sample, another P_ν distribution for induced fission is obtained applying the Terrel formula.[21] In the latter case a $\bar{\nu}_I$ value for induced fission of 3.25 instead of 3.07 is determined. This P_ν distribution leads after application of the code PENU to a new $P_\nu(p)$ distribution and to different numerical values of its factorial moments $\overline{\nu_{s(m)}(p)}$.

The resulting p (Ref. 22) (Table IV) is closer to the TIMOC p value and is less dependent on the size of the inspection interval τ. The obtained spontaneous fission rates $\bar{\nu}_s F_s$ do not increase significantly. The given errors are the standard deviations of the mean determined from the eight individually analyzed experimental runs.

IV.B. Factorial Moments of the Probability $n_x(\tau)$

Here the factorial moments of the $n_x(\tau)$ distribution are used to obtain an expression for $M^*_{n(0)}(\tau)$, $M^*_{n(1)}(\tau)$, and $M^*_{n(2)}(\tau)$ as a function of the measured quantities $M_{n(0)}(\tau)$, $M_{n(1)}(\tau)$, and $M_{n(2)}(\tau)$. With Eq. (81) it is

$$M^*_{n(1)}(\tau) = M_{n(1)}(\tau) - M_{b(1)}(\tau) \tag{91}$$

and

$$M^*_{n(2)}(\tau) = M_{n(2)}(\tau) - M_{b(2)}(\tau) - 2M^*_{n(1)}(\tau) M_{b(1)}(\tau) \quad . \tag{92}$$

Substituting for $M_{b(2)}(\tau)$ using Eq. (84), it follows that

TABLE III

Mean Values Obtained from Eight Runs Using Background Multiplets Only [$\bar{\nu}_I = 3.07$ (Ref. 10)]

	From Experiment			Reference Data	
	Interval Length				
	$\tau = 25.6\ \mu s$	$\tau = 51.2\ \mu s$	$\tau = 102.4\ \mu s$		Remarks
p	$(1.64 \pm 0.17) \times 10^{-2}$	$(1.38 \pm 0.13) \times 10^{-2}$	$(1.29 \pm 0.12) \times 10^{-2}$	1.070×10^{-2}	TIMOC (Ref. 17)
ϵ	0.260 ± 0.003	0.266 ± 0.002	0.267 ± 0.002	0.270 ± 0.001	Ref. 10
$\bar{\nu}_s F_s$ (1/s)	939 ± 6	943 ± 6	942 ± 6	916 ± 24	

TABLE IV

Mean Values Obtained from Eight Runs Using Background Multiplets Only ($\bar{\nu}_I = 3.25$ from TIMOC)

	Interval Length		
	$\tau = 25.6\ \mu s$	$\tau = 51.2\ \mu s$	$\tau = 102.4\ \mu s$
p	$(1.20 \pm 0.17) \times 10^{-2}$	$(1.34 \pm 0.13) \times 10^{-2}$	$(1.22 \pm 0.12) \times 10^{-2}$
$\bar{\nu}_s F_s$ (1/s)	945 ± 6	948 ± 6	946 ± 6

$$M^*_{n(2)}(\tau) = M_{n(2)}(\tau) - M^2_{b(1)}(\tau) - 2M^*_{n(1)}(\tau)M_{b(1)}(\tau) \times \left[1 + \frac{w(2,2,\tau)}{f(T,\tau)}\right] . \quad (93)$$

The values of $M^*_{n(1)}(\tau)$ and $M^*_{n(2)}(\tau)$ are numerically defined via Eqs. (91), (92), and (93) and are empirically determined.

The ratio $\beta(p)$ follows from Eq. (83) for $M^*_{n(q)}(\tau)$ with $q = 0,1,2$. It is

$$\beta(p) = \frac{3\overline{\nu_{s(2)}(p)}^2}{2\overline{\nu_{s(1)}(p)}\,\overline{\nu_{s(3)}(p)}} = \frac{2[M^*_{n(1)}(\tau)]^2}{M^*_{n(0)}(\tau)M^*_{n(2)}(\tau)} . \quad (94)$$

This ratio is again only a function of p. Using Eq. (94) and knowing the numerical values $M^*_{n(0)}(\tau)$, $M^*_{n(1)}(\tau)$, and $M^*_{n(2)}(\tau)$, p is obtained by interpolation from the factorial moments $\overline{\nu_{s(m)}(p)}$ $(m = 1,2,3)$. The neutron detection probability ϵ is determined by the ratio $M^*_{n(1)}(\tau)$ to $M^*_{n(0)}(\tau)$. It is

$$\epsilon = \frac{M^*_{n(1)}(\tau)}{M^*_{n(0)}(\tau)} \frac{2\overline{\nu_{s(1)}(p)}}{\overline{\nu_{s(2)}(p)}f(T,\tau)} . \quad (95)$$

Finally, the spontaneous fission neutron emission rate $\bar{\nu}_s F_s$ follows with known p and ϵ from Eq. (90).

The results obtained with the signal-triggered multiplets using a P_ν distribution for induced fission corresponding to $\bar{\nu}_I = 3.07$ are summarized in Table V. This distribution leads to p values (Table V) depending on the size of the inspection intervals τ. The values for ϵ and $\bar{\nu}_s F_s$ remain inside the error limits for these quantities. It appears, however, that there exists again a tendency to overestimate the spontaneous fission neutron emission rate. This is increased if the P_ν distribution for induced fission corresponding to a $\bar{\nu}_I$ of 3.25 determined with TIMOC is taken (Table VI).

In Ref. 10 the same plutonium sample is investigated using both the trigger and background multiplets to obtain values of $\bar{\nu}_s F_s$ and p for each analysis interval τ. The values of $\bar{\nu}_s F_s$ obtained applying this method are, given their error limits, just below the values obtained analyzing separately either the background or the trigger multiplets. This small discrepancy of the experimental data could be caused by the assumption made in the theory that the time response function of the detection head is the fundamental mode decay constant. Deviations from a pure exponential function exist during the slowing down of the fast source neutrons in the detection head, and during the decay of the higher modes immediately after and during the slowing down.

V. CONCLUSIONS

General expressions were obtained for the probability distribution $b_x(t - \tau, t, T_1, T_2)$ to have x signals

TABLE V

Mean Values Obtained from Eight Runs Using Trigger Multiplets Only [$\bar{\nu}_I = 3.07$ (Ref. 10)]

	From Experiment			Reference Data	
	Interval Length				
	$\tau = 25.6\ \mu s$	$\tau = 51.2\ \mu s$	$\tau = 102.4\ \mu s$		Remarks
p	$(1.53 \pm 0.2) \times 10^{-2}$	$(1.38 \pm 0.07) \times 10^{-2}$	$(1.15 \pm 0.1) \times 10^{-2}$	1.070×10^{-2}	TIMOC (Ref. 17)
ϵ	0.267 ± 0.004	0.267 ± 0.001	0.269 ± 0.003	0.270 ± 0.001	Ref. 10
$\bar{\nu}_s F_s$ (1/s)	937 ± 10	940 ± 4	939 ± 5	916 ± 24	

TABLE VI

Mean Values Obtained from Eight Runs Using Trigger Multiplets Only ($\bar{\nu}_I = 3.25$ from TIMOC)

	Interval Length		
	$\tau = 25.6\ \mu s$	$\tau = 51.2\ \mu s$	$\tau = 102.4\ \mu s$
p	$(1.32 \pm 0.2) \times 10^{-2}$	$(1.29 \pm 0.07) \times 10^{-2}$	$(1.32 \pm 0.1) \times 10^{-2}$
$\bar{\nu}_s F_s$ (1/s)	936 ± 10	943 ± 4	945 ± 5

inside a randomly triggered interval due to inhomogeneous Poisson distributed fission bursts occurring in the interval T_1, T_2; $T_1 \le T_2 \le t$. The same applies for the moments and factorial moments. This generalized theory permits a general time dependence of the probability $c(t,j,n,\xi)$ that of n-detected neutrons generated by a fission burst at ξ, j fall into an interval $t-\tau, t$. The theory is applied to practical cases in which $c(t,j,n,\xi)$ is calculated assuming a fundamental mode decay of the neutron population in the detection head after an injected neutron burst.

Rather complex analytical expressions are obtained for the probability distribution of multiplets inside fixed observation intervals τ. These apply for intervals triggered randomly or by each signal event.

The probability for a background multiplet $b_x(\tau)$ of order x depends on a polynomial of the order x of the source terms for spontaneous fission and (α,n) neutron emission. The probability to find inside an observation interval x trigger multiplets depends on a polynomial of the order $(x+1)$ in F_s and S_α. In both cases this polynomial is multiplied with $b_0(\tau)$, an exponential function with a linear dependence on F_s and S_α in the exponent. The detection probability ϵ appears together with the probabilities $P_{\alpha\nu}(p)$ and $P_{s\nu}(p)$ inside complicated expressions for Λ_j, however, which also contain various powers of $\exp(-\lambda\tau)$. This problem is overcome by forming the factorial moments of the $b_x(\tau)$ and $n_x(\tau)$ probability distributions $M_{b(m)}(\tau)$ and $M_{n(m)}(\tau)$. The moments of the $b_x(\tau)$ distribution are more complicated than the corresponding factorial moments. All types of moments have in common that the source terms of the primary neutrons appear as a linear function. The factorial moments of order m for the $b_x(\tau)$ and $n_x(\tau)$ distributions are proportional to ϵ^m and ϵ^{m+1} and the $P_\nu(p)$ distribution enters in the form of its factorial moments $\overline{\nu_{(m)}(p)}$ and $\overline{\nu_{(m+1)}(p)}$, respectively. This considerably simplifies the numerical efforts for the analysis of experimental data.

The derived theory is tested experimentally. All results obtained for $\bar{\nu}_s F_s$, p, and ϵ are with their respective error margins inside the known values of the used plutonium calibration sample. The determined values of p are very sensitive to the P_ν distribution for induced fission. This is not the case for ϵ and $\bar{\nu}_s F_s$. The numerical results show that the size of the inspection interval τ does not influence the values for the determined spontaneous fission neutron emission rate.

The choice of one inspection interval is sufficient for a data analysis at least in the low count rate range. At present the method is limited in its application to low neutron count rates in the absence of theoretical corrections for the dead-time losses of the neutron counters. Such corrections are of special importance for the probabilities with a higher number of signals inside the analysis interval.

APPENDIX A

In this Appendix, the validity of Eq. (24) and its compatibility with the probability generating function $\pi(z,T_1)$ of Eq. (20) for a generalized Poisson distribution with $j \le N$ are shown:

$$x b_x = \Lambda_1 b_{x-1} + 2\Lambda_2 b_{x-2} + \ldots N\Lambda_N b_{x-N} \qquad \text{(A.1)}$$

for $x \ge N$.

Multiplying both sides of Eq. (A.1) with z^{x-1} and summing the resulting expression over $N \le x \le \infty$, the following expression is obtained:

$$\sum_{x=N}^{\infty} z^{x-1} x b_x = \Lambda_1 \sum_{x=N}^{\infty} z^{x-1} b_{x-1} + 2\Lambda_2 \sum_{x=N}^{\infty} z^{x-1} b_{x-2} \ldots N\Lambda_N \sum_{x=N}^{\infty} z^{x-1} b_{x-N} \; . \qquad \text{(A.2)}$$

Equation (A.2) is written in the following form:

$$\frac{d}{dz} \sum_{x=N}^{\infty} z^x b_x = \Lambda_1 \left(\sum_{x=0}^{\infty} z^x b_x - \sum_{x=0}^{N-2} z^x b_x \right) + 2\Lambda_2 z \left(\sum_{x=0}^{\infty} z^x b_x - \sum_{x=0}^{N-3} z^x b_x \right) + N\Lambda_N z^{N-1} \sum_{x=0}^{\infty} z^x b_x \; . \qquad \text{(A.3)}$$

Putting

$$g(z) = \sum_{x=0}^{\infty} z^x b_x \; , \qquad \text{(A.4)}$$

it follows from Eqs. (A.3) and (A.4) that

$$\frac{d}{dz}\left[g(z) - \sum_{x=0}^{N-1} z^x b_x \right] = \Lambda_1 \left[g(z) - \sum_{x=0}^{N-2} z^x b_x \right] + 2\Lambda_2 z \left[g(z) - \sum_{x=0}^{N-3} z^x b_x \right] \ldots + N\Lambda_N z^{N-1} g(z) \qquad \text{(A.5)}$$

and

$$\frac{dg(z)}{dz} - \sum_{x=1}^{N-1} z^{x-1} x b_x = \sum_{j=1}^{N} j\Lambda_j z^{j-1} g(z) - \sum_{j=1}^{N-1} j\Lambda_j z^{j-1} \sum_{x=0}^{N-j-1} b_x z^x \; . \qquad \text{(A.6)}$$

With the initial conditions given in Eq. (25), the second terms of both sides of Eq. (A.6) are equal leading to the following differential equation for $g(z)$:

$$\frac{dg(z)}{dz} = \sum_{j=1}^{N} j\Lambda_j z^{j-1} g(z) \; . \qquad \text{(A.7)}$$

With the initial conditions of Eq. (25) for b_0, the solution of Eq. (A.7) is

$$g(z) = b_0 \exp\left(\sum_{j=1}^{N} \Lambda_j z^j\right) = \exp\left[\sum_{j=1}^{N} (z^j - 1)\Lambda_j\right] . \quad (A.8)$$

Equation (A.8) is identical to the probability generating function $\pi(z, T_1)$ [Eq. (20)] of a generalized Poisson distribution for $N \to \infty$.

APPENDIX B

In this section the first few analytical expressions of $w(n,j,\tau)$ for $1 \le n \le 4$ and $1 \le j \le n$ are summarized. According to Eq. (55) it is given by

$$w(n,j,\tau) = \binom{n}{j} \sum_{k=0}^{j-1} \binom{j-1}{k} (-1)^k \times \frac{1 - \exp[-\lambda\tau(n-j+k)]}{\lambda\tau(n-j+k)} . \quad (B.1)$$

From Eq. (B.1) follows

$$w(1,1,\tau) = 1 \quad (B.2)$$

$$w(2,1,\tau) = \binom{2}{1} \frac{1}{\lambda\tau} [1 - \exp(-\lambda\tau)] \quad (B.3)$$

$$w(3,1,\tau) = \binom{3}{1} \frac{1}{2\lambda\tau} [1 - \exp(-2\lambda\tau)] \quad (B.4)$$

$$w(4,1,\tau) = \binom{4}{1} \frac{1}{3\lambda\tau} [1 - \exp(-3\lambda\tau)] \quad (B.5)$$

$$w(2,2,\tau) = 1 - \frac{1}{\lambda\tau} [1 - \exp(-\lambda\tau)] \quad (B.6)$$

$$w(3,2,\tau) = \frac{3}{2\lambda\tau} [1 - 2\exp(-\lambda\tau) + \exp(-2\lambda\tau)] \quad (B.7)$$

$$w(4,2,\tau) = \frac{1}{\lambda\tau} [1 - 3\exp(-2\lambda\tau) + 2\exp(-3\lambda\tau)] \quad (B.8)$$

$$w(3,3,\tau) = 1 - \frac{1}{2\lambda\tau} [3 - 4\exp(-\lambda\tau) + \exp(-2\lambda\tau)] \quad (B.9)$$

$$w(4,3,\tau) = \frac{2}{3\lambda\tau} [2 - 6\exp(-\lambda\tau) + 6\exp(-2\lambda\tau) - 2\exp(-3\lambda\tau)] \quad (B.10)$$

$$w(4,4,\tau) = 1 - \frac{1}{6\lambda\tau} [11 - 18\exp(-\lambda\tau) + 9\exp(-2\lambda\tau) - 2\exp(-3\lambda\tau)] . \quad (B.11)$$

By means of the above equations, it is easily verified that the following relations hold for $1 \le n \le 4$:

$$\sum_{j=1}^{n} j_{(1)} w(n,j,\tau) = n_{(1)} w(1,1,\tau) , \quad (B.12)$$

$$\sum_{j=2}^{n} j_{(2)} w(n,j,\tau) = n_{(2)} w(2,2,\tau) , \quad (B.13)$$

and

$$\sum_{j=3}^{n} j_{(3)} w(n,j,\tau) = n_{(3)} w(3,3,\tau) . \quad (B.14)$$

In general it holds that

$$\sum_{j=k}^{n} j_{(k)} w(n,j,\tau) = n_{(k)} w(k,k,\tau) . \quad (B.15)$$

ACKNOWLEDGMENTS

Helpful discussions with L. Anselmi, N. T. Barrett, G. Birkhoff, L. Bondar, R. Dierckx, and A. Prosdocimi are gratefully acknowledged. Many thanks are due to K. Caruso for the execution of the numerical calculations and to S. Tenti and M. van Andel for typing the manuscript.

REFERENCES

1. K. BÖHNEL, "Die Plutoniumbestimmung in Kernbrennstoffen mit der Neutronen–Koinzidenzmethode," KFK-2203, Kernforschungszentrum Karlsruhe (1975).

2. N. ENSSLIN, M. L. EVANS, H. O. MENLOVE, and J. E. SWANSEN, *Nucl. Mater. Manage.*, **VII**, 43 (1978).

3. J. JACQUESSON, *Le Journal de Physique, Physique Appliquée, Suppl. au No. 6*, **24**, 112 (1963).

4. G. BIRKHOFF, L. BONDAR, J. LEY, R. BERG, R. SWENNEN, and G. BUSCA, "On the Determination of the ^{240}Pu in Solid Waste Containers by Spontaneous Fission Neutron Measurements, Application to Reprocessing Plant Waste," EUR-5158e, Commission of the European Communities, Joint Research Centre, Ispra (1974).

5. E. W. LEES and F. J. G. ROGERS, "Experimental and Theoretical Observations on the Use of the Euratom Variable Dead Time Neutron Counter for the Passive Assay of Plutonium," *Proc. Int. Symp. Nuclear Material Safeguards*, Vienna, October 2-6, 1978, SM 231/51, International Atomic Energy Agency, Vienna (1978).

6. L. BONDAR, "Time Correlation Analyser for Non-Destructive Plutonium Assay," *Proc. Int. Mtg. Monitoring of Plutonium Contaminated Waste*, Ispra, September 25-28, 1979, Commission of the European Communities, Ispra (1979).

7. L. BONDAR and B. G. R. SMITH, "Interpretation of Pu Waste Measurements by the Euratom Time Correlation

Analyser," *Proc. Int. Symp. Management of Alpha-Contaminated Waste*, Vienna, June 2-6, 1980, SM 246/50, International Atomic Energy Agency, Vienna (1980).

8. L. BONDAR, "Passive Neutron Assay," *Proc. Int. Symp. Recent Advances in Nuclear Material Safeguards*, Vienna, November 8-12, 1982, SM 260/54, International Atomic Energy Agency, Vienna (1982).

9. L. STANCHI, "Preliminary Report on a Device for Acquisition of Neutrons of Spontaneous Fissions," *Proc. Int. Symp. Nuclear Electronics*, JRC Dubna USSR, Warsaw (1971).

10. R. DIERCKX and W. HAGE, *Nucl. Sci. Eng.*, **85**, 325 (1983).

11. I. V. BASAWA and B. L. S. PRAKASA RAO, *Inference for Stochastic Processes*, p. 103, Academic Press, Inc., New York (1980).

12. M. O. DEIGHTON, *Nucl. Instrum. Methods*, 165 (1979).

13. E. J. DOWDY, C. N. HENRY, A. A. ROBBA, and J. R. PRATT," New Neutron Correlation Measurement Techniques for Special Nuclear Material Assay and Accountability," *Proc. Int. Symp. Nuclear Material Safeguards*, Vienna, October 2-6, 1978, SM-231/69, International Atomic Energy Agency, Vienna (1978).

14. L. ANSELMI and W. HAGE, "PENU—A Computer Programme for the Calculation of the Neutron Multiplicity of Prompt Neutrons of a Fission Cascade," Commission of the European Communities, Ispra (1983) (Report in preparation).

15. K. BÖHNEL, "The Effect of Multiplication on Neutron Coincidence Measurements," *Nucl. Sci. Eng.* (to be published).

16. W. HAGE and D. M. CIFARELLI, "On the Factorial Moments of the Neutron Multiplicity Distribution of Fission Cascades," Commission of the European Communities, Joint Research Centre, Ispra (to be published).

17. J. E. SWANSEN, P. R. COLLINSWORTH, M. S. KRICK, and D. L. PETERSON, "Multiplicity Sorter for Shift Register Coincidence Electronics," LA 9221-MS UC 15, Los Alamos National Laboratory (1982).

18. L. BONDAR, Private Communication, Joint Research Centre, Ispra (1982).

19. C. BUDTZ-JØRGENSEN and H. H. KNITTER, *Nucl. Sci. Eng.*, **79**, 380 (1981).

20. R. JAARSMA and H. RIEF, "TIMOC-72 Code Manual," EUR-5016e, Commission of the European Communities, Joint Research Centre, Ispra (1973).

21. J. TERREL, *Phys. Rev.*, **108**, 3 (1957).

22. F. BOGGIANI and A. SALLUSTIO, Thesis, Centro Studi Nucleari Enrico Fermi, Milano (1983).

NORTH-HOLLAND
PHYSICS
PUBLISHING

ON THE FACTORIAL MOMENTS OF THE NEUTRON MULTIPLICITY DISTRIBUTION OF FISSION CASCADES

W. HAGE

Commission of the European Communities, Joint Research Centre, Ispra Establishment, 21020 Ispra (Va), Italy

D.M. CIFARELLI

Università L. Bocconi, Istituto di Metodi Quantitativi, 20136 Milan, Italy

Received 10 July 1984

The effective number of combinations with which neutrons can be grouped together is an important quantity required for the interpretation of neutron time correlation or coincidence experiments with multiplying media. For this quantity analytical expressions are derived valid for a far subcritical assembly in a point and a one neutron energy group approximation. The derived expressions are applicable in models for the mass determination of spontaneous fission neutron emitters.

Reprinted from NUCLEAR INSTRUMENTS AND METHODS
IN PHYSICS RESEARCH A

Nuclear Instruments and Methods in Physics Research A236 (1985) 165–177
North-Holland, Amsterdam

ON THE FACTORIAL MOMENTS OF THE NEUTRON MULTIPLICITY DISTRIBUTION OF FISSION CASCADES

W. HAGE

Commission of the European Communities, Joint Research Centre, Ispra Establishment, 21020 Ispra (Va), Italy

D.M. CIFARELLI

Università L. Bocconi, Istituto di Metodi Quantitativi, 20136 Milan, Italy

Received 10 July 1984

The effective number of combinations with which neutrons can be grouped together is an important quantity required for the interpretation of neutron time correlation or coincidence experiments with multiplying media. For this quantity analytical expressions are derived valid for a far subcritical assembly in a point and a one neutron energy group approximation. The derived expressions are applicable in models for the mass determination of spontaneous fission neutron emitters.

1. Introduction

Neutron correlation techniques are used for the assay of those fissile materials which emit spontaneous fission neutrons. Applying this technique to small fissile samples analytical models [1–4] are in use for the interpretation of the measured data. These assume a Poissonian (α–n) and spontaneous fission distribution in space and energy independent models. Induced fission is considered as a fission cascade of negligible duration initiated by the (α–n) and spontaneous fission primary neutrons. With these assumptions the probability $P_\nu(p)$ is defined with which ν neutrons are emitted from the cascade inside the sample per primary (α, n) or spontaneous fission event, respectively, p being the probability that a neutron generates an induced fission event.

Of particular interest in the interpretation models is the effective number of combinations with which $1, 2 \cdots m$ neutrons from the same fission event can be grouped together. These effective numbers are computed [3] from the $P_\nu(p)$-distribution and depend on the probabilities $P_{s\nu}$ and P_ν with which ν neutrons are emitted per spontaneous and induced fission events, respectively. The present practice is to simulate the fission cascade for a limited number of generations by means of Monte Carlo methods [5], or analytical expressions [3] to obtain $P_\nu(p)$. Determined is then the probability $P_{s\nu}(p)$ for the emission of ν neutrons of a fission cascade triggered by spontaneous fission neutrons. From the numerical data the effective number of combinations with which 1, 2 or m neutrons are grouped together is computed. The principal disadvantage of this method is the rather long computing time required for these procedures even for a limited number of fission generations approximating the cascade. This disadvantage is avoided applying the analytical expressions derived in this paper for this effective number of combinations of order m. Two types of approximations are used concerning the fission cascade. In the first type of cascade only induced fission is considered, in the second all nuclear reactions in a space and energy independent model.

2. Theory

The derived models for the interpretation of neutron correlation measurements assume that the spontaneous fission and (α–n) events occurring in the sample appear as δ-bursts distributed in time according to a Poisson distribution. Return-neutrons from the neutron detection assembly into the sample,

0168-9002/85/$03.30

or moderation of neutrons with subsequent fissions inside the sample are excluded. Is further the neutron generation time of the sample much smaller than the fundamental mode decay time of the neutron detection assembly, then each neutron produced during a burst and detected cannot be distinguished from any other detected neutron of the same burst but produced during a different generation of the fission cascade. Are these three conditions fulfilled, neutron multiplication can be considered as a super-spontaneous fission event [1] with a new $P_\nu(p)$ distribution with bursts being Poisson distributed in time. This $P_\nu(p)$ distribution depends on the P_ν distribution of the primary neutrons, the P_ν distribution of the following generations and the probability p that a neutron generates an induced fission event.

An event tree simulating this physical cascade process generation by generation becomes already after the first generation of induced fission very complex for obtaining an explicit expression for $P_\nu(p)$ and from this the effective number of groups with m $(1 \leqq m \leqq \nu)$ neutrons escaping the cascade. For this reason an equivalent event tree of the cascade for groups of neutrons escaping the fission cascade is introduced. From this event tree analytical expressions for the effective number of groups with m neutrons leaving the cascade are derived.

In spontaneous fission events with the probability $P_{s\nu}$ for the emission of ν neutrons, groups with $m < \nu$ neutrons named effective multiplets can be formed. The effective number of these multiplets is $\overline{\nu_{s(m)}}$:

$$\overline{\nu_{s(m)}} = \overline{\binom{\nu_s}{m}} = \sum_{\nu=m}^{\infty} \binom{\nu}{m} P_{s\nu}. \tag{1}$$

Similarly, effective multiplets for induced fission are introduced with an effective number $\overline{\nu_{(m)}}$ defined by

$$\overline{\nu_{(m)}} = \overline{\binom{\nu}{m}} = \sum_{\nu=m}^{\infty} \binom{\nu}{m} P_\nu. \tag{2}$$

For this equivalent event tree, fission cascades are triggered by $\overline{\nu_{s(1)}}$ effective singlets, $\overline{\nu_{s(2)}}$ effective doublets, $\overline{\nu_{s(3)}}$ effective triplets $\cdots$ from spontaneous fission and continued with $\overline{\nu_{(1)}}$ effective singlets, $\overline{\nu_{(2)}}$ effective doublets $\cdots$ from induced fission in the following generations. This basic principle is applied in the following to determine the effective number of combinations with which multiplets escape the fission cascade. First a cascade with only neutron multiplication is considered. All neutrons escaping multiplication are regarded as detectable neutrons. The second type of cascade permits fission, capture, elastic and inelastic scattering and leakage.

2.1. Cascade with fissions only

First is considered a fission chain started with singlets from an average spontaneous fission event and continued with singlets only. In the first generation are $\overline{\nu_{s(1)}}$ singlets. A fraction $\overline{\nu_{s(1)}}l$ escapes directly from the sample with the probability $l = (1 - p)$. The other fraction causes via the probability p an induced fission generating $\overline{\nu_{s(1)}}\,p\overline{\nu_{(1)}}$ singlets in the second generation. In the nth generation are produced $\overline{\nu_{s(1)}}(p\overline{\nu_{(1)}})^{n-1}$ singlets of which $\overline{\nu_{s(1)}}(p\overline{\nu_{(1)}})^{n-1}l$ escape further fissions and become available for being detected.

The total number of singlets produced in a fission chain with an infinite number of generations is therefore:

$$s = \overline{\nu_{s(1)}}\left[1 + p\overline{\nu_{(1)}} + \left(p\overline{\nu_{(1)}}\right)^2 + \left(p\overline{\nu_{(1)}}\right)^3 \cdots\right] = \overline{\nu_{s(1)}}/\left(1 - p\overline{\nu_{(1)}}\right). \tag{3}$$

The total number of singlets escaping further fissions of the same chain is [4]:

$$\begin{aligned}\overline{\binom{\nu_s(p)}{1}} &= \overline{\nu_{s(1)}(p)} = \overline{\nu_{s(1)}}l\left[1 + p\overline{\nu_{(1)}} + \left(p\overline{\nu_{(1)}}\right)^2 + \cdots\right] \\ &= \overline{\nu_{s(1)}}l/\left(1 - p\overline{\nu_{(1)}}\right) = \overline{\nu_{s(1)}}M(p),\end{aligned} \tag{4}$$

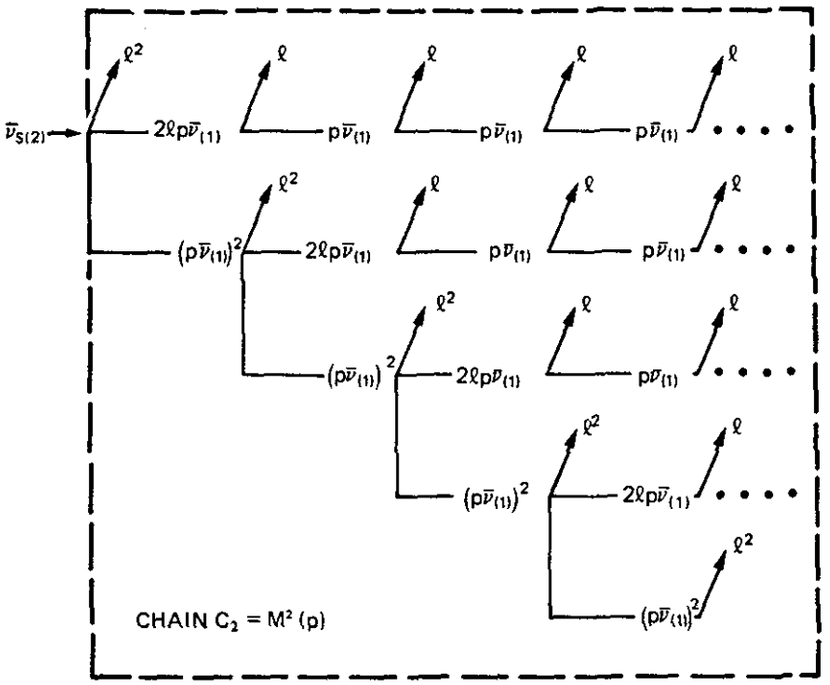

Fig. 1. Event tree 1 for $\overline{\binom{\nu_s(p)}{2}}$.

with

$$M(p) = \frac{l}{1 - p\overline{\nu_{(1)}}} = \frac{1-p}{1 - p\overline{\nu_{(1)}}}.$$

From a fission chain started with doublets, or singlets and continued with doublets, only groups of two neutrons escape the cascade. For this reason exist no contributions to $\overline{\nu_{s(1)}(p)}$ from chains containing $\overline{\nu_{s(m)}}$ or $\overline{\nu_{(m)}}$-terms with $m > 1$. $\overline{\nu_{s(1)}(p)}$ is the effective number of combinations with which singlets escape the fission cascade and become available for detection.

The fission chains of doublets escaping the fission cascade can be reduced to two typical event trees. Both are event trees in which after each generation occurs a term with l^2. One event tree is started by $\overline{\nu_{s(2)}}$ doublets (fig. 1), the other by $\overline{\nu_{s(1)}}$ singlets (fig. 2) and continued after 1 or 2 or 3 or $\cdots n$ generations by the event tree of fig. 1 initiated by $\overline{\nu_{s(2)}}$ doublets. The event tree 1 (fig. 1) gives to $\overline{\binom{\nu_s(p)}{2}}$ the contribution $S_1^{(2)}$:

$$S_1^{(2)} = \overline{\nu_{s(2)}} l^2 \left[1 + \frac{2p\overline{\nu_{(1)}}}{1 - p\overline{\nu_{(1)}}}\right] + \frac{\overline{\nu_{s(2)}}}{1 - \left(p\overline{\nu_{(1)}}\right)^2} l^2 \left[1 + \frac{2p\overline{\nu_{(1)}}}{1 - p\overline{\nu_{(1)}}}\right] \left(p\overline{\nu_{(1)}}\right)^2 \tag{5}$$

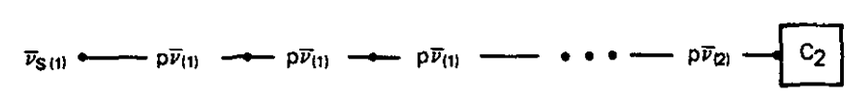

Fig. 2. Event tree 2 for $\overline{\binom{\nu_s(p)}{2}}$.

or

$$S_1^{(2)} = \overline{\nu_{s(2)}} M^2(p).$$

Event tree 2 of fig. 2 gives $S_2^{(2)}$:

$$S_2^{(2)} = \overline{\nu_{s(1)}} \frac{\overline{p\nu_{(2)}}}{1 - \overline{p\nu_{(1)}}} M^2(p). \tag{6}$$

This leads to

$$\left(\overline{\begin{matrix}\nu_s(p)\\ 2\end{matrix}}\right) = \overline{\nu_{s(2)}(p)} = S_1^{(2)} + S_2^{(2)} = M^2(p)\left[\overline{\nu_{s(2)}} + \overline{\nu_{s(1)}} \frac{\overline{p\nu_{(2)}}}{1 - \overline{p\nu_{(1)}}}\right]. \tag{7}$$

Terms with $\overline{\nu_{s(m)}}$ or $\overline{\nu_{(m)}}$ $m > 2$ do not contribute to $\overline{\nu_{s(2)}(p)}$ because these give rise to leakage of neutron groups with $m > 2$.

Eq. (7) gives the exact expression for $\left(\overline{\begin{matrix}\nu_s(p)\\ 2\end{matrix}}\right)$ of a cascade with fissions only. It is different from the

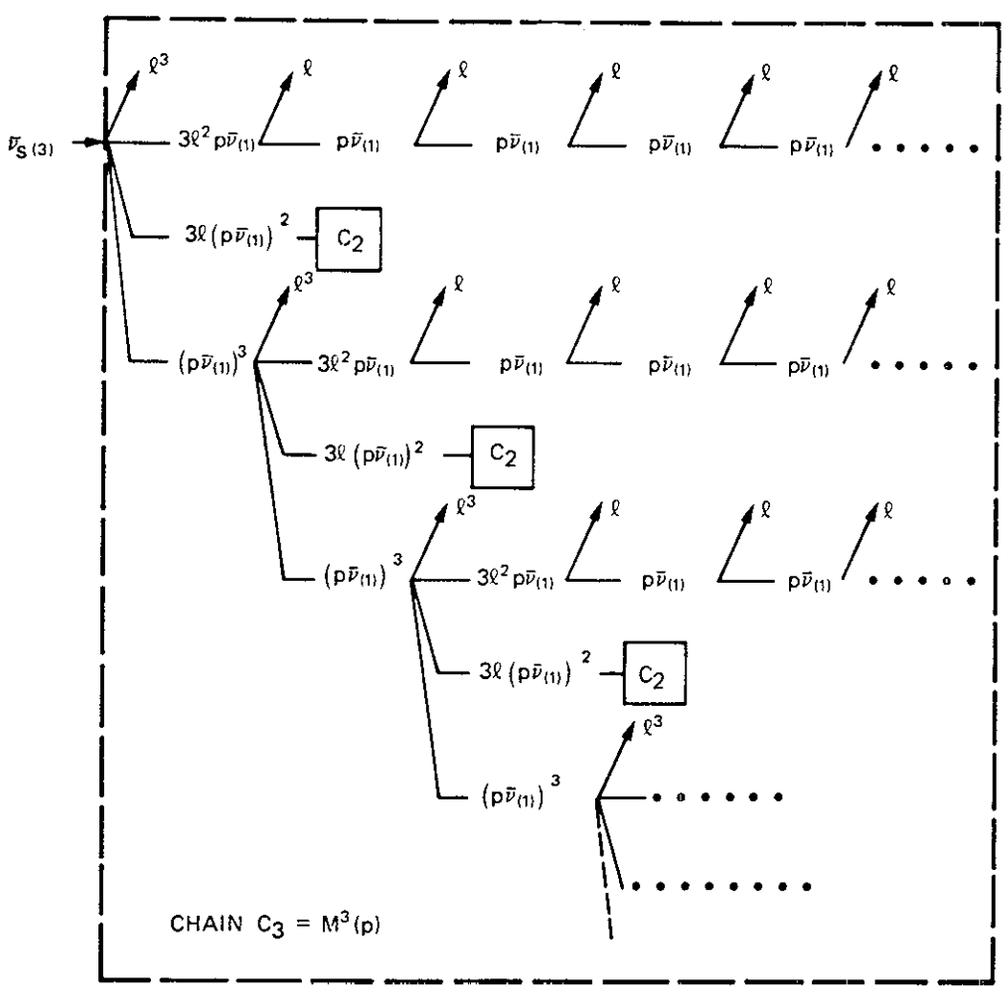

Fig. 3. Event tree 1 for $\left(\overline{\begin{matrix}\nu_s(p)\\ 3\end{matrix}}\right)$.

one used frequently in the literature of the type [6,7]:

$$\overline{\binom{\nu_s(p)}{2}} = M(p)\overline{\nu_{s(1)}}\left[M(p)\overline{\nu_{s(1)}} - 1\right]. \tag{8}$$

The fission chain of triplets escaping the fission cascade is based on three different event trees which lead in each generation to a term with l^3. Event tree 1 is started by $\overline{\nu_{s(3)}}$ triplets (fig. 3), event tree 2 by $\overline{\nu_{s(2)}}$ doublets (fig. 4), and event tree 3 by $\overline{\nu_{s(1)}}$ singlets (fig. 5). The event tree 1 gives to $\overline{\nu_{s(3)}(p)}$ the contribution:

$$\begin{aligned} S_1^{(3)} &= \overline{\nu_{s(3)}}l^3\left[1 + \frac{3p\overline{\nu_{(1)}}}{1 - p\overline{\nu_{(1)}}}\right] + 3\overline{\nu_{s(3)}}l\left(p\overline{\nu_{(1)}}\right)^2 M^2(p) \\ &\quad + \left[\overline{\nu_{s(3)}}l^3\left(1 + \frac{3p\overline{\nu_{(1)}}}{1 - p\overline{\nu_{(1)}}}\right) + 3\overline{\nu_{s(3)}}l\left(p\overline{\nu_{(1)}}\right)^2 M^2(p)\right]\frac{\left(p\overline{\nu_{(1)}}\right)^3}{1 - \left(p\overline{\nu_{(1)}}\right)^3}, \\ S_1^{(3)} &= \overline{\nu_{s(3)}}M^3(p). \end{aligned} \tag{9}$$

From the event tree 2 of fig. 4 follows:

$$\begin{aligned} S_2^{(3)} &= \overline{\nu_{s(2)}}\left[2lp\overline{\nu_{(1)}}\frac{p\overline{\nu_{(2)}}}{1 - p\overline{\nu_{(1)}}}M^2(p) + 2lp\overline{\nu_{(2)}}M^2(p) + 2p\overline{\nu_{(1)}}p\overline{\nu_{(2)}}M^3(p)\right] \\ &\quad + \overline{\nu_{s(2)}}\left[2lp\overline{\nu_{(1)}}\frac{p\overline{\nu_{(2)}}}{1 - p\overline{\nu_{(1)}}}M^2(p) + 2lp\overline{\nu_{(2)}}M^2(p) + 2p\overline{\nu_{(1)}}p\overline{\nu_{(2)}}M^3(p)\right]\frac{\left(p\overline{\nu_{(1)}}\right)^2}{1 - \left(p\overline{\nu_{(1)}}\right)^2}, \end{aligned} \tag{10}$$

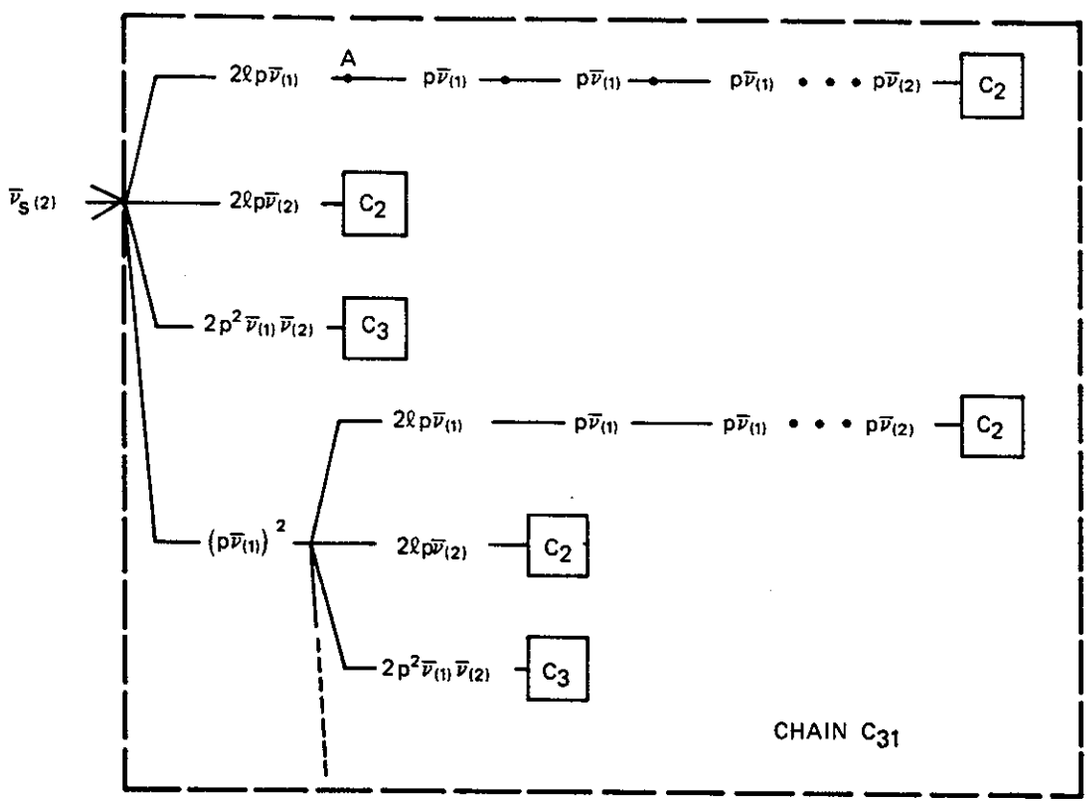

Fig. 4. Event tree 2 for $\overline{\binom{\nu_s(p)}{3}}$.

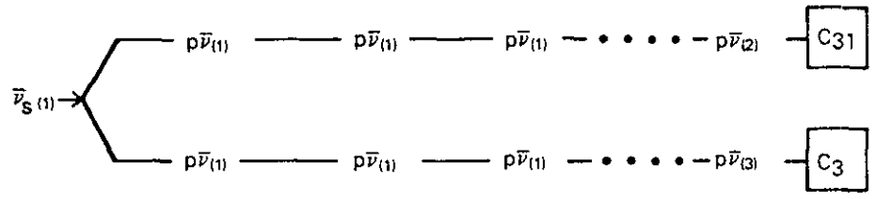

Fig. 5. Event tree 3 for $\overline{\binom{\nu_s(p)}{3}}$.

or

$$S_2^{(3)} = 2\overline{\nu_{s(2)}} M^3(p) \frac{p\overline{\nu_{(2)}}}{1 - p\overline{\nu_{(1)}}}.$$

The event tree 3 gives the contribution:

$$S_3^{(3)} = \overline{\nu_{s(1)}} \left[\frac{p\overline{\nu_{(2)}}}{1 - p\overline{\nu_{(1)}}} 2M^3(p) \frac{p\overline{\nu_{(2)}}}{1 - p\overline{\nu_{(1)}}} + \frac{p\overline{\nu_{(3)}}}{1 - p\overline{\nu_{(1)}}} M^3(p) \right],$$

or

$$S_3^{(3)} = \overline{\nu_{s(1)}} \left[\frac{p\overline{\nu_{(3)}}}{1 - p\overline{\nu_{(1)}}} + 2\left(\frac{p\overline{\nu_{(2)}}}{1 - p\overline{\nu_{(1)}}} \right)^2 \right] M^3(p). \tag{11}$$

The contributions $S_1^{(3)}$, $S_2^{(3)}$ and $S_3^{(3)}$ of the eqs. (9), (10) and (11) give finally:

$$\overline{\binom{\nu_s(p)}{3}} = \overline{\nu_{s(3)}(p)} = M^3(p) \left[\overline{\nu_{s(3)}} + 2\overline{\nu_{s(2)}} \frac{p\overline{\nu_{(2)}}}{1 - p\overline{\nu_{(1)}}} + \overline{\nu_{s(1)}} \left[\frac{p\overline{\nu_{(3)}}}{1 - p\overline{\nu_{(1)}}} + 2\left[\frac{p\overline{\nu_{(2)}}}{1 - p\overline{\nu_{(1)}}} \right]^2 \right] \right], \tag{12}$$

or

$$\overline{\nu_{s(3)}(p)} = M^3(p) \left[\overline{\nu_{s(3)}} + \overline{\nu_{s(1)}} \frac{p\overline{\nu_{(3)}}}{1 - p\overline{\nu_{(1)}}} \right] + 2M(p) \frac{p\overline{\nu_{(2)}}}{1 - p\overline{\nu_{(1)}}} \overline{\nu_{s(2)}(p)}. \tag{13}$$

Eqs. (4), (7) and (12) or (13) give the desired effective number of emitted neutrons of a fission cascade triggered by spontaneous fission neutrons for $1 \leqq m \leqq 3$. Higher order values of $\overline{\nu_{s(m)}(p)}$ are not required in a practical data analysis due to the low event rate for the detection of multiplets of order $m \geqq 4$.

The derived formulas use as primary neutrons of the fission cascade neutrons originating from spontaneous fission. Is the fission cascade triggered by neutrons from (α–n) reactions then in most cases $\overline{\nu_{s(m)}}$ can be put equal to $\overline{\nu_{(m)}}$. In these conditions the expressions for $\overline{\nu_{(m)}(p)}$ are considerably simplified. They are:

$$\overline{\nu_{(1)}(p)} = \overline{\nu_{(1)}} M(p), \tag{14}$$

$$\overline{\nu_{(2)}(p)} = \frac{\overline{\nu_{(2)}}}{1 - p\overline{\nu_{(1)}}} M^2(p), \tag{15}$$

$$\overline{\nu_{(3)}(p)} = \left[\frac{\overline{\nu_{(3)}}}{1 - p\overline{\nu_{(1)}}} + 2p\overline{\nu_{(2)}} \frac{\overline{\nu_{(2)}}}{\left(1 - p\overline{\nu_{(1)}}\right)^2} \right] M^3(p). \tag{16}$$

2.2. Cascade as fast fission threshold approximation

The fast neutron cascade inside a fuel item is triggered in this model again by a spontaneous fission event emitting $\overline{\nu_{s(m)}}$ multiplets of order m. These primary fast neutrons collide with the nuclei present in the sample and lead to nuclear reactions like inelastic scattering Σ_i, elastic scattering Σ_e, radiative capture Σ_γ and induced fission Σ_f. The total microscopic cross section Σ for the fast neutrons averaged over the respective spectrum of the neutrons inside the fuel is given by:

$$\Sigma = \Sigma_i + \Sigma_e + \Sigma_\gamma + \Sigma_f. \tag{17}$$

The neutrons collide with a collision probability $P(\Sigma, n)$ with the nuclei present in the fuel item. $P(\Sigma, n)$ depends on the generation number n of the neutrons in the cascade and on the total cross section Σ. In the following it is assumed that the sample size is such that the collision probability of the primary neutrons $P(\Sigma, 1) = P$ is valid for all generations of the cascade (primary collision approximation). Ref. [8] gives for the most common geometries (infinite slab, infinite cylinder, sphere, oblate spheroide) the analytical expressions of the collision probabilities and the respective numerical values relative to Σ.

The probability L that a neutron is emitted from a test item is either due to leakage $(1 - P)$ from the test item or due to inelastic scattering $\Sigma_i/\Sigma P$ below an assumed fast fission threshold. It is:

$$L = 1 - P + (\Sigma_i/\Sigma)P. \tag{18}$$

Elastic scattering events with the probability

$$E = (\Sigma_e/\Sigma)P \tag{19}$$

contribute along with the fission probability

$$F = (\Sigma_f/\Sigma)P \tag{20}$$

to the next generation of the cascade.

With this definition the value of $\overline{\nu_{s(1)}(P)}$ is determined. It is in analogy to eq. (4):

$$\overline{\nu_{s(1)}(P)} = \overline{\nu_{s(1)}}L[1 + A + A^2 \cdots] = \overline{\nu_{s(1)}}M(P), \tag{21}$$

with

$$M(P) = \frac{L}{1 - A}, \tag{22}$$

$$A = E + F\overline{\nu_{(1)}}. \tag{23}$$

In analogy to eq. (21) we find by means of slightly modified event trees of figs. 1–7:

$$\overline{\nu_{s(2)}(P)} = M^2(P)\left[\overline{\nu_{s(2)}} + \overline{\nu_{s(1)}}\frac{F\overline{\nu_{(2)}}}{1 - A}\right], \tag{24}$$

and

$$\overline{\nu_{s(3)}(P)} = M^3(P)\left[\overline{\nu_{s(3)}} + \overline{\nu_{s(1)}}\frac{F\overline{\nu_{(3)}}}{1 - A}\right] + 2M(P)\frac{F\overline{\nu_{(2)}}}{1 - A}\overline{\nu_{s(2)}(P)}. \tag{25}$$

For trigger neutrons of the fission cascade originating from (α–n) reactions it is again $\overline{\nu_{s(m)}} = \overline{\nu_{(m)}}$. It follows from eqs. (23)–(25):

$$\overline{\nu_{(1)}(P)} = \overline{\nu_{(1)}}M(P), \tag{26}$$

$$\overline{\nu_{(2)}(P)} = \frac{\overline{\nu_{(2)}}(1 - E)}{1 - A}M^2(P), \tag{27}$$

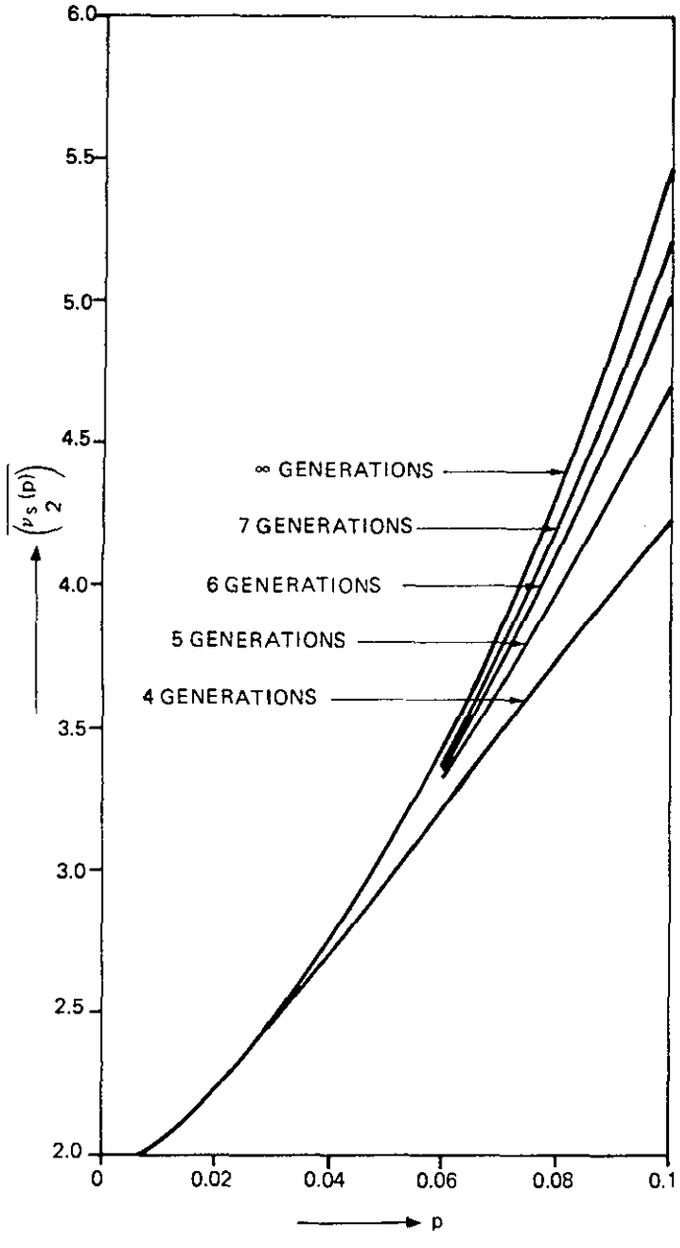

Fig. 6. $\overline{\binom{\nu_s(p)}{2}}$ as function of p (sample 1-22).

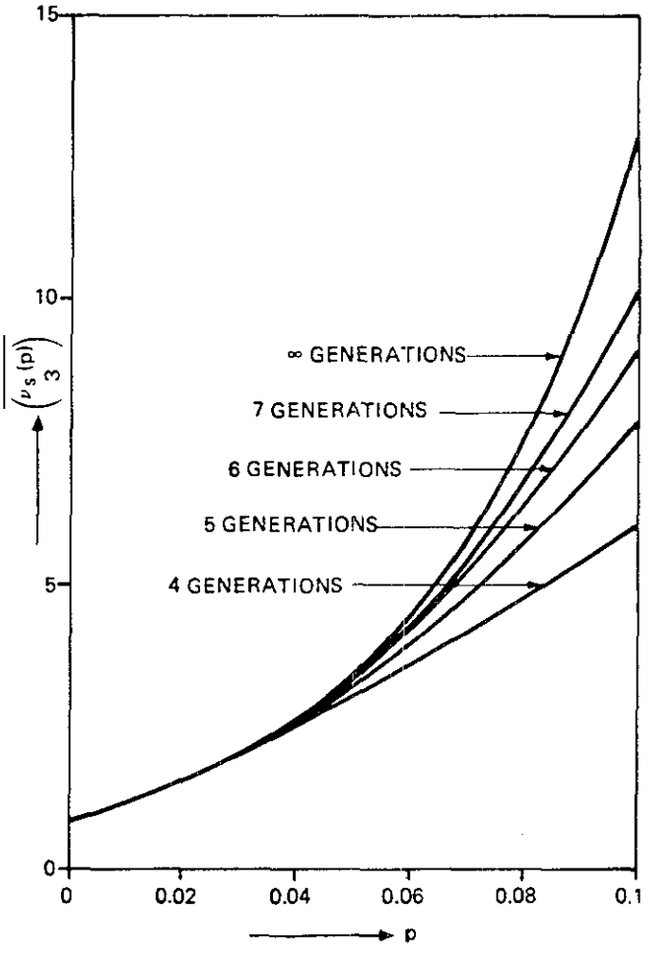

Fig. 7. $\overline{\binom{\nu_s(p)}{3}}$ as function of p (sample 1-22).

$$\overline{\nu_{(3)}(P)} = \left[\frac{\overline{\nu_{(3)}}(1-E)}{1-A} + 2F\overline{\nu_{(2)}}\frac{\overline{\nu_{(2)}}(1-E)}{(1-A)^2} \right] M^3(P). \tag{28}$$

In case of waste matrices the definition of the cross sections in a one group treatment is slightly different. First is assigned to all nuclear scattering phenomena which cause a substantial change of the neutron energy the cross section Σ_* [9]. Scattering events with small changes of the neutron energy are

defined again by Σ_e. Then the total cross section of the waste matrix is with ($\Sigma_f = 0$)

$$\Sigma = \Sigma_\gamma + \Sigma_* + \Sigma_e.$$

Neutrons with radiative capture and substantial energy loss cannot be detected in the detection head and are lost from the cascade. Let further the average chord length be

$$R = 4V/S, \tag{29}$$

with S the surface and V the volume of the waste item, where R is much smaller than $1/\Sigma$, then

$$L = 1 - P, \tag{30}$$

and

$$A = (\Sigma_e/\Sigma)P. \tag{31}$$

This leads to:

$$M(P) = \frac{1-P}{1-(\Sigma_e/\Sigma)P}. \tag{32}$$

In most waste categories $P\Sigma_e/\Sigma \ll 1$ holds, and the well known expression of ref. [10] is found

$$\overline{\nu_{s(m)}(P)} = \overline{\nu_{s(m)}}(1-P)^m. \tag{33}$$

3. Application of the theory

First the numerical results obtained with the analytical expressions of $\overline{\nu_{s(2)}(p)}$ and $\overline{\nu_{s(3)}(p)}$ are compared with the results using approximations of the $P_{s(\nu)}(p)$ distribution for a limited number of induced fission generations [4]. Then the derived formulas are applied to determine the spontaneous fission neutron emission rate using a neutron signal autocorrelator.

3.1. Numerical results of $\overline{\binom{\nu_s(p)}{2}}$ *and* $\overline{\binom{\nu_s(p)}{3}}$ *determinations*

In ref. [4] an analytical method is given which permits the determination of $P_\nu(p)$ for a limited number (max. 7) of fission generations based on a cascade model with fissions only. A computer code of this model used as input the $P_{s\nu}$ and P_ν distributions for spontaneous and induced fissions, respectively valid for a particular sintered PuO_2 calibration sample (table 1). Figs. 6 and 7 give the numerical results of $\overline{\binom{\nu_s(p)}{2}}$ and $\overline{\binom{\nu_s(p)}{3}}$ as a function of p. As curve parameter serves the number of fission generations used for the determination of $P_{s\nu}(p)$. The case for infinite generations is the numerical result of eqs. (7) and (13) using the $\overline{\nu_{s(m)}}$ and $\overline{\nu_{(m)}}$ values ($1 \leq m \leq 3$) of the P_ν distribution of table 1.

3.2. Determination of the spontaneous fission neutron emission rate with an autocorrelator

For the assay of fissile material the autocorrelator [1] has found wide-spread application under the name shift register. The instrument permits to measure the total number of neutrons T and to determine from the measured data the number of neutron signal doublets referred to as R. The model used for T and R is based on a one neutron energy group approximation considering the spontaneous fission neutron emitter

Table 1
P_ν distribution for spontaneous ($P_{s\nu}$) and induced (Pu) fission (P_ν)

ν	$P_{s\nu}$	P_ν
0	0.0677	0.0045
1	0.2120	0.0460
2	0.3479	0.1984
3	0.2639	0.3628
4	0.0924	0.2817
5	0.0149	0.0928
6	0.0011	0.0130
7	0.0001	0.0008

as point source. It is according to ref. [1]:

$$T = \left[F_s \overline{\nu_{s(1)}(p)} + S_\alpha \overline{M(p)} \right] \bar{\epsilon} T_M, \tag{34}$$

and

$$R = \left[F_s \overline{\nu_{s(2)}(p)} + p S_\alpha \overline{\nu_{(2)}(p)} \right] \overline{\epsilon^2} T_M e^{-\lambda\theta}(1 - e^{-\lambda\tau}), \tag{35}$$

with
F_s = spontaneous fission neutron emission rate,
S_α = (α–n) neutron emission rate,
ϵ = probability for the detection of one neutron,
T_M = measurement time,
θ = predelay of the shift register circuit [1],
τ = observation interval of the shift register circuit,
λ = fundamental mode decay constant of thermal neutron detection assembly.

With eqs. (4) $\overline{\nu_{s(1)}(p)}$ can be replaced in eq. (34); we find:

$$T = F_s \overline{\nu_{s(1)}} M(p)[1 + \alpha] \bar{\epsilon} T_M, \tag{36}$$

with

$$\alpha = \frac{S_\alpha}{F_s \overline{\nu_{s(1)}}}. \tag{37}$$

In a similar way using eqs. (7) and (15) $\overline{\nu_{s(2)}(p)}$ and $\overline{\nu_{(2)}(p)}$ are substituted in eq. (35) leading to:

$$R = F_s M^2(p) \frac{\overline{\nu_{s(2)}}}{1 - p\bar{\nu}_{(1)}} [1 + p\beta] \overline{\epsilon^2} T_M f(\theta, \tau), \tag{38}$$

with

$$\beta = (1 + \alpha) \frac{\bar{\nu}_{s(1)} \bar{\nu}_{(2)}}{\bar{\nu}_{s(2)}} - \bar{\nu}_{(1)},$$

and

$$f(\theta, \tau) = e^{-\lambda\theta}(1 - e^{-\lambda\tau}). \tag{39}$$

Forming the ratio

$$r = \frac{R}{T} \frac{\bar{\epsilon} \overline{\nu_{s(1)}}(1 + \alpha)}{\overline{\epsilon^2} \overline{\nu_{s(2)}} f(\theta, \tau)} = \frac{(1 - p)(1 + \beta p)}{(1 - p\bar{\nu}_{(1)})^2}, \tag{40}$$

a function is obtained which depends on the one side on quantities defined by the measured data (R, T), instrumental data (ϵ, $f(\theta T)$) and on nuclear data; the other side of the equation is a function of the probability that a neutron generates an induced fission p and of nuclear data. With a measurement of R_0 and T_0 of a known standard sample (p_0, $F_{0s}\overline{\nu_{0s(1)}}$), the instrumental constants can be eliminated forming the ratio:

$$\frac{r}{r_0} = \frac{\left(1 - p_0\overline{\nu_{0(1)}}\right)^2}{\left(1 - p\overline{\nu_{(1)}}\right)^2} \frac{(1-p)(1+\beta p)}{(1-p_0)(1+\beta_0 p_0)}. \tag{41}$$

Eq. (41) is a quadratic equation in p of the unknown sample and leads to:

$$p = \frac{(2\rho\bar{\nu}_{(1)} + \beta - 1) - \sqrt{(2\rho\bar{\nu}_{(1)} + \beta - 1)^2 - 4(\rho - 1)\left(\rho\bar{\nu}_{(1)}^2 + \beta\right)}}{2\left(\rho\bar{\nu}_{(1)}^2 + \beta\right)}, \tag{42}$$

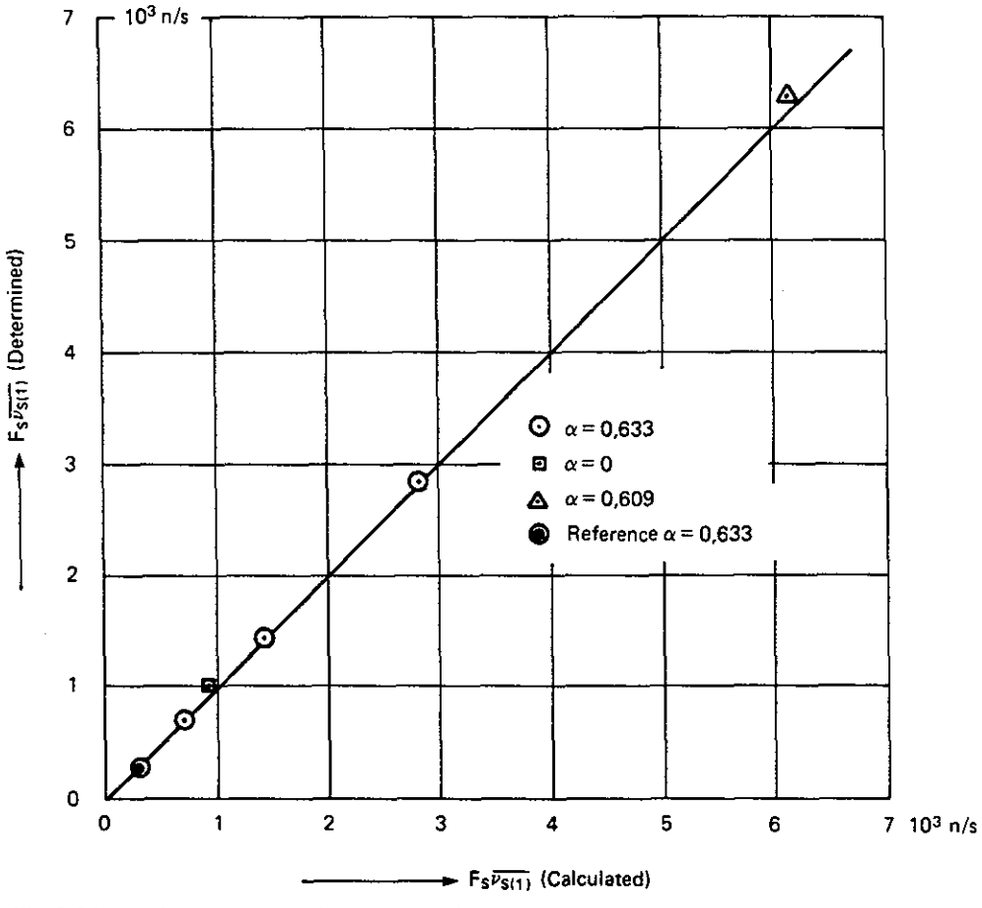

Fig. 8. Measured spontaneous fission neutron emission rate.

with

$$\rho = \frac{RT_0\bar{\epsilon}\overline{\epsilon_0^2\nu_{s(1)}}\,\overline{\nu_{0s(2)}}(1+\alpha)(1+p_0\beta_0)(1-p_0)}{R_0T\bar{\epsilon}_0\overline{\epsilon^2\nu_{0s(1)}}\,\overline{\nu_{s(2)}}(1+\alpha_0)(1-p\bar{\nu}_{0(1)})^2}. \tag{43}$$

Knowing p, the spontaneous fission neutron emission rate is obtained from the total number of counts relative to the emission rate of the standard sample

$$F_s\overline{\nu_{s(1)}} = F_{0s}\overline{\nu_{0s(1)}}\frac{TM_0(p)(1+\alpha_0)\bar{\epsilon}_0}{T_0M(p)(1+\alpha)\bar{\epsilon}}. \tag{44}$$

Eq. (43) was applied to the experimental data of a Pu and several PuO_2 samples given in ref. [7] in order to obtain p knowing p_0 of the standard sample 2. In the same reference are listed as well the required nuclear data. From the value of p the fission neutron emission rate is calculated by means of eq. (44). The results of this evaluation are given in fig. 8.

The emission rate calculated from the known isotopic weight of each sample is used as abscissa and as ordinate the result of eq. (44). The measured values of $F_s\bar{\nu}_{s(1)}$ have a statistical error of about 0.5%. All samples are accurate relative to the smallest sample within 0.6%. The three samples having the same α-ratio as the reference sample lie within 0.8% on the line with a slope of 45°. The metallic sample with an

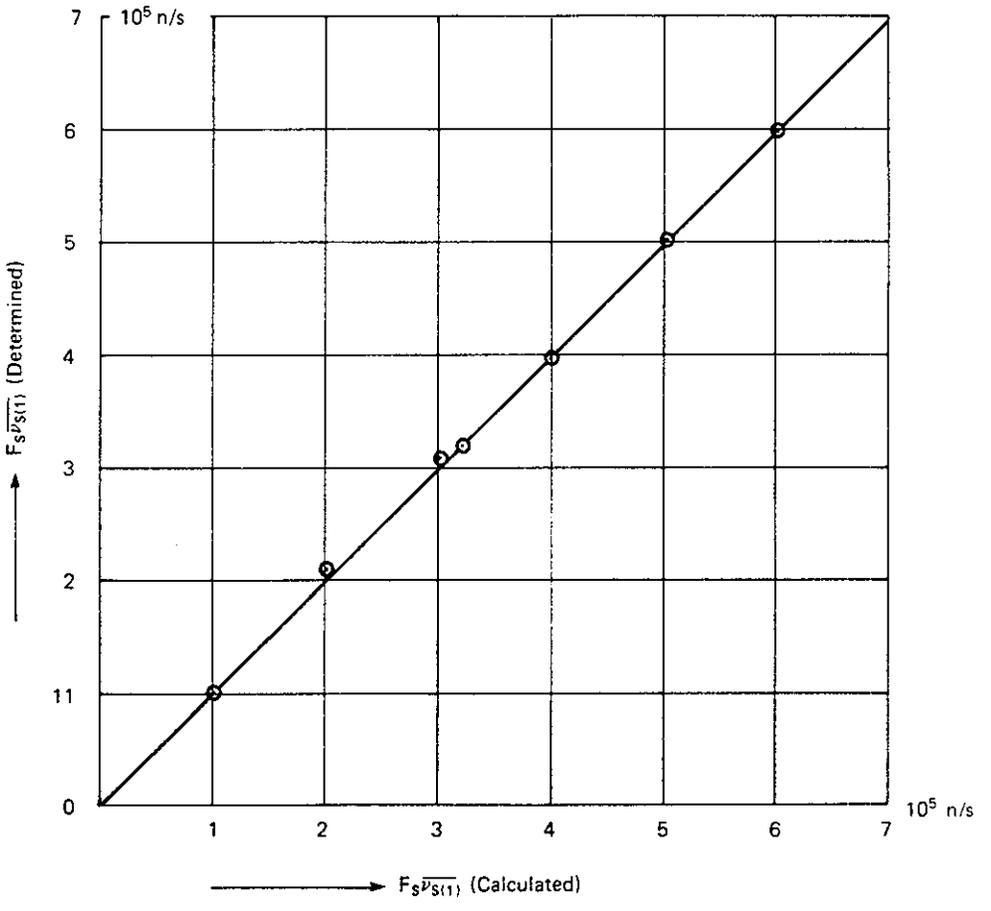

Fig. 9. Measured spontaneous fission neutron emission rate.

emission rate of 915 n/s is 11% and the largest PuO_2 sample with a different α-ratio is overestimated by about 2.8% by this approach. This discrepancy is believed to be due to the uncertainty of the α-ratio. The values derived for p lead to values which are about 10–15% smaller than those derived with the Monte Carlo code TIMOC.

Very satisfactory results were obtained analysing the measurement results of ref. [11]. In this experiment samples of 0.5–3 kg of PuO_2 were measured with the same isotopic composition. In the analysis the sample of 0.5 kg PuO_2 was used as the only reference and the spontaneous fission rate of the samples with 1, 1.5, 2, 2.5 and 3 kg PuO_2 were determined. Fig. 9 gives the experimentally determined spontaneous fission rate as a function of the spontaneous fission rate calculated from the isotopic composition. All samples except 2 (1.0 and 1.5 kg PuO_2) lie within 1% on the 45° straight line.

4. Conclusions

The derived equations for the effective number of emitted neutron multiplets $\overline{\binom{\nu_s(p)}{m}}$ of order m lead for the considered fission cascades to rather simple analytical expressions for $m \leqq 3$. Numerical checks show that the modelling of the $P_{s\nu}(p)$-distribution with 7 fission generations and the derivation of $\overline{\binom{\nu_s(p)}{m}}$ for $m \geqq 2$ from this distribution leads at $p > 0.04$ already to substantial deviations from the derived analytical expressions. The introduction of the formulas for $\overline{\binom{\nu(p)}{2}}$ ($m = 1, 2$) into the models used for the neutron signal autocorrelator, applied to far subcritical assemblies, leads to measured spontaneous fission rates with errors less than 1% in case that the calibration sample has the same α-ratio. Larger discrepancies occur for test samples with a different α-ratio.

Thanks are due to Dr. R. Dierckx for stimulating discussions, to Mrs. K. Caruso for performing the calculations and the preparation of the drawings. Acknowledged is further the typing of the manuscript by Mrs. G. Tenti and Mrs. M. van Andel.

References

[1] K. Böhnel, KFK-2203, Kernforschungszentrum Karlsruhe (1975).
[2] E.J. Dowdy, C.N. Henry, A.A. Robba and J.R. Pratt, Proc. Int. Symp. on Nuclear Material Safeguards, Vienna, SM-231/69 (IAEA, Vienna, 1978).
[3] R. Dierckx and W. Hage, Nucl. Sci. Eng. 85 (1983) 325.
[4] W. Hage and D.M. Cifarelli, Nucl. Sci. Eng. 89 (1985) 159.
[5] L. Bondar and B.G.R. Smith, Proc. Int. Symp. on Management of α-contaminated waste, Vienna, SM 246/50 (IAEA, Vienna, 1980).
[6] N. Ensslin, J. Stewart and J. Sapir, Nucl. Mater. Man. 8 (1979) 60.
[7] W. Hage, L. Anselmi and K. Caruso, EUR-9100EN, Commission of the European Communities, Joint Research Centre, Ispra (1983).
[8] K.M. Case, F. De Hoffmann and G. Placzek, Introduction to the theory of neutron diffusion, vol. 1, Los Alamos Scientific Laboratory, Los Alamos, New Mexico (June 1953).
[9] R.V. Meghreblian and D.K. Holmes, Reactor analysis (McGraw-Hill, New York, Toronto, London, 1960).
[10] G. Birkhoff and L. Bondar, EUR-6027e, Commission of the European Communities, Joint Research Centre, Ispra (1974).
[11] C. Beets et al., CEN/SCK Centre d'Etude de l'Energie Nucléaire Mol, Belgium, BLG 543 (Feb. 1981).

NUCLEAR SCIENCE AND ENGINEERING: 89, 159-176 (1985)

Correlation Analysis with Neutron Count Distributions in Randomly or Signal Triggered Time Intervals for Assay of Special Fissile Materials

W. Hage

Commission of the European Communities, Joint Research Centre
I-21020 Ispra (Varese), Italy

and

D. M. Cifarelli

Università L. Bocconi, Istituto di Metodi Quantitativi
I-20136 Milano, Italy

Received April 9, 1984
Accepted September 12, 1984

Abstract—*A mathematical model is derived for the probability distribution of neutron signal multiplets inside randomly and signal triggered time intervals for a generalized time response function of the neutron detector assembly. The theory is applied to assemblies with an exponential time decay of its neutron population. The probability distributions, their factorial moments, and moments are expressed as a function of the spontaneous fission rate, (α-n) reaction rate, neutron detection probability, probability that a neutron generates a fast fission, and nuclear data. Measurements with a plutonium sample are analyzed to check the derived algorithms for the factorial moments of the two probability distributions.*

Analyse de corrélation des distributions de comptes de neutrons dans des intervals de temps aléatoires ou déclenchés par les signaux pour l'essai des matériaux fissiles spéciaux

Résumé—*Un modèle mathématique est dérivé pour la distribution de probabilité des groupes de signaux neutroniques à l'intérieur d'intervals de temps. Ces intervals peuvent être déclenchés par des signaux neutroniques eux-mêmes ou par des signaux aléatoires. Le modèle est établi pour une réponse temporelle généralisée du détecteur neutronique. La théorie est appliquée pour des ensembles, pour lesquels la population neutronique décroit exponentiellement. Les distributions de probabilité, leurs moments factoriels et leurs moments dépendent du taux des fissions spontanées, du taux de la réaction (α-n), de la probabilité de détection neutronique, de la probabilité qu'un neutron donne lieu à une fission rapide et de données nucléaires. Des mesures faites sur un échantillon de Pu sont analysées pour tester les algorithmes dérivés pour les moments factoriels des distributions de probabilité.*

Korrelationsanalyse von Neutronenzählverteilungen in zufälligen oder signalgesteuerten Zeitintervallen für die Untersuchung von spaltbarem Material

Zusammenfassung—*Für eine allgemeine zeitliche Ausgleichsfunktion einer Neutronenzählanlage wurde ein mathematisches Modell für die Wahrscheinlichkeitsverteilung von Neutronensignalen innerhalb von zufälligen und signalgesteuerten Zeitintervallen hergeleitet. Die Theorie fand Anwendung für Zählanlagen mit einem exponentiellen Zerfallsgesetz der Neutronenbevölkerung. Die Wahrscheinlichkeitsverteilungen, ihre faktoriellen Momente, und ihre Momente erscheinen als Funktion der Spontanspaltrate, der (α-n)-Reaktionsrate, der Wahrscheinlichkeit für die Registrierung eines Neutrons, der Wahrscheinlichkeit daß ein Neutron eine Schnellspaltung erzeugt und kernphysikalischen Daten. Zur Überprüfung ihrer Gültigkeit wurden die abgeleiteten Gleichungen zur Interpretation von Messergebnissen mit einer Pu-Probe herangezogen.*

I. INTRODUCTION

The nondestructive assay of fissile material is a necessary tool to follow the flow of fissile material in a nuclear fuel cycle. In this paper, an analysis method for a passive neutron assay technique is elaborated. It is based on the determination of the spontaneous fission neutron emission rate of plutonium isotopes with even mass numbers (^{238}Pu, ^{240}Pu, ^{242}Pu) as an indicator for the fissile mass. This mass determination requires knowledge of the isotopic composition of the fuel, and needs a treatment of the neutrons generated by (α-n) reactions on light target nuclei (present in PuO_2) due to the strong alpha activity of most plutonium isotopes. A separation of the measured neutron signals generated by spontaneous fission from those of (α-n) reactions is achieved with time correlation analysis of these signals.

In this technique the neutrons emitted by a test item are slowed down in a moderator, diffuse there as thermal neutrons, and are partially absorbed by neutron detectors incorporated in the moderator assembly. The neutrons absorbed in the detectors are transformed in real time into electric signals and amplified, shaped, and converted into a signal pulse train. Two methods are in use for the analysis of this pulse train—the shift register[1,2] and the variable deadtime counter.[3-5] Both instruments deliver two experimental quantities—the total count and the correlated count. This permits the determination of the spontaneous fission rate F_s and either the (α-n) reaction rate S_α or the probability p that a primary source neutron generates an induced fission. For the assay of bulky fuel material containing plutonium, three experimental data are desired for a pure experimental determination of F_s, S_α, and p. In alpha-contaminated waste, neutron multiplication is less important; however, neutron absorption in the waste material modifies the neutron detection probability ϵ of the moderator detector assembly. In such measurement conditions a three-parameter analysis is suitable for a determination of F_s, S_α, and ϵ. Such a three-parameter analysis is performed in Refs. 6, 7, and 8.

In this technique the neutron signal pulse train is fed via a derandomizer[9] into a computer and analyzed to give the number of events with the same number of signals inside an analysis time interval τ. Two types of such intervals are used. One is triggered by each signal giving trigger multiplets; the other is triggered randomly to obtain the background multiplets.

In Refs. 6, 7, and 8, each of the two probability distributions is used to obtain F_s, S_α, p, or ϵ from their respective frequency distributions. One disadvantage of this treatment is that the probability distributions of both types of multiplets are complex expressions of these unknowns.

This disadvantage is avoided in Ref. 10 where the probability distributions of both the trigger and background multiplets are used together to obtain the factorial moments of the probability distribution of the correlated multiplets. This treatment leads to simple expressions for F_s, S_α, p, and ϵ. This method, however, requires the measurement of both the respective frequency distributions.

We avoid this by deriving both the moments and the factorial moments of the corresponding probability distributions. These lead to simple analytical expressions for F_s, S_α, p, and ϵ, which are then applied to the interpretation of the frequency distribution of the measured trigger and background multiplets.

II. THEORY

Section II gives a detailed derivation of a theory for the determination of the probability $b_x(t-\tau,t,T_1,T_2)$ to have x signals inside a randomly triggered time interval $t-\tau,t$. The fission events have an inhomogeneous Poisson distribution over the time interval T_1,T_2 where $0 \le T_1 \le T_2 \le t$. Furthermore, differential equations are derived giving the factorial moments and the moments of the $b_x(t-\tau,t,T_1,T_2)$ distribution.

II.A. Probability $b_x(t-\tau,t,T_1,T_2)$

To obtain an analytical expression for $b_x(t-\tau, t,T_1,T_2)$, it is assumed that the fission bursts occurring in the time interval $T_1,T_2(T_1<T_2<t)$ have an inhomogeneous Poisson distribution and are generated by a spontaneous fission point source, whose fission rate $F_s(s)$ varies with time s.

During a single fission burst, ν spontaneous fission neutrons are emitted with the probability $P_{s\nu}$. These ν neutrons are slowed down in a moderator detector assembly, referred to as the detection head, and diffuse there as thermal neutrons. Of these ν-emitted neutrons, n ($\nu \ge n$) are absorbed inside the neutron detectors and transformed into electric signals with the probability $\epsilon^n(1-\epsilon)^{\nu-n}$ in $\binom{\nu}{n}$ distinct orderings; ϵ is then the probability for the detection of a neutron originating from a fission event.

Of these n-detected neutrons originating from the fission event at time ξ (Fig. 1), j fall into the interval $t-\tau,t$ with the probability $c(t,j,n,\xi)$. With these definitions the probability generating function $G_\xi(z)$ for the number of neutrons from a single burst of fission neutrons at time ξ with probability $P_{s\nu}$, that ν neutrons are emitted of which n are detected and j fall into the interval $t-\tau,t$ where $\nu \ge n \ge j \ge 0$, is

$$G_\xi(z)=\sum_{\nu=0}^{\infty}\sum_{n=0}^{\nu}\sum_{j=0}^{n} z^j P_{s\nu}\binom{\nu}{n}\epsilon^n(1-\epsilon)^{\nu-n}c(t,j,n,\xi)\ . \tag{1}$$

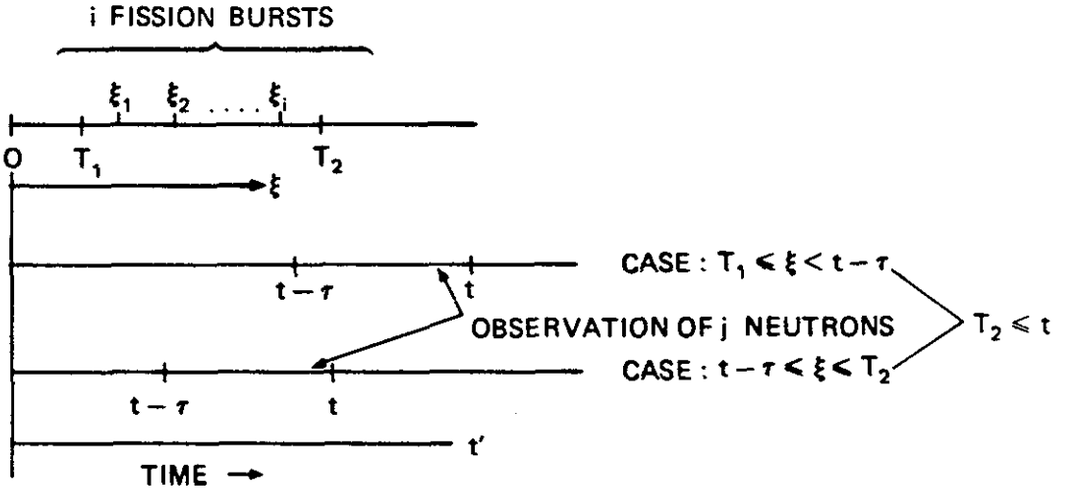

Fig. 1. Time diagram of fission bursts in $T_1 \le \xi \le T_2$ and observation of detected neutrons in $t-\tau \le t' \le t$.

If the neutron population originating from a single neutron burst decays in time according to the fundamental mode decay constant $1/\lambda$ of the detection head, then $c(t,j,n,\xi)$ is given by

$$c(t,j,n,\xi) = \binom{n}{j}\left\{\int_{max(\xi,t-\tau)}^{t} \exp[-\lambda(t'-\xi)]\lambda\,dt'\right\}^{j} \times\left\{1-\int_{max(\xi,t-\tau)}^{t} \exp[-\lambda(t'-\xi)]\lambda\,dt'\right\}^{n-j} . \tag{2}$$

The probability for detection of n neutrons from ν-emitted ones is

$$e_s(n) = \epsilon^n \sum_{\nu=n}^{\infty} P_{s\nu}\binom{\nu}{n}(1-\epsilon)^{\nu-n} . \tag{3}$$

The probability generating function $G_\xi(z)$ can then be written as

$$G_\xi(z) = \sum_{n=0}^{\infty}\sum_{j=0}^{n} z^j e_s(n)c(t,j,n,\xi) = \sum_{j=0}^{\infty} z^j \sum_{n=j}^{\infty} e_s(n)c(t,j,n,\xi) . \tag{4}$$

For $z=0$

$$G_\xi(0) = \sum_{n=0}^{\infty} e_s(n)c(t,o,n,\xi) , \tag{5}$$

which is the probability that from n-detected neutrons from a fission burst at ξ, none fall into the interval $t-\tau, t$.

The probability generating function $\pi[z|\xi_1,\xi_2,\ldots,\xi_i,N(T_1,T_2)=i]$ to register j signals in the interval $t-\tau,t$ produced by i fission bursts at i different times $\xi_1,\xi_2,\ldots,\xi_i$ inside the interval T_1,T_2 is formed by the product of the individual generating functions because the fissions occur independently one from the other. It is

$$\pi[z|\xi_1,\xi_2,\ldots,\xi_i,N(T_1,T_2)=i] = G_{\xi_1}(z)G_{\xi_2}(z)G_{\xi_3}(z)\ldots G_{\xi_i}(z) \tag{6}$$

and

$$\pi[z|\xi_1,\xi_2,\ldots,\xi_i,N(T_1,T_2)=i] = \sum_{n_1=0}^{\infty} e_s(n_1)\sum_{j_1=0}^{n_1} c(t,j_1,n_1,\xi_1)z^{j_1} \times \sum_{n_2=0}^{\infty} e_s(n_2)\sum_{j_2=0}^{n_2} c(t,j_2,n_2,\xi_2)z^{j_2} \ldots \sum_{n_i=0}^{\infty} e_s(n_i)\sum_{j_i=0}^{n_i} c(t,j_i,n_i,\xi_i)z^{j_i} , \tag{7}$$

with $T_1 \le \xi_1 \le \xi_2,\ldots, \le \xi_i \le T_2$ and $i=1,2,3,\ldots$.

Let us consider the time $\xi_1,\xi_2,\xi_3,\ldots,\xi_i$ to be subordinated by the i fissions in the interval T_1,T_2, $N(T_1,T_2)=i$. It is known that these random variables are distributed according to the density[11]

$$\varphi_i(\xi_1,\xi_2,\ldots,\xi_i) = i!\,\frac{F_s(\xi_1)F_s(\xi_2),\ldots,F_s(\xi_i)}{\left[\int_{T_1}^{T_2} F_s(s)\,ds\right]^i} \qquad T_1 \le \xi_1 \le \xi_2 \ldots \le \xi_i \le T_2 . \tag{8}$$

The probability generating function of i fission bursts $\pi[z|\xi_1,\xi_2,\ldots,\xi_i,N(T_1,T_2)=i]$ is now multiplied with its density function $\varphi_i(\xi_1,\xi_2,\ldots,\xi_i)$ and

integrated over the respective time intervals: $T_1 \le \xi_1 \le \xi_2 \le \xi_3 \ldots \le \xi_{i-1} \le \xi_i \le T_2$. It is given by

$$\pi_i(z, T_1) = \pi[z|N(T_1, T_2) = i] \tag{9}$$

$$= \int_{T_1}^{T_2} d\xi_1 \int_{\xi_1}^{T_2} d\xi_2 \ldots \int_{\xi_{i-1}}^{T_2} d\xi_i \pi[z|\xi_1, \xi_2, \ldots, \xi_i, N(T_1, T_2) = i] \varphi_i(\xi_1, \xi_2, \ldots, \xi_i) \ . \tag{10}$$

With Eqs. (7) and (8), Eq. (10) becomes

$$\pi_i(z, T_1) = \frac{i!}{\left[\int_{T_1}^{T_2} F_s(s)\, ds\right]^i} \left[\sum_{n_1=0}^{\infty} e_s(n_1) \sum_{j_1=0}^{n_1} z^{j_1} \int_{T_1}^{T_2} F_s(\xi_1) c(t, j_1, n_1, \xi_1)\, d\xi_1 \right.$$
$$\times \sum_{n_2=0}^{\infty} e_s(n_2) \sum_{j_2=0}^{n_2} z^{j_2} \int_{\xi_1}^{T_2} F_s(\xi_2) c(t, j_2, n_2, \xi_2)\, d\xi_2$$
$$\vdots$$
$$\left. \times \sum_{n_i=0}^{\infty} e_s(n_i) \sum_{j_i=0}^{n_i} z^{j_i} \int_{\xi_{i-1}}^{T_2} F_s(\xi_i) c(t, j_i, n_i, \xi_i)\, d\xi_i \right] \ . \tag{11}$$

This can be rearranged as follows:

$$\pi_i(z, T_1) = \frac{i}{\left[\int_{T_1}^{T_2} F_s(s)\, ds\right]^i} \sum_{n_1=0}^{\infty} e_s(n_1) \sum_{j_1=0}^{n_1} z^{j_1} \int_{T_1}^{T_2} F_s(\xi_1) c(t, j_1, n_1, \xi_1)\, d\xi_1 \left[\int_{\xi_1}^{T_2} F_s(s)\, ds\right]^{i-1}$$

$$\times \left\{ \frac{(i-1)!}{\left[\int_{\xi_1}^{T_2} F_s(s)\, ds\right]^{i-1}} \left[\sum_{n_2=0}^{\infty} e_s(n_2) \sum_{j_2=0}^{n_2} z^{j_2} \int_{\xi_1}^{T_2} F_s(\xi_2) c(t, j_2, n_2, \xi_2)\, d\xi_2 \right.\right.$$
$$\vdots$$
$$\left.\left. \times \sum_{n_i=0}^{\infty} e_s(n_i) \sum_{j_i=0}^{n_i} z^{j_i} \int_{\xi_{i-1}}^{T_2} F_s(\xi_i) c(t, j_i, n_i, \xi_i)\, d\xi_i \right] \right\} \ . \tag{12}$$

The last part of Eq. (12) is $\pi_{i-1}(z, \xi_1)$; hence,

$$\pi_i(z, T_1) = \frac{i}{\left[\int_{T_1}^{T_2} F_s(s)\, ds\right]^i} \sum_{n_1=0}^{\infty} e_s(n_1) \sum_{j_1=0}^{n_1} z^{j_1} \int_{T_1}^{T_2} F_s(\xi_1) c(t, j_1, n_1, \xi_1) \left[\int_{\xi_1}^{T_2} F_s(s)\, ds\right]^{i-1} \pi_{i-1}(z, \xi_1)\, d\xi_1 \ , \tag{13}$$

with $\pi_0(z, T_1) = 1$.

The probability generating function $\pi_i(z, T_1)$ is now multiplied by the probability of i fissions inside T_1, T_2 and summed over $0 \le i \le \infty$. It is

$$\pi(z, T_1) = \sum_{i=1}^{\infty} \pi_i(z, T_1) \frac{\left[\int_{T_1}^{T_2} F_s(s)\, ds\right]^i}{i!} \exp\left[-\int_{T_1}^{T_2} F_s(s)\, ds\right] + \pi_0(z, T_1) \exp\left[-\int_{T_1}^{T_2} F_s(s)\, ds\right] \ . \tag{14}$$

With Eq. (13) this becomes

$$\pi(z, T_1) = \sum_{i=1}^{\infty} \exp\left[-\int_{T_1}^{T_2} F_s(s)\, ds\right] \sum_{n_1=0}^{\infty} e_s(n_1) \sum_{j_1=0}^{n_1} z^{j_1} \int_{T_1}^{T_2} \left\{ F_s(\xi_1) c(t, j_1, n_1, \xi_1) \right.$$
$$\left. \times \frac{\left[\int_{\xi_1}^{T_2} F_s(s)\, ds\right]^{i-1}}{(i-1)!} \pi_{i-1}(z, \xi_1) \right\} d\xi_1 + \pi_0(z, T_1) \exp\left[-\int_{T_1}^{T_2} F_s(s)\, ds\right] \ . \tag{15}$$

Expression (15) simplifies after summation over i to the following integral equation (putting $n_1 = n$; $j_1 = j$; $\xi_1 = \xi$):

$$\pi(z,T_1) = \exp\left[-\int_{T_1}^{T_2} F_s(s)\,ds\right]\sum_{n=0}^{\infty} e_s(n) \times \sum_{j=0}^{n} z^j \int_{T_1}^{T_2} F_s(\xi)c(t,j,n,\xi)\pi(z,\xi) \times \exp\left[\int_{\xi}^{T_2} F_s(s)\,ds\right] d\xi + \pi_0(z,T_1)\exp\left[-\int_{T_1}^{T_2} F_s(s)\,ds\right] . \quad (16)$$

Equation (16) is transformed into a differential equation after partial differentiation with respect to T_1:

$$\frac{\partial\pi(z,T_1)}{\partial T_1} = \pi(z,T_1)\left[1 - \sum_{n=0}^{\infty} e_s(n) \times \sum_{j=0}^{n} z^j c(t,j,n,T_1)\right]F_s(T_1) . \quad (17)$$

The term inside the brackets of Eq. (17) is simplified as follows:

$$\sum_{n=0}^{\infty} e_s(n)\sum_{j=0}^{n} z^j c(t,j,n,T_1) = e_s(0)c(t,0,0,T_1) + \sum_{n=1}^{\infty} e_s(n)\sum_{j=0}^{n} z^j c(t,j,n,T_1) . \quad (18)$$

Thus, with $c(t,0,0,T_1) = 1$,

$$e_s(0) = 1 - \sum_{n=1}^{\infty} e_s(n) ,$$

and using Eq. (18), Eq. (17) reduces to the following expression:

$$\frac{d\pi(z,T_1)}{dT_1} = \pi(z,T_1)F_s(T_1)\sum_{j=1}^{\infty}(1-z^j) \times \sum_{n=j}^{\infty} e_s(n)c(t,j,n,T_1) . \quad (19)$$

The solution of the differential equation for $0 \le T_1 \le T_2$ is given by

$$\pi(z,T_1) = \exp\left[\sum_{j=1}^{\infty}(z^j-1)\Lambda_j(t-\tau,t,T_1,T_2)\right] , \quad (20)$$

with

$$\Lambda_j(t-\tau,t,T_1,T_2) = \sum_{n=j}^{\infty} e_s(n)\int_{T_1}^{T_2} F_s(s)c(t,j,n,s)\,ds . \quad (21)$$

Here, $\pi(z,T_1)$ is the probability generating function of a generalized Poisson distribution with the parameters $\Lambda_1(t-\tau,t,T_1,T_2)$, $\Lambda_2(t-\tau,t,T_1,T_2)\ldots$. It is identical with the expression presented in Ref. 1 for the case where $T_1 = 0$ and $T_2 = t$ and a time-independent spontaneous fission source. This starts directly with a difference equation similar to Eq. (17) without using explicitly the properties of the Poisson distribution of the spontaneous fission events.

Using

$$b_x(t-\tau,t,T_1,T_2) = \frac{1}{x!}\left[\frac{d^x\pi(z,T_1)}{dz^x}\right]_{z=0} , \quad (22)$$

the probability distribution $b_x(t-\tau,t,T_1,T_2)$ is obtained via Eqs. (20) and (21); $\pi(z,T_1)$ corresponds to the random variable X defined by

$$X = X_1 + 2X_2 + 3X_3 + \ldots , \quad (23)$$

where the X_j $(j = 1,2,3,\ldots)$ are mutually independent random variables distributed according to Poisson statistics with parameter $\Lambda_j(t-\tau,t,T_1,T_2)$.

If

$$e_s(n) = 0 \quad \text{for } n \ge N+1 ,$$

then the exponent of Eq. (20) becomes a sum limited by N.

The corresponding probability distribution then satisfies (as demonstrated in Appendix A)

$$xb_x = \Lambda_1 b_{x-1} + 2\Lambda_2 b_{x-2} + \ldots N\Lambda_N b_{x-N} , \quad (24)$$

with the abbreviations

$$b_x = b_x(t-\tau,t,T_1,T_2)$$

and

$$\Lambda_j = \Lambda_j(t-\tau,t,T_1,T_2)$$

for $x \ge N$.

The initial conditions are

$$b_0 = \exp\left(-\sum_{j=1}^{N}\Lambda_j\right)$$

$$1b_1 = \Lambda_1 b_0$$

$$2b_2 = \Lambda_1 b_1 + 2\Lambda_2 b_0$$

$$3b_3 = \Lambda_1 b_2 + 2\Lambda_2 b_1 + 3\Lambda_3 b_0$$

$$\vdots$$

$$(N-1)b_{N-1} = \sum_{j=1}^{N-1} j\Lambda_j b_{N-1-j} . \quad (25)$$

Equation (24) was presented in Ref. 1 to describe spontaneous fissions as a homogeneous Poisson process.

If $\Lambda_j \ne 0$ for each $j \ge 1$, then it follows from Eqs. (20), (21), and (22) that

$$xb_x = \sum_{j=1}^{x} j\Lambda_j b_{x-j} \tag{26}$$

for $x \geq 1$ and

$$b_0 = \exp\left(-\sum_{j=1}^{\infty} \Lambda_j\right) . \tag{27}$$

The explicit solution for b_x for $1 \leq j \leq N$ is

$$b_x = b_0 \sum_{\substack{1i_1+2i_2+\ldots Ni_N=x \\ 0 \leq i_j < \infty}} \frac{\Lambda_1^{i_1}\Lambda_2^{i_2}\ldots\Lambda_N^{i_N}}{i_1!i_2!\ldots i_N!} . \tag{28}$$

In Ref. 12, expressions are given for b_x for $T_1 = 0$, $T_2 = t$, $t \to \infty$ with $\Lambda_1 \neq 0$, $\Lambda_2 \neq 0$, $\Lambda_j = 0$ for $j > 2$ and a homogeneous Poisson process. This special case is covered by Eq. (28).

The figures i_j and the corresponding index j of the Λ_j $(1 \leq j \leq N)$ in Eq. (28) have a specific physical meaning. The value i_j is the number of fission events that contributes j signals to the x signals present in the interval $t-\tau, t$. For example, with $x = 4$ we have

$$\begin{aligned}
&i_1 = 4 \quad \text{and} \quad i_2 = i_3 = i_4 = 0 \\
&2i_2 = 4 , \quad i_2 = 2 , \quad \text{and} \quad i_1 = i_3 = i_4 = 0 \\
&i_1 + 2i_2 = 4 , \quad i_1 = 2 , \quad i_2 = 1 , \quad \text{and} \quad i_3 = i_4 = 0 \\
&i_1 + 3i_3 = 4 , \quad i_1 = 1 , \quad i_3 = 1 , \quad \text{and} \quad i_2 = i_4 = 0 \\
&4i_4 = 4 , \quad i_4 = 1 , \quad \text{and} \quad i_1 = i_2 = i_3 = 0 .
\end{aligned}$$

This leads to

$$b_4 = b_0\left(\frac{\Lambda_1^4}{4!} + \frac{\Lambda_2^2}{2!} + \frac{\Lambda_2^1\Lambda_1^2}{1!2!} + \frac{\Lambda_1^1\Lambda_3^1}{1!1!} + \frac{\Lambda_4^1}{1!}\right) . \tag{29}$$

When there are only single neutrons $j = 1$, Eq. (28) is then the well-known Poisson distribution for a time-dependent source emitting one neutron per burst.

Equations (24), (27), and (28) give the probability for x neutron signals inside the interval $t-\tau, t$ generated by fission bursts distributed according to an inhomogeneous Poisson distribution in the interval T_1, T_2. The derivation of the expressions shows that the neutron signals can appear in a different time sequence than the respective fissions generating the neutrons; i.e., overlapping of fission neutron signals can occur.

II.B. Moments of the $b_x(t-\tau, t, T_1, T_2)$ Distribution

To simplify Eqs. (27) and (28), we use their moments. The factorial moment of order m of the $b_x(t-\tau, t, T_1, T_2)$ distribution is defined by

$$M_{b(m)} = \sum_{x=m}^{\infty} x(x-1)\ldots(x-m+1)b_x , \qquad m \geq 0 , \tag{30}$$

using the abbreviations

$$M_{b(m)} = M_{b(m)}(t-\tau, t, T_1, T_2)$$

and

$$b_x = b_x(t-\tau, t, T_1, T_2) .$$

To get an analytical expression for $M_{b(m)}$, a differential equation for b_x is derived first using Eqs. (19) and (22). This leads to the following system of differential equations:

$$\frac{\partial b_x}{\partial T_1} = b_x F_s(T_1) \sum_{j=1}^{\infty}\sum_{n=j}^{\infty} e_s(n)c(tj,n,T_1) - \sum_{j=1}^{x} b_{x-j}F_s(T_1)\sum_{n=j}^{\infty} e_s(n)c(t,j,n,T_1) . \tag{31}$$

Equation (31) is transformed into a system of differential equations for $M_{b(m)}$ by multiplying both sides with the polynomial

$$x_{(m)} = x(x-1)(x-2)\ldots(x-m+1) \tag{32}$$

and summing over x starting with $x = m$. It is then

$$\frac{\partial M_{b(m)}}{\partial T_1} = M_{b(m)}F_s(T_1)\sum_{j=1}^{\infty}\sum_{n=j}^{\infty} e_s(n)c(t,j,n,T_1) - \sum_{x=m}^{\infty}\sum_{j=1}^{x} x_{(m)}b_{x-j}F_s(T_1) \times \sum_{n=j}^{\infty} e_s(n)c(t,j,n,T_1) . \tag{33}$$

The order of summation of the second expression on the right side of Eq. (33) is now interchanged. First, it is summed over the index j and then over $q = x - j$.

$$\frac{\partial M_{b(m)}}{\partial T_1} = M_{b(m)}F_s(T_1)\sum_{j=1}^{\infty}\sum_{n=j}^{\infty} e_s(n)c(t,j,n,T_1) - \sum_{j=m}^{\infty}\sum_{q=0}^{\infty}(j+q)_{(m)}b_q F_s(T_1)\sum_{n=j}^{\infty} e_s(n)c(t,j,n,T_1) - \sum_{j=1}^{m-1}\sum_{q=m-j}^{\infty}(j+q)_{(m)}b_q F_s(T_1)\sum_{n=j}^{\infty} e_s(n)c(t,j,n,T_1) . \tag{34}$$

The polynomial $(j+q)_{(m)}$ in Eq. (34) is replaced by

$$(j+q)_{(m)} = \sum_{r=0}^{m}\binom{m}{r} j_{(m-r)}q_{(r)} . \tag{35}$$

Furthermore, the following relation is used:

$$\frac{\partial \Lambda_j}{\partial T_1} = -F_s(T_1)\sum_{n=j}^{\infty} e_s(n)c(t,j,n,T_1) . \tag{36}$$

Inserting Eqs. (35) and (36) in Eq. (34) yields the following differential equation:

$$\frac{\partial M_{b(m)}}{\partial T_1} = \sum_{r=0}^{m-1}\sum_{j=m-r}^{\infty}\binom{m}{r} j_{(m-r)}M_{b(r)}\frac{\partial \Lambda_j}{\partial T_1} . \tag{37}$$

The integration is performed directly in the limits $T_1^* \le T_1 \le T_2$.

For the solution of Eq. (37) an abbreviation is first introduced for a factorial moment $M^*_{b(k)}$ of order k defined by

$$M^*_{b(k)} = \sum_{j=k}^{\infty} j_{(k)} \int_{T_1^*}^{T_2} F_s(T_1) \sum_{n=j}^{\infty} e_s(n) c(t,j,n,T_1)\, dT_1 = \sum_{j=k}^{\infty} j_{(k)} \Lambda_j \tag{38}$$

for $k \ge 1$, and using the abbreviation $\Lambda_j = \Lambda_j(t-\tau, t, T_1^*, T_2)$. Equation (38) is uniquely defined by the characteristics of the source, the detector assembly, and the time intervals of fission and neutron detection.

With this factorial moment of the physical properties, Eq. (37) becomes after integration

$$M_{b(m)} = \sum_{r=0}^{m-1} \binom{m}{r} \int_{T_1^*}^{T_2} M_{b(r)} \frac{\partial M^*_{b(m-r)}}{\partial T_1}\, dT_1 \tag{39}$$

for $m \ge 1$ and $M_{b(0)} = 1$.

From Eq. (39) the following solutions are obtained:

$$M_{b(1)} = M^*_{b(1)}$$

and

$$M_{b(2)} = M^*_{b(2)} + M^*_{b(1)} M_{b(1)}\ , \tag{40}$$

or in general

$$M_{b(m)} = \sum_{r=0}^{m-1} \binom{m-1}{r} M^*_{b(m-r)} M_{b(r)} \tag{41}$$

for $m \ge 1$.

A system of equations for the moments of the b_x distribution of order m is found following the same procedure as indicated for the factorial moments. It is

$$\mu_{bm}(t-\tau, t, T_1, T_2) = \sum_{x=1}^{\infty} x^m b_x(t-\tau, t, T_1, T_2)\ . \tag{42}$$

The corresponding differential equation is

$$\frac{\partial \mu_{bm}}{\partial T_1} = \sum_{j=1}^{\infty} \sum_{r=0}^{m-1} \binom{m}{r} j^{m-r} \mu_{br} \frac{\partial \Lambda_j}{\partial T_1}\ , \tag{43}$$

using $\mu_{bm} = \mu_{bm}(t-\tau, t, T_1, T_2)$ and $\Lambda_j = \Lambda_j(t-\tau, t, T_1, T_2)$.

Defining again a moment $\mu^*_{bk}(t-\tau, t, T_1, T_2)$ of order k characterizing the source and the neutron detection process,

$$\mu^*_{bk} = \sum_{j=1}^{\infty} j^k \int_{T_1^*}^{T_2} F_s(T_1) \sum_{n=j}^{\infty} e_s(n) c(t,j,n,T_1)\, dT_1 = \sum_{j=1}^{\infty} j^k \Lambda_j\ , \tag{44}$$

using the abbreviation $\mu^*_{bk} = \mu^*_{bk}(t-\tau, t, T_1, T_2)$, for $k \ge 1$, the following general expression for μ_{bm} is found:

$$\mu_{bm} = \sum_{r=0}^{m-1} \binom{m-1}{r} \mu^*_{b,m-r} \mu_{br} \tag{45}$$

for $m \ge 1$.

The great advantage in using the factorial moments or the moments of the b_x distribution [Eqs. (41) and (45)] for the interpretation of the measured moments $M_{b(m)}$ or μ_{bm} is that the source term $F_s(s)$ occurs as a linear term in $M^*_{b(k)}$ and μ^*_{bk}. This is not the case if the analytical expressions for b_x are directly used for the interpretation of the measured distribution.

III. APPLICATION OF THE THEORY TO SIGNAL MULTIPLETS WITH TIME CONSTANT SOURCES

In this section, the general theory is applied to specific cases in order to arrive at algorithms suitable for the interpretation of specific neutron correlator devices. Considered are correlator devices based on the measurement of the number of signals existing inside fixed time intervals τ. The intervals are triggered either randomly or by each neutron signal.[1,2,6-10] The quantities obtained experimentally are the background multiplets $B_x(\tau)$ and the trigger multiplets $N_x(\tau)$ $(x = 1,2,3,\dots)$, respectively, defined by[10]

$B_x(\tau)$ = number of events with x signals inside k randomly triggered inspection intervals τ

$N_x(\tau)$ = number of events with x signals inside the inspection intervals of duration τ obtained during an observation time T_M. Each neutron signal triggers an inspection time interval $\tau (T_M \gg \tau)$.

The frequency counterpart $b_x^+(\tau)$ to the probability $b_x(\tau)$ has x measured signals inside randomly triggered inspection intervals of duration τ and is

$$b_x^+(\tau) = \frac{B_x(\tau)}{k}\ . \tag{46}$$

Correspondingly, the frequency counterpart $n_x^+(\tau)$ to the probability $n_x(\tau)$, $n_x^+(\tau)$ has x signals inside signal triggered intervals of duration τ

$$n_x^+(\tau) = \frac{N_x(\tau)}{N_T}\ , \tag{47}$$

where N_T is the number of counts collected during the measurement time T_M, referred to as gross counts, and where

$$b_x(\tau) = b_x(t-\tau, t, T_1, T_2) \tag{48}$$

and

$$n_x(\tau) = n_x(t-\tau, t, T_1, T_2) \ , \tag{49}$$

for $T_1 = 0$, $T_2 = t$, $t \to \infty$.

The value of $n_x(\tau)$ is decomposed[10] into the probability $b_{x-y}(\tau)$ and the probability $r_y(\tau)$; $r_y(\tau)$ is the probability of having inside a triggered interval of duration τ, y other correlated signals, i.e., signals originating from the same fission event. Thus,[10]

$$n_x(\tau) = \sum_{y=0}^{x} r_y(\tau) b_{x-y}(\tau) \ , \tag{50}$$

with

$$\sum_{y=0}^{\infty} r_y(\tau) = 1 \ .$$

Reference 10 gives analytical expressions for $R_y(\tau) = r_y(\tau) N_T$ with neutron multiplication and $(\alpha\text{-}n)$ neutrons in the sample. The objective is therefore now limited to find, using the derived theory, analytical expressions for $b_x(\tau)$. Algorithms for $n_x(\tau)$ and the moments of $b_x(\tau)$ and $n_x(\tau)$ are then easily found.

III.A. Probability $b_x(\tau)$

The probability $b_x(\tau)$ is derived from the probability $b_x(t-\tau, t, T_1, T_2)$ for homogeneous Poisson distributed fission bursts in the interval $T_1 = 0$, $T_2 = t$ with neutron signals of these fissions registered in the interval $t-\tau, t$ with $t \to \infty$. Furthermore, it is assumed that the neutron population in the detection head generated by a neutron burst decays in time with its fundamental mode decay time $1/\lambda$. It then follows from Eqs. (2) and (21) for a time constant spontaneous fission rate F_s that for fission bursts in the interval $0 = T_1 \le \xi \le t-\tau$

$$\Lambda_j(t-\tau, t, 0, t-\tau) = F_s \sum_{n=j}^{\infty} e_s(n) \binom{n}{j} \sum_{k=0}^{n-j} \binom{n-j}{k} (-1)^k (e^{\lambda\tau} - 1)^{j+k} \times \frac{\exp[-\lambda\tau(j+k)] - \exp[-\lambda t(j+k)]}{\lambda(j+k)} \ , \tag{51}$$

and for fission bursts in the interval $t-\tau \le \xi \le t$

$$\Lambda_j(t-\tau, t, t-\tau, t) = F_s \sum_{n=j}^{\infty} e_s(n) \binom{n}{j} \sum_{k=0}^{j} \binom{j}{k} (-1)^k \times \frac{1 - \exp[-\lambda\tau(n+k-j)]}{\lambda(n+k-j)} \ . \tag{52}$$

With $t \to \infty$ the following expression for $\Lambda_j(\tau)$ is found:

$$\Lambda_j(\tau) = F_s \sum_{n=j}^{\infty} e_s(n) \binom{n}{j} \times \left(\sum_{k=0}^{n-j} \binom{n-j}{k} (-1)^k \left[\frac{1 - \exp(\lambda\tau)}{\lambda(j+k)} \right]^{j+k} + \sum_{k=0}^{j} \binom{j}{k} (-1)^k \times \frac{\{1 - \exp[-\lambda\tau(n+k-j)]\}}{\lambda(n+k-j)} \right) \ . \tag{53}$$

This leads, after rearranging the sums over k, to

$$\Lambda_j(\tau) = F_s \tau \sum_{n=j}^{\infty} e_s(n) w(n, j, \tau) \ , \tag{54}$$

with

$$w(n, j, \tau) = \binom{n}{j} \sum_{k=0}^{j-1} \binom{j-1}{k} (-1)^k \times \frac{\{1 - \exp[-\lambda\tau(n+k-j)]\}}{\lambda\tau(n+k-j)} \ . \tag{55}$$

Some expressions of $w(n, j, \tau)$ are listed in Appendix B.

The value of $\Lambda_j(\tau)$ is easily generalized for the case that the neutron source emits, in addition to the spontaneous fission neutrons, single neutrons generated by $(\alpha\text{-}n)$ reactions. If S_α is the time constant $(\alpha\text{-}n)$ neutron emission rate and ϵ_α the detection probability for neutrons from this process, then Eq. (54) for $\Lambda_j(\tau)$ reads

$$\Lambda_j(\tau) = S_\alpha \tau \epsilon_\alpha \delta_{1j} + F_s \tau \sum_{n=j}^{\infty} e_s(n) w(n, j, \tau) \ , \tag{56}$$

with $j \ge 1$, and

$$\delta_{1j} = \begin{cases} 1 & \text{for } j = 1 \\ 0 & \text{for } j \ne 1 \end{cases} \ ,$$

where δ_{1j} is the Kronecker symbol.

The effect of neutron multiplication inside the fissile source can be taken into account in Eq. (56) with the simplifications of Ref. 10. In this approximation each primary source neutron of a homogeneous Poisson distributed spontaneous fission burst triggers with a certain probability p [or p_α for $(\alpha\text{-}n)$ neutrons] a fission cascade of short duration compared to the decay time $1/\lambda$ of the neutron detection system. All neutrons escaping from this fission cascade enter into the detection head and give in this approximation a contribution to a new $P_\nu(p)$ distribution. This distribution is a complex function of the probability p that a fission neutron generates an induced fission and of the probabilities $P_{s\nu}$ and P_ν for the emission of ν neutrons due to spontaneous and induced fissions, respectively. With this model a term appears in Eq. (56) as

$$A = S_\alpha \tau (1 - p_\alpha) \epsilon_\alpha \delta_{1j} \ , \tag{57}$$

i.e., the number of neutrons from (α-n) reactions escaping with the probability $(1 - p_\alpha)$ an induced fission and being detected with the probability ϵ_α. The part $p_\alpha S_\alpha \tau$ triggers a fission cascade of which n neutrons are detected and j fall inside the interval τ. This contribution is

$$B = p_\alpha S_\alpha \tau \sum_{n=j}^{\infty} e_\alpha(n,p) w(n,j,\tau) \ , \tag{58}$$

with

$$e_\alpha(n,p) = \epsilon^n \sum_{\nu=n}^{\infty} \binom{\nu}{n} P_{\alpha\nu}(p) (1-\epsilon)^{\nu-n} \tag{59}$$

and

$$\sum_{\nu=0}^{\infty} P_{\alpha\nu}(p) = 1 \ ,$$

where $P_{\alpha\nu}(p)$ is the probability for the emission of ν neutrons per primary (α-n) source neutron, $(0 \le \nu < \infty)$ allowing fast neutron multiplication.[10]

The detection probability $e_\alpha(n,p)$ becomes a function of p via the $P_{\alpha\nu}(p)$ distribution of the fission cascade escape neutrons. For a fission cascade triggered by spontaneous fission events with a $P_{s\nu}$ distribution of the primary neutrons, a detection probability similar to Eq. (59) is found:

$$e_s(n,p) = \epsilon^n \sum_{\nu=n}^{\infty} \binom{\nu}{n} P_{s\nu}(p) (1-\epsilon)^{\nu-n} \tag{60}$$

and

$$\sum_{\nu=0}^{\infty} P_{s\nu}(p) = 1 \ ,$$

where $P_{s\nu}(p)$ is the probability for the emission of ν neutrons per spontaneous fission event with fast neutron multiplication. With fast neutron multiplication of the primary source neutrons, Eq. (56) then reads

$$\Lambda_j(\tau,p) = \tau \Big[S_\alpha (1 - p_\alpha) \epsilon_\alpha \delta_{1j} + p_\alpha S_\alpha \sum_{n=j}^{\infty} e_\alpha(n,p) w(n,j,\tau) + F_s \sum_{n=j}^{\infty} e_s(n,p) w(n,j,\tau) \Big] \tag{61}$$

for $j \ge 1$.

The probability $b_x(\tau)$ is according to Eqs. (28) and (61), respectively, proportional to $b_0(\tau)$ and to a polynomial of the order x in F_s and S_α with coefficients depending on powers in ϵ and $\exp(-\lambda\tau)$. In extreme cases of $\lambda\tau$, the equation system is considerably simplified.

Consider first a detection head with a very long decay time $1/\lambda$ and a relatively short observation interval $\tau(\lambda\tau \ll 1)$. With these conditions, $\Lambda_1(\lambda\tau \ll 1)$ is identical to the average number of counts collected during τ. The $\Lambda_j(\lambda\tau \ll 1)$ values for $j > 1$ are zero. Thus, $b_x(\tau)$ follows with Eq. (28) in the limit $\lambda\tau \to 0$, a pure homogeneous Poisson distribution.

In the other extreme case $(\lambda\tau \gg 1)$, the decay time of the detection head $1/\lambda$ is very short with respect to τ. In the limit $\lambda\tau \to \infty$, it follows that

$$\Lambda_j(\lambda\tau \to \infty) = \tau [S_\alpha (1 - p_\alpha) \epsilon_\alpha \delta_{1j} + p_\alpha S_\alpha e_\alpha(j,p) + F_s e_s(j,p)] \ .$$

These $\Lambda_j(\tau)$ values lead to a $b_x(\tau)$ distribution, which is still a generalized Poisson distribution.

III.B. Factorial Moments $M_{b(m)}(\tau)$ and $M^*_{b(m)}(\tau)$

Factorial moments $M_{b(m)}(\tau)$ and $M^*_{b(m)}(\tau)$ are derived from moments $M_{b(m)}(t-\tau, t, T_1, T_2)$ and $M^*_{b(m)}(t-\tau, t, T_1, T_2)$ for homogeneous Poisson distributed fission bursts in the interval $T_1 = 0$ and $T_2 = t$. Signal detection occurs in the interval $t-\tau, t$ with $t \to \infty$. With these conditions and time-independent spontaneous fission and (α-n) reaction rates F_s and S_α, Eq. (38) reads

$$M^*_{b(m)}(\tau) = \sum_{j=m}^{\infty} j_{(m)} \Lambda_j(\tau) \tag{62}$$

for $m \ge 1$.

The value of $\Lambda_j(\tau)$ is defined in Eq. (54) leading to the following expression for a pure spontaneous fission neutron source with a spontaneous fission rate F_s:

$$M^*_{b(m)}(\tau) = F_s \tau \sum_{j=m}^{\infty} j_{(m)} \sum_{n=j}^{\infty} e_s(n) w(n,j,\tau) \tag{63}$$

for $m \ge 1$.

With neutron multiplication and (α-n) reactions inside the sample, the expression for $\Lambda_j(\tau,p)$ of Eq. (61) must be used in Eq. (62). It is then

$$M^*_{b(m)}(\tau) = \tau \Big[S_\alpha (1 - p_\alpha) \epsilon_\alpha \delta_{1m} + p_\alpha S_\alpha \sum_{j=m}^{\infty} j_{(m)} \sum_{n=j}^{\infty} e_\alpha(n,p) w(n,j,\tau) + F_s \sum_{j=m}^{\infty} j_{(m)} \sum_{n=j}^{\infty} e_s(n,p) w(n,j,\tau) \Big] \tag{64}$$

for $m \ge 1$.

With the relation (see Appendix B)

$$\sum_{j=m}^{\infty} j_{(m)} w(n,j,\tau) = n_{(m)} w(m,m,\tau) \ , \qquad (65)$$

Eq. (64) reads

$$M^*_{b(m)}(\tau) = \tau \Big[S_\alpha (1-p_\alpha)\epsilon_\alpha \delta_{1m} + p_\alpha S_\alpha \sum_{n=m}^{\infty} e_\alpha(n,p) n_{(m)} w(m,m,\tau) + F_s \sum_{n=m}^{\infty} e_s(n,p) n_{(m)} w(m,m,\tau) \Big] \ . \qquad (66)$$

It is

$$\sum_{n=m}^{\infty} e_\alpha(n,p) n_{(m)} = \sum_{n=m}^{\infty} \sum_{\nu=n}^{\infty} P_{\alpha\nu}(p) \binom{\nu}{n} \epsilon^n (1-\epsilon)^{\nu-n} n_{(m)} = \epsilon^m \sum_{\nu=m}^{\infty} \nu_{(m)} P_{\alpha\nu}(p) = \epsilon^m \overline{\nu_{\alpha(m)}(p)} \ . \qquad (67)$$

In Eq. (67), $\overline{\nu_{\alpha(m)}(p)}$ is the effective factorial moment of the $P_{\alpha\nu}(p)$ distribution. Similarly, it follows that

$$\sum_{n=m}^{\infty} e_s(n,p) n_{(m)} = \epsilon^m \overline{\nu_{s(m)}(p)} \ , \qquad (68)$$

where $\overline{\nu_{s(m)}(p)}$ is the effective factorial moment of the $P_{s\nu}(p)$ distribution. Using Eqs. (67) and (68), Eq. (66) becomes

$$M^*_{b(m)}(\tau) = \tau \{ S_\alpha (1-p_\alpha)\epsilon_\alpha \delta_{1m} + [p_\alpha S_\alpha \overline{\nu_{\alpha(m)}(p)} + F_s \overline{\nu_{s(m)}(p)}] \epsilon^m w(m,m,\tau) \} \qquad (69)$$

for $m \geq 1$.

For $\overline{\nu_{\alpha(1)}(p)}$ and $\overline{\nu_{s(1)}(p)}$ exist the explicit expressions[10]

$$\overline{\nu_{\alpha(1)}(p)} = \frac{\bar{\nu}_{I\alpha}(1-p)}{1-p\bar{\nu}_I} = \sum_{\nu=1}^{\infty} P_{\alpha\nu}(p)\nu \qquad (70)$$

and

$$\overline{\nu_{s(1)}(p)} = \frac{\bar{\nu}_s(1-p)}{1-p\bar{\nu}_I} = \sum_{\nu=1}^{\infty} P_{\alpha\nu}(p)\nu \ , \qquad (71)$$

where

$\bar{\nu}_I$ = average number of emitted neutrons per induced fission event caused by neutrons with a fission neutron spectrum

$\bar{\nu}_{I\alpha}$ = average number of emitted neutrons per induced fission event caused by neutrons with an (α-n) neutron spectrum

$\bar{\nu}_s$ = average number of emitted neutrons per spontaneous fission event.

The factorial moment $M_{b(m)}(\tau)$ of order m of the measured distribution is obtained from Eq. (41) with fission bursts in the interval $0 = T_1 \leq \xi \leq T_2 = t$ and with $t \to \infty$. It is

$$M_{b(m)}(\tau) = \sum_{r=0}^{m-1} \binom{m-1}{r} M^*_{b(m-r)}(\tau) M_{b(r)}(\tau) \qquad (72)$$

for $m \geq 1$.

The analytical expressions for the moments of the $b_x(\tau)$ distribution are obtained as well directly from

$$M_{b(m)}(\tau) = \sum_{x=m}^{\infty} x_{(m)} b_x(\tau) \ , \qquad (73)$$

using Eq. (24) or (26) and Eq. (61).

The factorial moment $M^*_{b(1)}(\tau)$ gives with Eq. (69) the obvious expression for the gross counts collected during the interval τ. The factorial moment $M_{b(2)}(\tau)$ depends on $M^*_{b(2)}(\tau)$, $M^*_{b(1)}(\tau)$, and $M_{b(1)}(\tau)$. The measurement of this moment is known as the enhanced variance method[12] or the reduced variance method.[13] Reference 13 gives an analytical expression for this analysis method including an approximation for a fixed counter dead time. Without this approximation Ref. 13 gives the same results as Eqs. (69) and (72).

The moments $\mu^*_{bm}(\tau)$ and $\mu_{bm}(\tau)$ are obtained from Eqs. (44) and (45), respectively, for fission bursts in the interval $0 \leq T_1 \leq \xi \leq T_2 = t$ with $\lim t \to \infty$.

For a source with neutron multiplication and primary neutrons due to the spontaneous fission and (α-n) reactions, $\mu_{bm}(\tau)$ is given by

$$\mu^*_{bm}(\tau) = \sum_{j=1}^{\infty} j^m \Lambda_j(\tau) = \tau \Big[S_\alpha (1-p_\alpha)\epsilon_\alpha \delta_{1m} + p_\alpha S_\alpha \sum_{n=1}^{\infty} \sum_{n=j}^{\infty} j^m e_\alpha(n,p) w(n,j,\tau) + F_s \sum_{n=1}^{\infty} \sum_{n=j}^{\infty} j^m e_s(n,p) w(n,j,\tau) \Big] \qquad (74)$$

for $m \geq 1$.

After some algebraic operations it follows with Eqs. (55), (59), and (60) that

$$\mu^{*}_{bm}(\tau) = \tau\Bigg[S_\alpha(1-p_\alpha)\epsilon_\alpha\delta_{1m} + p_\alpha S_\alpha \sum_{q=1}^{m} \epsilon^q \frac{\overline{\nu_{\alpha q}(p)}}{q!} w(q,q,\tau) \times \sum_{n=1}^{q}\binom{q}{n}(-1)^{q-n}n^m + F_s \sum_{q=1}^{m} \epsilon^q \frac{\overline{\nu_{sq}(p)}}{q!} w(q,q,\tau) \times \sum_{n=1}^{q}\binom{q}{n}(-1)^{q-n}n^m\Bigg] \quad (75)$$

for $m \geq 1$.

The determination of $\mu_{bm}(\tau)$ is analogous to that of $M_{b(m)}(\tau)$.

Equation (75) is much more complicated than Eq. (69); therefore, an interpretation of the experimental data in the form of the moments $\mu_{bm}(\tau)$ is less advisable.

The analytical expressions found for the probability distribution $b_x(\tau)$ to have x signal events inside randomly triggered time intervals are rather complex expressions of S_α, F_s, ϵ, and p. A determination of these parameters from a measured distribution leads to rather extensive numerical efforts.[6-8] This is avoided by forming factorial moments of the $b_x(\tau)$ distribution. These lead to the simplest expressions for a practical data reduction. The $P_\nu(p)$ distribution does not appear explicitly, but its factorial moments do. These are calculated with the PENU code[14] for up to seven fission events. Recently, analytical expressions for these factorial moments have been derived[15,16] in a fast fission approximation.

III.C. Probability $n_x(\tau)$

The probability to find x signals inside a signal-triggered interval of duration τ is $n_x(\tau)$. According to Eq. (50), it is expressed as a product of $b_{x-y}(\tau)$ to have $(x-y)$ uncorrelated neutron signals inside randomly triggered time intervals and the probability $r_y(\tau)$ to have y correlated signals inside τ; i.e., these y signals are generated by the same fission burst. This latter quantity is taken from Ref. 10 and is reported without derivation. It is

$$r_y(\tau) = \frac{T_M}{N_T}\Bigg\{S_\alpha(1-p_\alpha)\epsilon_\alpha\delta_{0\alpha} + f^y(T,\tau)\sum_{n=y+1}^{\infty}[p_\alpha S_\alpha e_\alpha(n,p) + F_s e_s(n,p)] \times \sum_{k=1}^{n-y}\binom{n-k}{y}[1-f(T,\tau)]^{n-y-k}\Bigg\}, \quad (76)$$

with

$$N_T = M_{b(1)}(\tau)\frac{T_M}{\tau}$$

$$\delta_{0y} = \begin{cases} 1 & \text{for } y=0 \\ 0 & \text{for } y\neq 0 \end{cases}$$

$$f(T,\tau) = \exp(-\lambda T)[1-\exp(-\lambda\tau)] \quad \text{for } y \geq 0\ , \quad (77)$$

and where

T = delay time between signal trigger and initiation of inspection interval

T_M = total measurement time.

Equation (76) is valid for a point source with $(\alpha$-$n)$ and spontaneous fission primary neutrons, and fast neutron multiplication generating the neutron signal pulse train. It is considered that the first arriving signal triggers with a delay T the inspection interval τ. The number of signals y arriving in the inspection interval τ, being correlated with the trigger signal, determines the order of the multiplet $R_y(\tau)$ or the probability for its occurrence $r_y(\tau)$.

The probability $n_x(\tau)$ is defined by Eq. (50) and the expressions for $b_x(\tau)$ [Eq. (28)] and $r_y(\tau)$ [Eq. (76)]. As $\lambda\tau \to 0$, the distribution of the probability $n_x(\tau)$ approaches a homogeneous Poisson distribution. It is

$$r_0(\lambda\tau\to 0) = \frac{T_M}{N_T}[S_\alpha(1-p_\alpha)\epsilon_\alpha + p_\alpha S_\alpha\overline{\nu_{\alpha(1)}(p)} + F_s\overline{\nu_{s(1)}(p)}] \quad (78)$$

$$r_y(\lambda\tau\to 0) = 0 \quad \text{for } y>0$$

and

$$n_x(\lambda\tau\to 0) = r_0(\lambda\tau\to 0)b_x(\lambda\tau\to 0)\ . \quad (79)$$

A direct interpretation of the measured $n_x(\tau)$ distribution requires extensive computations, due to the complex expressions for $b_x(\tau)$ [Eq. (28)] and $r_y(\tau)$ [Eq. (76)].

III.D. Factorial Moments $M_{n(m)}(\tau)$ and $M^{*}_{n(m)}(\tau)$

The factorial moment of the $n_x(\tau)$ distribution of order m is defined by

$$M_{n(m)}(\tau) = \sum_{x=m}^{\infty} x(x-1)\ldots(x-m+1)n_x(\tau) = \sum_{x=m}^{\infty} x_{(m)}n_x(\tau) \quad (80)$$

for $m \geq 1$.

Replacing $n_x(\tau)$ in Eq. (80) with Eq. (50), the following general expression for the factorial moment of order m is found:

$$M_{n(m)}(\tau) = \sum_{q=0}^{m} \binom{m}{q} M^*_{n(q)}(\tau) M_{b(m-q)}(\tau) \ , \quad (81)$$

with

$$M^*_{n(q)}(\tau) = \sum_{x=q}^{\infty} x_{(q)} r_x(\tau) \quad (82)$$

$$M^*_{n(0)}(\tau) = 1$$

and $m \geq 1$.

The factorial moment $M^*_{n(q)}(\tau)$ is expressed as a function of the characteristics of the source, the neutron detection head, and the signal recording system.

With Eq. (76) it follows from Eq. (82), after some algebraic operations, that

$$M^*_{n(q)}(\tau) = \frac{\tau}{M_{b(1)}(\tau)} \left\{ S_\alpha (1 - p_\alpha) \epsilon_\alpha \delta_{0q} + \frac{\epsilon^{q+1}}{q+1} f^q(T,\tau) \times [p_\alpha S_\alpha \overline{\nu_{\alpha(q+1)}(p)} + F_s \overline{\nu_{s(q+1)}(p)}] \right\} \quad (83)$$

for $q \geq 0$. With Eq. (83) and the factorial moments $M^*_{b(m)}(\tau)$ and $M_{b(m-q)}(\tau)$ of the $b_{(m-q)}(\tau)$ distribution given in Eqs. (69) and (72), respectively, the factorial moment of the $n_x(\tau)$ distribution is completely defined.

It is not necessary that the moments $M_{b(m-q)}(\tau)$ are known by measurement. They can be expressed by combinations of factorial moments of the probability for trigger and background multiplets of lower order. Using Eq. (72) for $m = 2$, an expression for $M_{b(2)}(\tau)$ as a function of $M^*_{b(2)}(\tau)$ and $M_{b(1)}(\tau)$ is obtained. Replacing in this expression $M^*_{b(2)}(\tau)$ using Eq. (69) for $m = 2$ and Eq. (83) with $q = 1$, the following expression is found:

$$M_{b(2)}(\tau) = 2M_{b(1)}(\tau) M^*_{n(1)}(\tau) \frac{w(2,2,\tau)}{f(T,\tau)} + M^2_{b(1)}(\tau) \ . \quad (84)$$

In a similar way follows that

$$M_{b(3)}(\tau) = 3M_{b(1)}(\tau) M^*_{n(2)}(\tau) \frac{w(3,3,\tau)}{f^2(T,\tau)} + M^3_{b(1)}(\tau) + 3M^2_{b(1)}(\tau) 2M^*_{n(1)}(\tau) \frac{w(2,2,\tau)}{f(T,\tau)} \ . \quad (85)$$

The equations for the trigger multiplets and their factorial moments are derived for inspection intervals, being triggered by the first arriving signal of the part of the pulse train under investigation. The signals forming the multiplets normally arrive later than the trigger signal (Fig. 2). This, however, is not always the case. In some multiplet analyzers[17] the signal trigger of the inspection interval occurs with a delay T after the signal has left the inspection interval. In this case signals that have arrived earlier than the trigger signal but are still inside τ form the multiplet.

IV. VERIFICATION OF THE THEORY BY AN EXPERIMENT

The theory derived for the factorial moments of the probabilities $b_x(\tau)$ and $n_x(\tau)$ was tested with a metallic plutonium reference sample of 8.45 g. This permitted a test of the theory for a time-independent spontaneous fission rate in the absence of $(\alpha\text{-}n)$ reactions. This sample was measured inside a hollow cylindrical detection head with a polyethylene moderator and thirty-two 100-cm-long ^{3}He proportional counters. Four counters were connected to an amplifier discriminator chain to reduce dead-time losses. The

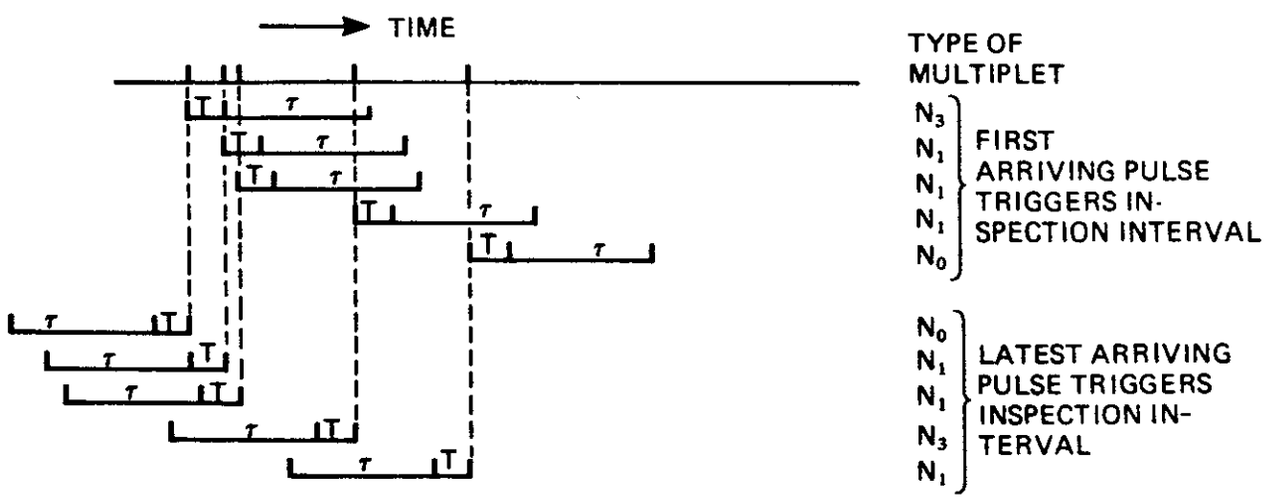

Fig. 2. Trigger multiplet types.

resulting pulse train of the eight channels was fed into a computer programmed to measure trigger and background multiplets.[6-8] Each signal from the amplifier chain triggered with a predelay of 6.4-μs three time channels ($\tau_1 = 25.6$ μs, $\tau_2 = 51.2$ μs, $\tau_3 = 102.4$ μs) to obtain three trigger multiplets for each order x. The background multiplets were obtained from periodically triggered not overlapping inspection intervals τ_1, τ_2, and τ_3. The obtained frequencies $b_x^+(\tau)$ and $n_x^+(\tau)$ and their respective standard deviations from the mean obtained during eight runs each with a measurement time of 8 min are given in Tables I and II (Ref. 18), respectively, for $x \leq 5$.

IV.A. Factorial Moments of the Probabilities $b_x(\tau)$

The factorial moments of the $b_x(\tau)$ distribution are then used to obtain an expression for $M^*_{b(2)}(\tau)$ and $M^*_{b(3)}(\tau)$ as a function of the measured quantities $M_{b(m)}(\tau)$ $(m = 1,2,3)$. It is

$$M^*_{b(2)}(\tau) = M_{b(2)}(\tau) - M^2_{b(1)}(\tau) \tag{86}$$

and

$$M^*_{b(3)}(\tau) = M_{b(3)}(\tau) - 2M^*_{b(2)}(\tau)M_{b(1)}(\tau) - M^*_{b(1)}(\tau)M_{b(2)}(\tau) \ . \tag{87}$$

The value of $M^*_{b(m)}(\tau)$ is from Eq. (69), a function of the source, detector, and signal register data. Using Eq. (69), for $m = 1$, 2, 3 and assuming for the measured plutonium sample $S_\alpha = 0$, the following ratio $\beta(p)$ is obtained[10]:

$$\beta(p) = \frac{3\overline{\nu_{s(2)}(p)}^2}{2\overline{\nu_{s(1)}(p)}\,\overline{\nu_{s(3)}(p)}} = \frac{3[M^*_{b(2)}(\tau)]^2 w(3,3,\tau)}{2M^*_{b(1)}(\tau)M^*_{b(3)}(\tau)w^2(2,2,\tau)} \ . \tag{88}$$

This ratio is a function of the probability p that a neutron generates an induced fission and of nuclear data. The value p is found by interpolation using the tabulated values of $\overline{\nu_{s(m)}(p)}$ given in Ref. 10 and the numerical values of $M^*_{b(m)}(\tau)$ defined by the factorial moments of the $b_x^+(\tau)$ distribution. These tables for $\overline{\nu_{s(m)}(p)}$ are obtained from the PENU code,[14] which

TABLE I

Frequency Distribution of Signals $b_x^+(\tau)$ Inside Randomly Triggered Intervals (Mean Values of Eight Runs)

	Interval Length					
	$\tau = 25.6$ μs		$\tau = 51.2$ μs		$\tau = 102.4$ μs	
x	$b_x^+(\tau)$	$\sigma[b_x^+(\tau)]$	$b_x^+(\tau)$	$\sigma[b_x^+(\tau)]$	$b_x^+(\tau)$	$\sigma[b_x^+(\tau)]$
0	9.9374×10^{-1}	2.0×10^{-5}	9.8798×10^{-1}	2.9×10^{-5}	9.7722×10^{-1}	5.3×10^{-5}
1	5.9134×10^{-3}	1.63×10^{-5}	1.0888×10^{-2}	3.7×10^{-5}	1.9503×10^{-2}	6.7×10^{-5}
2	3.2762×10^{-4}	1.7×10^{-6}	1.0417×10^{-3}	1.0×10^{-5}	2.9136×10^{-3}	1.7×10^{-5}
3	1.4703×10^{-5}	7.5×10^{-7}	7.8695×10^{-5}	2.9×10^{-6}	3.2868×10^{-4}	6.4×10^{-6}
4	5.2053×10^{-7}	1.5×10^{-7}	5.2736×10^{-6}	7.4×10^{-7}	3.1462×10^{-5}	2.9×10^{-6}
5	---	---	3.0724×10^{-7}	2.1×10^{-7}	3.3938×10^{-6}	7.4×10^{-7}

TABLE II

Frequency Distribution of Signals $n_x^+(\tau)$ Inside Signal Triggered Intervals (Mean Values of Eight Runs)

	Interval Length					
	$\tau = 25.6$ μs		$\tau = 51.2$ μs		$\tau = 102.4$ μs	
x	$n_x^+(\tau)$	$\sigma[n_x^+(\tau)]$	$n_x^+(\tau)$	$\sigma[n_x^+(\tau)]$	$n_x^+(\tau)$	$\sigma[n_x^+(\tau)]$
0	9.1033×10^{-1}	8.7×10^{-4}	8.6005×10^{-1}	9.9×10^{-4}	8.0983×10^{-1}	6.9×10^{-4}
1	8.4492×10^{-2}	9.4×10^{-4}	1.2693×10^{-1}	8.5×10^{-4}	1.6512×10^{-1}	5.3×10^{-4}
2	4.9677×10^{-3}	2.2×10^{-4}	1.2007×10^{-2}	3.2×10^{-4}	2.2186×10^{-2}	4.5×10^{-4}
3	2.1866×10^{-4}	6.1×10^{-5}	9.8487×10^{-4}	9.1×10^{-5}	2.3925×10^{-3}	5.4×10^{-4}
4	1.3545×10^{-5}	7.4×10^{-6}	4.9340×10^{-5}	1.8×10^{-5}	2.3511×10^{-4}	1.0×10^{-4}
5	1.5467×10^{-5}	---	7.7293×10^{-6}	5.9×10^{-9}	1.5469×10^{-5}	9.8×10^{-6}

calculates for specified p values the $P_\nu(p)$ distribution and the respective factorial moments. This code requires as input the P_ν distribution of the primary source neutrons and the P_ν distribution of the neutrons generated by induced fission events. From the ratio of $M^*_{b(2)}(\tau)$ and $M^*_{b(1)}(\tau)$, it follows that the probability for the detection of a neutron in the detection head is

$$\epsilon \simeq \frac{M^*_{b(2)}(\tau)}{M^*_{b(1)}(\tau)} \frac{\overline{\nu_{s(1)}(p)}}{\overline{\nu_{s(2)}(p)}\, w(2,2,\tau)} \quad . \tag{89}$$

The spontaneous fission neutron emission rate $\bar{\nu}_s F_s$ is finally derived from the gross counts $M_{b(1)}(\tau) = M^*_{b(1)}(\tau)$:

$$\bar{\nu}_s F_s \simeq \bar{\nu}_s \frac{M^*_{b(1)}(\tau)}{\epsilon \overline{\nu_{s(1)}(p)} \tau} \quad . \tag{90}$$

Table III summarizes the mean values of p, ϵ, and $\bar{\nu}_s F_s$ and the respective standard deviations of the mean. The obtained results agree with the reference data of the plutonium foil using a ^{240}Pu spontaneous fission half-life of 1.15×10^{11} yr given in Ref. 19. For the analysis of the measured data, the same $P_\nu(p)$ distribution as in Ref. 10 was used leading to a $\bar{\nu}_I$ for induced fission of 3.07.

It appears that the method tends to overestimate p and to underestimate ϵ leading to a slight overestimation of $\bar{\nu}_s F_s$. Calculating [using TIMOC (Ref. 20)] the fission probabilities for each individual isotope present in the plutonium sample, another P_ν distribution for induced fission is obtained applying the Terrel formula.[21] In the latter case a $\bar{\nu}_I$ value for induced fission of 3.25 instead of 3.07 is determined. This P_ν distribution leads after application of the code PENU to a new $P_\nu(p)$ distribution and to different numerical values of its factorial moments $\overline{\nu_{s(m)}(p)}$.

The resulting p (Ref. 22) (Table IV) is closer to the TIMOC p value and is less dependent on the size of the inspection interval τ. The obtained spontaneous fission rates $\bar{\nu}_s F_s$ do not increase significantly. The given errors are the standard deviations of the mean determined from the eight individually analyzed experimental runs.

IV.B. Factorial Moments of the Probability $n_x(\tau)$

Here the factorial moments of the $n_x(\tau)$ distribution are used to obtain an expression for $M^*_{n(0)}(\tau)$, $M^*_{n(1)}(\tau)$, and $M^*_{n(2)}(\tau)$ as a function of the measured quantities $M_{n(0)}(\tau)$, $M_{n(1)}(\tau)$, and $M_{n(2)}(\tau)$. With Eq. (81) it is

$$M^*_{n(1)}(\tau) = M_{n(1)}(\tau) - M_{b(1)}(\tau) \tag{91}$$

and

$$M^*_{n(2)}(\tau) = M_{n(2)}(\tau) - M_{b(2)}(\tau) - 2M^*_{n(1)}(\tau) M_{b(1)}(\tau) \quad . \tag{92}$$

Substituting for $M_{b(2)}(\tau)$ using Eq. (84), it follows that

TABLE III

Mean Values Obtained from Eight Runs Using Background Multiplets Only [$\bar{\nu}_I = 3.07$ (Ref. 10)]

	From Experiment			Reference Data	
	Interval Length				
	$\tau = 25.6\ \mu$s	$\tau = 51.2\ \mu$s	$\tau = 102.4\ \mu$s		Remarks
p	$(1.64 \pm 0.17) \times 10^{-2}$	$(1.38 \pm 0.13) \times 10^{-2}$	$(1.29 \pm 0.12) \times 10^{-2}$	1.070×10^{-2}	TIMOC (Ref. 17)
ϵ	0.260 ± 0.003	0.266 ± 0.002	0.267 ± 0.002	0.270 ± 0.001	Ref. 10
$\bar{\nu}_s F_s$ (1/s)	939 ± 6	943 ± 6	942 ± 6	916 ± 24	

TABLE IV

Mean Values Obtained from Eight Runs Using Background Multiplets Only ($\bar{\nu}_I = 3.25$ from TIMOC)

	Interval Length		
	$\tau = 25.6\ \mu$s	$\tau = 51.2\ \mu$s	$\tau = 102.4\ \mu$s
p	$(1.20 \pm 0.17) \times 10^{-2}$	$(1.34 \pm 0.13) \times 10^{-2}$	$(1.22 \pm 0.12) \times 10^{-2}$
$\bar{\nu}_s F_s$ (1/s)	945 ± 6	948 ± 6	946 ± 6

$$M^*_{n(2)}(\tau) = M_{n(2)}(\tau) - M^2_{b(1)}(\tau) - 2M^*_{n(1)}(\tau)M_{b(1)}(\tau) \times \left[1 + \frac{w(2,2,\tau)}{f(T,\tau)}\right] . \quad (93)$$

The values of $M^*_{n(1)}(\tau)$ and $M^*_{n(2)}(\tau)$ are numerically defined via Eqs. (91), (92), and (93) and are empirically determined.

The ratio $\beta(p)$ follows from Eq. (83) for $M^*_{n(q)}(\tau)$ with $q = 0,1,2$. It is

$$\beta(p) = \frac{3\overline{\nu_{s(2)}(p)}^2}{2\overline{\nu_{s(1)}(p)}\,\overline{\nu_{s(3)}(p)}} = \frac{2[M^*_{n(1)}(\tau)]^2}{M^*_{n(0)}(\tau)M^*_{n(2)}(\tau)} . \quad (94)$$

This ratio is again only a function of p. Using Eq. (94) and knowing the numerical values $M^*_{n(0)}(\tau)$, $M^*_{n(1)}(\tau)$, and $M^*_{n(2)}(\tau)$, p is obtained by interpolation from the factorial moments $\overline{\nu_{s(m)}(p)}$ $(m = 1,2,3)$. The neutron detection probability ϵ is determined by the ratio $M^*_{n(1)}(\tau)$ to $M^*_{n(0)}(\tau)$. It is

$$\epsilon = \frac{M^*_{n(1)}(\tau)}{M^*_{n(0)}(\tau)} \frac{2\overline{\nu_{s(1)}(p)}}{\overline{\nu_{s(2)}(p)}f(T,\tau)} . \quad (95)$$

Finally, the spontaneous fission neutron emission rate $\bar{\nu}_s F_s$ follows with known p and ϵ from Eq. (90).

The results obtained with the signal-triggered multiplets using a P_ν distribution for induced fission corresponding to $\bar{\nu}_I = 3.07$ are summarized in Table V. This distribution leads to p values (Table V) depending on the size of the inspection intervals τ. The values for ϵ and $\bar{\nu}_s F_s$ remain inside the error limits for these quantities. It appears, however, that there exists again a tendency to overestimate the spontaneous fission neutron emission rate. This is increased if the P_ν distribution for induced fission corresponding to a $\bar{\nu}_I$ of 3.25 determined with TIMOC is taken (Table VI).

In Ref. 10 the same plutonium sample is investigated using both the trigger and background multiplets to obtain values of $\bar{\nu}_s F_s$ and p for each analysis interval τ. The values of $\bar{\nu}_s F_s$ obtained applying this method are, given their error limits, just below the values obtained analyzing separately either the background or the trigger multiplets. This small discrepancy of the experimental data could be caused by the assumption made in the theory that the time response function of the detection head is the fundamental mode decay constant. Deviations from a pure exponential function exist during the slowing down of the fast source neutrons in the detection head, and during the decay of the higher modes immediately after and during the slowing down.

V. CONCLUSIONS

General expressions were obtained for the probability distribution $b_x(t-\tau, t, T_1, T_2)$ to have x signals

TABLE V

Mean Values Obtained from Eight Runs Using Trigger Multiplets Only [$\bar{\nu}_I = 3.07$ (Ref. 10)]

	From Experiment			Reference Data	
	Interval Length				
	$\tau = 25.6\ \mu s$	$\tau = 51.2\ \mu s$	$\tau = 102.4\ \mu s$		Remarks
p	$(1.53 \pm 0.2) \times 10^{-2}$	$(1.38 \pm 0.07) \times 10^{-2}$	$(1.15 \pm 0.1) \times 10^{-2}$	1.070×10^{-2}	TIMOC (Ref. 17)
ϵ	0.267 ± 0.004	0.267 ± 0.001	0.269 ± 0.003	0.270 ± 0.001	Ref. 10
$\bar{\nu}_s F_s$ (1/s)	937 ± 10	940 ± 4	939 ± 5	916 ± 24	

TABLE VI

Mean Values Obtained from Eight Runs Using Trigger Multiplets Only ($\bar{\nu}_I = 3.25$ from TIMOC)

	Interval Length		
	$\tau = 25.6\ \mu s$	$\tau = 51.2\ \mu s$	$\tau = 102.4\ \mu s$
p	$(1.32 \pm 0.2) \times 10^{-2}$	$(1.29 \pm 0.07) \times 10^{-2}$	$(1.32 \pm 0.1) \times 10^{-2}$
$\bar{\nu}_s F_s$ (1/s)	936 ± 10	943 ± 4	945 ± 5

inside a randomly triggered interval due to inhomogeneous Poisson distributed fission bursts occurring in the interval T_1, T_2; $T_1 \le T_2 \le t$. The same applies for the moments and factorial moments. This generalized theory permits a general time dependence of the probability $c(t,j,n,\xi)$ that of n-detected neutrons generated by a fission burst at ξ, j fall into an interval $t-\tau, t$. The theory is applied to practical cases in which $c(t,j,n,\xi)$ is calculated assuming a fundamental mode decay of the neutron population in the detection head after an injected neutron burst.

Rather complex analytical expressions are obtained for the probability distribution of multiplets inside fixed observation intervals τ. These apply for intervals triggered randomly or by each signal event.

The probability for a background multiplet $b_x(\tau)$ of order x depends on a polynomial of the order x of the source terms for spontaneous fission and (α,n) neutron emission. The probability to find inside an observation interval x trigger multiplets depends on a polynomial of the order $(x+1)$ in F_s and S_α. In both cases this polynomial is multiplied with $b_0(\tau)$, an exponential function with a linear dependence on F_s and S_α in the exponent. The detection probability ϵ appears together with the probabilities $P_{\alpha\nu}(p)$ and $P_{s\nu}(p)$ inside complicated expressions for Λ_j, however, which also contain various powers of $\exp(-\lambda\tau)$. This problem is overcome by forming the factorial moments of the $b_x(\tau)$ and $n_x(\tau)$ probability distributions $M_{b(m)}(\tau)$ and $M_{n(m)}(\tau)$. The moments of the $b_x(\tau)$ distribution are more complicated than the corresponding factorial moments. All types of moments have in common that the source terms of the primary neutrons appear as a linear function. The factorial moments of order m for the $b_x(\tau)$ and $n_x(\tau)$ distributions are proportional to ϵ^m and ϵ^{m+1} and the $P_\nu(p)$ distribution enters in the form of its factorial moments $\overline{\nu_{(m)}}(p)$ and $\overline{\nu_{(m+1)}}(p)$, respectively. This considerably simplifies the numerical efforts for the analysis of experimental data.

The derived theory is tested experimentally. All results obtained for $\bar{\nu}_s F_s$, p, and ϵ are with their respective error margins inside the known values of the used plutonium calibration sample. The determined values of p are very sensitive to the P_ν distribution for induced fission. This is not the case for $\bullet$ and $\bar{\nu}_s F_s$. The numerical results show that the size of the inspection interval τ does not influence the values for the determined spontaneous fission neutron emission rate.

The choice of one inspection interval is sufficient for a data analysis at least in the low count rate range. At present the method is limited in its application to low neutron count rates in the absence of theoretical corrections for the dead-time losses of the neutron counters. Such corrections are of special importance for the probabilities with a higher number of signals inside the analysis interval.

APPENDIX A

In this Appendix, the validity of Eq. (24) and its compatibility with the probability generating function $\pi(z, T_1)$ of Eq. (20) for a generalized Poisson distribution with $j \le N$ are shown:

$$xb_x = \Lambda_1 b_{x-1} + 2\Lambda_2 b_{x-2} + \ldots N\Lambda_N b_{x-N} \qquad \text{(A.1)}$$

for $x \ge N$.

Multiplying both sides of Eq. (A.1) with z^{x-1} and summing the resulting expression over $N \le x \le \infty$, the following expression is obtained:

$$\sum_{x=N}^{\infty} z^{x-1} x b_x = \Lambda_1 \sum_{x=N}^{\infty} z^{x-1} b_{x-1} + 2\Lambda_2 \sum_{x=N}^{\infty} z^{x-1} b_{x-2} \ldots N\Lambda_N \sum_{x=N}^{\infty} z^{x-1} b_{x-N} \; . \qquad \text{(A.2)}$$

Equation (A.2) is written in the following form:

$$\frac{d}{dz} \sum_{x=N}^{\infty} z^x b_x = \Lambda_1 \left(\sum_{x=0}^{\infty} z^x b_x - \sum_{x=0}^{N-2} z^x b_x \right) + 2\Lambda_2 z \left(\sum_{x=0}^{\infty} z^x b_x - \sum_{x=0}^{N-3} z^x b_x \right) + N\Lambda_N z^{N-1} \sum_{x=0}^{\infty} z^x b_x \; . \qquad \text{(A.3)}$$

Putting

$$g(z) = \sum_{x=0}^{\infty} z^x b_x \; , \qquad \text{(A.4)}$$

it follows from Eqs. (A.3) and (A.4) that

$$\frac{d}{dz}\left[g(z) - \sum_{x=0}^{N-1} z^x b_x \right] = \Lambda_1 \left[g(z) - \sum_{x=0}^{N-2} z^x b_x \right] + 2\Lambda_2 z \left[g(z) - \sum_{x=0}^{N-3} z^x b_x \right] \ldots + N\Lambda_N z^{N-1} g(z) \qquad \text{(A.5)}$$

and

$$\frac{dg(z)}{dz} - \sum_{x=1}^{N-1} z^{x-1} x b_x = \sum_{j=1}^{N} j\Lambda_j z^{j-1} g(z) - \sum_{j=1}^{N-1} j\Lambda_j z^{j-1} \sum_{x=0}^{N-j-1} b_x z^x \; . \qquad \text{(A.6)}$$

With the initial conditions given in Eq. (25), the second terms of both sides of Eq. (A.6) are equal leading to the following differential equation for $g(z)$:

$$\frac{dg(z)}{dz} = \sum_{j=1}^{N} j\Lambda_j z^{j-1} g(z) \; . \qquad \text{(A.7)}$$

With the initial conditions of Eq. (25) for b_0, the solution of Eq. (A.7) is

$$g(z) = b_0 \exp\left(\sum_{j=1}^{N} \Lambda_j z^j\right) = \exp\left[\sum_{j=1}^{N} (z^j - 1)\Lambda_j\right] . \quad (A.8)$$

Equation (A.8) is identical to the probability generating function $\pi(z, T_1)$ [Eq. (20)] of a generalized Poisson distribution for $N \to \infty$.

APPENDIX B

In this section the first few analytical expressions of $w(n,j,\tau)$ for $1 \le n \le 4$ and $1 \le j \le n$ are summarized. According to Eq. (55) it is given by

$$w(n,j,\tau) = \binom{n}{j} \sum_{k=0}^{j-1} \binom{j-1}{k} (-1)^k \times \frac{1 - \exp[-\lambda\tau(n-j+k)]}{\lambda\tau(n-j+k)} . \quad (B.1)$$

From Eq. (B.1) follows

$$w(1,1,\tau) = 1 \quad (B.2)$$

$$w(2,1,\tau) = \binom{2}{1} \frac{1}{\lambda\tau} [1 - \exp(-\lambda\tau)] \quad (B.3)$$

$$w(3,1,\tau) = \binom{3}{1} \frac{1}{2\lambda\tau} [1 - \exp(-2\lambda\tau)] \quad (B.4)$$

$$w(4,1,\tau) = \binom{4}{1} \frac{1}{3\lambda\tau} [1 - \exp(-3\lambda\tau)] \quad (B.5)$$

$$w(2,2,\tau) = 1 - \frac{1}{\lambda\tau} [1 - \exp(-\lambda\tau)] \quad (B.6)$$

$$w(3,2,\tau) = \frac{3}{2\lambda\tau} [1 - 2\exp(-\lambda\tau) + \exp(-2\lambda\tau)] \quad (B.7)$$

$$w(4,2,\tau) = \frac{1}{\lambda\tau} [1 - 3\exp(-2\lambda\tau) + 2\exp(-3\lambda\tau)] \quad (B.8)$$

$$w(3,3,\tau) = 1 - \frac{1}{2\lambda\tau} [3 - 4\exp(-\lambda\tau) + \exp(-2\lambda\tau)] \quad (B.9)$$

$$w(4,3,\tau) = \frac{2}{3\lambda\tau} [2 - 6\exp(-\lambda\tau) + 6\exp(-2\lambda\tau) - 2\exp(-3\lambda\tau)] \quad (B.10)$$

$$w(4,4,\tau) = 1 - \frac{1}{6\lambda\tau} [11 - 18\exp(-\lambda\tau) + 9\exp(-2\lambda\tau) - 2\exp(-3\lambda\tau)] . \quad (B.11)$$

By means of the above equations, it is easily verified that the following relations hold for $1 \le n \le 4$:

$$\sum_{j=1}^{n} j_{(1)} w(n,j,\tau) = n_{(1)} w(1,1,\tau) , \quad (B.12)$$

$$\sum_{j=2}^{n} j_{(2)} w(n,j,\tau) = n_{(2)} w(2,2,\tau) , \quad (B.13)$$

and

$$\sum_{j=3}^{n} j_{(3)} w(n,j,\tau) = n_{(3)} w(3,3,\tau) . \quad (B.14)$$

In general it holds that

$$\sum_{j=k}^{n} j_{(k)} w(n,j,\tau) = n_{(k)} w(k,k,\tau) . \quad (B.15)$$

ACKNOWLEDGMENTS

Helpful discussions with L. Anselmi, N. T. Barrett, G. Birkhoff, L. Bondar, R. Dierckx, and A. Prosdocimi are gratefully acknowledged. Many thanks are due to K. Caruso for the execution of the numerical calculations and to S. Tenti and M. van Andel for typing the manuscript.

REFERENCES

1. K. BÖHNEL, "Die Plutoniumbestimmung in Kernbrennstoffen mit der Neutronen–Koinzidenzmethode," KFK-2203, Kernforschungszentrum Karlsruhe (1975).

2. N. ENSSLIN, M. L. EVANS, H. O. MENLOVE, and J. E. SWANSEN, *Nucl. Mater. Manage.*, **VII**, 43 (1978).

3. J. JACQUESSON, *Le Journal de Physique, Physique Appliquée, Suppl. au No. 6*, **24**, 112 (1963).

4. G. BIRKHOFF, L. BONDAR, J. LEY, R. BERG, R. SWENNEN, and G. BUSCA, "On the Determination of the ^{240}Pu in Solid Waste Containers by Spontaneous Fission Neutron Measurements, Application to Reprocessing Plant Waste," EUR-5158e, Commission of the European Communities, Joint Research Centre, Ispra (1974).

5. E. W. LEES and F. J. G. ROGERS, "Experimental and Theoretical Observations on the Use of the Euratom Variable Dead Time Neutron Counter for the Passive Assay of Plutonium," *Proc. Int. Symp. Nuclear Material Safeguards*, Vienna, October 2-6, 1978, SM 231/51, International Atomic Energy Agency, Vienna (1978).

6. L. BONDAR, "Time Correlation Analyser for Non-Destructive Plutonium Assay," *Proc. Int. Mtg. Monitoring of Plutonium Contaminated Waste*, Ispra, September 25-28, 1979, Commission of the European Communities, Ispra (1979).

7. L. BONDAR and B. G. R. SMITH, "Interpretation of Pu Waste Measurements by the Euratom Time Correlation

Analyser," *Proc. Int. Symp. Management of Alpha-Contaminated Waste*, Vienna, June 2-6, 1980, SM 246/50, International Atomic Energy Agency, Vienna (1980).

8. L. BONDAR, "Passive Neutron Assay," *Proc. Int. Symp. Recent Advances in Nuclear Material Safeguards*, Vienna, November 8-12, 1982, SM 260/54, International Atomic Energy Agency, Vienna (1982).

9. L. STANCHI, "Preliminary Report on a Device for Acquisition of Neutrons of Spontaneous Fissions," *Proc. Int. Symp. Nuclear Electronics*, JRC Dubna USSR, Warsaw (1971).

10. R. DIERCKX and W. HAGE, *Nucl. Sci. Eng.*, **85**, 325 (1983).

11. I. V. BASAWA and B. L. S. PRAKASA RAO, *Inference for Stochastic Processes*, p. 103, Academic Press, Inc., New York (1980).

12. M. O. DEIGHTON, *Nucl. Instrum. Methods*, 165 (1979).

13. E. J. DOWDY, C. N. HENRY, A. A. ROBBA, and J. R. PRATT," New Neutron Correlation Measurement Techniques for Special Nuclear Material Assay and Accountability," *Proc. Int. Symp. Nuclear Material Safeguards*, Vienna, October 2-6, 1978, SM-231/69, International Atomic Energy Agency, Vienna (1978).

14. L. ANSELMI and W. HAGE, "PENU—A Computer Programme for the Calculation of the Neutron Multiplicity of Prompt Neutrons of a Fission Cascade," Commission of the European Communities, Ispra (1983) (Report in preparation).

15. K. BÖHNEL, "The Effect of Multiplication on Neutron Coincidence Measurements," *Nucl. Sci. Eng.* (to be published).

16. W. HAGE and D. M. CIFARELLI, "On the Factorial Moments of the Neutron Multiplicity Distribution of Fission Cascades," Commission of the European Communities, Joint Research Centre, Ispra (to be published).

17. J. E. SWANSEN, P. R. COLLINSWORTH, M. S. KRICK, and D. L. PETERSON, "Multiplicity Sorter for Shift Register Coincidence Electronics," LA 9221-MS UC 15, Los Alamos National Laboratory (1982).

18. L. BONDAR, Private Communication, Joint Research Centre, Ispra (1982).

19. C. BUDTZ-JØRGENSEN and H. H. KNITTER, *Nucl. Sci. Eng.*, **79**, 380 (1981).

20. R. JAARSMA and H. RIEF, "TIMOC-72 Code Manual," EUR-5016e, Commission of the European Communities, Joint Research Centre, Ispra (1973).

21. J. TERREL, *Phys. Rev.*, **108**, 3 (1957).

22. F. BOGGIANI and A. SALLUSTIO, Thesis, Centro Studi Nucleari Enrico Fermi, Milano (1983).

ESARDA

EUROPEAN SAFEGUARDS RESEARCH AND DEVELOPMENT ASSOCIATION

Reprinted from the Proceedings of the

9th ESARDA Symposium on Safeguards and Nuclear Material Management

London, U.K., 12-14 May 1987

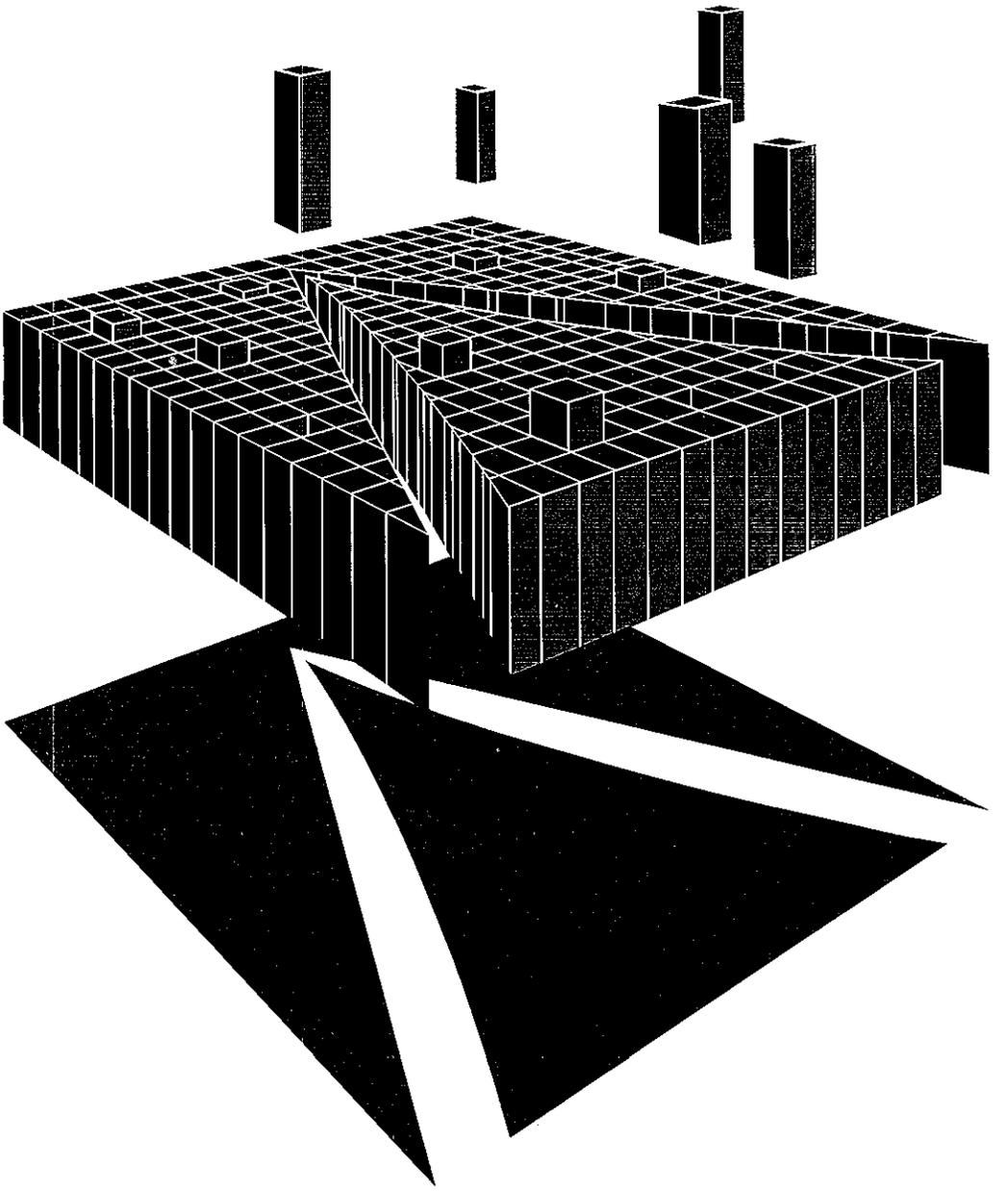

COMMISSION OF THE EUROPEAN COMMUNITIES

JOINT RESEARCH CENTRE

VERIFICATION OF THE INTERPRETATION MODELS OF THE NEUTRON AUTO-CORRELATOR WITH MONTE CARLO CALCULATIONS

F. Bevacqua, F.V. Frazzoli
Università degli Studi di Roma, La Sapienza
Facoltà di Ingegneria
Via A. Scarpa 14, 00161 Rome - Italy

W. Hage
Commission of the European Communities
Joint Research Centre - Ispra Establishment
21020 Ispra (Va) - Italy

9th ESARDA Symposium, London 1987

Abstract

For the interpretation of the experimental data obtained with the neutron signal auto-correlator, two methods were applied in order to obtain the Pu-240 equivalent mass of PuO_2 and MOX samples with known isotopic composition and weight. The assay results agree in most cases with the known data of the PuO_2 samples. Remarkable deviations were observed with MOX samples. Modifications of the existing model did not lead to an improvement of these results.

Introduction

The neutron correlation technique has found wide-spread application for the non-destructive assay of Pu containing fuel material. The present existing models[1,2] for the interpretation of measurement results obtained with the shift register take into account neutron multiplication. It is further assumed that the ratio (α-n) reaction rate to spontaneous fission neutron emission rate can be determined from the known isotopic composition. This model has been applied successfully to PuO_2 powder fuel[3,4] but showed rather large deviations assaying MOX fuel[3]. For this reason, two different approaches for the assay were tested[5].

In method A it is assumed that the fission probability p_α for neutrons originating from (α-n) reactions is different from the fission probability p of fission neutrons and that the ratio p/p_α can be determined with sufficient precision with neutron transport codes.

In method B the (α-n) reaction rate and the spontaneous fission rate are determined from the experimental data calculating the neutron multiplication factor M absolutely with the neutron transport Monte Carlo code TIMOC[6]. For both methods a well-characterized standard sample of similar type as the assay samples is required. Results of sensitivity calculations on the neutron multiplication factor are included for humidity and density effects of the test samples[5].

Theory

The basic equations of the interpretation models of the dead time corrected singlets T and correlated doublets R (usually referred to as "totals" T and "reals" R) were modified such that (α-n) neutrons have a different fission probability p_α as the fission neutrons. With these modifications it is:

$$T = \varepsilon T_M F_s \nu_{s(1)} M(1+\alpha\delta) \qquad (1)$$

$$R = \varepsilon^2 T_M f(\Theta,\tau) F_s \nu_{s(2)} M^2 [1+\beta(1+\alpha\gamma)(M-1)] \qquad (2)$$

with

$$M = \frac{1-p}{1-p\nu_{I(1)}}$$

$$\alpha = \frac{S_\alpha}{F_s \nu_{s(1)}}$$

$$\delta = \frac{1}{M}\,[1+\gamma(M-1)]$$

$$\gamma = \frac{p_\alpha}{p}$$

$$f(\Theta,\tau) = e^{-\lambda\Theta}(1-e^{-\lambda\tau})$$

$$\beta = \frac{\nu_{s(1)}\nu_{I(2)}}{\nu_{s(2)}(\nu_{I(1)}-1)}$$

The symbols used are:

- S_α = (α,n) neutron emission rate of test item,
- F_s = spontaneous fission rate of test item,
- p, p_α = probability that a neutron generates an induced fission event,
- M = neutron multiplication factor,
- T_M = measurement time,
- ε = probability for detection of a neutron,
- τ = observation interval,
- Θ = delay between trigger signal and start of observation interval τ,
- λ = fundamental mode decay constant of moderator-detector assembly,
- $P_{j\nu}(p)$ = probability for the emission of ν fast neutrons per prompt fission caused by a primary neutron generated by reaction j (j = α or I then (α,n) reaction or induced fission; j = s spontaneous fission),
- $\nu_{j(\mu)}$ = μ^{th} factorial moment of the $P_{j\nu}$ distribution,

$$\nu_{j(\mu)} = \sum_{\nu=\mu}^{\infty} \binom{\nu}{\mu} P_{j\nu}$$

Method A

In method A the two quantities T_1 and R_1 derived from the measurements of an unknown sample are used together with T_o and R_o of a reference sample to determine first the neutron multiplication factor M_1 of the unknown sample. Using Eqs.(1) and (2) for the reference sample (index o) and the test sample (index 1), the following equation for M_1 is obtained:

$$A_1 M_1^3 + M_1^2(1-A_1) - \rho_1 M_1(1+\alpha_1\gamma_1) + \rho_1\alpha_1(\gamma_1-1) \qquad (3)$$

with

$$\rho_1 = \frac{T_o R_1 \nu_{s(1)1} \nu_{s(2)o} M_o}{T_1 R_o \nu_{s(1)o} \nu_{s(2)1} (1+\alpha_o\delta_o)} [1+(M_o-1)A_o]$$

$$A_1 = \beta_1(1+\alpha_1\gamma_1)$$

$$\beta_1 = \frac{\nu_{s(1)1}\nu_{I(2)1}}{\nu_{s(2)1}(\nu_{I(1)1}-1)}$$

With $\gamma_1 = 1$ follows from Eq.(3) the well-known expression of refs.1 and 4.

Having determined M_1, the corresponding spontaneous fission rate F_{s1} is obtained applying Eq.(2) for the known and unknown sample. The correction factors for the "Totals" and "Reals" are:

$$\frac{T_1(M_1=1)}{T_1(M_1)} = C_T = \frac{1}{M_1(1+\alpha_1\delta_1)} \qquad (4)$$

and

$$\frac{R_1(M_1=1)}{R_1(M_1)} = C_R = \frac{1}{M_1^2[1+\beta_1(M_1-1)(1+\alpha_1\gamma_1)]} \qquad (5)$$

Method B

In method B Eqs.(1) and (2) are solved for the two unknowns F_{s1} and $S_{\alpha 1}$ knowing the neutron multiplication factor M_1 of the unknown sample and the data of the reference sample. For this purpose Eqs.(1) and (2) are written in the following form:

$$\frac{1}{\varepsilon} = \frac{1}{T}[F_s b_{11} + S_\alpha b_{12}] \qquad (6)$$

$$\frac{1}{\varepsilon^2 f(\theta\tau)} = \frac{1}{R}[F_s b_{21} + S_\alpha b_{22}] \qquad (7)$$

with

$$b_{11} = T_M M \nu_{s(1)}$$

$$b_{12} = T_M M \delta$$

$$b_{21} = T_M M^2 \nu_{s(2)}[1+\beta(M-1)]$$

$$b_{22} = T_M M^2 \nu_{I(2)} \frac{M-1}{\nu_{I(1)}-1} \cdot \gamma$$

Introducing the quantities r_1 and r_2 the detector head characteristics are eliminated with the data of the reference sample (index o)

$$r_1 = \frac{T_1}{T_o}[b_{110}F_{so} + b_{120}S_{\alpha o}] \qquad (8)$$

or

$$r_1 = b_{111}F_{s1} + b_{121}S_{\alpha 1} \qquad (9)$$

and

$$r_2 = \frac{R_1}{R_o}[b_{210}F_{so} + b_{220}S_{\alpha o}] \qquad (10)$$

or

$$r_2 = b_{211}F_{s1} + b_{221}S_{\alpha 1} \qquad (11)$$

Solving Eqs.(9) and (11) with respect to F_{s1}, the following relation is found:

$$F_{s1} = \frac{1}{\left[1-\beta_1(M_1-1)\left(\frac{\gamma_1}{\delta_1}-1\right)\right]T_M \nu_{s(2)1}} \cdot \left[\frac{r_2}{M_1^2} - \frac{r_1}{M_1}\frac{\beta_1\gamma_1}{\nu_{s(1)}\delta_1}(M_1-1)\right] \qquad (12)$$

This equation serves to determine the spontaneous fission rate of the unknown sample. It uses the measured T_o, T_1, R_o and R_1 values of the reference and test sample, respectively, via r_1 and r_2 defined in Eqs.(8) and (10). The constants b_{ij} (i=1,2 and j=1,2) are determined knowing the neutron multiplication factors of both the reference and test sample.

In the following the present analysis method of refs.1 and 4 will be confronted with procedure A and B[5].

Confrontation of the Various Methods

Experimental and nuclear data

For the verification of the different corrections applied to the balance equations for the "Totals" and "Reals", the experimental results of ref.3 were utilized. The updated sample weights and isotopic compositions are summarized in Tables 1 and 2, respectively. For this confrontation, two sample families were used, PuO_2 powder samples and mixed oxide samples with a strongly varying uranium content. The "Totals" T and "Reals" R corrected for dead time and background are listed in Table 3 for both sample assay families. Table 4 summarizes the nuclear constants. α is determined directly from the isotopic composition of the Pu. The γ-value has been determined with the TIMOC code[6] for the geometry of the samples and the HLNCC-II detector head. Its numerical value does not vary substantially for the PuO_2 powder samples. It increases, however, markedly with increasing isotopic abundance of U-238 in MOX samples. For the calculation of β an approximated procedure

TABLE 1 - Sample weights

Sample Nr.	$\frac{Pu}{Pu+U}$	Pu (metal) mass (g)	$M_{eD}(240)$ (g)	Sample type
XN 1097	1	2783.04	1063.17	PuO_2
XN 1062	1	2734.87	1041.62	PuO_2
XN 1059	1	2679.51	1041.65	PuO_2
XN 1123	1	2659.70	950.00	PuO_2
XN 1064	1	2536.71	972.86	PuO_2
XN 1025	1	2502.13	848.23	PuO_2
XN 1055	1	2106.69	821.44	PuO_2
XN 1066	1	1460.28	567.68	PuO_2
VO 2202	22.745	1337.29	273.92	MOX
VO 2212	26.745	979.94	206.30	MOX
VO 2027	16.633	669.39	170.94	MOX
VO 2030	16.633	562.39	143.61	MOX
VO 2067	4.613	247.13	49.76	MOX
VO 2066	4.613	109.76	22.10	MOX

TABLE 2 - Updated isotopic composition of PuO_2 and MOX samples

Sample Nr.	Updated isotopic composition W/W								Remarks
	Pu^{238}	Pu^{239}	Pu^{240}	Pu^{241}	Pu^{242}	U^{238}	U^{235}	Am^{241}	
XN 1097	1.490	59.191	24.987	9.042	5.290	-	-	3.401	
XN 1062	1.596	58.407	25.550	8.727	5.718	-	-	3.309	Refer.
XN 1059	1.596	58.407	25.550	8.727	5.718	-	-	3.309	
XN 1123	1.199	60.844	24.972	8.264	4.737	-	-	3.036	
XN 1064	1.596	58.407	25.550	8.727	5.718	-	-	3.309	
XN 1025	1.630	62.975	24.382	7.392	4.187	-	-	2.826	
XN 1055	1.588	58.282	25.551	8.836	5.740	-	-	3.235	
XN 1066	1.596	58.407	25.550	8.727	5.718	-	-	3.309	
VO 2202	0.135	77.991	19.083	2.147	0.643	99.514	0.486	1.456	Refer.
VO 2212	0.196	77.298	19.262	2.455	0.788	99.550	0.450	1.715	
VO 2027	0.401	72.111	21.710	4.068	1.701	99.441	0.559	1.245	
VO 2030	0.401	72.111	21.710	4.068	1.701	99.441	0.559	1.245	
VO 2067	0.129	78.524	18.758	1.950	0.639	99.396	0.602	1.542	
VO 2066	0.129	78.524	18.758	1.950	0.639	99.398	0.602	1.542	

TABLE 3 - Measurement data of UO_2 and MOX fuel samples corrected for dead time and background

Sample Nr.	Sample type	t(s)	T (c/s)	R (c/s)	$\sigma_{R/R}$	$\sigma_{T/T}$
XN 1097	PuO_2	600	403189	38779	0.005	0.0015
XN 1062	PuO_2	300	416741	40681	0.004	0.0015
XN 1059	PuO_2	600	408032	38961	0.005	0.0015
XN 1123	PuO_2	600	347349	33523	0.005	0.0017
XN 1064	PuO_2	600	384313	35984	0.005	0.0016
XN 1025	PuO_2	600	321159	33322	0.004	0.0017
XN 1055	PuO_2	600	323943	29629	0.005	0.0017
XN 1066	PuO_2	600	217725	18891	0.005	0.0021
VO 2202	MOX	400	93549	9193	0.012	0.0032
VO 2212	MOX	400	84201	6117	0.013	0.0034
VO 2027	MOX	400	59657	4450	0.013	0.0041
VO 2030	MOX	400	49690	3617	0.013	0.0044
VO 2067	MOX	400	5086	1341	0.012	0.014
VO 2066	MOX	300	6814	566	0.012	0.012

TABLE 4 - Nuclear constants of samples

Sample Nr.	α	γ	β	β_{TIMOC}	M_{TIMOC}	M_{EX}
XN 1097	1.0639	1.0126	2.1208	2.1222	1.508	1.1468
XN 1062	1.0698	1.0287	2.1209	2.1263	1.1499	1.1499
XN 1059	1.0698	1.0120	2.1209	2.1179	1.1461	1.1448
XN 1123	0.9657	1.0335	2.1217	2.1566	1.1538	1.1379
XN 1064	1.0698	1.0850	2.1209	2.1072	1.1278	1.1367
XN 1025	1.1470	1.0052	2.1196	2.1047	1.1387	1.1752
XN 1055	1.0545	1.0684	2.1209	2.1367	1.1240	1.1297
XN 1066	1.0639	1.0466	2.1209	2.1959	1.1162	1.1171
VO 2202	0.6463	1.1678	2.0405	2.0541	1.1033	1.1033
VO 2212	0.7107	1.1433	2.0559	2.0273	1.0896	1.0323
VO 2027	0.7342	1.2493	2.067	2.0525	1.0663	1.0409
VO 2030	0.7342	1.2493	2.0267	2.0553	1.0641	1.0352
VO 2067	0.6642	1.3481	1.9711	1.9821	1.0410	1.0770
VO 2066	0.6642	1.3761	1.9711	1.9992	1.0306	1.0588

has been set up. The values obtained agree very well for both sample families with those of TIMOC. A rather good agreement between the multiplication factor M determined with TIMOC and the value derived from the experimental data M_{ex}[1,4] was found for the PuO_2 powder samples excluding one case. A much less good agreement was found for the MOX samples. This discrepancy has not yet been identified and demands further investigations.

Assay results

For the assay results it was considered useful to present the measured mass of the Pu-240 equivalent as a function of its declared value m_{eD}. Having a perfectly characterized reference sample the measured values of the Pu-240 mass equivalent must lie on a straight line passing through 0 with an inclination of 45° (Fig. 1).

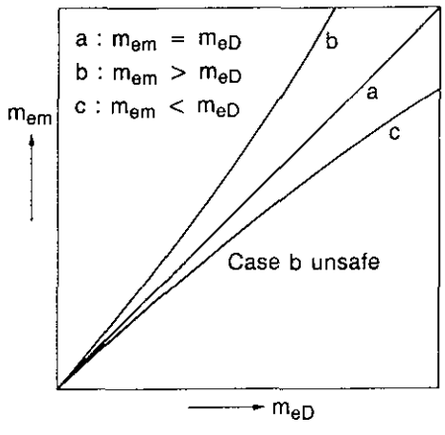

Fig. 1. Measured Pu-240 mass equivalent m_{em} as a function of declared value m_{eD}.

If the values are systematically above this line the measured mass equivalent is greater than its declared value and could be a warning for control authorities. In Fig. 2 are summarized the assay results of the PuO_2 powder samples for methods A and B. There has been no difference taking $p_\alpha = p$ or $p_\alpha \neq p$ in both methods. In method A the spread of the individual results is in the mean about ± 30 g and would be ± 15 g eliminating one outlying point at about 850 g. In this case the assay result of an inspection sample

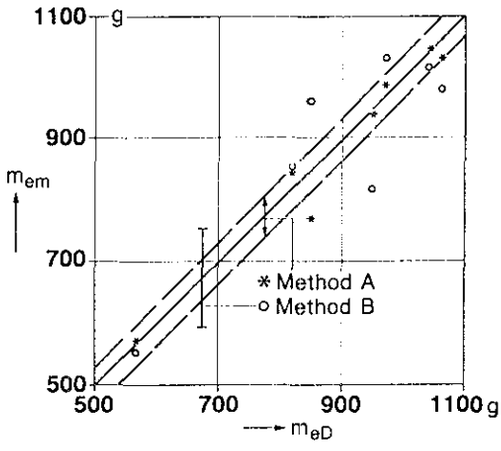

Fig. 2. Measured Pu-240 mass equivalent m_{em} as a function of declared value m_{eD} for PuO_2 samples.

size with 5420 g of Pu-240 equivalent would have a final error of +10 g. With method B, i.e. using not the measured multiplication factor M_1 but the TIMOC value, the assay result would lead to three times larger errors.

For MOX samples (Fig. 3) considerable deviations were observed. The modifications of the

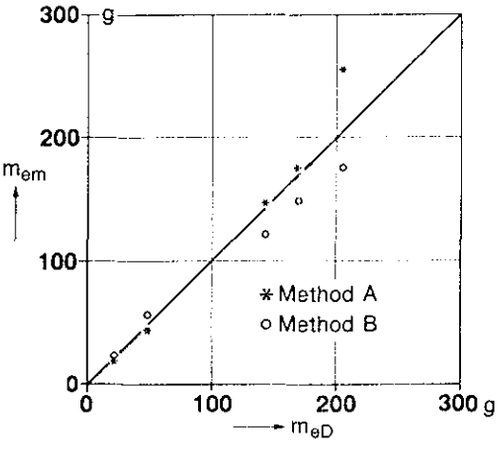

Fig. 3. Measured Pu-240 mass equivalent m_{em} as a function of declared value m_{eD} for MOX samples.

models have not led to satisfactory results even taking into account the marked variations of β and γ with the variation of the U-238 isotopic abundance. Fig. 4 gives the neutron multiplication factor M_1 of three different origins as a function of the fissile Pu mass for the PuO_2 powder samples. Excluding the value of sample XN 1025, all determined M_1 values are in reasonable agreement.

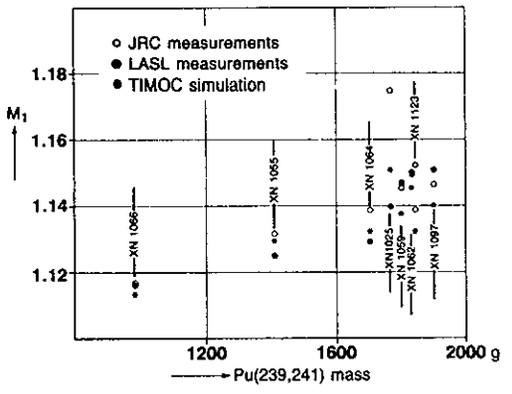

Fig. 4. Neutron multiplication factor M_1 as a function of total fissile Pu mass Pu(239,241).

The large discrepancies of m_{em} found for the MOX fuel suggested a parametric investigation of humidity and density effects on the neutron multiplication. Fig. 5 shows that if there is any important effect in the neutron multiplication, it could come not from the sample humidity but rather from the unknown MOX sample density. The neutron detection head had in this case a maximum of 2% influence on the neutron multiplication factor.

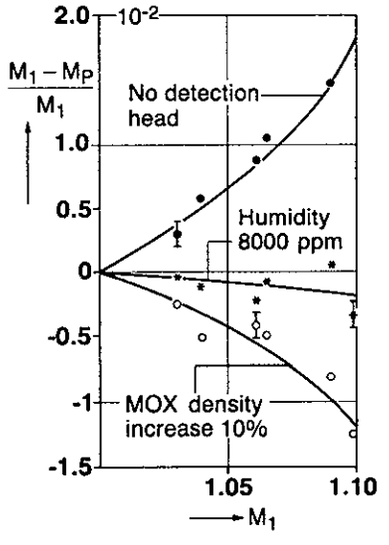

Fig. 5. Coefficients of multiplication factor for HLNCC II MOX fuel.

Conclusions

The procedure used for the calculation of the constant β has been confirmed with respect to its numerical outcome by Monte Carlo neutron transport calculations. The simple method used for the assay of PuO_2 powder of refs.1 and 4 gives identical results with method A. For this reason it is possible to take $p_0 = p$. The assay results of MOX could not be improved nor by method A nor by B. It turned out that realistic sample density variations influence more the neutron multiplication factor than humidity variations. This might explain why method A leads to better results than method B.

Acknowledgements

The authors are grateful to Mrs. K. Caruso for her assistance during the preparation of this work and to Mrs. G. Castagnetti and Mrs. M. van Andel for typing the manuscript.

References

1. N. Ensslin, "A simple self-multiplication correction for in-plant use", Proc. ESARDA, Liège (Belgium), 21-23 May 1985, p.233.
2. W. Hage and D.M. Cifarelli, "On the factorial moments of the neutron multiplicity distribution of fission cascades", Nucl. Inst. Meth. A236, 165-177 (1985).
3. B.G.R. Smith, H.O. Menlove, M.S. Krick and R. Ingels, "Field test and calibration of the HLNCC-II for high burn-up plutonium samples", in 7th ESARDA Annual Symposium on Safeguards and Nuclear Material Management, Liège (Belgium), 1985, L. Stanchi (Ed.), Joint Research Centre, Ispra (Italy), Vol.19, pp.177-183.
4. W. Hage and K. Caruso, "An analysis method for the neutron auto-correlator with multiplying samples", EUR 9792 EN (1984).
5. F. Bevacqua, "Tecniche di correlazione neutronica per la misura di materiali fissili: interpretazione dei dati sperimentali con codici di simulazione Monte Carlo", Tesi di Laurea, Università di Roma, La Sapienza, 85/86.
6. H. Rief and H. Kschwendt, "TIMOC, a general purpose Monte Carlo code for stationary and time dependent neutron transport", EUR 4519e, 1970.

ESARDA

EUROPEAN SAFEGUARDS RESEARCH AND DEVELOPMENT ASSOCIATION

Reprinted from the Proceedings of the
9th ESARDA Symposium on Safeguards and Nuclear Material Management
London, U.K., 12-14 May 1987

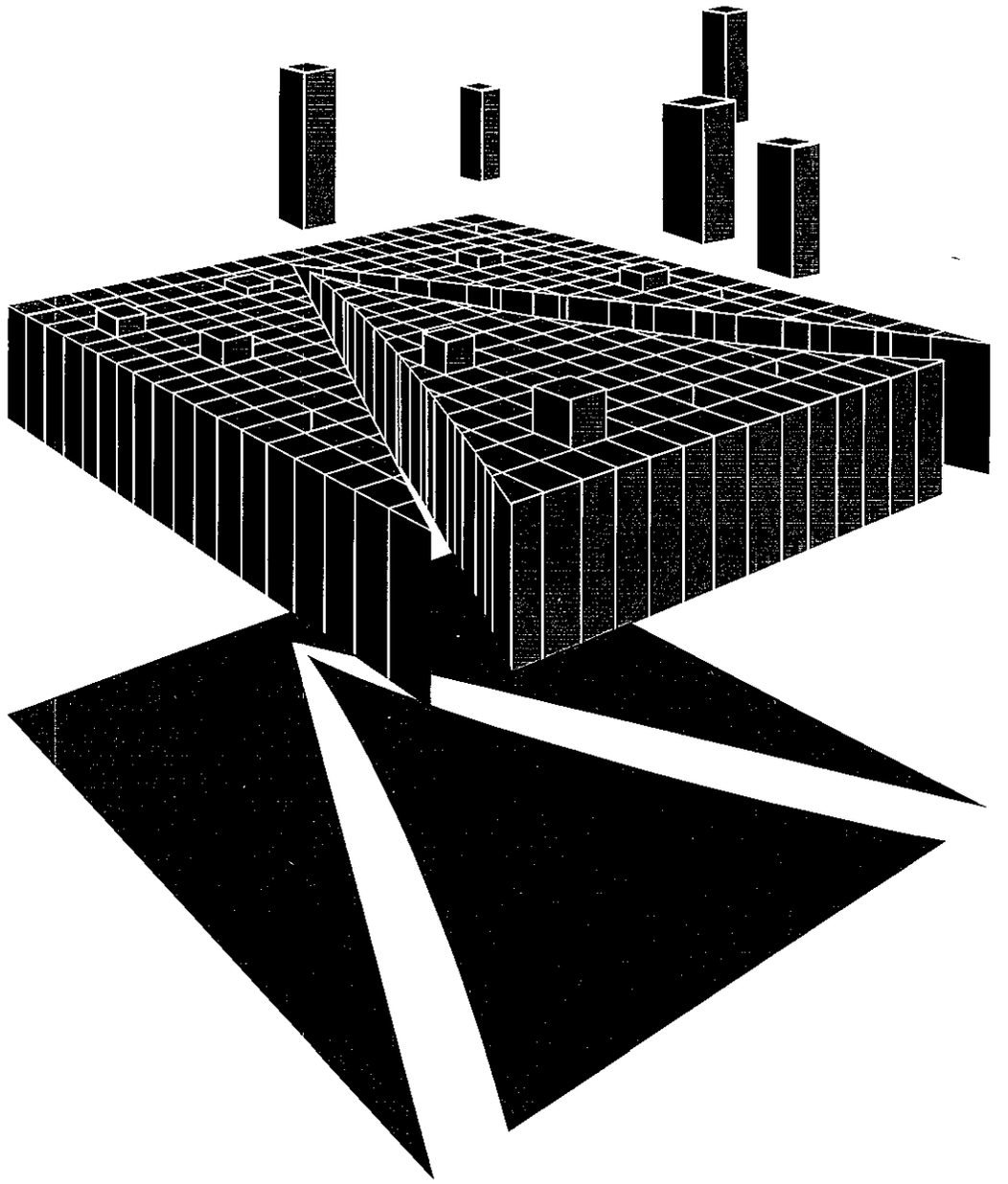

COMMISSION OF THE EUROPEAN COMMUNITIES
JOINT RESEARCH CENTRE

MULTIPLICATION AND ABSORPTION CORRECTION OF AUTO CORRELATOR MEASUREMENT DATA

W. Hage, A. Prosdocimi, V. Vocino
Commission of the European Communities
Joint Research Centre - Ispra Establishment
21020 Ispra (Va) - Italy

9th ESARDA Symposium, London 1987

Abstract

This paper gives the derivation of a simple interpretation model for the neutron signal auto correlator for the assay of fuel samples with fast neutron multiplication and absorption.

1. Introduction

The non-destructive assay of plutonium can be made by a determination of the spontaneous fission rate of its even isotopes. These isotopes emit per spontaneous fission event groups of ν neutrons with the probability P_ν $(0 \leq \nu \leq 10)$. By means of neutron correlation techniques single neutron signal events from (α,n)-reactions of plutonium with the oxide (^{17}O, ^{18}O) or contaminants can be eliminated from signal events with more than one neutron per spontaneous fission event[1-5].

In this technique the neutrons emitted by a test item are slowed down in a moderator, diffuse there as thermal neutrons, and are partially absorbed by neutron detectors incorporated in the moderator assembly. The neutrons absorbed in the detectors are transformed in real time into electric signals amplified, shaped, and converted into a signal pulse train.

Widest application to analyse this pulse train has found the shift register[3]. This instrument delivers two experimental quantities: the total counts T and the effective number of doublets R+A measured in a sequence of observation intervals τ. Each signal of the observation interval opens with a small delay θ and a large delay of about 1 ms such observation intervals.

The difference of the measured doublets in the gates with the small and large delay gives the effective number of correlation doublets R. For the assay of bulky fissile material containing Pu the measured quantities T and R can be expressed as function of the spontaneous fission rate F_S of the (α,n)-reaction rate S_α and the probability p that a neutron generates an induced fission event[6-9]. In this paper the model of the shift register is extended to the case that the neutrons have a finite probability for absorption a inside the sample. Such an extension can be of interest for the assay of mixed oxide fuel with a low Pu and ^{235}U content.

2. Theory

The theory starts from the dead time and background corrected counts of the singlets T and of the correlated doublets R. The counts T are composed of three components:

- the spontaneous fission rate F_S generating $\nu_{S(1)}(p,a)$ neutrons per spontaneous fission event of which the fraction ε is detected;
- the (α,n)-reaction rate S_α of which the fraction (1-p-a) enters into the detector head to be detected with probability ε;
- the fraction pS_α producing $\nu_{I(1)}(p,a)$ neutrons per induced fission event which is detected in the detector head with probability ε

$$T = \varepsilon[F_S\nu_{S(1)}(p,a)+S_\alpha(1-p-a)+pS_\alpha\nu_{I(1)}(p,a)]T_m \quad (1)$$

a = probability that a fast neutron is absorbed inside the test sample;
p = probability that a fast neutron generates an induced fission event inside the test sample;
T_m = measurement time.

The factorial moments $\nu_{S(\mu)}(p,a)$ and $\nu_{I(\mu)}(p,a)$ were determined in ref.7 considering a fast fission approximation for $\mu = 1,2$ and 3.

For samples with only fission and absorption it is:

$$\nu_{S(1)}(p,a) = \nu_{S(1)}\frac{1-p-a}{1-p\nu_{I(1)}} = \nu_{S(1)}M \quad (2)$$

$$\nu_{I(1)}(p,a) = \nu_{I(1)}M$$

with $\nu_{J(\mu)} = \sum_{\nu=\mu}^{\infty}\binom{\nu}{\mu}P_{J\nu}$

$P_{J\nu}$ = probability for emission of ν neutrons per spontaneous (J=S) and induced (J=I) fission.

Combining Eqs.(1) and (2) the well-known equation for the single counts T is obtained

$$T = \varepsilon F_S\nu_{S(1)}M(1+\alpha) \quad (3)$$

$$\alpha = \frac{S_\alpha}{F_S\nu_{S(1)}}$$

T is frequently referred to as "Totals".

The only difference to earlier expressions[7-9] is that the multiplication factor M contains the probability a that a fast neutron is absorbed inside the test sample.

The effective number of correlated doublets R usually referred to as "Reals" is given by the well-known expression

$$R = \varepsilon^2 e^{-\lambda\theta}(1-e^{-\lambda\tau})[F_S\nu_{S(2)}(p,a)+pS_\alpha\nu_{I(2)}(p,a)]T_m \quad (4)$$

The second factorial moments $\nu_{S(2)}(p,a)$ and $\nu_{I(2)}(p,a)$ are now dependent on the probability that a fast neutron generates an induced fission and on the probability that a fast neutron is absorbed inside the test item.

From ref.7 follow the second factorial moments replacing p by M.

$$p = \frac{M-1}{M\nu_{I(1)}-g} \qquad g = 1 + \frac{a}{p} \tag{5}$$

It is then

$$\nu_{S(2)}(p,a) = \nu_{S(2)}M^2[1+\beta(M-1)] \tag{6}$$

and

$$\nu_{I(2)}(p,a) = \frac{\nu_{S(2)}}{\nu_{S(1)}} M^2\beta(M-1) \tag{7}$$

$$\text{with } \beta = \frac{\nu_{S(1)}\nu_{I(2)}}{\nu_{S(2)}(\nu_{I(1)}-g)} \tag{8}$$

With Eqs.(5) till (7) the Reals R become

$$R = \varepsilon^2 e^{-\lambda\theta}(1-e^{-\lambda\tau})F_S\nu_{S(2)}M^2[1+(1+\alpha)\beta(M-1)] \tag{9}$$

Forming the ratio R/T of an unknown test sample and normalizing this ratio on R_o/T_o of a known sample, the well-known expression for the neutron multiplication factor M is obtained[7-9]. It is

$$M = \frac{(A-1) + \sqrt{(A-1^2 + 4A\rho}}{2A} \tag{10}$$

$$\text{with } A = \beta(1+\alpha) \tag{11}$$

$$\text{and } \rho = \frac{RT_o(1+\alpha)\nu_{S(2)0}\nu_{S(1)}}{R_oT(1+\alpha_o)\nu_{S(2)}\nu_{S(1)0}} M_o[1+A(M_o-1)] \tag{12}$$

The only difference taking into account fast neutron absorption is that the quantity β depends on g which is 1 neglecting any absorption and becomes in the limit 1.3 for very low Pu contents in MOX. The "Totals" T_c and "Reals" R_c corrected for neutron multiplication and (α,n)-reactions remain as before.

Only that now β and M depend on $g > 1$. It is:

$$T_c(M=1) = T(M)\kappa_T \tag{13}$$

$$R_c(M=1) = R(M)\kappa_R \tag{14}$$

$$\text{with } \kappa_T = \frac{1}{M(1+\alpha)}$$

$$\text{and } \kappa_R = \frac{1}{M^2[1+A(M-1)]}$$

An interesting relation is obtained determining directly the ratio of the spontaneous fission rate F_S of a test sample relative to the one of well-characterized standard. For this purpose the totals relative to those of a reference sample T_o are used with Eq.(3) to obtain an expression for the neutron multiplication factor M of the unknown sample

$$M = M_o \frac{TF_{S0}(1+\alpha_o)\nu_{S(1)0}}{T_oF_S(1+\alpha)\nu_{S(1)}} \tag{15}$$

With Eq.(8) the ratio of the "Reals" R and R_o of a test and a reference sample can be formed. Replacing in the resulting expression the neutron multiplication of the unknown sample, an equation of second degree for the ratio of the spontaneous fission rates of a test and reference sample is obtained. It is:

$$\left(\frac{F_S}{F_{S0}}\right)^2 + \frac{F_S}{F_{S0}}(A-1) - A\rho = 0 \tag{16}$$

or

$$\frac{F_S}{F_{S0}} = \frac{R_oT^2(1+\alpha_o)^2}{2RT_o^2(1+\alpha)^2[1+A_o(M_o-1)]} \left[\sqrt{(A-1)^2 + 4AM_o \frac{RT_o(1+\alpha)}{R_oT(1+\alpha_o)}[1+A_o(M_o-1)] \frac{\nu_{S(1)}\nu_{S(2)0}}{\nu_{S(1)0}\nu_{S(2)}}} - [A-1]\right] \tag{17}$$

The spontaneous fission rate ratio has nearly a quadratic dependence of the total counts T. For this reason it is important to measure this quantity very accurately and to perform the necessary corrections especially due to background with great care. Eq.(17) is particularly useful for the measurement of fuel pins and cans with approximately the same Pu isotopic composition and weight.

With $R = R_o$, $T = T_o$, Eq.(17) can be used to determine the uncertainty of F_S/F_{S0} due to errors of the neutron multiplication factor M[10], the α-ratio and the β-value[11].

Fig. 1 gives the error

$$\frac{F_S - F_{S0}}{F_S}$$

as a function of the neutron multiplication factor M due to neglection of neutron absorption. The case with $g = 1.3$ corresponds to a sample with a very low Pu content in MOX fuel. If the Pu content is greater than about 50% in MOX, then the systematic error due to a neglection of neutron absorption remains below 1%.

The largest uncertainties of F_S are due to errors made in the assessment of the α-value especially for high burn-up fuel with $\alpha \gtrsim 1$ (Fig. 2).

An error of α of about 30% causes an uncertainty of F_S which is about 15%. Neutron multiplication has little influence on this error.

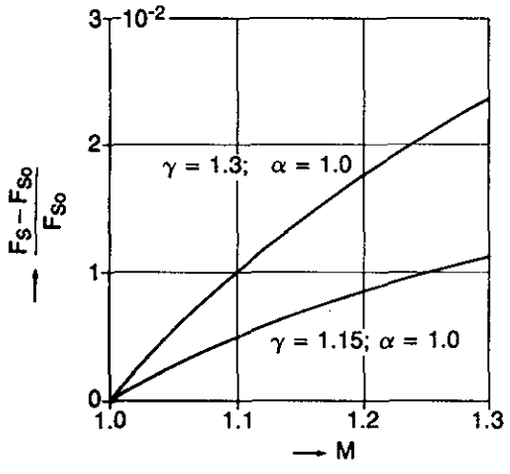

Fig. 1 - Systematic error of F_S neglecting neutron absorption for $T/T_o \approx 1$ and $R/R_o = 1$.

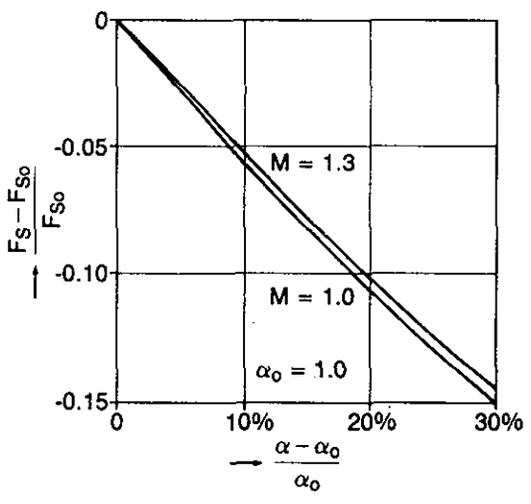

Fig. 2 - Systematic error of F_S due to error of α.

3. Conclusions

The inclusion of fast neutron absorption in the algorithm for the interpretation of shift register measurements does not alter appreciably the mathematical expressions (Eq.(10)).

The numerical results show that the error introduced remains for practical applications below 1%.

Other matrix effects of fast neutrons are at present under investigation.

The paper gives with Eq.(17) an expression which is particularly useful for the interpretation of measurement data obtained with samples of similar weight and isotopic composition.

4. Acknowledgements

Many thanks are due to Mrs. K. Caruso for her assistance and to Mrs. G. Castagnetti and Mrs. M. van Andel for typing the manuscript.

5. References

1. G. Birkhoff, L. Bondar, N. Coppo, "Variable dead time neutron counter for tamper resistant measurements of spontaneous fission neutrons", EUR 4801e (1972).
2. E.W. Lees, F.J.G. Rogers, "Experimental and theoretical observations on the use of the Euratom variable dead time neutron counter for passive assay of plutonium", IAEA SM 231/51, Vienna (1981).
3. K. Böhnel, "Die Plutoniumbestimmung in Kernbrennstoffen mit der Neutronen - Koinzidenzmethode", KfK 2203 (1975).
4. N. Ensslin, J. Stewart, J. Sapir, "Self multiplication correction factors for neutron coincidence counting", Nucl. Mat. Man. VIII, 2 (60-73) (1979).
5. E.J. Dowdy, C.N. Henry, A.A. Robba, J.R. Pratt, "New neutron correlation measurement techniques for special nuclear material assay and accountability", Proc. Int. Symp. on Nuclear Material Safeguards, Vienna, SM-231/69 (IAEA, Vienna, 1978).
6. K. Böhnel, "The effect of multiplication on neutron coincidence measurements", Nucl. Sci. Eng. 90, 75 (1985).
7. W. Hage, D.M. Cifarelli, "On the factorial moments of the neutron multiplicity distribution of fission cascades", Nucl. Inst. Meth. A236, 165-177 (1985).
8. N. Ensslin, "A simple self-multiplication correction for in-plant use", Proc. ESARDA, Liège (Belgium), 21-23 May 1985, p.233.
9. W. Hage, K. Caruso, "An analysis method for the neutron auto correlator with multiplying samples", EUR 9792 EN (1984).
10. M.T. Swinhoe, "Multiplication effects in neutron coincidence counting: uncertainties and multiplying reference samples", ESARDA, Liège (Belgium), 21-23 May 1985, p.223.
11. M.S. Zucker, N.E. Holden, "Neutron multiplicity for neutron induced fission of U235, U238 and Pu239 as a function of neutron energy", Proc. Int. Symp. on Nuclear Material Safeguards, IAEA, Vienna (Austria), 10-14 November 1986, SM-293-122.

ESARDA

EUROPEAN SAFEGUARDS RESEARCH AND DEVELOPMENT ASSOCIATION

Reprinted from the Proceedings of the
9th ESARDA Symposium on Safeguards and Nuclear Material Management
London, U.K., 12-14 May 1987

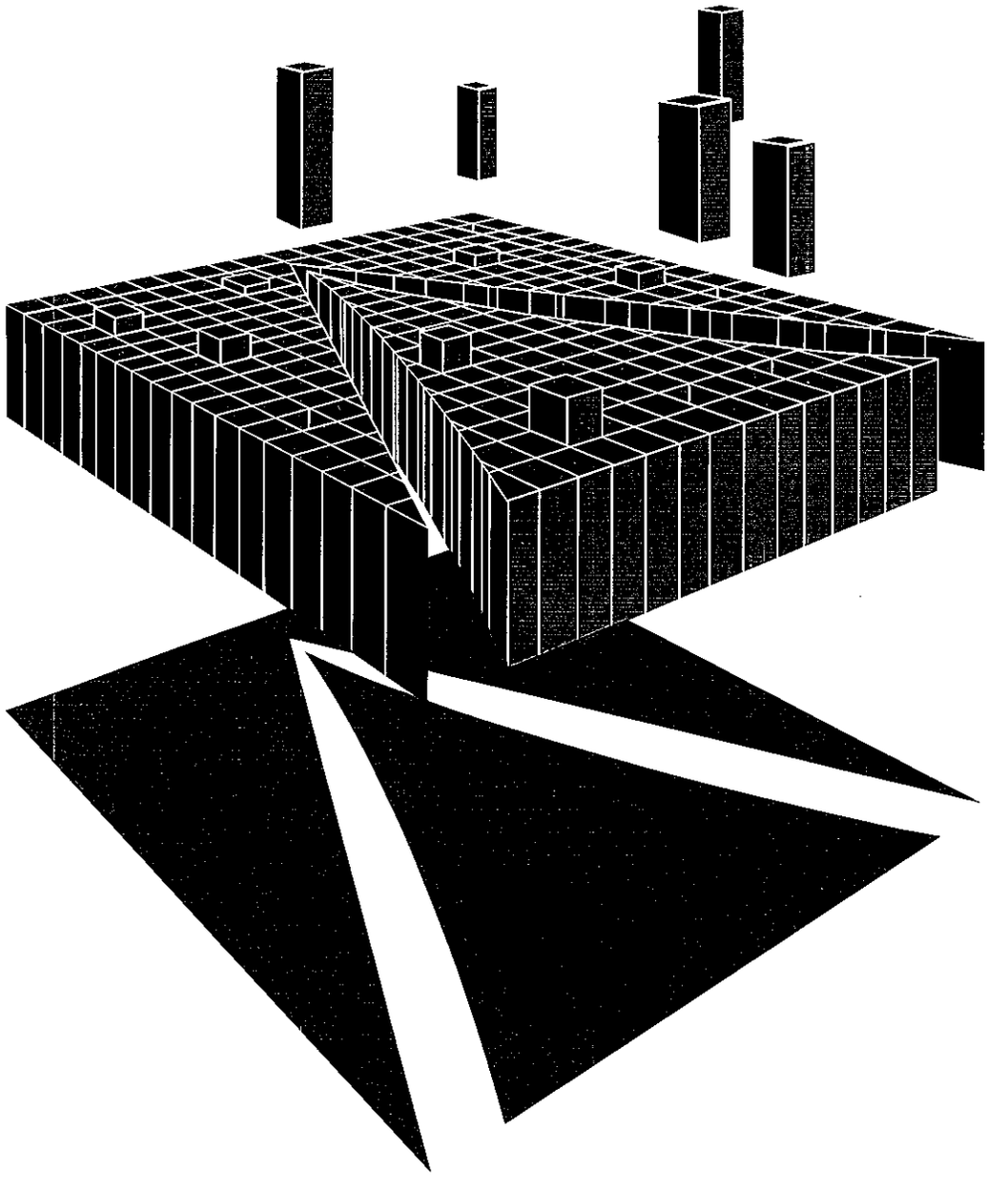

COMMISSION OF THE EUROPEAN COMMUNITIES
JOINT RESEARCH CENTRE

A COMPUTER CONTROLLED SHIFT REGISTER SYSTEM FOR THE AUTOMATIC ASSAY OF PLUTONIUM OXIDE BY PASSIVE NEUTRON INTERROGATION

R. Benoit, R. Haas*, W. Hage, A. Prosdocimi, B.L. Thaurel**, V. Vocino
Commission of the European Communities
Joint Research Centre - Ispra Establishment
21020 Ispra (Va) - Italy
*CEC Safeguards Directorate, Luxembourg
**CEA CEN, Saclay

9 th ESARDA Symposium, London 1977

Abstract

An instrument has been assembled such to implement an NDA procedure for the passive neutron interrogation of plutonium, consistent with the needs of safeguards inspection procedures. The method adopted is that of correlated neutron counting by means of shift-register circuitry, applied to samples of canned PuO_2 only. The instrumentation, most in the NIM modular configuration, is controlled by micro computer which handles all the measuring procedure and the data treatment of the results with the associated corrections and the statistical checks. The algorithms, the assay procedure and the calibration method are presented.

Introduction

The purpose of this paper is to present a complete system for the passive interrogation of plutonium oxide, assembled about a neutron correlation analyser of the shift register type. For such a system an open configuration has been chosen in order to be able to utilize either already available components or to make operators able to match future compatible ones. For the complete system it is intended a whole chain beginning with the neutron detection head as far as an on-line computer, the latter implemented by the suitable software and procedure to put any operator in condition to use the instrument, continuously assisted by the computer.

1. The Neutron Interrogation System

1.1 The shift register analyser could have a rather compact electronic package and, furthermore, it can constitute a device integrated with the neutron detector and its analog electronics. Nevertheless, the compactness of the electronics finds its limits in the size and weight of the neutron detection head which cannot be reduced further if the fast neutrons of fission have to be slowed down to thermal energies. Anyway, also an on-line computer with its peripherals constitutes a limit of portability despite the fact that more and more compact hardware becomes available today.

1.2 Our effort has been to look at the compatibility of the various components available to the safeguards authorities, either because some of them are already existing and operating, or because the evolution of some components is still running and they cannot be defined for ever. Moremover, the method of electronic analysis could be improved as in the typical case of the multiplicity sorter.

For all these reasons a modular structure has been adopted such as NIM plug-in units for the electronics and serial interfacing for the computer (Fig. 1).

1.3 A first advantage achieved by our system has been a larger availability of material offered by the market for most of the components. This can have an impact both on the choice and on the cost, together with the possibility to assemble a system in different ways. Thus, for instance, many kinds of analog electronics and connections of the preamplifiers are compatible with the unique condition to deliver, as output, standard signals.

The possibility to implement a shift

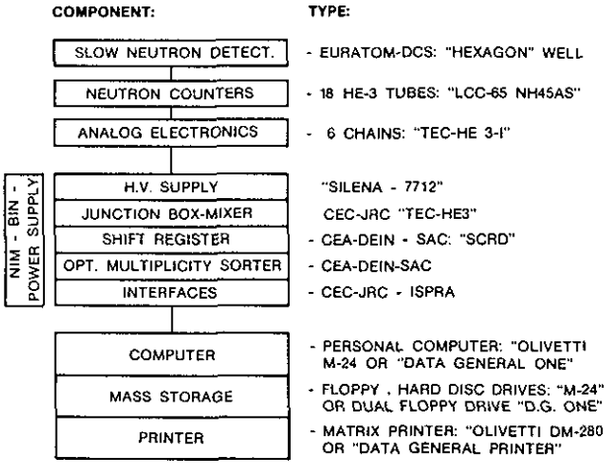

Fig. 1. Block scheme of the system hardware.

register only, or a shift register with multiplicity sorter, is ope :. Also the computer can be whatever after a suitable software of data transfer is devised. But, on the other hand, the fact of having renounced to an integrated system has increased the size of the whole system, and a larger amount of connection cables has become inevitable.

2. Instrumental Components

2.1 In order to carry out a campaign of experiments, a typical hexagonal detection head has been matched to the interrogation system[2] (Fig. 1). Six slabs of polyethylene moderator, with three proportional counters embedded in each slab, form a hexagonal well where small cans of plutonium oxide powder, or drums of plutonium waste, can be placed. The 18 proportional counters are connected three by three to six amplifying chains of the TEC-I type[1]. The electronics package of each chain contains preamplifier, main amplifier and discriminator, a common junction box distributes H.V. and L.V. supplies, then it mixes all the detector signals into a single output. Generally, the detection head, the counter tubes and the associated electronics could be whichever when their output is compatible with the shift register input requirement.

2.2 The neutron correlation analysis is performed by a shift register circuitry, mounted in a NIM module of three units, designed by CEA-DEIN Saclay; its timer can be controlled externally, while predelay and gate widths can be selected by the front panel over a large range, and read electronically. The three scalers accumulating total, real plus accidental and accidental counts are both displayed on the panel and transferred to a BCD output.

As an option, a multiplicity sorter can be added in order to count the neutron real coincidences according to their order of multiplicity, from one to eight, while the residual counts are accumulated in another scaler. This multiplicity sorter has no display, but its memories can be read by an interfaced computer.

2.3 The BCD output of the shift register unit is converted into a RS-232-C serial output by an interface unit, so that a computer can be connected to receive the reading of the three scalers. Furthermore, it can read the selected predelay and gate positions and preset the counting time in a recycle mode. In the same way the computer can read the memories of the multiplicity sorter.

A suitable software implements the whole procedure for operating the instrument and it can control all data handling procedures of the results as described further on in chapters 4 and 5.

2.4 Some of the physical characteristics about the performances of the system will be given here, with the exception of the neutron detection head and its analog electronics, because this part of the system is not typical and could be replaced by other components. The shift register unit accepts positive pulses of more than 50 ns, the predelay can be set to 16 values from 1 to 15 µs, in two ranges with steps of about 1 µs, the gate width has a range of 8 values from 15 µs to 122 µs, in steps of about 16 µs. A special output can count the total input, just before the synchronizer, so that it can be compared with the total scaler of the instrument and checked for possible slight counting losses.

2.5 Two types of computer have been matched to the instrument so far, both based on a MS-DOS system and programmed in BASIC for an easier utilization. A desk computer OLIVETTI type M-24 with color CRT screen, a 5.25" floppy and a hard disc; a line printer writes a full or a shortened record of the interrogation assay.

Otherwise, the same software can be run by a DATA GENERAL ONE portable computer, with two 3.5" disc drives and a LCD screen; an associated printer can produce the same records as before.

3. Operation Procedure for Assay

3.1 The procedure begins with some preliminary checks of the instrument, namely sensitivity and background[3]. The former is checked by means of either a reference Cf-252 fission source or a plutonium sample (Fig. 2). It is merely displayed a warning when the observed real coincidence rate differs from its expected value more than 2.6 times the standard deviation.

For every measurement the good operation of

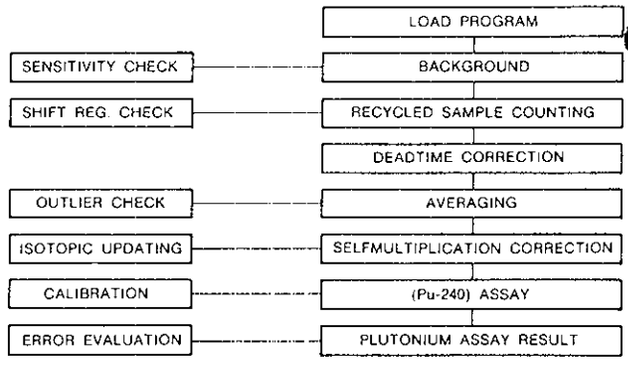

Fig. 2. Flow chart of the assay procedure.

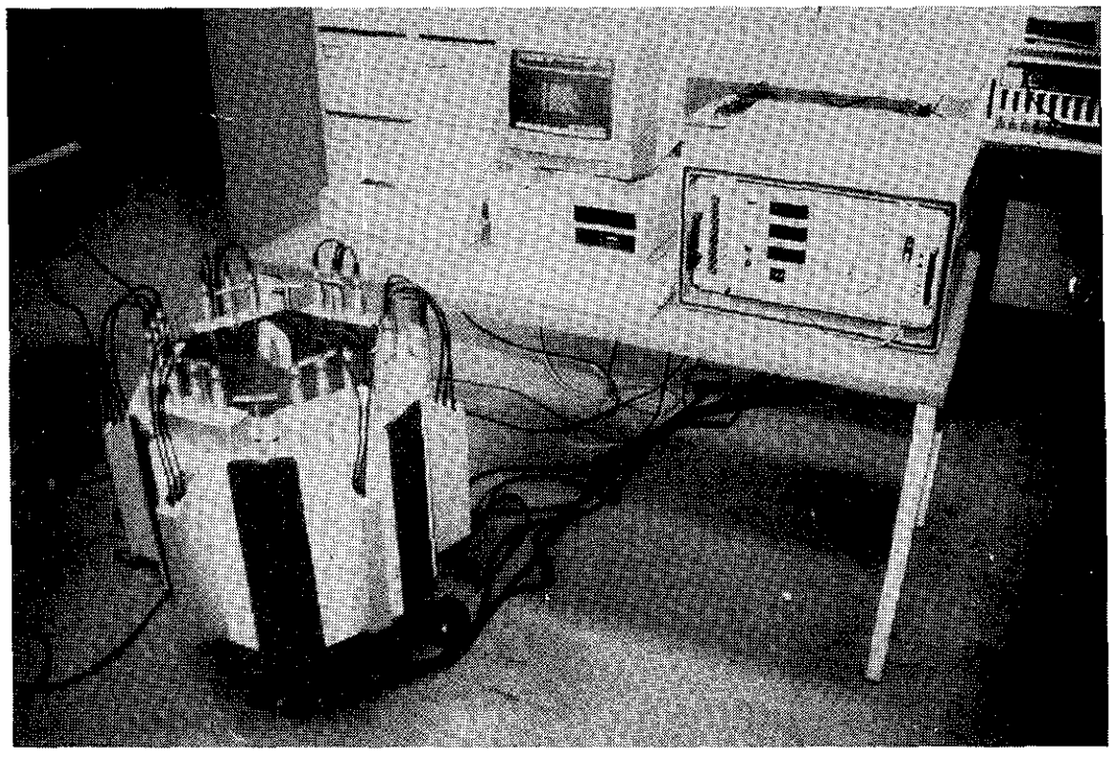

Fig. 3. Overall view of the interrogation system.

the register is checked by comparing the observed with the calculated accidental coincidence rate; when the difference becomes higher than three times the standard deviation, the measurement is rejected and repeated.

Eventually, a background determination for the total count rate is required for further corrections.

3.2 In assying a plutonium sample, a run of preset repeated measurements is performed automatically, the accepted results are analyzed statistically and a warning is given for possible outliers. Both total and real coincidence rates are retained and dead time corrections are applied to both on the basis of the resolution time of a single electronic chain. The effective dead time of more chains is evaluated taking into account also the count rate.

3.3 After a measurement cycle is achieved, the total and real coincidence rates are utilized for a self-multiplication correction, on the basis of a reference sample assumed as no-multiplying.

Both quantities depend on the neutron multiplication which is very marked in the case of the reals. With the model for the neutron multiplication[4,5] of a point source, the following relations are valid

$$T = \varepsilon T_M F_s \nu_{s(1)} M(1+\alpha) \qquad (1)$$

$$R = \varepsilon^2 T_M e^{-\lambda\theta}(1-e^{-\lambda\tau}) F_s \nu_{s(2)} [1+\beta(M-1)(1+\alpha)] \qquad (2)$$

with

$\beta = \nu_{s(1)}\nu_{I(2)}/\nu_{s(2)}(\nu_{I(1)}-1)$

F_s = spontaneous fission neutron emission rate

$S\alpha$ = (α,n) neutron emission rate

ε = probability for the detection of one neutron

T_M = measurement time

θ = predelay of the shift register circuit

τ = observation interval of the shift register circuit

λ = fundamental mode decay constant of thermal neutron detection assembly

$P_{Kj\nu}$ = probability for emission of ν neutrons due to fissions by isotope K (j = s spontaneous, j = I induced)

α = (α,n) to S.F. neutron ratio

$$\nu_{j(m)} = \sum_{\nu=m}^{\infty} \binom{\nu}{m} P_{Kj\nu}$$

Equations (1) and (2) hold for practical samples where the total mean values of $\nu_{s(m)}$ are defined as independent of the Pu-240 equivalent mass.

With the measured data T_o, R_o and T,R from a well-characterized standard sample and a test sample, respectively, an equation for the determination of the multiplication factor M of the test sample is obtained following the procedures of refs.4 and 5.

The multiplication factor is then determined

for a subset of samples using the same standard as a reference. The determined multiplication factor is used to correct the reals R(M) of this subset for neutron multiplication to get a value R(M=1). All values should then be a linear function of the declared Pu-240 mass equivalent.

3.4 It is important to state that the Pu-240 mass equivalent to be used must be the mass equivalent $m_e(240)$ defined by the spontaneous fission rate F_s

$$m_e(240) = F_s/f_s(240) \qquad (3)$$

f_s = spontaneous fission rate of isotope Pu-240 per unit mass.

All other definitions of the Pu-240 mass equivalent are found not correct with neutron multiplication. For this reason, Eq.(3) is used for the definition of $m_e(240)$ in the elaborated software.

4. Operation Procedure for Calibration

4.1 A first application to safeguards is devised for Pu oxide cans, therefore calibrating samples over a large range of masses would be available. One of the samples will be assumed as a reference for self-multiplication and the remaining items will be corrected for self-multiplication. The responses are expected to be linear versus the Pu-240 equivalent mass, then the calibration results will be fitted to a straight line and the parameters derived together with the fit errors.

4.2 Every assayed or calibrating sample is characterized by its Pu mass and its isotopic composition, the latter is updated and the equivalent Pu-240 mass can be calculated.

During the assay mode the calibration parameters should be known and it is essential to refer to the same experimental conditions both for calibration and assay. Therefore, such conditions must be well described when calibration parameters are given.

4.3 Last but not least, the error of the assayed Pu-240 equivalent is calculated on the basis of the statistical count errors of the raw measurements, of the calibration parameters error due to the least square fit, and eventually through the error propagation up to the Pu mass.

References

1. Y. Haurie, J. Tourneix, "Tête électronique pour compteur à He 3 modèle I", EUR 7655 FR (1982).
2. P. Hansen, "Characterization of the neutron detection head Hexagon for safeguards purposes", report FMM-113-NDA (1985).
3. A. Prosdocimi, W. Hage, "Procedures for the treatment of shift register measurements", report FMM-105-NDA (1985).
4. N. Ensslin, "A simple self multiplication correction for in-plant use", Proc. ESARDA, May 1985, Liège (Belgium), p.233.
5. W. Hage, D.M. Cifarelli, "On the factorial moments of the neutron multiplicity distribution of fission cascades", Nucl. Instr. Meth., A-236, 165-177 (1985).

ESARDA

EUROPEAN SAFEGUARDS RESEARCH AND DEVELOPMENT ASSOCIATION

Reprinted from the Proceedings of the
9th ESARDA Symposium on Safeguards and Nuclear Material Management
London, U.K., 12-14 May 1987

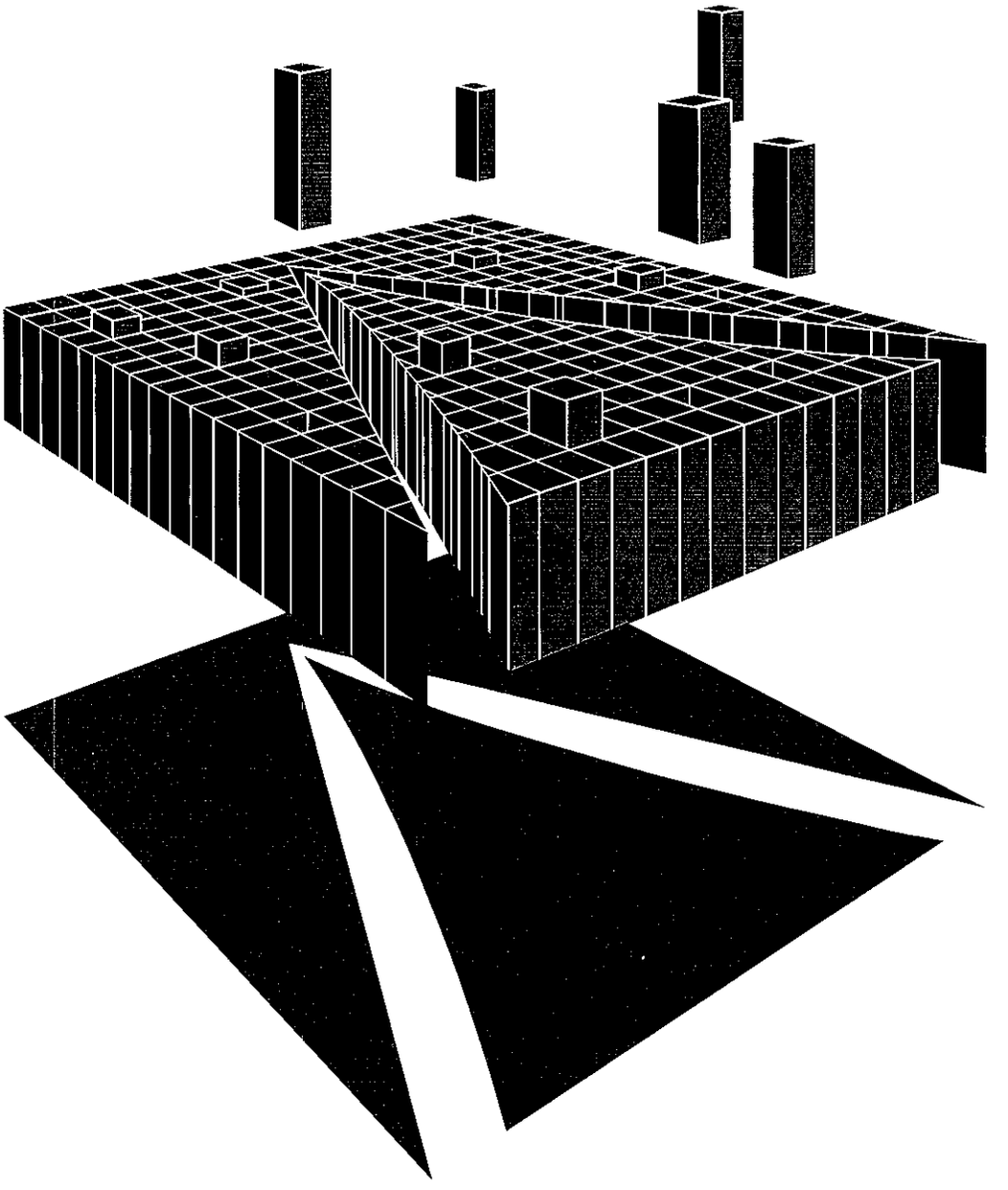

COMMISSION OF THE EUROPEAN COMMUNITIES
JOINT RESEARCH CENTRE

A TRANSPORTABLE INSTRUMENT FOR DETERMINATION OF URANIUM CONTENT IN POWDERS OR PELLETS BY DELAYED NEUTRON TECHNIQUE: DUCA

R. Adam, P. Agostini, L. Caldon, G. Cordani, M. Cuypers, N. Farese, R. Haas*, V. Vocino
Commission of the European Communities
Joint Research Centre - Ispra Establishment
21020 Ispra (Va) - Italy

*EURATOM Safeguards Directorate
Luxemburg

9th ESARDA Symposium; London 1987

Abstract

An instrument has been developed in order to assay U by NDA according to the needs of safeguards inspections. The method adopted uses delayed neutron counting of samples containing U oxide in small cylindrical capsules. The instrumentation is controlled by an on-line microprocessor. It is connected to a personal computer so that all the measurement procedures, the management of measurement results, the associated corrections and the statistical checks are carried out automatically. The performance of the instrument has been checked with LEU UO_2 powders and pellets.

1. Introduction

The delayed neutron technique has been used for many years. For uranium assay the implementation of this technique for an in-field instrument used in routine inspections is shown. On the basis of a request for a transportable instrument, the instrument DUCA (Determination Uranium Content Apparatus) has been developed[1,4].

2. Brief Description of the Instrument System[3]

(Fig. 1). The main parts of the system are:

2.1 Loading-Unloading Sample System (Fig. 2)

This equipment is used to transfer the sample from the loading container into the irradiation counting zone and thereafter to withdraw it into the unloading container. The main parts of this device are: the loading container which contains a maximum of 25 capsules, the unload container which is similar to the load container and is used to store the capsules after irradiation, and the sample transfer drawer which transports one capsule at a time to the centre of the ^3He detector block and discharges it into the unload container.

2.2 Source Transfer Device (Fig. 2)

This device is made up essentially of a stepping motor which controls the source transfer rod. This rod contains the four californium sources and it will be moved so that the sources can be placed rapidly in the irradiation zone or in parking zone position. The rod is made up of various sections with different materials of different lengths depending on the functions which they fulfill: neutron moderator or neutron and gamma shielding.

2.3 Sources Parking Compartment (Fig. 2)

The sources are shielded radially by a hollow lead cylinder surrounded by water near their parking position. The source parking compartment itself is separated by a Cd shield from the counting irradiation zone to prevent penetration of thermal neutrons.

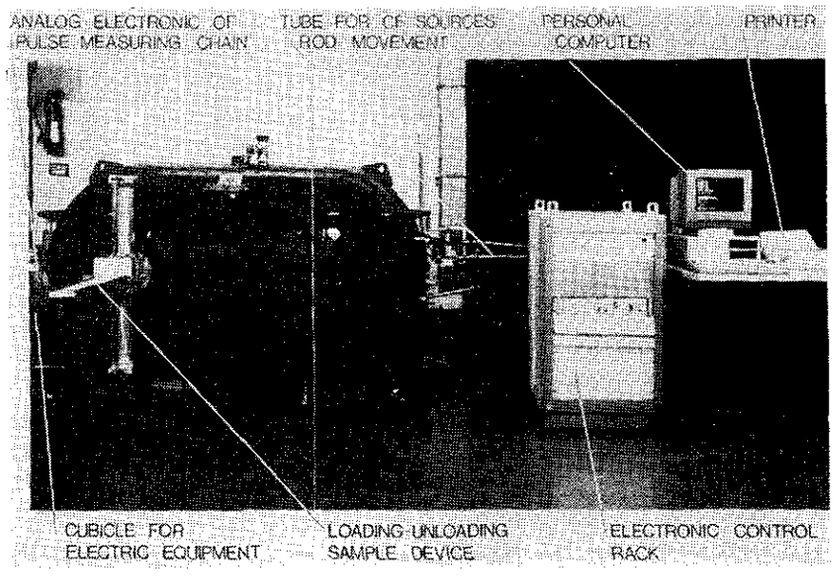

Fig. 1. DUCA instrument.

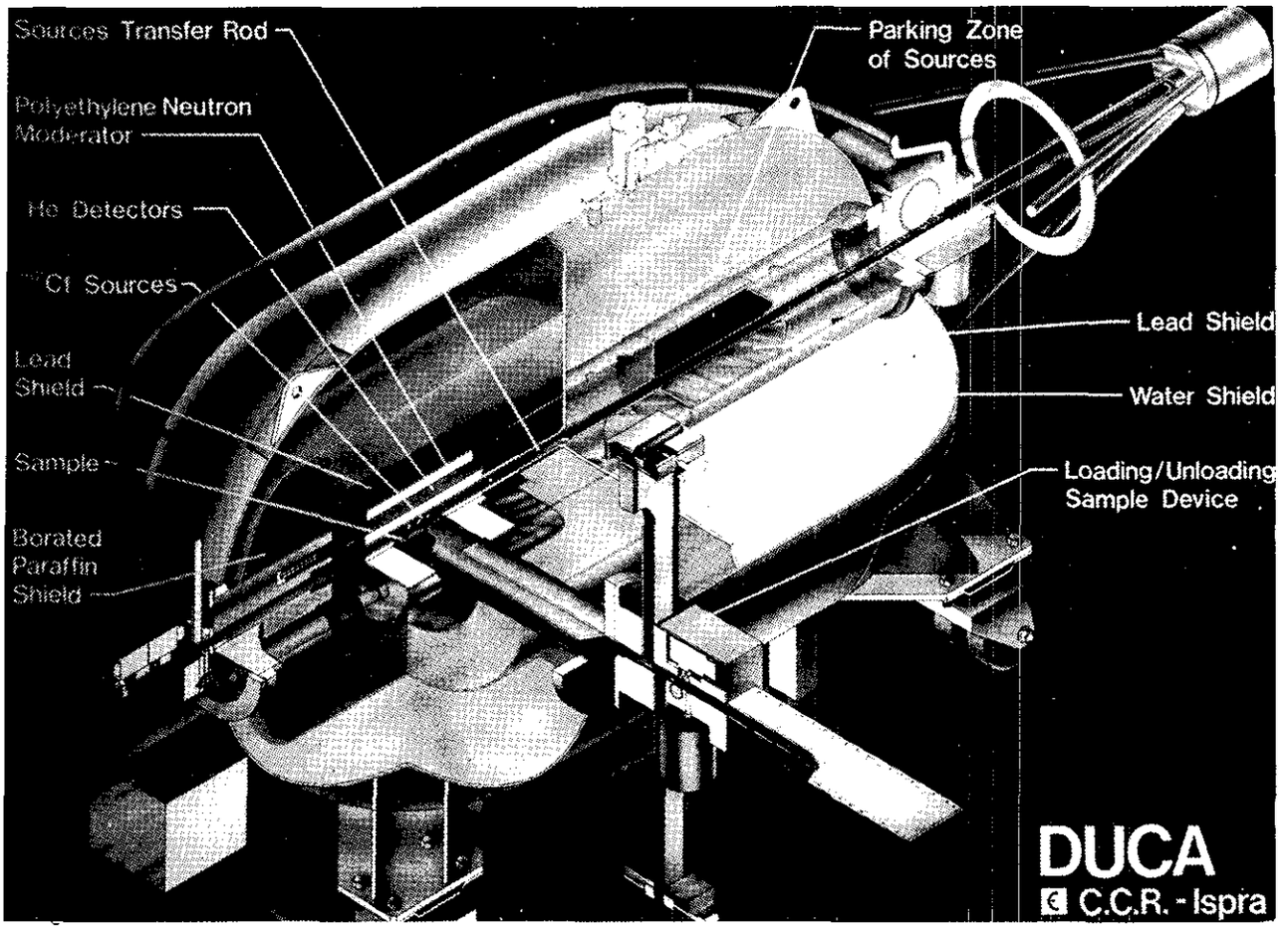

Fig. 2. Schematic representation of DUCA instrument.

2.4 Irradiation/Counting Compartment (Fig. 2)

This zone serves to irradiate the sample by means of the ^{252}Cf sources and to count the delayed neutrons coming from the irradiated sample. The counting position is inside a cylindrical polyethylene block with 5 incorporated ^{3}He counters. This is surrounded by hollow cylinders first of lead, then of borated paraphine.

2.5 Container (Fig. 2)

The parking compartment and the counting irradiation compartment are contained inside a cylindrical container with two hemispherical covers. The interspace between these compartments and the container is filled with water for shielding purposes.

2.6 Sample Holder (Fig. 3)

The DUCA device serves for measurement on sampling material such as, for example, powders or pellets of LWR. This material usually up to 25 g of powder and 100 g for pellets has to be put into special holders such as that of Fig. 3. The holder is a special cylindrical capsule closed by a plug. Its main characteristics are: length: 83 mm; external diameter: 18 mm; internal diameter: 13 mm; inner volume; 9.7 cm^3; material: polycarbonate.

2.7 Electric Equipment (Fig. 4)

The system is constituted of:

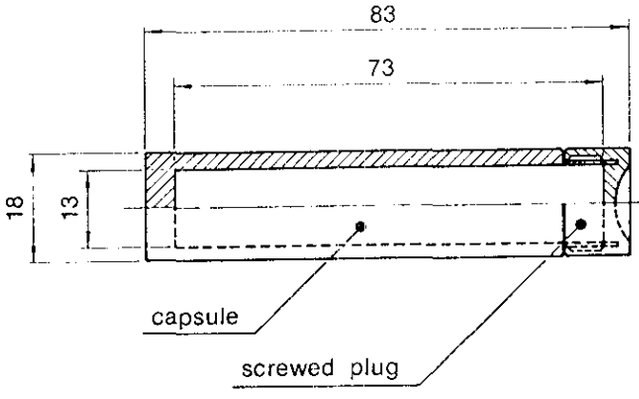

Inner volume: 9.7 cm^3; Material: polycarbonate; Weight of powders up to 40 g of UO_x; Weight of pellets up to 100 g of UO_x. Dimensions in mm.

Fig. 3. Sample holders.

- two motors to move the californium source rod (A1) and to move the samples in and out the irradiation zone (C4);
- several microswitches:
  . for safety (B3, E12),
  . to communicate that the sample is in "IRRAD" or "LOADING" or in "UNLOADING" position (C5, C6, C7),
  . to communicate that the sources are in "REST" or in "IRRAD" position (B2, E13);

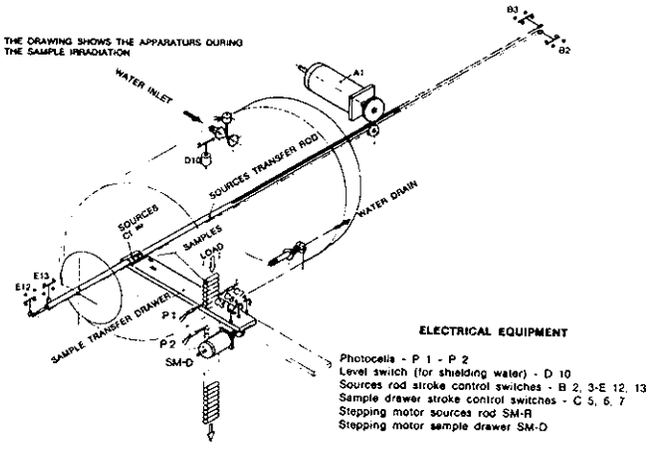

Fig. 4. Electrical equipment.

- photocells, to check if the loading container is empty (C8) and/or if the unloading container is full (C9), with a switch to communicate if the shielding container is full of water (D10).

2.8 Electronics and Detectors (Fig. 5)

The five ^{3}He detectors of the DUCA instrument are connected in parallel to the input of a single charge preamplifier. The preamplifier is blocked during the irradiation phase of the sample and it becomes active after the ^{252}Cf sources are moved away, otherwise the analog chain would be saturated. The whole system of preamplifier, amplifier and discriminator is represented by a simple monoblock located on the detector head. All the operating parameters such as, for example, gain at threshold, are prefixed. The dead time of the electronic chain is about 1 μs.

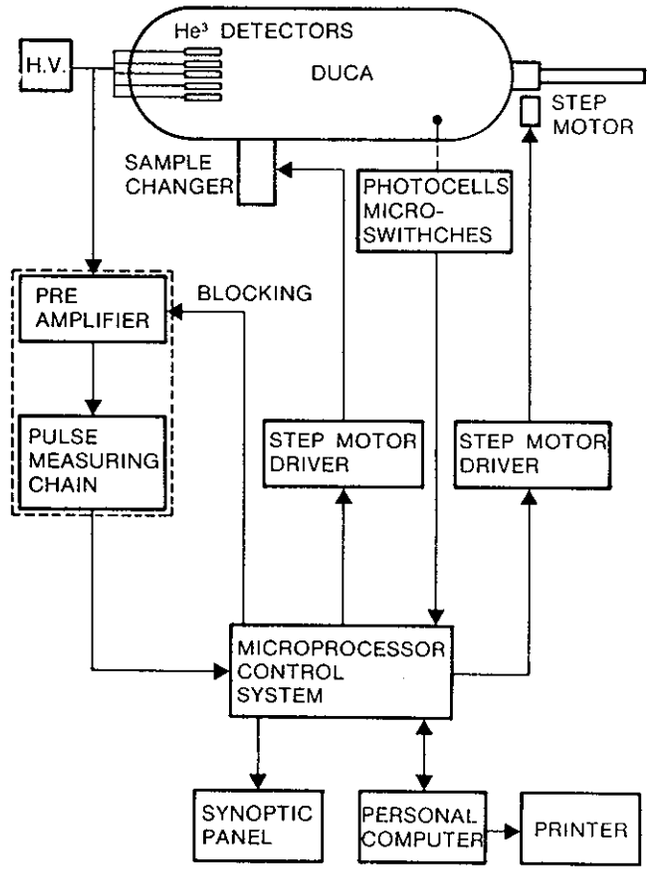

Fig. 5. Block diagram of DUCA electronic equipment.

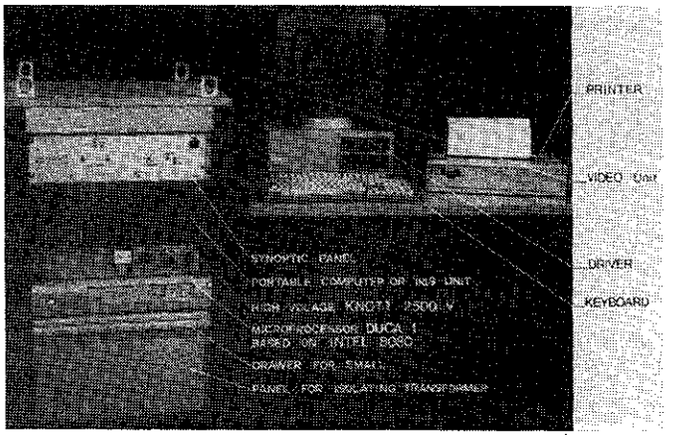

Fig. 6. DUCA control rack and personal computer.

2.9 Control System and Personal Computer (Figs. 6 and 7)

The software to control the running operation of the DUCA instrument is implemented on an INTEL 8080 system. The data acquisition, elaboration, management and storage of the measurements are made on an IBM compatible PC and are based on an MS DOS operating system. All the raw data are stored on floppy disc. The personal computer used

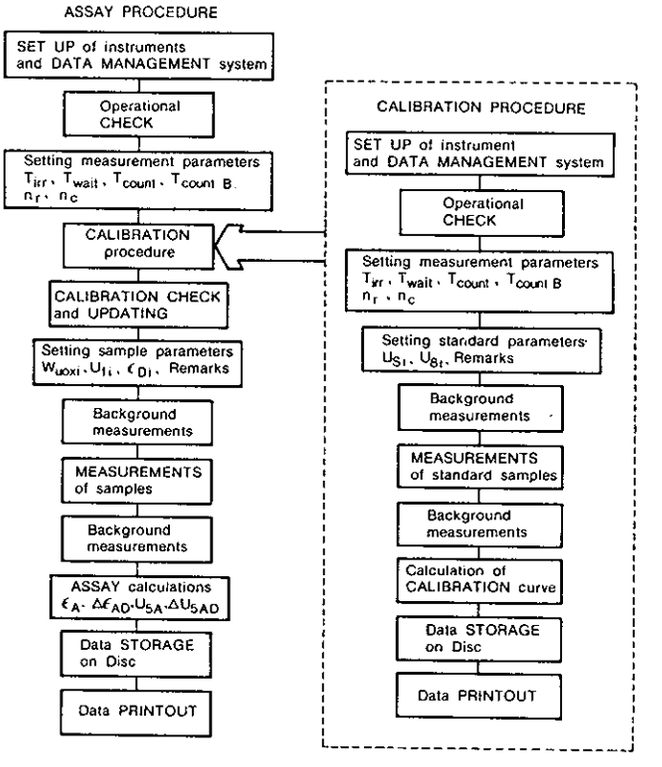

Fig. 7. Schematic block diagram of DUCA procedures.

up to now is typically an IBM PC XT, OLIVETTI M24SP or Data General one. The schematic block diagram of the procedures used for DUCA acquisition and analyser of the results are shown in Fig. 7.

3. Calibration Curve (Fig. 8)

The irradiation counting cycle of DUCA, as described below, refers to the so-called one shot condition which means that each sample is irradiated for t_i seconds and delayed neutrons are counted for t_c seconds with a waiting interval between irradiation and counting of t_w seconds to allow for removal of the irradiation source[2]. The number of delayed neutron precursors of group g present in the sample after an irradiation time t_i is

$$P_g(t_i) = PR_g(1-e^{-\lambda_g t_i})/\lambda_g$$

with
PR_g = production rate of group g
λ_g = decay constant of group g

and at the beginning of the counting interval

$$P_g(t_i+t_w) = PR_g(1-e^{-\lambda_g t_i})e^{-\lambda_g t_w}/\lambda_g$$

The source strength of delayed neutrons emitted by precursors of group g during the counting interval (beginning with t=0) is given by

$$S_g(t) = P_g(t)\lambda_g = PR_g(1-e^{-\lambda_g t_i})e^{-\lambda_g t_w}e^{-\lambda_g t}$$

The production rates PR_g can be expressed as

$$PR_g = F.Q.AB_g$$

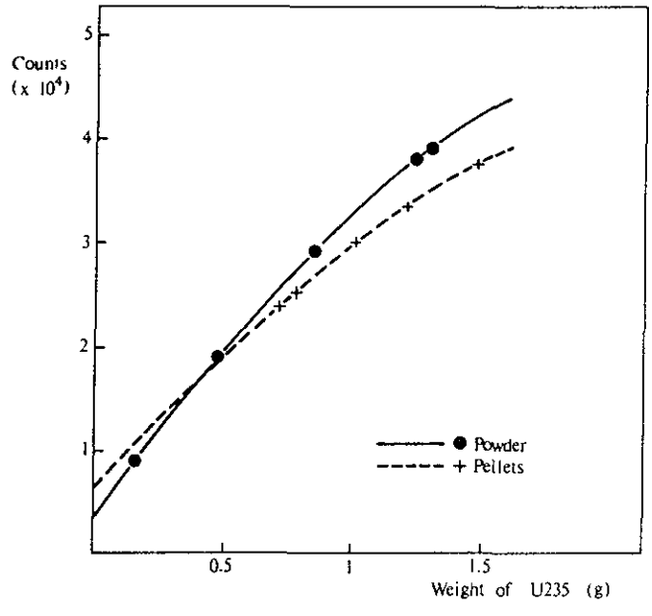

DUCA CALIBRATION CURVE WITH U238 = 22 g

Fig. 8. Calibration curves.

where AB_g is the relative abundance of the precursors of the group g and Q is the irradiation source strength. The factor F takes into account experimental conditions such as geometry, neutron moderation, U content, enrichment of the sample and flux depression in the sample.

The number of delayed neutrons of group g recorded during the counting interval td is

$$C_g(t_c) = \varepsilon FQAB_g(1-e^{-\lambda_g t_i})e^{-\lambda_g t_w}\int_0^{t_c} e^{-\lambda_g t}dt =$$

$$= \varepsilon FQAB_g(1-e^{-\lambda_g t_i})e^{-\lambda_g t_w}(1-e^{-\lambda_g t_c})/\lambda_g =$$

$$= \varepsilon FQN_g$$

where ε = detection probability of delayed neutrons.

If we assume that ε has the same value for all delayed neutrons independent of their origin (group of precursors), we can group ε together with F

$$\varepsilon F = F_T$$

and obtain for the total (T) number of delayed neutrons recorded during the counting interval

$$C_T(t_c) = F_T Q \sum_1^6 {}_g\, AB_g(1-e^{-\lambda_g t_i})e^{-\lambda_g t_w}(1-e^{-\lambda_g t_c})/\lambda_g =$$

$$= F_T Q N$$

It has to be remembered that no dead time losses are taken into account. F_T and Q are sample and instrument specific factors which are independent of the choice of the irradiation-counting cycle. The influence of the latter on the total counts is represented by N.

Form of Calibration Curve

When relating the total counts of a DUCA measurement to the U weight and enrichment of the sample, one has to take into account the variation of the average thermal neutron flux in the sample with density ρ and with relative ^{235}U content C of the material. The flux depression is negligible as far as the fast source neutrons are concerned $\left(\sigma^{238}_{fast} = 0.6 \text{ bar}\right)$. The thermal flux depression is in a first approximation proportional to $e^{-\Sigma_{abs}\bar{d}}$ where Σ_{abs} is the macroscopic cross section and $\bar{d}$ is a "representative" length which depends only on the dimensions of the sample container.

$$\Sigma_{abs}\bar{d} = \text{const}\,\rho\,\sigma^{tot}_{abs}\bar{d} = \rho\,\sigma^{tot}_{abs}\alpha$$

$$\sigma^{tot}_{abs} = (1-c)\sigma^{238}_{abs} + c\,\sigma^{235}_{abs}$$

$$\sigma^{238}_{abs} \simeq 2.5 \text{ barns} \qquad \sigma^{235}_{abs} \simeq 700 \text{ barns}$$

Since $\sigma_{abs}^{238} \ll \sigma_{abs}^{235}$ we can simplify the above expression for in the c range of interest ($0 < c < 0.06$) to be

$$\sigma_{abs}^{tot} = 2.5 + 700\ c$$

The thermal flux depression is then given by

$$e^{-(2.5+700c)\rho\alpha} \simeq 1 - (2.5+700c)\rho\alpha$$

where α is one of the calibration constants.

This leads to the following general expression for the total counts of a DUCA measurement corrected for dead time losses and background:

$$C_T = \left((1-(2.5+700c)\rho\alpha)\beta c+\gamma c + (1-c)\delta\right) U\, Q$$

where
thermal flux depression is $(1-(2.5+700c)\rho\alpha)$
thermal fission in ^{235}U βc
fast fission in ^{235}U γc
fast fission in ^{238}U $(1-c)\delta$
U = U weight
U_5 = ^{235}U weight
U_8 = ^{238}U weight.

Since the samples are contained in standard size containers, ρ is proportional to W. In view of the result of the foregoing chapter ($C_T = F_T Q N$ with Q and N being independent of sample features) one can rearrange the above formula with new calibration constants a,b,c,d in the form:

$$C_T = (aU_5^2+bU_5+cU_8+dU_5U_8)Q\cdot N = F_T Q\, N$$

The calibration constants are determined experimentally measuring at least four different standard samples of known U weight and ^{235}U concentration.

4. Results (Fig. 9)

The DUCA instrument has been tested up to now only in the laboratory. The samples used are obtained from powders and pellets of LWR's. In the following Table 1, the main characteristics, the net counts detected and the assay errors in % of ^{235}U are given. In Fig. 9 the discrepancies for the assayed samples are shown. Two calibration curves were made: one for powder and the other for pellets. The following values for the constants a,b,c,d, as already defined, were found:

For powder: a = -6561.9
b = 35689.0
c = 156.78
d = 27.80

For pellets: a = -5565.2
b = 28302.3
c = 263.8
d = 76.8

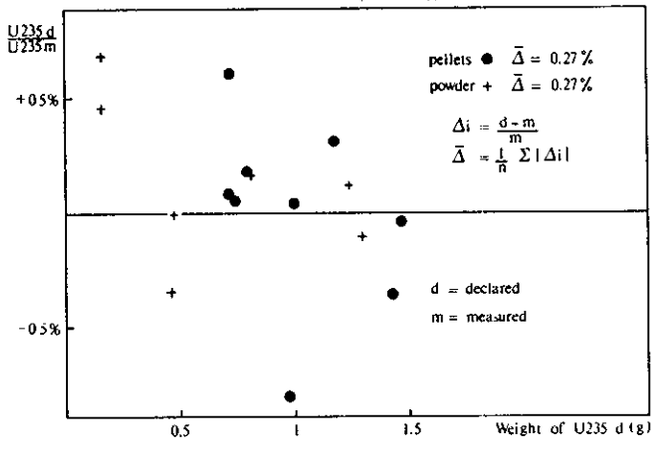

Fig. 9. Comparisons ^{235}U declared vs measured.

TABLE 1 - ^{235}U declared vs ^{235}U measured

Sample No.	Phys. form	Enrichment (%)	U_{tot}(g)	Net counts	Δ %
1	powder	0.713	21.581	8734	0.45
3	"	1.99	23.43	19153	-0.35
5	"	4.022	20.22	28126	0.16
19	"	3.592	34.577	40555	0.10
20	"	4.309	30.074	40812	-0.12
2	"	0.713	21.794	8824	0.68
4	"	1.99	23.268	18994	-0.053
11	pellets	5.08	23.248	33338	0.3
12	"	4.309	22.669	29809	-0.8
13	"	6.41	22.972	37729	-0.06
14	"	3.206	22.238	24179	0.071
16	"	3.592	20.464	24081	0.05
21	"	3.206	22.279	24156	0.61
22	"	3.592	21.732	25426	0.17
23	"	4.309	23.40	30411	0.03
25	"	6.41	22.388	37059	-0.37

$$\Delta\% = \frac{^{235}U \text{ declared} - {}^{235}U \text{ measured}}{^{235}U \text{ measured}} \%$$

The mean value $\bar{\Delta}$ of the $|\Delta_i|$ values is for pellets and for powder the same. It is

$$\bar{\Delta} = 0.27\%$$

The mean values of the Δ_i values were determined as well and their standard deviations for both powders and pellets. The following values were found:

For powders: $\frac{1}{n}\sum_i^n \Delta_i = 0.14\%$ with standard deviation 0.34%;

For pellets: $\frac{1}{n}\sum_i^n \Delta_i = 0.0001\%$ with standard deviation 0.40%.

Usually the powder is more hygroscopic if confronted with pellets. If we do not correct the uranium content for the water content generally with powders we can have a higher error than with pellets. Greater errors will be obtained for powders if no corrections are made for their water content.

5. Conclusions

The DUCA instrument provides an automatic control and data evaluation system, to simplify the inspector's in-field activity. The following has been achieved:

- higher reliability by means of the selection of high quality components and regular execution of automatic test sequences;
- easier operation of the measurement system, used by the inspector, via personal computer, guided step by step and with the aid of a symbolic panel;
- the very fast system of movement of the ^{252}Cf sources, the fast neutron counting chain (dead time about 1 μs) and a good calibration formula for low enriched uranium provide the possibility for accurate measurements (0.3%).

References

1. V. Vocino et al., "Latest development and implementations of instruments for uranium assay by delayed neutron techniques", IAEA - SM-293/8, November 1986.
2. R. Adam, B. Benoit and H. Meister, "Etude pour la réalisation de DUCA", FMM/N. 53 NDA.
3. P. Agostini, L. Caldon and G.F. Cordani, "DUCA-TN N. ES 4.1300.A.003, June 1985".
4. R. Adam, N. Farese and V. Vocino, "Field Manual for DUCA", NE.80.1571.A.001, May 1986.

ESARDA

EUROPEAN SAFEGUARDS RESEARCH AND DEVELOPMENT ASSOCIATION

1st ANNUAL SYMPOSIUM on Safeguards and Nuclear Material Management

PALAIS DES CONGRES, Salle Albert 1er
Entrance Mont des Arts, BRUSSELS, BELGIUM
APRIL 25/27, 1979

Cosponsored by
COMMISSION OF THE EUROPEAN COMMUNITIES

JOINT RESEARCH CENTRE

A PHOTONEUTRON ACTIVE INTERROGATION DEVICE: PHYSICAL DESIGN, CALIBRATION AND OPERATIONAL EXPERIENCE

A. Prosdocimi, P. Dell'Oro

Commission of the European Communities

Joint Research Centre - Ispra Establishment
21020 Ispra (Varese) - Italy

1st. ESARDA Symposium, Brussels 1979

Abstract

A non-destructive assay of bulk uranium samples can be performed through the active interrogation by neutrons having energies in the keV range. Photoneutrons from ^{124}Sb-γ-Be reaction are used to irradiate the ^{235}U isotope of uranium samples, thus arrangements are taken in order to have a uniform irradiation of the sample volume. The counting of the fission neutrons is carried out with energy sensitive neutron detectors. The response of the method is dependent on many parameters and features of the sample, like chemical composition, physical form, volume, shape, isotopic enrichment. For these reasons, specific calibration curves have been established for several fissile materials and ranges of ^{235}U amounts. This method has been operational in safeguards procedures and it has shown its good practicability and a direct interpretation of the measuring results.

1. Introduction

The method here described is applicable to uranium samples even of large volume and with considerable contents of the ^{235}U isotope, it is based on the active interrogation of the fissile isotope by neutrons of high penetrability but having a subthreshold energy compared to the ^{238}U fission cross section. When bulk samples of fissile material are to be assayed, the irradiating flux is required to have good uniformity over the whole volume of the sample, and enough strength to make the instrument sensitive to small contents of ^{235}U. The neutrons emitted by the induced fissions, as a result of interrogation, will be detected by an array of neutron counters, sensitive to the neutron energy too, therefore able to discriminate fission neutron counts against a background of source neutrons.

Under such conditions, the neutron count can be directly related to the ^{235}U masses on the basis of appropriate calibrations. Being the samples to be assayed so different as chemical composition, physical form and sizes, the response of the interrogation depends on the penetrability of the primary neutrons through the sample and on the degree of moderation the source neutrons undergo while crossing the matrix material. For these reasons, calibration curves have to be established for every type of fissile material. The field of applicability of this method is very wide, covering large ranges of materials, enrichments and masses.

2. Physical Principle

A suitable interrogating neutron source has been found out to be the well known ^{124}Sb-γ-Be photoneutron source; the ^{124}Sb isotope produced by irradiation of antimony in a thermal reactor, decays with a half-life of 60.2 days emitting gamma rays of 1.692 MeV (50%) and 2.088 MeV (11%). At these energies neutrons of 27 keV and 423 keV, respectively, can be yielded by a beryllium target, it can be remarked that these energies are far below the fission threshold of ^{238}U. In the absence of moderating materials, the neutron energy spectrum has a narrow peak able to interrogate the ^{235}U isotope only, and at the same time it assures a satisfactory penetrability as the neutron mean free path in metal ^{235}U is about 12 cm. Assumed the neutron yield of such source to be $3 \cdot 10^6$ n/s. Ci, a photoneutron source loaded with 5 Ci of ^{124}Sb can deliver 1.5×10^7 n/s.

The design of the primary neutron source must take care to introduce the minimum amounts of moderating materials, for this reason the thickness of the beryllium targets is to be kept to a minimum compatible with the efficiency of the (γ, n) reaction, moreover, only heavy materials are employed: tungsten to get an efficient gamma shielding of the source, lead for the biological shielding and titanium as neutron reflector.

In spite of the fact that the photoneutron source requires heavy and cumbersome gamma shields, nevertheless it has the advantage that it can be disactivated by extracting the antimony capsules out of the beryllium targets.

As the uranium samples to be assayed could have volumes as large as several dm^3, the cavity where the sample has to be interrogated must have a larger volume with well defined boundaries. For this purpose, an irradiation chamber is provided for just in front of the photoneutron source, surrounded by thick iron walls that have the task both to reflect fast neutrons back into the chamber and to constitute a valid biological shield for the operator.

Particular care is requested by the neutron detectors that must assure the best amplitude discrimination between the pulses produced by fission neutrons and pulses belonging to the strong background of gammas and source neutrons. In spite of the fact that background pulses have low amplitude, they can pile-up and reach

the fission neutron amplitude spectrum.

Gas recoil proportional counters filled with ^4He have been chosen for their good characteristics.

High efficiency in neutron detection is reached by high gas pressure, moreover the ^4He neutron scattering cross section displays a broad peak between 1 and 2 MeV and fits rather well the fission energy spectrum.

Even the angular differential cross section is advantaging the head-on collissions in He(n, n) scattering, which gives higher pulses.

The sensitivity to the γ background, particularly important in order to minimize the pulse pile-up, has been found low enough for the ^4He counter to allow a satisfactory discrimination.

Nevertheless, owing to the multiplicity of large ^4He tubes required to get a good overall efficiency, it could be necessary to join several tubes by groups on more amplifying chains in order to improve the signal to noise ratio.

An estimation of the sensitivity of the instrument can be obtained by examining the following figures referring to an actual instrument already in operation and to a sample of UO_2 enriched at 93% of ^{235}U:

- specific sensitivity, net count = 0.5 $[s^{-1}.Ci^{-1}.g^{-1}]$;
- background count = 0.9 $[s^{-1}.Ci^{-1}]$, equivalent to 2 g of ^{235}U.

An upper limit to the ^{235}U content of the sample is given only by practical conditions, samples up to 5 kg of ^{235}U have been measured so far.

General lay-out. Following the experience of a prototype of photoneutron interrogating device, in operation for a few years, a new machine was designed in 1977 and built at Ispra by the JRC of CEC in 1978. The schedule is to put it into operation within this year.

In Fig. 1 a photo and a general view of this machine is reported.

From a design point of view, attention must be drawn on the fact that the features of the present machine are just one out of many other possible solutions meeting the same task and based on the same physical principles. In our particular case, some basic requirements have partly conditioned the project. The most important was the machine to be transportable either unloaded or loaded with the ^{124}Sb sources (2.5 + 2.5)Ci. Also small autonomous movements along the laboratories were to be foreseen. Nevertheless, during the present project, many different solutions were devised, but the final choice was a large compromise between the availability of the machine and the above mentioned requirements. The present machine is composed by four main parts:

- wheeled trolley and basement;
- source block;
- movable cover of the irradiation chamber;
- counter bench.

The total weight of the ensemble is approximately 3 tons, but it is not difficult to wheel it

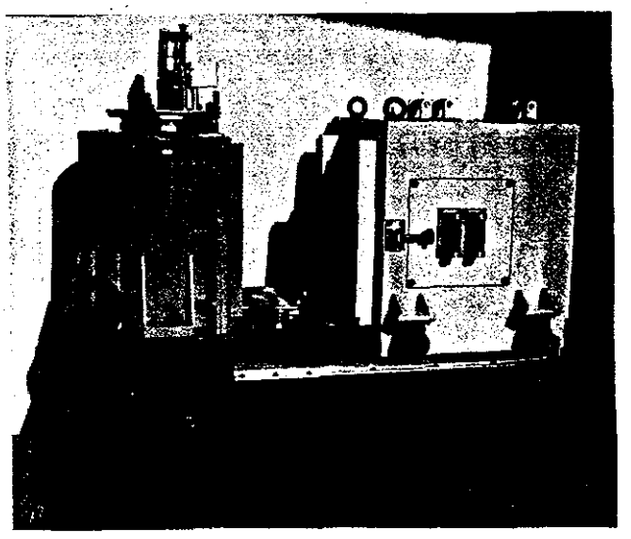

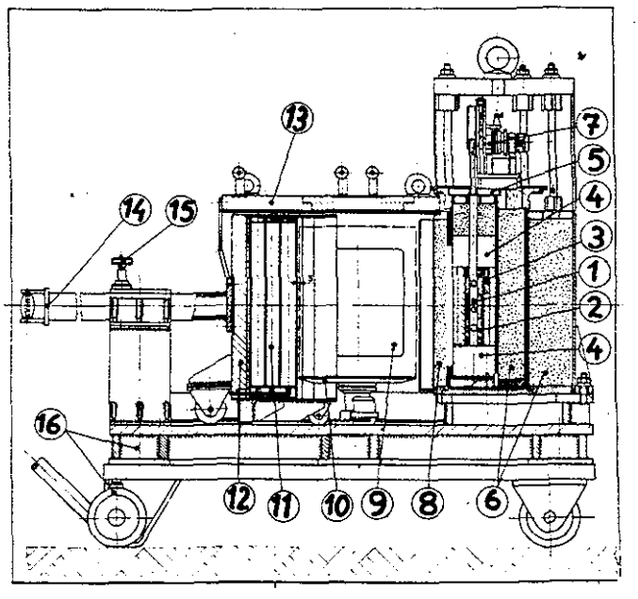

Fig. 1 : View and cross section of the photoneutron interrogating device.

1. ^{124}Sb sources
2. Be thimbles
3. Ti neutron reflector
4. W upper and lower shield
5. Rotating excentric plug
6. Pb biological shield
7. Photo neutron on-off mechanism
8. Front source wall
9. Measuring chamber
10. Turn-table disc (38 cm)
11. Neutron detector bench
12. Fe detector wall
13. Fe chamber cover
14. Detector bench handle
15. Detector adjusting pin
16. Wheeled trolley and basement

along a flat hard floor.

For transport it can be readily disassembled in the above said main parts and in other smaller subassemblies. The 27 counter tubes are the only fragile part of the machine and during transport they are arranged in a special protecting box.

When disassembled, the heaviest part is the source block weighing 1320 Kg. The source block is meant for shielding the gamma radiations of the two ^{124}Sb sources. It is mainly constituted by lead, but a great many parts are tungsten. This metal was chosen both for its good gamma shielding properties and its low neutron scattering section.

A schematic view of the source block is shown in Fig. 2. The source block is provided with two motors. One motor is meant to turn the excentric shield. By means of this excentric disposition of the sources, the radiation dose rate can be strongly reduced during opening of the machine for sample loading and unloading. An interlock system, both electric and mechanical, prevents undue opening of the measuring chamber when the shield is not closed. The second motor drives the sources via a magnetic clutch. When neutrons have to be yielded, "source on", the Sb is drawn into the two beryllium thimbles (outer diameter 45, inner diameter 15, height 60 mm). In order to switch off the source, the clutch current is cut and the Sb capsules drop by gravity inside a tungsten thimble of the same inner and outer diameter as the beryllium ones.

For any undue operation, the sources are automatically scrammed in their recovered position inside the W shield. Health-physics measurements performed in Ispra on the new built machine have given very good results; with (2.5 + 2.5) Ci of ^{124}Sb, no place of the machine surface is above normal dose rate of 2.5 mR/h for gamma, and when neutrons are yielded, it is sufficient to keep a distance of one metre from the machine to stay below permissible exposure.

Both the cover of the measuring chamber and the counter bench are movable and roll on wheels along rails fixed on the basement. The cover is pushed open during operation any time a measuring sample must be loaded or unloaded from the machine. The two bolts on the cover sides are normally not in use during operation, but fastened only during transport.

At the centre of the measuring chamber a motorized turn-table is placed. The purpose of rotating the sample during the irradiation is to get a more uniform response when the sample has not a cylindrical mass symmetry. The measuring samples are placed on the turn-table disc which supports up to 100 Kg. Though its weight is about 650 Kg, opening and closing the chamber cover is fairly light when the machine is well horizontally settled.

In normal operative conditions, the machine can perform about thirty samples on hour. The two main functions of the chamber cover are:
- biological shielding;
- reflecting neutrons to increase countrate.

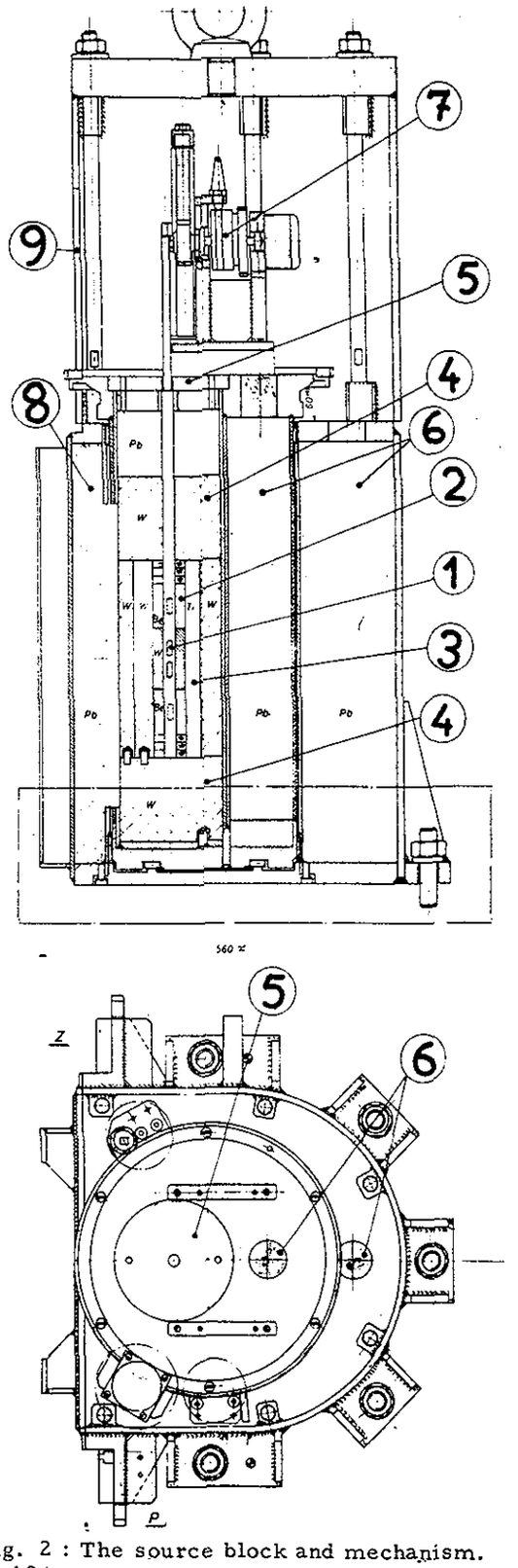

Fig. 2 : The source block and mechanism.

1. ^{124}Sb sources
2. Be thimbles
3. Ti neutron reflector
4. W shields
5. Rotating excentric plug
6. Pb biological shield
7. Photoneutron on-off mechanism
8. Pb front source wall
9. Transport cap

The wall of the chamber cover is made of iron, 5 cm thick, and internally sheathed by 1 cm stainless steel. Since iron is a good reflector for neutrons around the energies of the Sb-Be source (24 KeV) and also for fission neutrons, an increasing of about 50% in count rate is due to neutron saving of reflector.

Also the neutron counter bench is movable along the bottom of the basement. It is driven by means of a long handling rod. Its position is set by means of a pin blocking directly the rod to a column in which the rod slides and is guided.

The position of the counter bench is set in function of the diameter of the turn-table disc in order to keep the counter as close as possible to the measuring sample and the sample as close as possible to the source wall. (Fig. 3b). Since the efficiency of the instrument is strongly decreasing as soon as counters, sample and source are put far apart from each other, the assays are performed using the smallest possible disc for every family of samples. Yet sometimes it is impossible to get the sample diameter (or its general outer dimensions) fit the disc diameter.

Three discs are foreseen: diameter 12, 20 and 38 cm. Following the operation experience of the prototype machine (six inventory campaigns were already performed with that machine), the disc which is likely to be most used is the smallest one. About 95% of samples we have dealt with are canned into iron tins of maximum outer diameter of 12 cm. Only few stainless steel bottles have an outer diameter of 15 cm.

When a disc has to be mounted on the turntable, the position of the turn-table has to be readjusted on the machine basement and the counter bench has to be moved in the new position according to the disc diameter. Five mm clearance is allowed between the disc and the counters and the source wall. The turn-table height is not adjustable. There are only two possible levels. One bottom position is used only in case of very high samples (max. height 50 cm). The response of the machine is not good in the very low positions. Some 50% or more is to be expected as response decreasing in this area. The normal operative level of the turn-table is about 15 cm above the first one (about 30 cm above the bottom of the chamber).

In this position, samples of about 30 cm height can still be measured and the response curve along vertical axis is mostly high and flat. During the first laboratory tests on the machine the following data were measured:

Table I : Relative response of a ^{235}U sample along the vertical axis of the discs in their respective geometries

Disc diam. (cm)	Normalized minimum count	Normalized maximum count	$\frac{\text{min}}{\text{max}}$
12	0.82	1.00	0.82
20	0.57	0.66	0.86
38	0.27	0.30	0.89

The support of the counter bench is a heavy iron wall. It is internally sheathed with 1 cm of stainless steel and carries the 9 boxes of the neutron counters.

Besides holding and driving the counters, the function of the support of the counter bench is the same as for the chamber cover, i.e. both to shield the radiations inside the measuring chamber and to act as a reflector for inner neutrons.

4. Detectors and Electronics

Suitable neutron detectors to be employed in this instrument should have a high neutron efficiency together with a low gamma sensitivity, furthermore they should be able to discriminate the pulses of the fission neutrons against the pulses of the 27 keV photoneutron source. Proportional counter tubes of 5 cm diameter and 50 cm length, filled with Helium-4 gas pressurized at 15 atm , have been adopted;

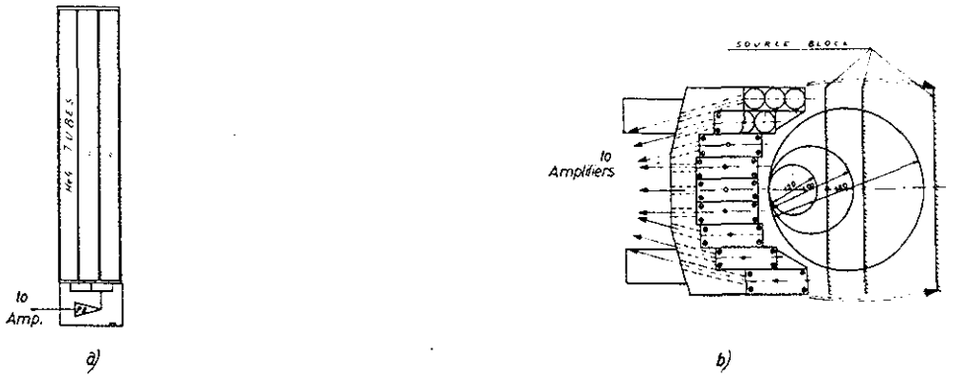

a) b)

Fig. 3 : The neutron detector: a) three counter tubes assembled in a modular supply and preamplifier unit; b) the array of nine units around the sample plates in the irradiation chamber.

indeed the elastic cross section of ^4He has a peak which emphasizes the detector sensitivity to fission neutrons.

Because of the high filling pressure, the signal pulses are rather long, fortunately we have seldom high counting rates, but the pulse length could produce unwanted pile-up effects. It will be for reducing the pile-up of gammas and source neutron pulses that the counters have been ganged together by groups of three, each group having individual analog electronic chain as far as the threshold discriminator. Eventually the 0.5 µs shaped pulses delivered by the nine chains are mixed and counted. One scaler-timer is sufficient to read the result of the measurement, but a microprocessor will soon replace the readout unit and it will be able to calculate the net counting rate, to select the most appropriate calibration parameters delivering as final reading the ^{235}U mass contained in the assayed sample. Some care should be devoted to set the discriminator threshold at a suitable level for counting the most of the fission spectrum with a high rejection of gamma and photoneutron pile-up background (Fig. 4). The neutron recoil spectrum obtained with a ^{252}Cf source of spontaneous fission has to be compared to the similar spectrum of an irradiated ^{235}U sample under active interrogation where the primary source background is present. The threshold level setting gives an idea of the efficiency of the useful count (Fig. 4).

Each counter box, containing three tubes, (Fig. 3a), is interchangeable with any other one and it can be replaced easily by a spare box in case of failure. The H.V. supply line and the preamplifier are common to the counters of the same box and all the circuitry is well protected against mechanical injuries and environmental moisture. The total of 27 counters, distributed among nine boxes, is arranged in vertical position into the irradiation chamber (Fig. 3b), according to a packed semicircular array surrounding closely the sample.

Practically the whole counting efficiency, estimated at 1.5% of the total of fission neutron emitted, is rather uniformly shared among the nine units, namely at ± 8%.

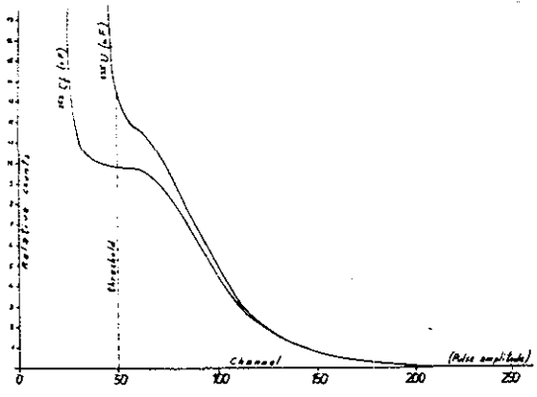

Fig. 4 : Pulse amplitude spectra of the ^4He recoil proportional counter produced by a ^{252}Cf (S.F.) source and by a ^{235}U (n, F.) sample irradiated by photoneutrons.

5. Calibration

The method of active ^{235}U assaying is essentially a relative measurement when the following conditions are satisfied:

a) the irradiating source must have the same energy and intensity;
b) the counting efficiency of the electronics must remain constant, in other words, good stability of H.V. supply, amplifier gain and discriminator threshold should be assured;
c) the counter bench must have a well defined geometry around the sample;
d) the sample must have the same composition and to be in the same mass range as required by the calibration;
e) the sample must occupy the same position and the same volume in the irradiation chamber.

The conditions a) and b) are assured by adopting a normalization sample, which always measured in the same manner before every assay, checks the sensitivity of the instrument, taking into account in such a way the ^{124}Sb source decay and any other drift inherent to electronics and geometry.

To satisfy the conditions d) and e), actual samples with a wide ^{235}U mass range should be available, in order to cover all the practical cases. The ^{235}U contents of the calibration samples must be known with sufficient precision and without any systematic error, indeed random errors on the masses could be minimized by a least square fitting of the calibration points. Fig. 5 displays a typical calibration curve.

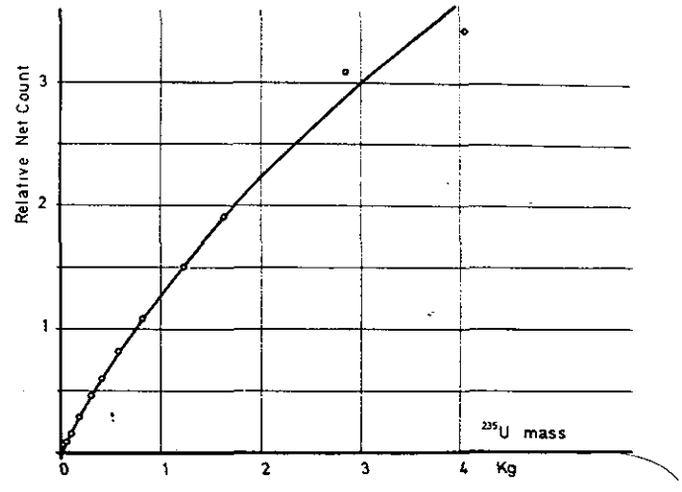

Fig. 5 : A typical calibration curve holding for 93% enriched U oxide powder in 12 cm diameter iron can.

By assuming as independent variables of a calibration the ^{235}U mass, say M235, and the correspondent net count N, as it will be defined in no. 6, the experimental points can be fitted satisfactorily by a power function of the type

$$M_{235} = a \cdot N^b \qquad (1)$$

where of the two parameters a represents the amplitude and b the shape of the calibration curve, both to be calculated by a least square fitting. By this procedure, different sets of calibration parameters a and b have been established for several materials, particularly for

uranium metal
uranium tetrafluoride
uranium oxide powder
uranium oxide pellets
uranium carbon coated particles
uranium and thorium oxide
uranium and aluminium cores

with enrichments up to 93% ^{235}U and mass ranges up to about 5 Kg of ^{235}U. Of course, one has to take into account also the nature and the size of the container for possible neutron energy degradation.

The calibrations established until now and able to satisfy the most of the practical cases are in the order of fifteen, anyway when their precision has to be checked the shape of the calibration curve, namely the b parameter, is hold unchanged, while the a parameter will be renormalized on a point corresponding to a sample the mass of which has been well measured by destructive analysis.

6. Measuring Procedure

Before carrying out any assay on uranium samples, two preliminary measurements have to be performed, namely the background counting rate C_b due to gammas and neutrons from the source, and the counting rate C_o of the normalisation sample. In our case, it has been adopted as normalisation sample a set of five U-Al cores assembled vertically on a rack which holds them parallel and apart one from the other. The total amount of ^{235}U contained in the normalisation sample M_o is of the order of 75 g; such a type of fissile material has been preferred because its good mechanical definition and stability assures a long term reproducibility.

To assay an unknown sample of uranium, the gross counting rate obtained by its active interrogation will be corrected and reduced to the net specific count

$$N = \frac{C - C_b}{\frac{C_o - C_b}{M_o}} \qquad (2)$$

Afterwards the most appropriate calibration should be chosen after having taken into account the nature and the characteristics of the fissile sample, then the result of the ^{235}U assay can be derived by the net count through the relationship (1).

The procedure described here is currently applied during the physical inventory taking and this method of active interrogation has proved to have a rather wide application field and to give results of the precision of few percents.

7. References

/1/ O. Menlove et al., Nucl. Techn. Vol. 19 p. 181, 1973.

/2/ G. Birkhoff et al., Euratom Internal Report, Ispra 1661, 1975.

ESARDA

EUROPEAN SAFEGUARDS RESEARCH AND DEVELOPMENT ASSOCIATION

2nd ANNUAL SYMPOSIUM on Safeguards and Nuclear Material Management

Adam Ferguson Building
EDINBURGH, SCOTLAND
26th–28th March, 1980

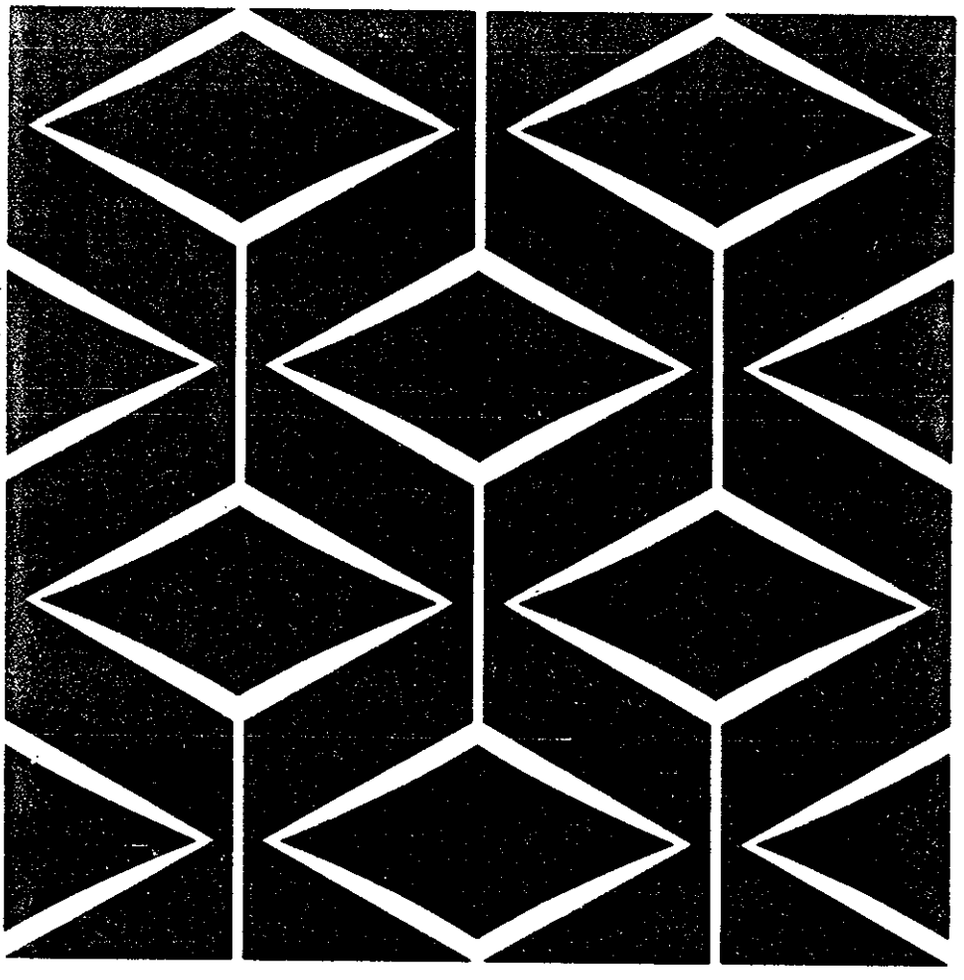

Cosponsored by
COMMISSION OF THE EUROPEAN COMMUNITIES

JOINT RESEARCH CENTRE

PERFORMANCES AND OPERATION OF A PHOTONEUTRON ACTIVE INTERROGATION SYSTEM FOR NON-DESTRUCTIVE ASSAY OF U-235

A. Prosdocimi, P. Dell'Oro
Commission of the European Communities
Joint Research Centre - Ispra Establishment
I-21020 Ispra (Va), Italy

2nd ESARDA Symposium, Edinburgh 1980

Abstract

A NDA instrument operating on the basis of the subthreshold neutron interrogation of uranium has been constructed to fulfill the requirements of the physical inventories in the framework of nuclear safeguards.

Laboratory measurements carried out on the instrument assessed its performances according to the sensitivity of the neutron detectors to the fission neutrons and to the response of the whole system to a sample of U-235.

Calibration procedures are described, and the results obtained with actual uranium samples are commented in view of the practical utilisation of such NDA system.

1. Field of Application

The method of active neutron interrogation using subthreshold neutrons yielded by a (γ, n) source, has typical applications in the assay of the U-235 content of fissile materials.

In this case such a method has been implemented by PHONID, PHOtoneutron Interrogation Device[1], the application field of which is defined both by its specific features, i.e.

- strength of the neutron source,
- volume of the irradiation chamber,
- gamma counting background of the neutron detectors,
- sensitivity of the neutron detectors,

and by factors such as

- neutron mean free path in the sample,
- homogeneity of the sample over its whole volume.

PHONID in version No. 2 may be loaded with 5 Ci (in any case with no more than 10 Ci), of radioactive Sb-124 and by taking into account the overall sensitivity of the device, a response equivalent to the background counting corresponds to an amount of about 2 g of U-235.

The measuring cavity can accommodate cylindrical samples up to a diameter of 38 x 40 cm, however, in the current applications, an upper limit is imposed to the sample size by neutron multiplication effects; it is recalled here that samples up to 8 kg U-235 have been assayed so far.

In order to give an idea of the neutron propagation through a fissile sample, it is remarked that the mean free path of 25 keV neutrons in U-235 with a density of 18.9 g/cm^3 is of the order of 5 cm, to be compared with the transversal radius of a cylindrical sample.

Furthermore, also plutonium could be assayed by PHONID in the active mode, taking into account the background of spontaneous neutrons which is counted together with the interrogation count. The former is a fraction of about 60% of the latter. Practical assays of plutonium are still to be investigated.

2. Operation of PHONID

Such a device has the disadvantage of being rather heavy and cumbersome and it has to be considered a stationary instrument to be installed permanently in a plant. This is essentially due both to heavy γ-shielding of the photoneutron source and to the fast neutron reflectors. In practice, the instrument has demonstrated a high degree of versatility: it accommodates samples of different shape and size; it operates with the neutron reflectors removed; and assays are also possible with a part of the counter tubes removed or not operating. The only limitation is the need of specific calibration for every kind of fissile material to be assayed, the mass content of U-235 being the only variable to be referred to the response of the instrument.

The reproducibility of the detection efficiency of PHONID is not a constraint as each run of assays is normalised to a measurement of a reference standard. This normalisation has the advantage of also correcting for the decay of the γ-source and for every drift in the detector and in the electronic chains.

Practically, each half-day run is preceded by a measurement of the source background, i.e. gamma pile-up and photoneutrons, and by a normalisation standard assaying. This is sufficient to correct and normalise with adequate accuracy a run of assays for half a day.

It is mentioned here that the normalisation sample is made of a set of five plates of U-Al cermets containing a total of 74.85 g U-235; the precise value of this mass is not required by the assaying procedure.

3. Calibrating Techniques

Calibrating PHONID is a rather delicate operation, because the response of the active interrogation depends upon many factors,

- homogeneity of the sample,
- volume occupied by the sample in the interrogating neutron field,
- moderating and absorbing power of the material for the 25 keV neutrons,
- the same properties of the material for the fission neutrons.

For these reasons individual calibrations should be established for every family of samples, taking account of chemical composition, U-235 enrichment, matrix materials, canning, etc.

Practically, a calibration requires several samples of the same nature, able to cover the whole U-235 mass range with useful calibration points. Furthermore, by a least-squares fitting the curve is smoothed to an algebraic function, which procedure minimises possible random inaccuracy of the masses. In order to detect systematic errors, it should be sufficient to determine precisely just one sample and to normalise the entire curve to it.

A function which suitably fits the relationship between the U-235 mass M_{235}, and the response N of the interrogation[1], is the power function

$$M_{235} = a\, N^{b}$$

where a and b are the parameters to be determined by the calibration. On a "log-log" graph, b represents the slope of the straight line and a produces a translation of the line. Fig. 1 displays a set of calibration curves for different materials holding for given mass ranges.

4. Assaying of U-235

During a physical inventory taking it is of

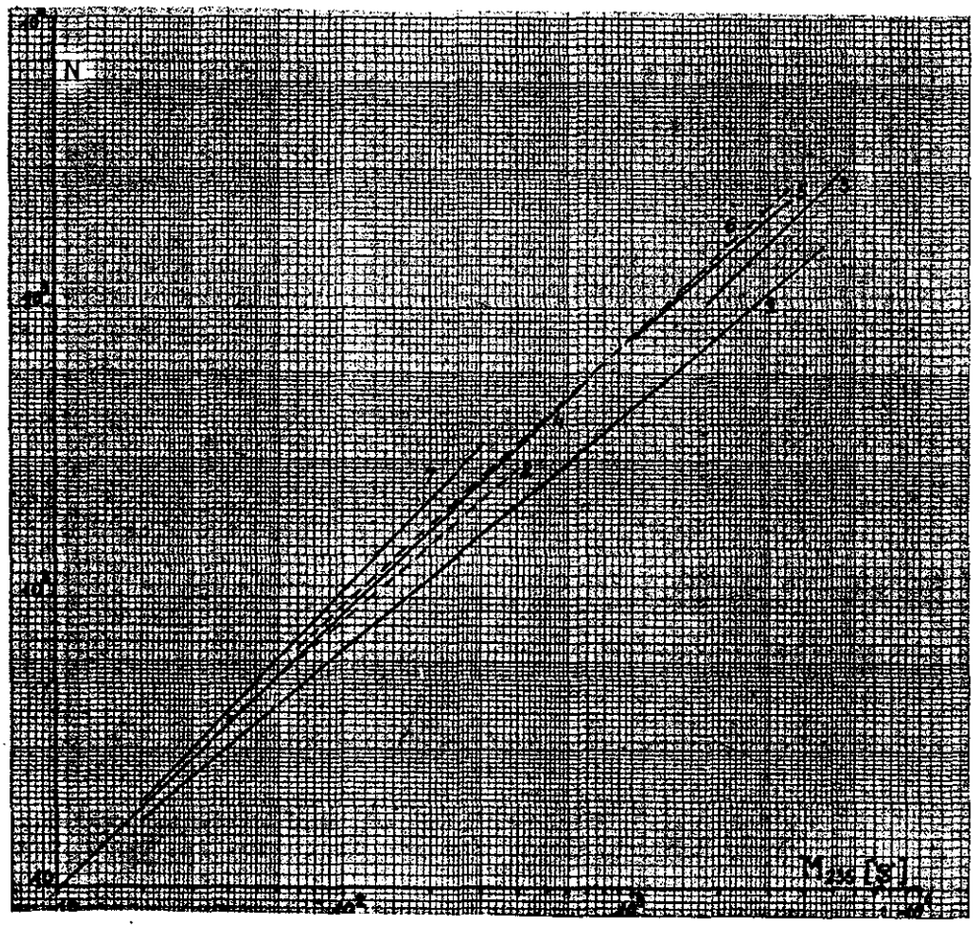

Fig. 1 - Calibration Curves of PHONID-2 for HEU: 1 = metal uranium; 2 = U-Th oxide; 3 = U_3O_8 powder; 4 = U-Al cermet cores; 5 = UF_4 powder; 6 = U_3O_8 powder; 7 = U-Th oxide, carbon coated. All samples enriched at 93% U-235, except No. 6 which is enriched at 80%.

utmost importance to make a good choice for the calibration curve to be adopted, in order to get the mass of U-235 derived from the instrument response, i.e. from the count rate produced by the assayed sample, referred to the count rate of the normalisation sample, when all the remaining conditions are reproduced.

Afterwards, the measurement procedure is straightforward, attending furthermore to the range of validity of the calibration for the U-235 mass.

In order to give an idea of the different effects, some response curves are displayed. Fig. 2 shows the softening effect of matrix materials on the energy spectrum of the interrogating neutrons.

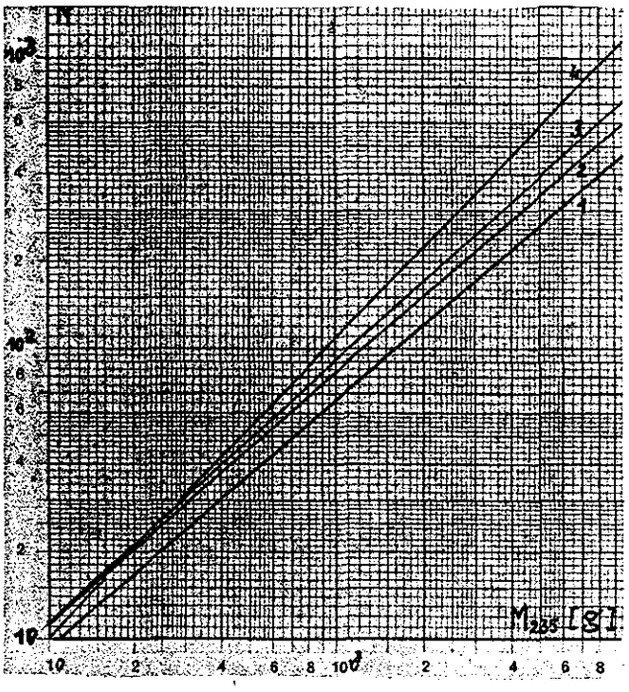

Fig. 2 - Influence of a matrix material added to uranium: 1 = none (i.e. pure uranium); 2 = thorium; 3 = oxygen or aluminium; 4 = thorium and carbon.

Fig. 3 has been obtained with the same material in two different physical forms.
Fig. 4, finally, shows the enrichment effect on the response of metal uranium.

It must be pointed out that such comparisons are not exhaustive and it would not be advisable to draw from them conclusions of general validity.

5. References

1. A. Prosdocimi, P. Dell'Oro, "A Photoneutron active interrogation device: Physical Design, Calibration and Operational Experience", Proc. of ESARDA Symposium, Brussels 1979, p. 297.

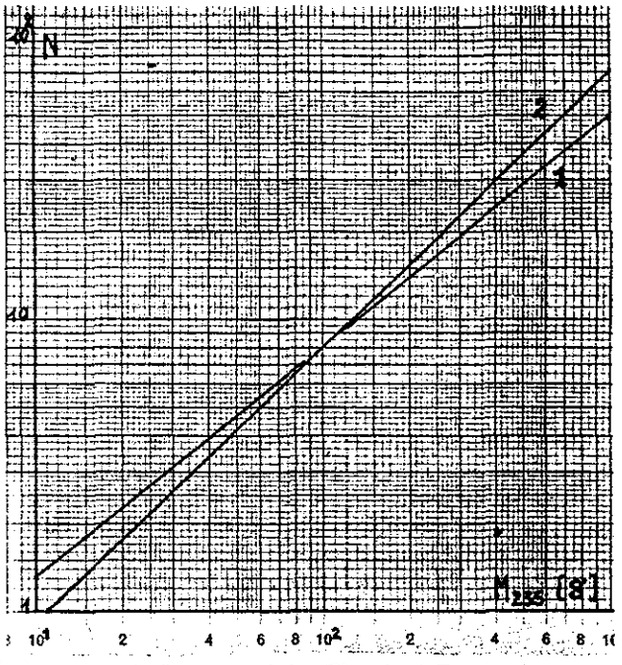

Fig. 3 - Influence of the Physical Form: 1 = UO_2 pellets, 35% U-235; 2 = UO_2 powder, 35% U-235.

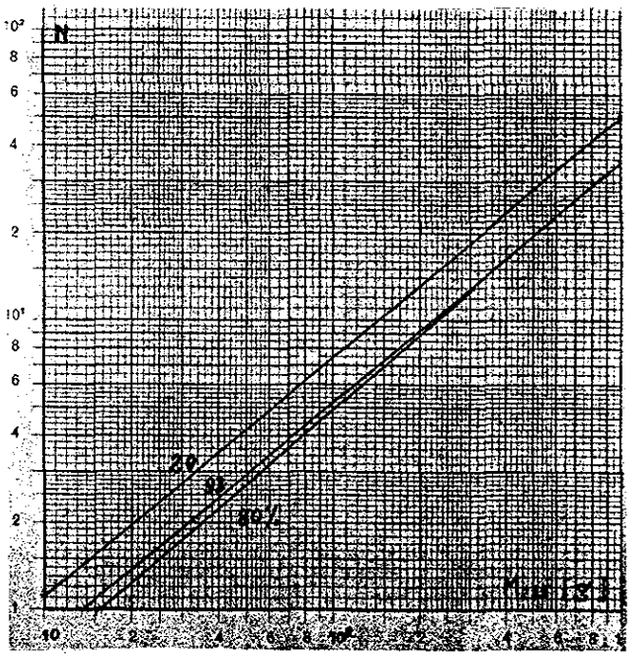

Fig. 4 - Influence of U-235 Enrichment for Metal Uranium.

Progress in PERLA

S. Guardini
CEC, JRC-Ispra

1. Introduction

The last occasion on which we wrote about the **PER**formance **LA**boratory (PERLA) in the ESARDA Bulletin was in No. 9 of 1985 /1/. That article was a rather comprehensive view of one of the tasks of PERLA, i.e. performance assessment, showing the importance of studying Safeguards instrument performances in a field environment, where the error behaviour is not the same as in the laboratory.

It was from a practical point of view a proposal, the realization of the laboratory being still distant.

Now, after two years, we can say that we have an operational facility PRE PERLA where all the tasks of PERLA can be pursued, and have been already initiated.

The general aim of PERLA /2,3/ was identified from the beginning as bridging the gap between the laboratory development and the application of Safeguards instruments and techniques in an industrial environment.

The laboratory is oriented specifically to NDA and C/S techniques; this paper is mainly concerned with NDA aspects.

The main themes of concern are :

- assessment of the performances of instruments and methods in near field conditions;
- periodic calibrations under well defined conditions of instruments used routinely by inspectors and operators in industrial facilities;
- training of inspectors and operators;
- development of new methods according to needs.

The aim of this paper is to give a progress report of the status of PERLA. Four aspects are mainly treated here :

1. the set up of the laboratories and their structures in the ESSOR complex (section 2),
2. the procurement and characterization of PERLA Standards (PS) (section 3),
3. construction of user oriented instruments (section 4),
4. training (section 5).

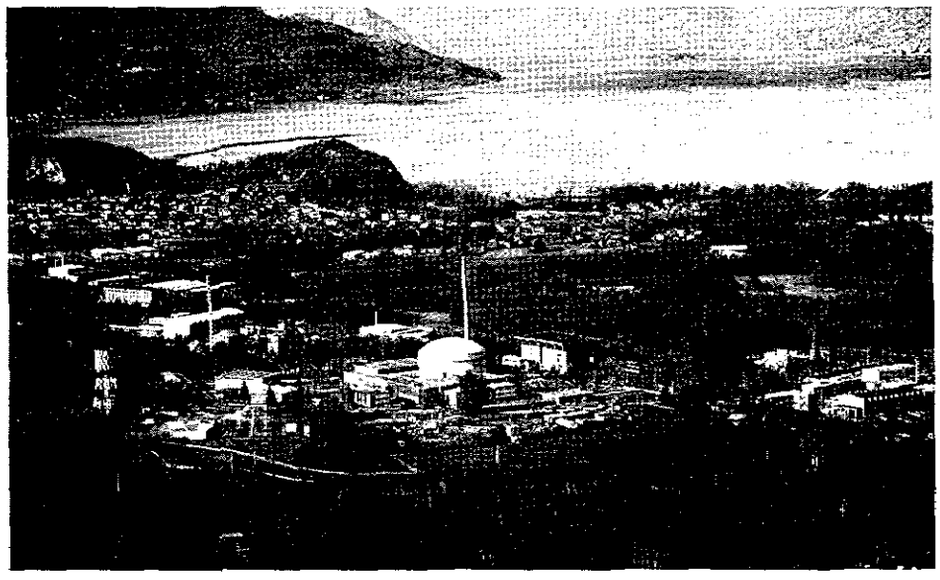

Fig. 1 - JRC-Ispra with a view of ESSOR complex

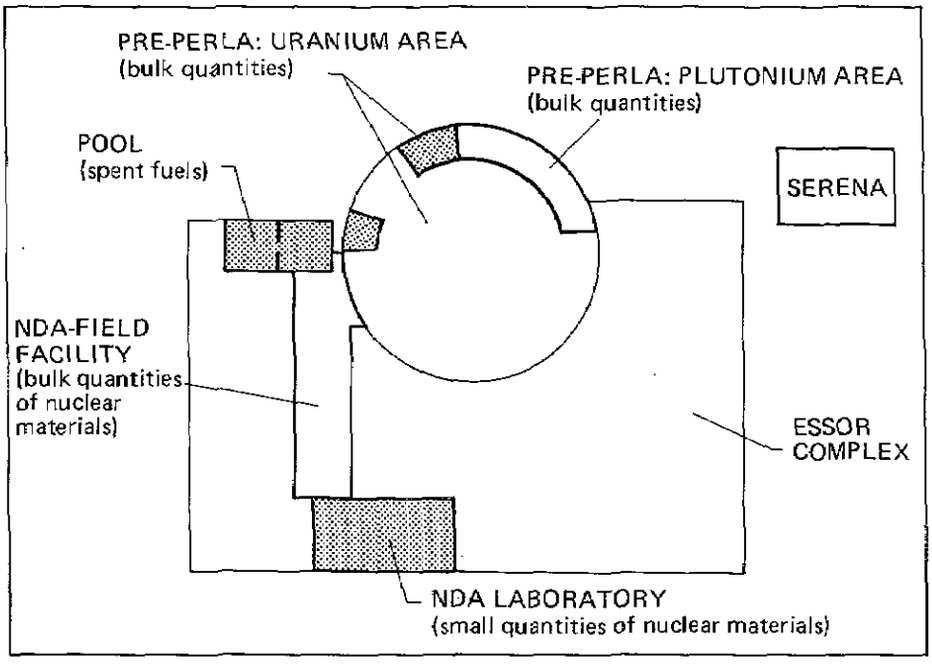

Fig. 2 - PERLA laboratory - general view

2. Set-up of Laboratories

PERLA is a laboratory which uses different facilities : PRE PERLA, the Non Destructive Assay (NDA) laboratory, the spent fuel pool, the NDA-field facility and SERENA (Figs. 1 and 2).

Some of the facilities are used only and specifically for Safeguards purposes (e.g. PRE PERLA), others (e.g. the pool) are shared with other programmes.

2.1 PRE PERLA facility

The PRE PERLA laboratory (Fig. 3) has been built inside the ESSOR reactor containment building. It has been equipped to measure bulk quantities of fissile materials (U and Pu). Its name comes from the fact that as the NDA-field facility has still to be constructed in another room, it was decided

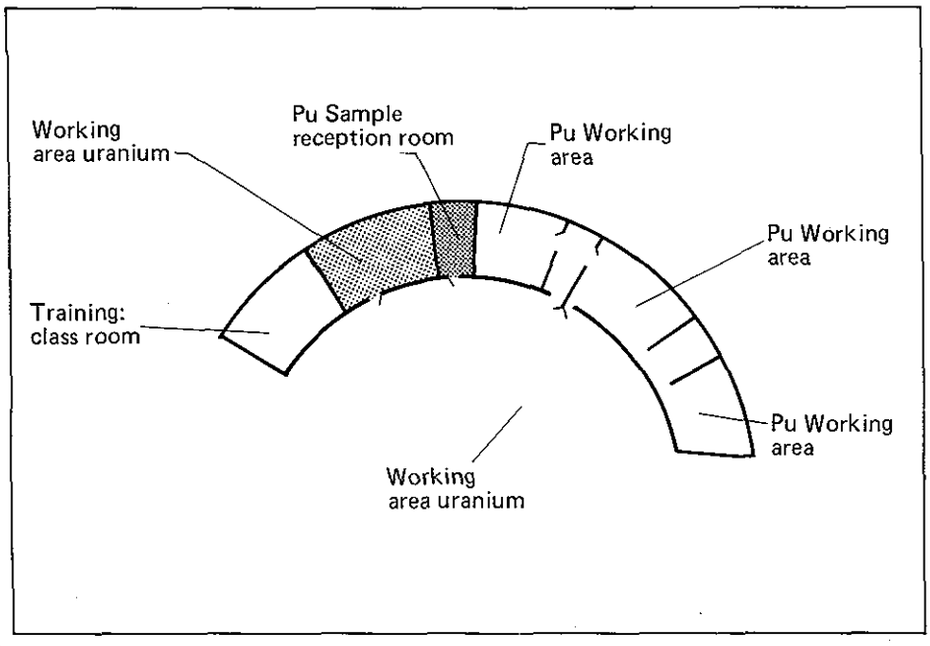

Fig. 3 - Schematic view of PRE PERLA

in 1985 to anticipate the beginning of PERLA type experiments. For this purpose four laboratories, storage rooms, handling rooms have been made available for the Safeguards programme in an already protected zone, where bulk quantities of fissile materials in sealed samples could be measured. PRE PERLA could then be set up and became operative at the beginning of 1987.

Calibration experiments with the ^{235}U inventory have already been carried out, as well as training (see section 5). In Fig. 4, PRE PERLA is shown during the simulated High Enriched Uranium (HEU) Physical Inventory Verification (PIV) training course / 4 / of July 1987.

2.2 NDA laboratory

It is a complex of 7 laboratory rooms where small quantities of fissile materials (~ 200 g) can be measured. Operative since 1986, it is dedicated to research and development of NDA techniques.

2.3 The spent fuel storage pool

Six spent MTR fuels from the ESSOR reactor were discharged in the pond. Four additional LWR spent fuels will also be procured and stored. Training and development of NDA techniques for spent fuels will take place in the pond. The ESSOR spent fuel pool is shown in Fig. 5.

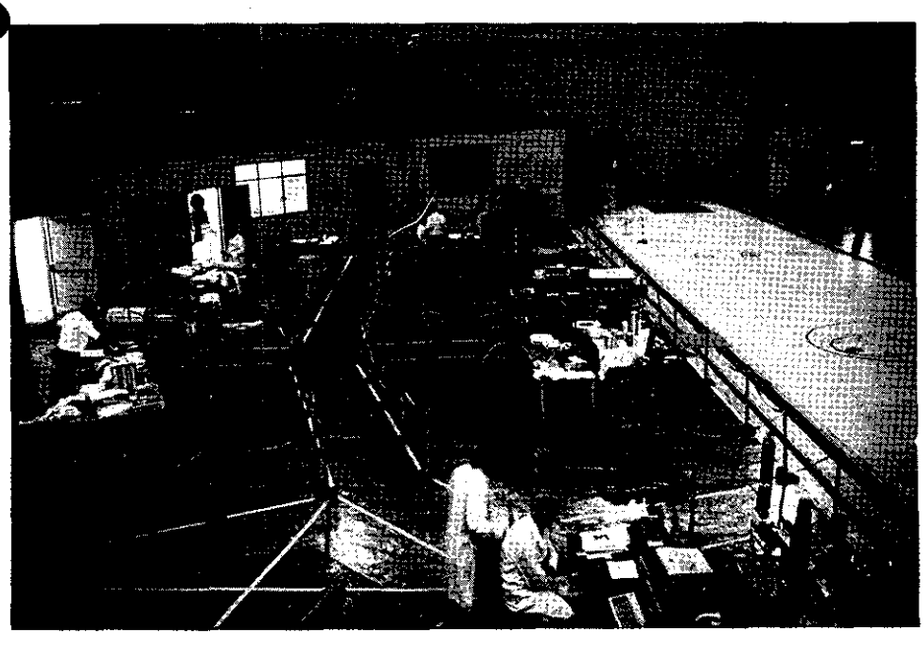

Fig. 4 - Picture of PRE PERLA during HEU Physical Inventory Training course of July 1987

2.4 NDA-field facility

The NDA-field facility will be realized modifying a large existing laboratory. It will have the same characteristics of PRE PERLA, i.e. measurement of bulk quantities of U and Pu.

The modification works will start in 1988 and will be finished in 1990 giving the facility the appearance shown in Fig. 6.

2.5 SERENA

SERENA is a Safeguards exhibition and training facility which will be fully equipped in 1988, joining other training facilities in the PERLA area, besides the nuclear laboratories where a large part of the practical training is carried on. SERENA is shown in Fig. 7.

3. Procurement and Characterization of PERLA Standards (PS)

3.1 Generalities

The first absolute necessity of a laboratory that aims to act as a calibration and training laboratory in the field of Safeguards is to have available a large inventory of well characterized and reference materials, representing to the largest possible extent samples that are most commonly encountered in the fuel cycle.

Identifying this inventory was actually the first task of the PERLA team. A further important task was to acquire fissile materials and to characterize them at a high level /5/.

Nevertheless, PERLA cannot and does not intend to substitute the field as far as instrument performance determination is concerned : as mentioned earlier it represents a bridge between the laboratory and the field. Neither can PERLA materials fully replace plant specific reference materials (PSRMs) like those standards that were obtained in a joint effort by Euratom Safeguards Directorate, IAEA and the JRC /6,7/.

That was an exercise which, as well as giving tools for really quantitative accountancy with NDA, gave us all much experience in preparing working standards. It was a positive experience which has been abandoned, maybe too early, if one thinks of the importance of having a frame of well characterized standards for authentication purposes, for the detection of biases, resolution of discrepancies, and, in general terms, for carrying out really quantitative NDA.

Nevertheless, that experience was very useful for acquiring the PERLA standards inventory, because the main rules followed were those suggested by that exercise /8/.

We now have a new task in front of us in the near future : to create close links

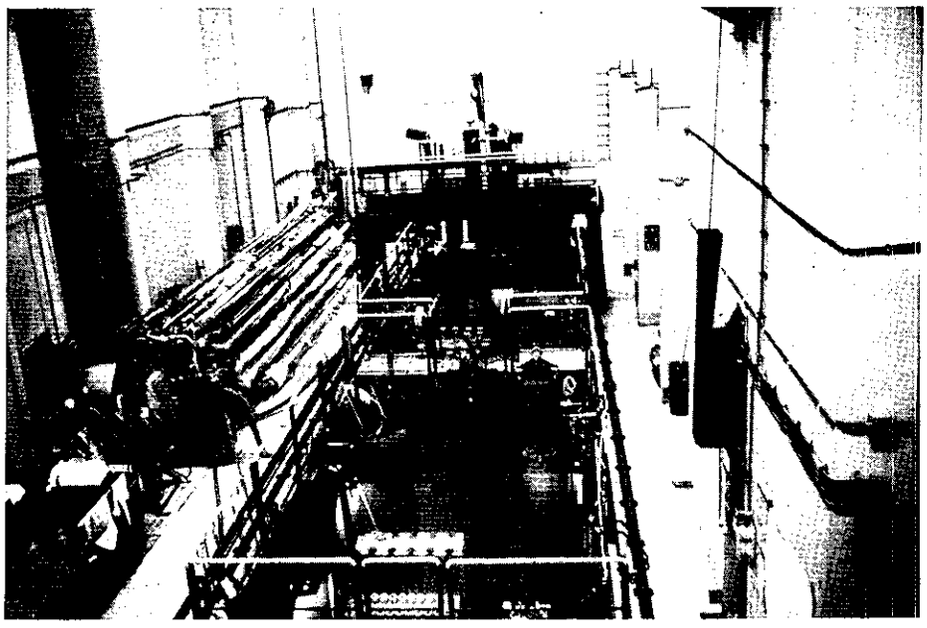

Fig. 5 - View of the ESSOR spent fuel pool

with the field, correlating the large inventory of samples of PERLA with standards already existing or to be prepared in European laboratories and plants.

3.2 Characterization of PERLA standards

Basic criteria for the characterization

As said before, in establishing procurement and characterization schemes for PERLA standards we followed very much the general criteria established when characterizing the PSRMs /8/. Detailed flow schemes were somehow different obviously, because of the different experimental situations encountered for PERLA and the different final use, but many procedures were the same.

The general requirements for PERLA standards we established were :

a. they must be representative of plant samples (e.g. PuO_2 cans, MOX industrial pins, MTR assemblies, etc.).
b. they should be prepared and characterizec for specific NDA methods with defined "performance values" /9/ or "expected overall uncertainty values" /10/. Therefore overall random and systematic uncertainty must be a priori planned so that calibrations with these standards do not introduce an appreciable uncertainty component in the NDA measurements.
c. most of them must belong to the same family, i.e. come from the same original production batch so having the same chemical and isotopic characteristics. In this way, for instance, the gamma spectrometrist can measure the same sample in the form of powder and pellets and pins excluding any influence from the above chemical and physical parameters.
d. their characterization must be traceable back to primary standards.

General guidelines followed in the procurement schemes were :

- define the scopes of specific samples, i.e. the NDA measurement techniques for which the PS were prepared;
- define consequent uncertainty levels taking in mind the above "performance values ";

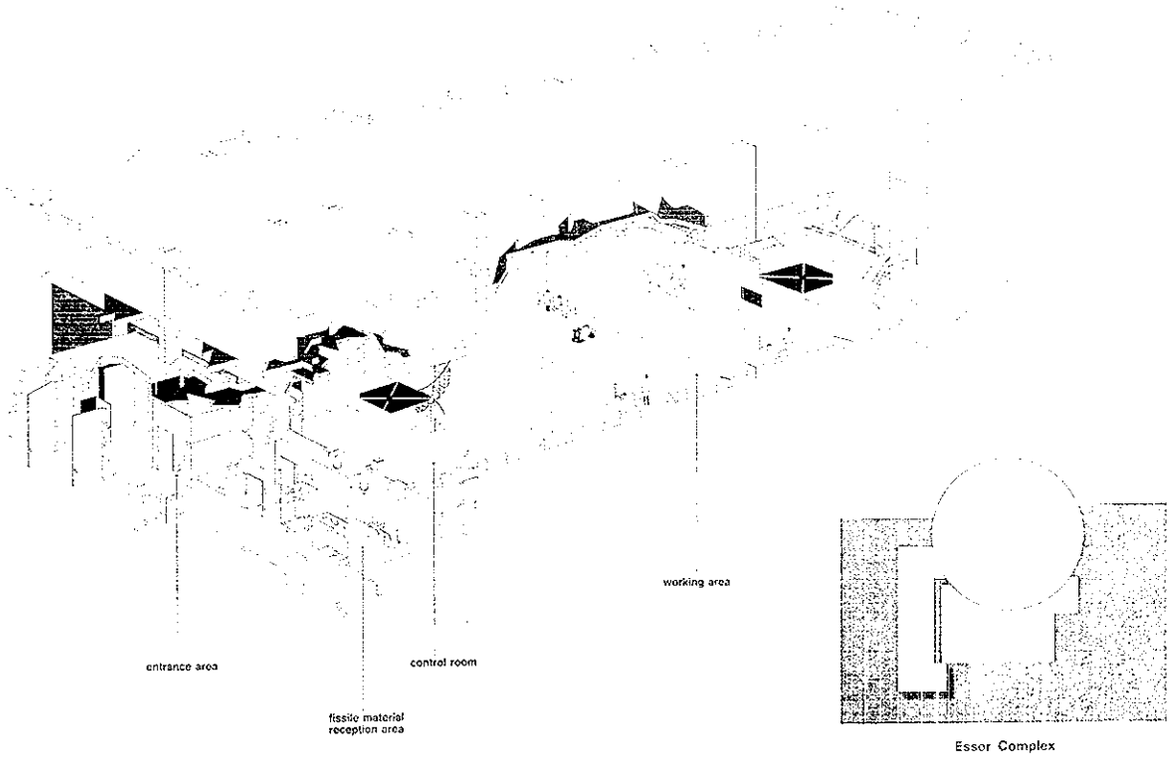

Fig. 6 - View of the future NDA-field facility

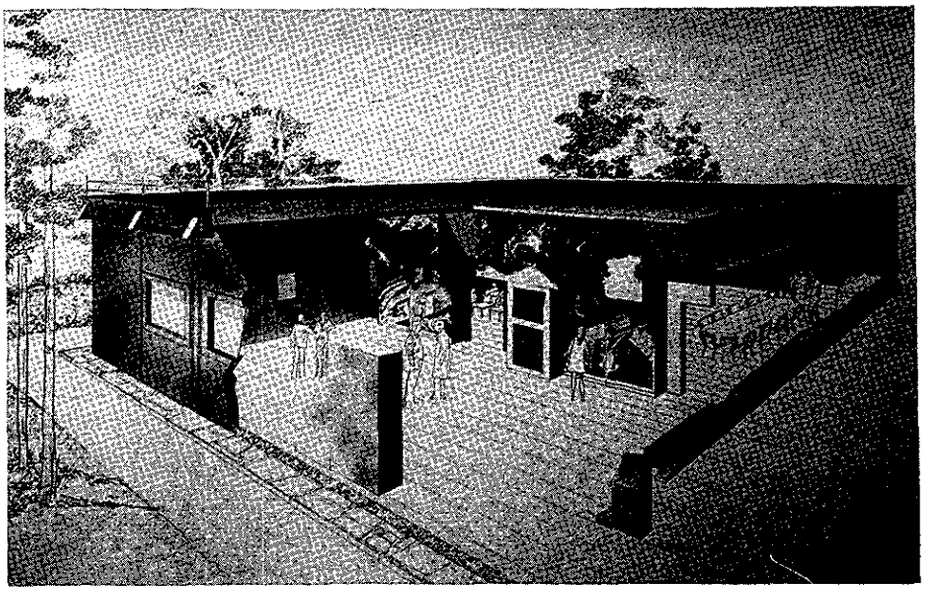

Fig. 7 - The Safeguards exhibition and training facility SERENA

- define preparation and characterization procedures to achieve such levels of accuracy;
- define error propagation schemes and statistical data evaluation schemes;
- define analytical instructions for the DA laboratories;
- prepare PERLA certificates and protocols to fully describe the PS and the procedures followed in their preparation and characterization and to record the traceability to primary standards.

The method followed in characterizing PERLA standards

1. The first important aspect to start with in the logical approach defined above to procure and characterize the standards was to a priori define the required level of accuracy in connection with the NDA technique applied to those standards and with the "expected overall uncertainty values" /10/ of that technique.
   In Table I a list of required accuracies for Pu standards is given together with the so-called "limiting factor", i.e. the technique and the parameter /11/ that imposes such a level.
2. The next step was to study the possibility of reaching such a degree of characterization, looking at the level of accuracy attainable by DA, which is the basis for any characterization. In Table II the typical expected accuracies for different techniques are shown, as defined by the three laboratories taking part in the characterization on the basis of attainable accuracies in DA /12,13/.

Table I - Required overall uncertainty for PuO_2

Parameter	Uncertainty (%)	Limiting factor
Pu content	0.2	calorimetry
^{238}Pu abundance	0.5	calorimetry, γ spectrometry
^{239}Pu abundance	0.2	calorimetry, γ spectrometry
^{240}Pu abundance	0.3	γ spectrometry
^{241}Pu abundance	0.3	γ spectrometry
^{241}Am	0.5	calorimetry, γ spectrometry

Table II - Typical Expected Accuracies of DA Methods

Measurement	Material	Method	σ
Pu-conc.	PuO_2	AgO or Mc. Don.	0.15
	MOX		0.15
U-conc.	MOX	Davies & Gray	0.1
Pu-238	PuO_2	Mass. spect.	0.5
	MOX	α-spec.	1.5
Pu-239	all	Mass. spect.	0.05
Pu-240			0.1
Pu-241			0.3
Pu-242			0.3
Am-241	all	γ-spec.	1.0
U-235	low	Mass. spectr.	0.1
	high		0.03
U-234	high	Mass. spect.	1.0
U-236	high		1.0
U-234	nat.		10
U-236	nat.		?

3. The third step was to define "accurate procedures" for the preparation of the standards and for their characterization with DA and NDA techniques suitable for attaining the required levels of accuracy. "Accurate procedures" means first of all identifying a priori on a preparation flow scheme the possible uncertainty sources; then one must reduce that error component and quantify it.

One example : Pu bearing samples

The preparation and characterization schemes were different for different families of standards; in Fig. 8 one of the five different scenarios is given showing the procurement of an LWR family of MOX powder-pellets-pins from the same batch.

An uncertainty build-up model was then developed which contained all the most important error sources predicted for that family. In Fig. 9, a generalized model for PuO_2 samples is presented showing, in a condensed fashion, the most important steps from where uncertainty could come. Each step was then developed in terms of: a) procedures to be followed to reduce uncertainty in preparation and b) quantitative definition of the error component. With reference to that PuO_2 family the most delicate points were identified as follows :

1. Homogeneity
   - a definition of homogeneity has been developed in /11/ again for different limiting factors or techniques applied; in other words, calorimetry, for instance, is not influenced by an inhomogeneity inside a PuO_2 box, while gamma spectrometry gives an answer on the internal homogeneity of a can.
   - preliminary DA/NDA measurements were done on the original PuO_2 production batches ensuring that internal/external homogeneity was acceptable /14,15,16/.
   - the sampling and DA scheme were worked out and implemented for homogeneity checks (Fig. 10), that gave the sampling component of the uncertainty.
2. Sampling and DA
   A sampling and analytical scheme was prepared taking into account the overall uncertainty required, the error propagation model and the statistical evaluation of the final overall uncertainty that takes into account errors : in the single determination, in the sampling homogeneity and in the interlaboratory difference (Fig. 10).
   Very detailed instructions were discussed with and then given to the DA laboratories, going from the number of repetitions, to the expected uncertainty from

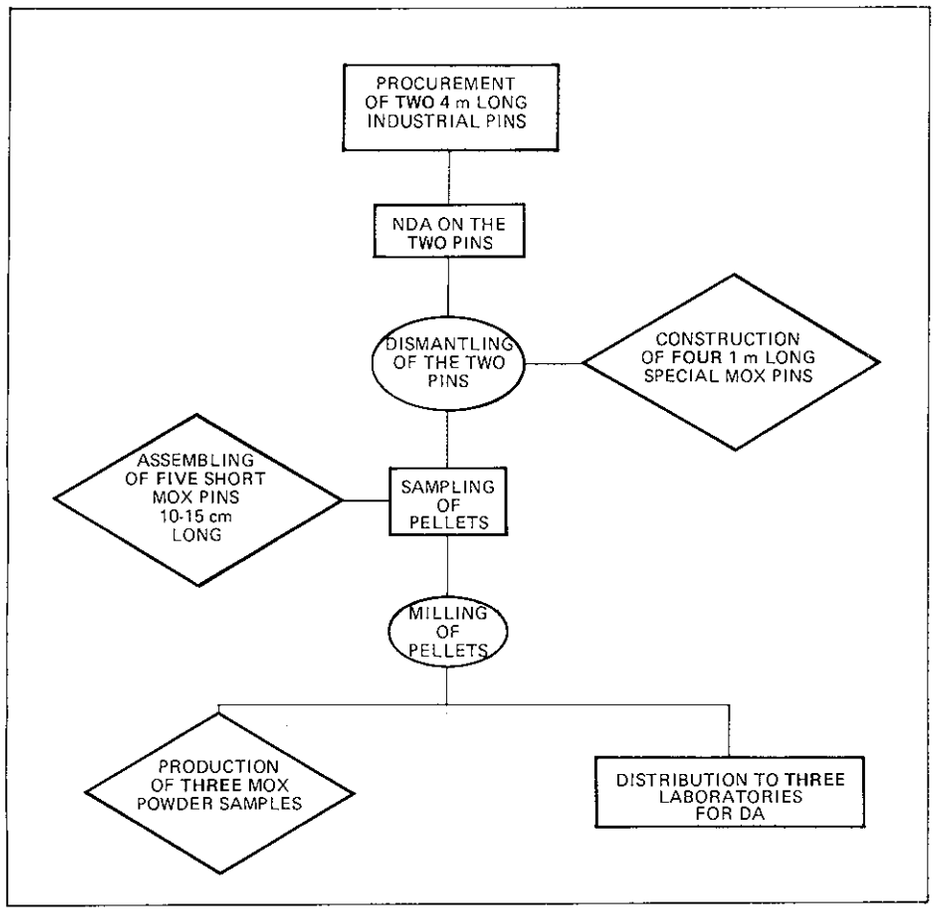

Fig. 8 - Procurement scenario for a reduced-size family concept (Light-water reactor DWR)

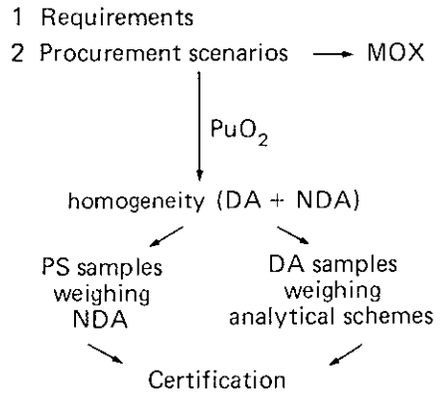

Fig. 9 - Characterization procedures for PuO_2 powder standards

DA (Table II), the nuclear data to be used, down to details such as the type of vial to be used in the analytical treatment (see a typical working protocol in Fig. 11).

3. Weighing
Careful sample weighing protocols have been established both for DA and NDA samples. The laboratories were also required to establish carefully documented balance control based upon standard weights.

4. Humidity
One of the most important parameters which could affect NDA neutron measurements is humidity content. General H_2O content limits were imposed as well as a strict check of the fabrication and sampling procedures, so as to ensure on the one hand a representative sampling and DA analysis, and on the other hand that no further H_2O pick-up could occur after sampling. Actually, the whole preparation and sampling process was carried out in inert atmosphere.

The PERLA inventory

In Table III, the total inventory envisaged for PERLA is summarized. At present, only HEU and Pu bearing samples are in the inventory; LEU and spent fuels are under study and their procurement schemes under preparation. They are expected to be procured for the end of 1989.

4. Construction of Safeguards Oriented Instruments

For some years it has been pointed out and it can increasingly be seen on the basis

Table III - Nuclear Materials for PERLA

Material type			Certification level*
HEU	MTR plates, plates	3 enrichments	4
	MTR assemblies (*8)		4
	UO_2 powders, pellets (g/kg)	6 enrichments	3
	HTR particles, pebbles		3
	Metal buttons (g)		4
LEU	UO_2 powders, pellets (g/kg)		
	UO_2 pins	not yet procured	
	Short assemblies		
	UO_2 CBNM NBS	5 enrichments	*
PuO_2	Small cans (g)	3 burnup	2
	Large cans (kg)	3 burnup	2
	CBNM	5 samples	*
	PIDIE	7 samples	*
MOX	Pins	fast, thermal	2
	Pellets	recycle	2
	powders		4

*) The certification levels are as follows:
1: International reference material or many labs
2: PERLA certificate (3 labs)
3: PERLA certificate (2 labs)
4: PERLA certificate (1 lab)
5: others

of the experience built-up over the years, that the main problem in transferring Safeguards instruments and methods from the developing laboratory to the field is that of producing reliable Safeguards instruments. It is, in fact, evident that most of the techniques when applied have a different (ower) accuracy in the field than they do when used in the laboratory.

It has only recently been realized that, generally speaking, this is due to objective reasons rather than to incorrect application of the instrument. The lack of extensive structurec measurement data bases and appropriate error models delayed the process of understanding. The last point is particularly delicate: we must have in Safeguards a great concern for experimental error definition, particularly in NDA where the error behaviour is quite complex /17,18/.

The definition of target errors in DA for Safeguards was possible without detailed error models, because the samples are always measured in the same laboratory conditions: DA always has the "same" sample. These unmodelled parameters such as homogeneity, sampling errors, etc., from time to time lead anyhow to unexplicable discrepancies.

In NDA where the items to be measured are extremely variable an error model which assigns the same overall error to almost all different combinations of instrument and measured items cannot represent the complexity of the error phenomenology which generally exists when measuring a complex population.

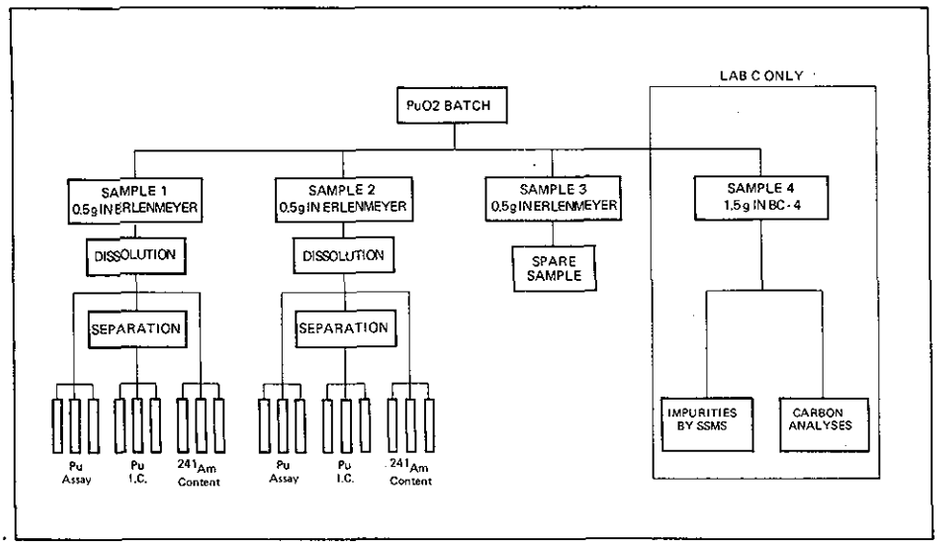

Fig. 10 - Analytical scheme for PuO_2. Same for labs A, B, C

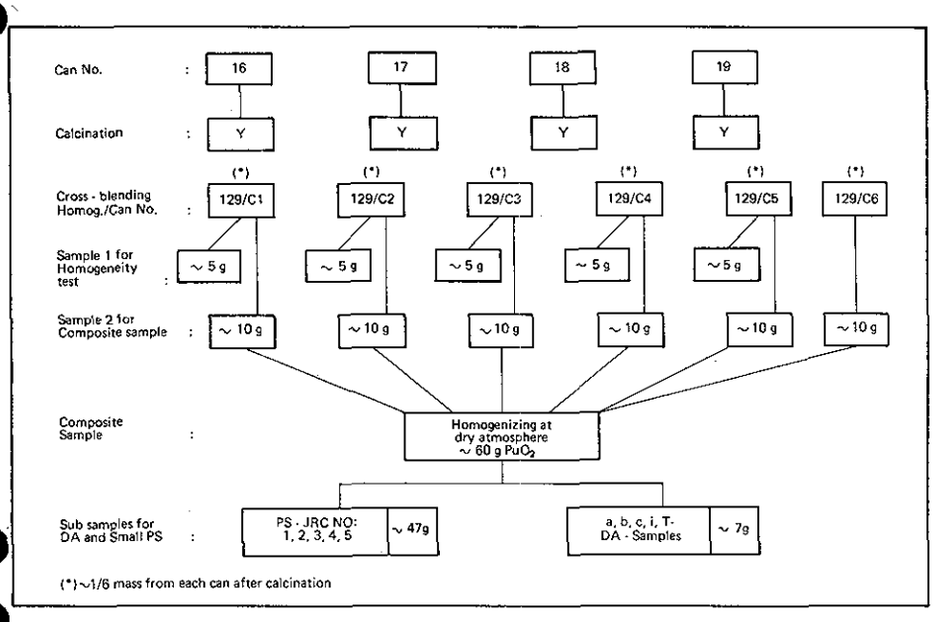

Fig. 11 - Preparation of small PERLA standards (PS) and DA-samples of PuO_2-lot 129/LB

Furthermore, the lack of time for performing measurements, forces sometimes the inspectors to reduce the counting time. In the absence of an analytical model quantifying the importance of the statistical counting variance on the overall uncertainty, subjective judgement could lead to contradictory results: sometimes the counting time reduction leads to an obvious degradation of the results, sometimes not.

But, finally, the fundamental reason for field-laboratory discrepancies resides in the fact that frequently the physical and statistical error models were lacking or were borrowed from applications different from those used in Safeguards, or again no model existed, therefore "intercomparison" experiments could not be extrapolated to experimental situations different from those actually checked.

Furthermore, traditionally a good experimentalist, when in doubt, overestimates his uncertainty without having negative effects /17/. But Safeguards control is based on 1) a sampling plan and 2) comparisons with declared values.

Overestimating the uncertainty in Safeguards means disturbing both the above procedures leading to a series of regrettable side effects, such as :

- artificially low false alarm rate
- unnecessarily high sample sizes
- waste of resources
- perturbed detection probabilities.

This means that, as well as besides specific statistics tools, we must also develop a new experimentalist mentality that could be resumed by saying that a good measurement may be useless without a good evaluation of uncertainty.

Or, to express the same concept in other words, a good laboratory physical instrument might be a poor Safeguards instrument, if it is not properly equipped with Safeguards procedures and ad hoc statistical error propagation, suitably tailored for use by inspectors and for HQ reanalysis. Being conscious of the above needs for field NDA instruments the JRC-Ispra has been constructing for some years integrated systems where together with a sound physical approach other Safeguards aspects are contained, namely :

- sampling parameters (to allow an error propagation to substrata, strata, whole inventory);
- tailored error models specifically developed for the instrument concerned and the way it is used;
- Safeguards verification procedures (calibration, recalibration, normalization) through which the error propagation is built accounting for random error, short and long term systematic errors, etc.;
- software protocols, data bases and data base managers, software supports, allowing acquisition-recording-transmission-field analysis and HQ reanalysis.

The various aspects of such multi-disciplinary instruments are regulated by the so-called FIDES rules /19,20,21/, FIDES being the **F**unctional **I**ntegrated **D**ata **E**valuation **S**cheme.

Examples of FIDES implementation are :

SIGMA (Fig. 12), a device in operation at HOBEG since 1974 for the monitoring of HTGR pebbles /22,23,24/, recently completely reviewed following FIDES criteria.

PU METER (Fig. 13) for the determination of Pu isotopic composition /25,26/.

PHONID (Fig. 14) for monitoring U and Pu bearing samples, from grams of waste up to kg samples. An exemplar of PHONID belonging to Luxembourg Safeguards Directorate has been performing measurements in the NUKEM plant since 1974. Another PHONID is operated by JRC-Ispra to support the Safeguards Directorate during physical inventories in European LEU fabrication plants /27,28/.

GAMMA SCANNER (Fig. 15) is a device for monitoring ^{235}U in MTR fuel elements. Two units have been working since 1972 in HEU plants. The instrument is now being thoroughly modified and improved to meet FIDES criteria /29/.

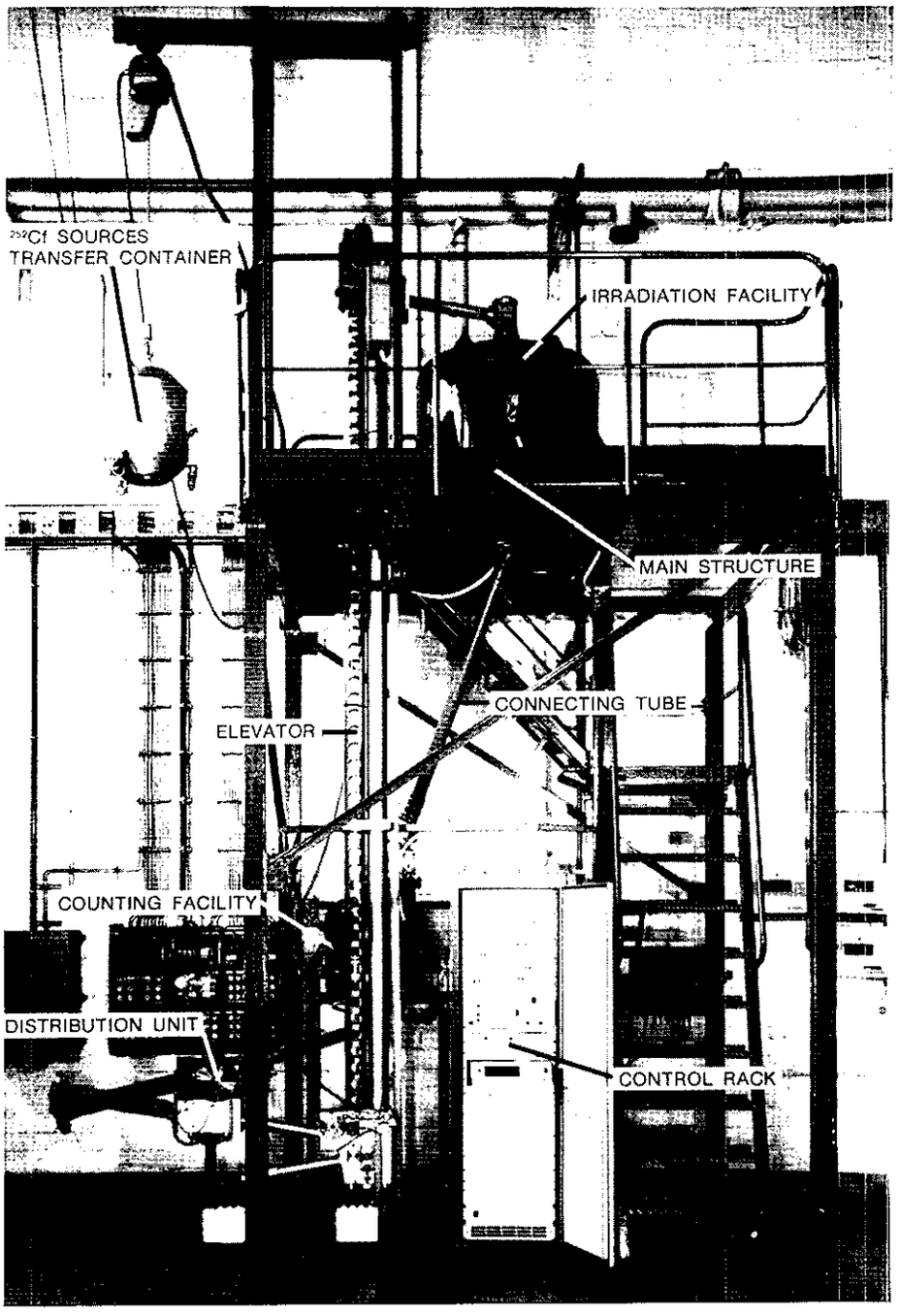

Fig. 12 - View of the delayed neutron counting device for monitoring THTR fuel pebbles SIGMA

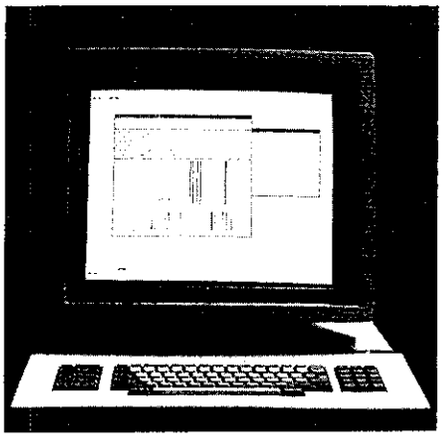

Fig. 13 - View of the Pu meter, an instrument for the determination of plutonium isotopic ratios

5. Training

The JRC-Ispra had in the past an intensive training activity. About 50 training courses have been given to Euratom (some to IAEA) inspectors, mostly oriented on NDA techniques and instruments such as :

- uranium enrichment determination
- plutonium isotopic composition determination.
- neutron coincidence counting (Variable Dead Time Counters and Shift Registers).
- uranium 235 content determination in THTR pbbles : (SIGMA and DUCA /30/)
- integrated training on HEU Physical Inventory Verification (PIV).

Much attention has been paid recently to training courses which, besides teaching the correct use of instruments, also provide a more integrated view of verification activities. Typically the PIV type courses on plutonium and uranium where inspectors are taught to plan an inspection, perform measurements and draw conclusions on a statistical basis, are being encouraged.

Following this trend, the training activity at Ispra is being restructured along the lines of PERLA, i.e. of a service and support provided by the Joint Research Centre of the Commission of the European Communities to other General Directions, particularly DG XVII, to European laboratories and installations and to IAEA.

A typical example of the new kind of training in PERLA was the course held at Ispra in July 1987 where eight IAEA and four Euratom inspectors were taught how to take a complete PIV on PERLA HEU Inventory /31/.

The training "menu" in PERLA will contain

- basic disciplinary courses on neutron detection, gamma spectrometry, calorimetry, statistics;
- instrument oriented courses at various levels of complexity;
- integrated courses, i.e. advanced courses on material type verification with combined techniques (e.g. Pu monitoring through combined calorimetry + gamma spectrometry) and complete PIVs.

The courses will be held by Commission officers when teaching JRC techniques and instruments, and/or by outside scientists in other cases.

6. Conclusions

The picture of the PERLA laboratory that we have tried to give with this presentation is that of an **open laboratory**, where calibration and training activities can be carried out by JRC staff together with officers from other institutions : inspectors, European and non-European scientists. They will find in PERLA well characterized fissile materials, specialized support and suitable laboratories.

References

/1/ M. CUYPERS, S. GUARDINI — Performance Assessment Method for NDA, A Challenge for PERLA. ESARDA Bulletin No. 9, October 1985

/2/ M. CUYPERS, T. DOYLE, S. GUARDINI, J. LEY — PERLA, a Laboratory for Training and Performance Assessment of Safeguards Technique. Proc. of INMM Intern. Symp., June 1986, New Orleans, La. (USA)

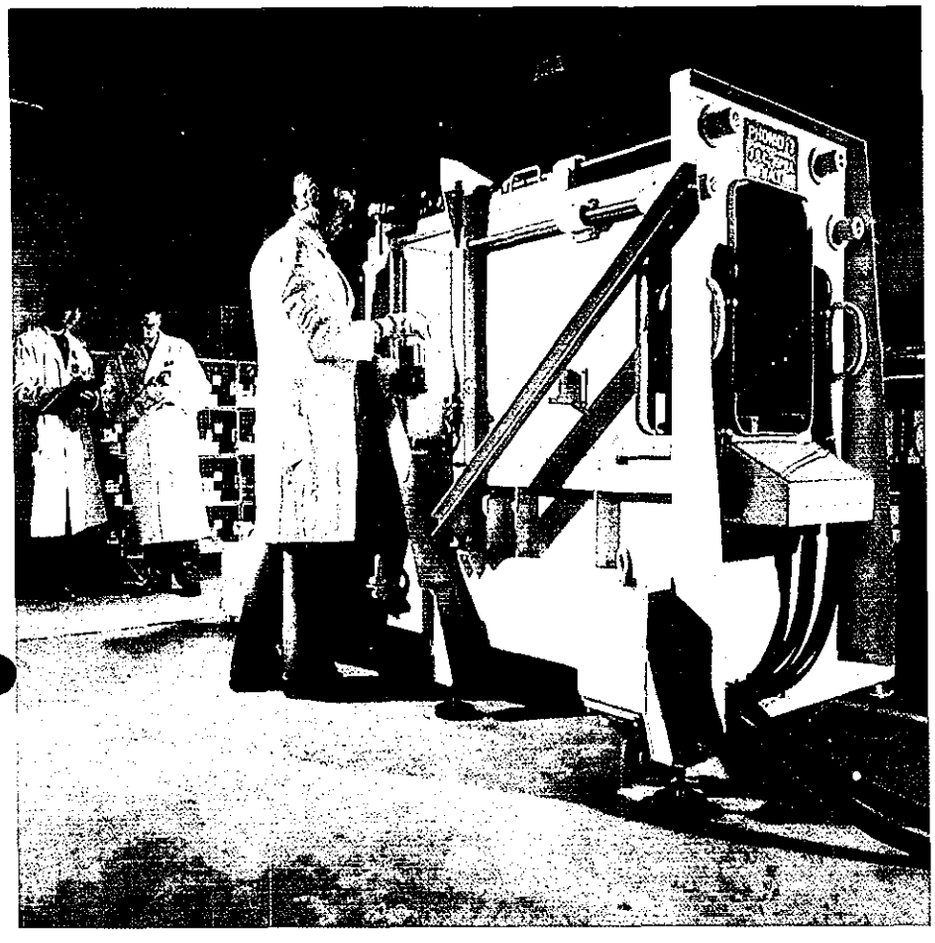

Fig. 14 - View of the PHONID 3 instrument, photoneutron interrogation device to monitor plutonium and uranium bulk samples

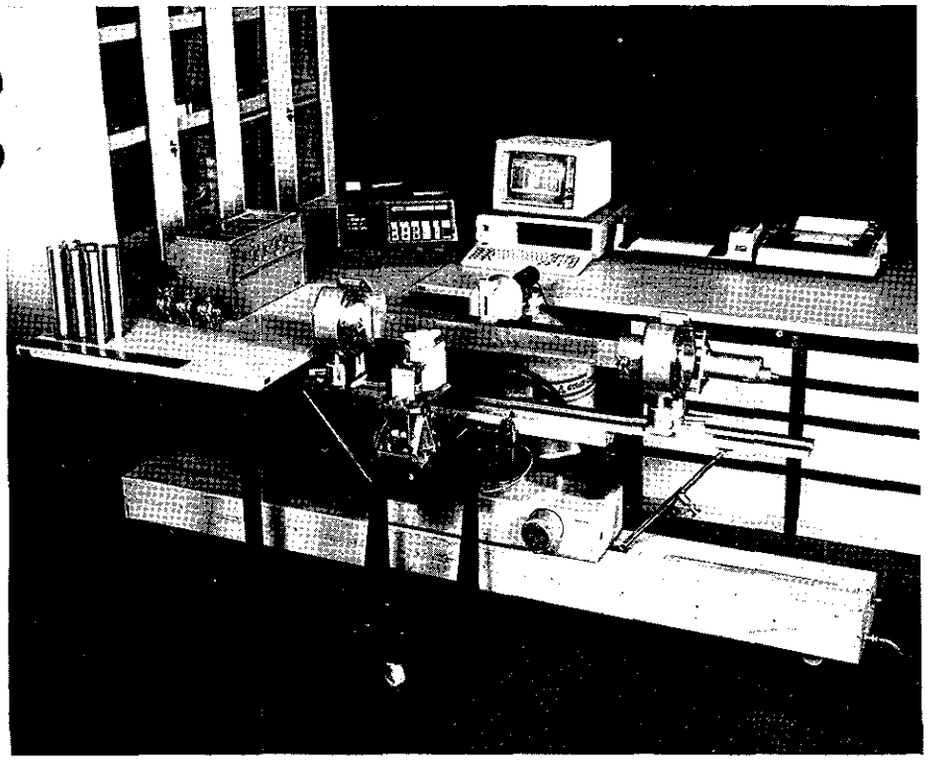

Fig. 15 - View of the MTR gamma scanner

/3/ M. CUYPERS, E. CELANT, J. LEY, J.L. BOURDON, S. CARUSO, T. DOYLE, V. VOCINO, F. SOREL, S. CRUTZEN, S. GUARDINI — PERLA, Safeguards Performance, Calibration and Training Laboratory at JRC-Ispra. Proc. 6th ESARDA Symp., 14-18 May 1984, Venice (Italy)

/4/ M. FRANKLIN — A Training Course for IAEA Inspectors at JRC-Ispra. ESARDA Bulletin No. 13. October 1987

/5/ M. CUYPERS, T. DOYLE, S. GUARDINI, G. GUZZI, J. LEY, S. ZANELLA — Procurement and Characterization of Nuclear Materials for the Performance Assessment of Measurement Techniques in PERLA. Intern. Symp. on Nuclear Material Safeguards, 10-14 November 1986, Vienna (A)

/6/ R. ABEDIN-ZADEH et al. — Preparation of a Plant Specific Standard for MOX Pins. Proc. of the ESARDA Specialists Meeting on Harmonization and Standardization in Nuclear Safeguards, 1982, Petten (NL)

/7/ R. ABEDIN-ZADEH, T. BEETLE, G. BUSCA, S. GUARDINI, E. KUHN, D. TERREY — Preparation and Characterization of Plant Specific Reference Materials: Results and Progresses. 5th Annual ESARDA Symp., 19-21 April 1983, Versailles (France)

/8/ G. BUSCA, M. CUYPERS, S. GUARDINI — General Criteria for the Procurement of Plant Specific Reference Materials. Proc. of the 4th Annual ESARDA Symp., Specialists Meeting on Harmonization and Standardization for Nuclear Safeguards, 1982, Petten (NL)

/9/ Report of the Working Group on NDA. Working document of the 8th Annual ESARDA Meeting, p. 45, Copenhagen, 13-15 May 1986

/10/ A. SANDSTROEM — Third Advisory Group Meeting on Evaluation on Quality of Safeguards NDA Measurement Data, p. 40, IAEA, Vienna 1983

/11/ Working Group "Definition of Procedures for the Preparation of PERLA Standards" — Modified Procurement and Characterization Scheme for the Pu PERLA standards. JRC Special Activities Report No. I.07.C3.85.26, FMM/C-109, Nov. 1985

/12/ P. DE BIEVRE et al. — How Well Can Uranium and Plutonium from Irradiated Fuel be Assayed by the Nuclear Community ? Final Results of the IDA-80 Programme. Proc. of the 7th ESARDA Symposium, Liège (Belgium), 21-23 May 1985, p. 339

/13/ W. BEYRICH et al. — The IDA-80 Measurement Evaluation Programme on Mass Spectrometric Isotope Dilution Analysis of Uranium and Plutonium, Vol. 1,2,3. EUR 7990.EN (1984), EUR 7991.EN (1984), EUR 7992.EN (1985)

/14/ S. BAUMANN, Alkem GmbH, private communication 1987

/15/ A. PROSDOCIMI, V. VOCINO — Personal communication, JRC-Ispra, 1987

/16/ G. CARAVATI, D. D'ADAMO — Personal *communication, JRC-Ispra, 1987*

/17/ M. CUYPERS, M. FRANKLIN, S. GUARDINI — Methodology for NDA Performance Assessment. Proc. INMM Intern. Symp., June 1986, New Orleans, La. (USA)

/18/ P. DE BIEVRE et al. — Random Uncertainties in Sampling and Element Assay of Nuclear Materials. Target Values *1988. ESARDA Bulletin No. 13, October* 1987

/19/ M. CUYPERS, G. DE GRANDI, M. FRANKLIN, K. MÜLLER, S. GUARDINI, M. MONTAGNI — An Integrated Scheme for NDA Data Evaluation. Proc. 5th ESARDA Symp., 19-21 April 1983, Versailles (France)

/20/ G. DE GRANDI, M. FRANKLIN, S. GUARDINI, G. CORTELLAZZI, M. MONTAGNI — Software, Data Structures and Data Evaluation Algorithms for a Verification Data Management System. Proc. 6th ESARDA Symp., 14-18 May 1984, Venice (Italy)

/21/ M. FRANKLIN — Sampling Plans in Attribute Mode with Multiple Levels of Precision. Proc. 27th Annual Meeting of *the Institute of Nuclear Materials* Management, 22-25 June 1986, New Orleans, La. (USA)

/22/ M. CUYPERS, E. VAN DER STRICHT, M. BOURSIER, M. CORBELLINI — The Verification of the ^{235}U Flow at the Output of the THTR Fuel Fabrication Plant. IAEA Symp., October 1975, IAEA-SM-201/173.

/23/ P. AGOSTINI et al. — SIGMA-R, an *Improved Version of the Device for THTR* Fuel Element Monitoring. Proc. 9th ESARDA Symp., 12-14 May 1987, London (UK)

/24/ P. AGOSTINI et al. — SIGMA-R, an Improved Version of the Delayed Neutron Counting Device for THTR Fuel Element Monitoring. To be published as EUR report (1988)

/25/ D. D'ADAMO — Topical Report on Pu Isotopic Ratios Determination. Joint Research Centre Progress Report 1986

/26/ G. DE GRANDI — A Software Tool for the Post-Evaluation of Plutonium Isotopic Composition Measurements. Proc. 9th ESARDA Symp., 12-14 May 1987, London (UK)

/27/ A. PROSDOCIMI, P. DELL'ORO — A Photoneutron Active Interrogation Device : Physical Design, Calibration and Operation Experience. Proc. 1st ESARDA Symp., Brussels 1979

/28/ R. CARCHON, R. COLOMBO, P. DELL'ORO, S. GUARDINI, A. PROSDOCIMI, G. SMAERS — Active Interrcgation of Pu and U Bulk Samples with PHONID Devices. Proc. 7th ESARDA *Symp., 21-23 May 1985, Liège (Belgium)*

/29/ G.B. CONTI, M. CORBELLINI, D. D'ADAMO, S. GUARDINI, M. KRUEGER — Two Gamma Scanning Devices for MTR Fuel Flements and Fuel Rods Monitoring. Proc. 9th ESARDA Symp., 12-14 May 1987, London (UK)

/30/ R. ADAM et al. — A Transportable Instrument for Determination of Uranium Content in Powders or Pellets by Delayed Neutron Technique. Proc. 9th ESARDA Symp., 12-14 May 1987, London (UK)

/31/ M. CUYPERS et al. — High Enriched Uranium Physical Inventory Verification Exercise in JRC-Ispra. Submitted to INMM Annual Meeting, June 1988, Las Vegas, Nev. (USA)

Monitoring of Field Data

R. Haas
Euratom Safeguards Directorate, Luxembourg
Y. Haurie, H.J. Metzdorf
CEC, Joint Research Centre Ispra, Italy
H. Reuters
PROCOM, Aachen, F.R. Germany

Abstract

Euratom is developing presently a modular monitoring system in order to enhance containment and surveillance measures in nuclear plants. Since this monitoring system includes the authenticable transfer of measurement data it will also be applicable for the monitoring of NRTA field data.

In the paper the functional design of the modular monitoring system is described together with an application to a tank store.

Introduction

With the scope of improving the efficiency of todays safeguards and to cope with the evolution of the fuel cycle in the European Communities, Euratom invests some effort to further develop containment and surveillance (C/S) methods /1/. These efforts also include the further development of the technical means. It had been proposed that the integration of monitoring, or data logging into C/S significantly improves the assurance which is obtained from the application of C/S measures.

We are in the process of completing the development of a monitoring system which we consider suited for a large range of applications. The collection of NRTA field data should be another useful application for this monitoring system.

Requirements for a Safeguards Monitoring System

Data from different measurement instruments, which will be called sensors, must be collected in a central station or in substations. The sensors may be distributed over large areas of the plant. The monitoring system which collects these data must fulfill the following requirements ;

- reliability (data must not get lost or modified),
- tamper resistance, data authentication,
- functional reliability,
- possibility for adaptation to field requirements and for extension,
- user-friendliness,
- cost efficiency (use of standard components).

Except for the authentication problem, commercial monitoring systems exist in industrial plants (so called Building Automation Systems), for instance, for the collection and evaluation of infrastructure related data. This experience had been incorporated into the design of the VACOSS fiber optic seal /2/ which started to enter safeguards use some five years ago.

Structure of the VACOSS Monitoring System

A design proposal for a Safeguards Monitoring was made in the early 1980s /3/ and a demonstration prototype was built for the continual verification of VACOSS seals, named Local Verification System (LOVER). Maintaining the basic structure, the system was redesigned and has been extended to accept as sensor also any ON/OFF sensor /5/. Presently also general measurements sensors are being included. Fig. 1 shows the layout of the basic system with its 4 levels. The combination of several systems in a fifth level, central station, is of course possible but not the scope of this presentation.

The system operates in a strictly hierarchical way, i.e. each level has direct access to the next lower level only. Each level operates autonomously after initialisation, surveils the lower level, retrieves and stores any new information and keeps it available for the next higher level. Since each level is equipped with suitable memory capacities the failure of a higher level does not cause a system failure.

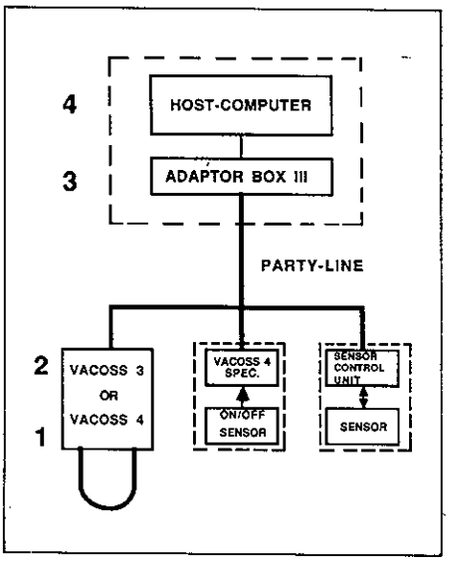

Fig. 1 - Modular Monitoring System

The sensor data is read by the level 2 sensor control unit (SUE); both are integrated into one, tamper resistant housing. Upon request by level 3 the SUE sends the requested information on the party-line to the adaptor box III (ADBIII) as clear text and encrypted text. By decryption and comparison the ADBIII authenticates the message, adds it to its own data set and in case the data set had been requested by the host computer the latter receives the message.

The VACOSS 3 and the improved VACOSS 4 seals are both fiber optic sensors combined with a SUE of limited capacity. The VACOSS 4 special is essentially the SUE which may surveil any ON/OFF sensor (motion detector, threshold detector, etc.). This presentation is concerned with the general SUE.

Description of the Monitor Components

Sensor

Any device which produces an information signal (electric current, voltage, frequency, or digital signal) may be used as sensor. There may be several signals, representing measurement information and dynamic or static states of the sensor. Dynamic states may change repeatedly between ON and OFF (fiber loop, sensor power supply, etc.); a static variable can only change once after initialisation and it is normally used to indicate tamper conditions or component failure.

Sensor Control Unit (SUE)

Figure 2 shows a symbolic diagram of the SUE. The main component is a single chip microcomputer (8 k Byte memory). The SUE continuously surveils the state of the sensor, it keeps the time and a record of the last status changes with the time when they occurred. Upon request of level 3 the SUE may give control information to the sensor and read measurement information.

The SUE number (the sensor address) and the identifier are fixed data; the encryption key and initialisation date and time are data which the SUE receives upon

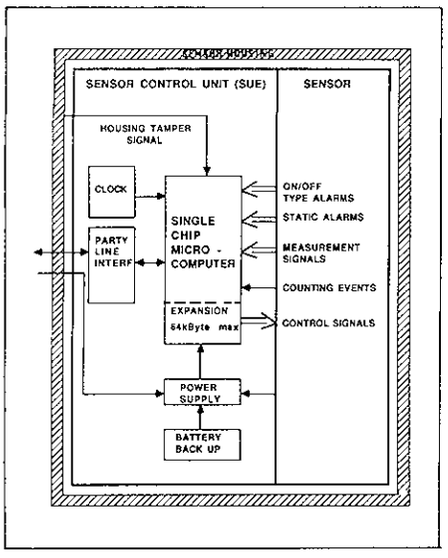

Fig. 2 - Schematic Diagram of Sensor Control Unit

initialisation.

The SUE may be extended (64 k Byte maximum) which allows it to perform quite complex data collection and evaluation functions.

Adaptorbox III (ADBIII)

The originally developed adaptor boxes I and II were designed for manual interrogation of the VACOSS seals; the ADBIII has been developed for automated interrogation of VACOSS seals and the VACOSS compatible SUEs. The ADBIII is an interface unit, a single board microcomputer (FALCON from Digital Equipment Corporation), which executes all the routine work required for the interrogation of the SUEs. Its basic functions are as follows :

- management of the party-line communication,
- encryption/decryption and authentication,
- maintaining of the data required for addressing and communication with the SUEs,
- date and time keeping,
- cyclic surveillance of the SUEs for changes of status and updating of the alarm table (table of status changes obtained from SUEs and detected by the ADBIII),
- communication with SUEs upon specific request from the host computer,
- communication with the host computer via an RS-232 port.

The frequency of SUE interrogation, the encryption key, the identifier (encryption key for the first initialisation), and the configuration of the SUE status change table can be defined individually for each of the SUEs.

Host Computer

With the routine work being executed by the adaptor box the host computer can be selected in view of the

- amount of data to be processed and the evaluation software,
- the required input/output facilities and periferals; one port (presently RS 232 C) is required for the communication with the ADBIII.
- the environmental conditions.

Multiple I/O ports, multitasking or parallel processors will normally not be required for the monitoring task.

The application software of the host computer must satisfy the following functions :

a) initialisation of all components (ADBIII and SUEs),
b) retrieval of status change information from the ADBIII, evaluation and storage,
c) retrieval of measurement information from the SUEs (through the ADBIII), evaluation and storage,
d) user-friendly inspector interface and preparation of output (hard copy, floppy disc, etc.).

We have used a HP41CX computer for a demonstration of the monitoring system with several VACOSS seals and a motion detector (VACOSS 4 special), satisfying functions a), b) and d) /4/. For laboratory test and development an IBM compatible PC is used presently.

Application of the Monitoring System

A first application of the monitoring system is presently developed for a Pu-nitrate store. The liquid arrives in small containers and is accumulated in 300 l tanks. Sealing of the tanks for Safeguards purposes ist not feasible technically.

In order to reduce the remeasurement effort the liquid volume will be monitored continuously using the operators level gauges (capacitance sensors). With the knowledge of

- the present volume and
- the volume changes since the last verification measurement,

the Pu content can be calculated if there were no volume additions in the mean time. Fig. 3 shows the system layout. The capacitance signal is converted to frequency and then converted into current to supply the operators control instrumentation. The output of the capacitance-frequency converter (sensor) is read by the SUE and transferred through the ADBIII to the host computer. The SUE will also monitor the status of the power supply of the converter. Since the frequency-current converter includes variable range adjustments it is better for safeguards purposes to pick-up the frequency signal. The electronic units and the positioning devices for the capacitive sensors will be protected by VACOSS seals.

The SUE in this application is equipped with an external memory expansion so that 2 types of measurement signals can be generated upon request of the host computer :

- single frequency readings,
- the average frequency and standard deviation of N readings at T/sec interval.

The host computer will obtain from the ADBIII the alarm information such as VACOSS seal events, power supply failures of converters, party-line continuity problems, etc. It will request through the ADBIII at regular intervals the results of the frequency measurement of the different SUEs.

The interpretation of the frequency values in volume is done by the host computer, using experimentally obtained calibration constants.

Calibration tests have shown that also temperature information is required for each tank in order to improve the volume calculation. This information is collected by different SUEs, which are not indicated in Fig. 3.

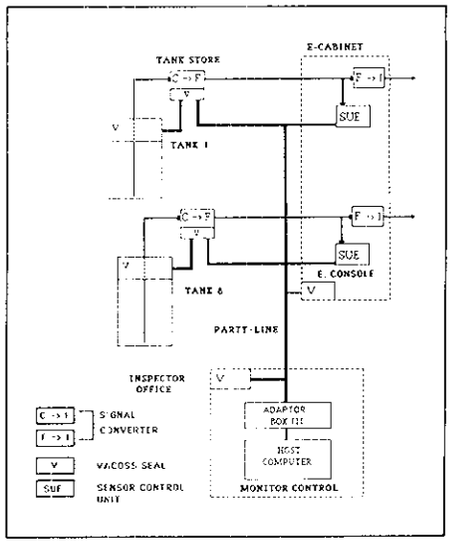

Fig. 3 - Liquid Level Monitor

With suitable algorithms the volumes, volume changes and the periods of stable volume are evaluated and stored.

Other software packages in support of the inspector are planned for the review, consolidation and documentation of the tank history. Together with inspection data from other sources the inspector will eventually be able to arrive at a complete safeguards analysis of the tank store. For this reason, a multitasking micro-computer has been chosen as host computer.

In the present project, 8 tanks will be read for level (frequency) and for temperature (current) and 5 VACOSS seals will be monitored, i.e. all together 21 sensors. In the long term the number of tanks will be increased.

No basic problems are expected in that respect. Since the data communication will always use the same party-line, no modification of the installations will be required.

Conclusion

The above described modular monitoring system will permit to collect field data in authenticable way making use of operators sensors (and measurement equipment) and of standard components for data communication. Addressable sensor control units which are connected by a single party-line and the encrypted data transfer simplify installation, operation and verification of the monitoring systems. This system will be suited also for the monitoring of NRTA field data.

References

/1/ CUYPERS, M., HAAS, R. — Can Containment and Surveillance Play a more Important Role in Safeguards? ANS Intern. Conf., San Diego, December 1987

/2/ ARNING, F., REUTERS, H., BUEKER, H. — Remote Verifiable Sealing System for Safeguards Application. ESARDA Bulletin No. 2 (1982)

/3/ REUTERS, H., WOLF, M. — Entwicklung eines Fernüberwachungssystems für Containment- und Surveillance-Instrumentierung zum Zwecke der internationalen Spaltstoff-Flußkontrolle. Forschungsbericht BMFT-EB (KWA 2040/3), F.R. Germany (1981)

/4/ METZDORF, H.J., HAAS, R., REUTERS, H., BUEKER, H. — Modular Monitoring System. 9th ESARDA Symposium, London (UK) 1987

CBNM Information

Central Bureau for Nuclear Measurement
Commission of the European Communities
Joint Research Centre
Geel Establishment

Regular European Interlaboratory Measurement Evaluation Programme (REIMEP)

After the interruption of the US Safeguards Analytical Laboratory Evaluation (SALE) Programme, CBNM took the initiative to organize an enquiry among former SALE participants and the ESARDA-WGDA members (European Safeguards Research and Development Association - Working Group for Techniques and Standards in Destructive Analysis). Many laboratories announced their interest for such a programme and it was decided to launch a Regular European Interlaboratory Measurement Evaluation Programme (REIMEP) in 1986. Still the same year PuO_2 and UF_6 measurement rounds were organized and the results discussed with participants in June 1987. Both were very revealing, in view of comparing gas mass- and thermionic mass spectrometry with γ-ray spectrometry in the case of UF_6, or Pu element determinations on samples in different containers. Measurement rounds on UO_2 powder, UO_2 pellets, and Uranyl- and Pu-nitrate solutions are in an advanced state of preparation for 1988 (Fig. 1).

The objectives and characteristics of REIMEP can be summarized as follows :

a. Provide state-of-the-practice pictures for the assay of a given fissile isotope abundance or element content of a given nuclear material (Example, Fig. 2). It is not primarily intended to perform the evaluation of a particular method, nor is it intended to demonstrate state-of-the-art or ultimately achievable, optimum performance.
b. Officially guaranteed coded participation; individual results only to concerned participants.
c. Limited frequency; to be discussed with participants.
d. Participants to work under normal working conditions (their own choice).
e. Reporting of results in graphical display (again only to participants).
f. Conclusions to be drawn by participants for themselves; assistance is given if requested.
g. Provide characterization value with a provable total uncertainty which should be smaller than the interlaboratory spread.

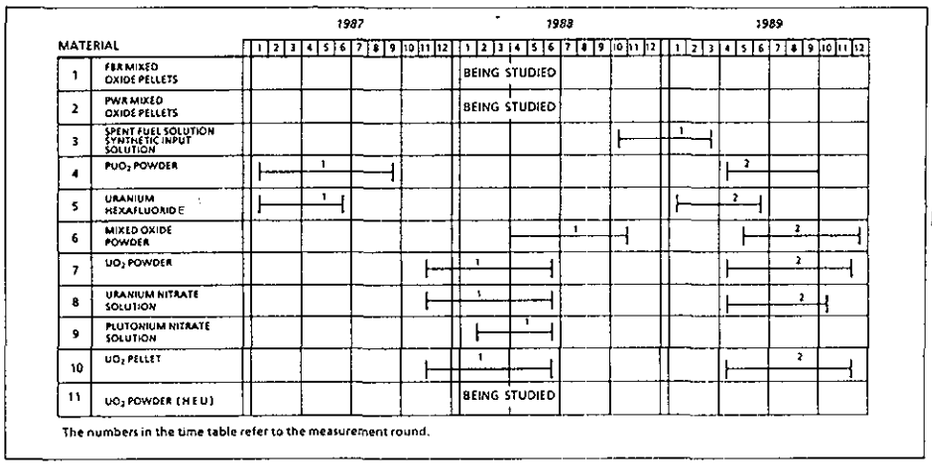

Fig. 1 - Approximate frequency of measurement rounds (status February 1988)

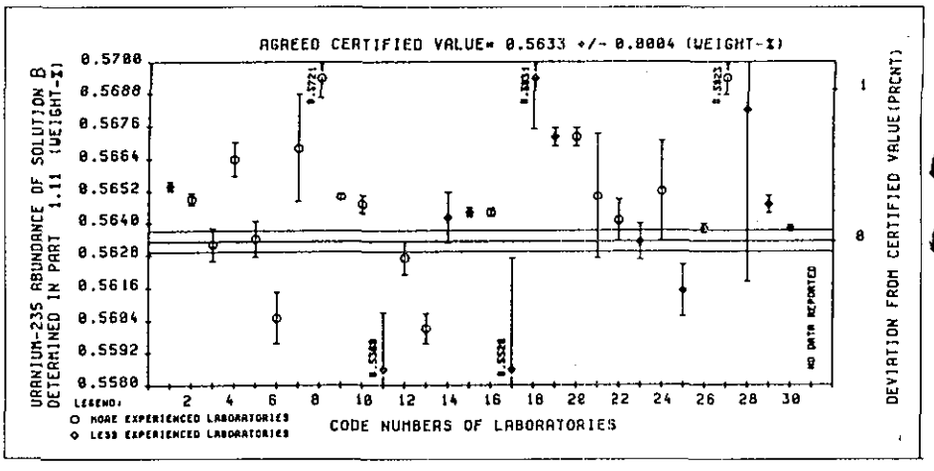

Fig. 2 - Typical example (taken from IDA-80) how a graph with REIMEP results will be presented

CBNM, supported by a few experienced European laboratories, is responsible for coordination, test sample preparation, dispatching and characterization of the material. Coding of participants, collection of results and evaluation is performed only by CBNM for reasons of its independence.

Participation is open to all laboratories within the European Community and - depending on the number of European participants - also open for some non-EC applicants. A participation fee is requested.

For further information, please address to :
Central Bureau for Nuclear Measurements,
Materials Division, Steenweg op Retie,
B-2440 Geel (Belgium)
Tel.: (014)571271. Telefax : (014)584278.
Telex . 33589 EURAT B

A Joint European-American Certified Reference Material for Uranium Isotopic Measurements by Gamma Ray Spectrometry

International collaboration co-ordinated by the Central Bureau for Nuclear Measurements of the Commission of the European Communities and the U.S. National Bureau of Standards has resulted in the preparation and joint certification of a Reference Material for gamma-ray spectrometric measurements of the U-235 isotope abundance in homogeneous bulk material.

The RM is designed both as EC-NRM 171 (European Community Certified Nuclear Reference Material No. 171) and NBS SRM 969 (National Bureau of Standards Standard Reference Material No. 969). It consists of a set of five sealed cans, each of which contains 200 g U_3O_8 with one of five different U-235/U isotope abundances. Their nominal values are 0.31, 0.71, 1.94, 2.95 and 4.46 mass percent. The set includes an empty can for measurements of material of unknown U-235/U abundance under similar geometric conditions. In addition, each reference sample prossesses an ultrasonic identification system which generates a unique ultrasonic spectrum. This system can be used to verify the identity and integrity of each can.

Detailed reports have been issued which describe the preparation and certification of the RM. The European report is published as report COM 4153; the corresponding U.S. report is NBS Special Publication 260-96. A User's Manual has been prepared by the Kernforschungszentrum Karlsruhe (KfK), Federal Republic of Germany,. and is published as KfK 3752 (May 1985).

The Reference Materials set costs 4224 ECU. Additional information is obtainable from : Central Bureau for Nuclear Measurements, Steenweg op Retie, B-2440 Geel (Belgium).

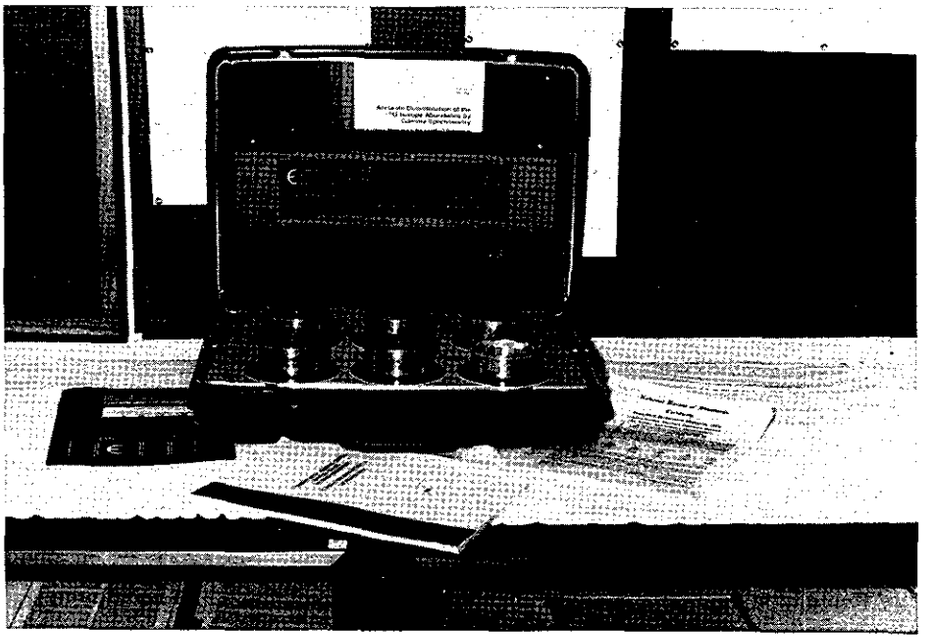

CHARACTERIZATION OF THE Pu-BEARING PERLA STANDARD

C. Bigliocca, S. Guardini, G. Guzzi, L. Haemers, F. Mousty
CEC-JRC, Ispra (Italy)

E. Kuhn, N. Doubek, R. Fiedler, A. Zoigner
IAEA, Vienna (Austria)

S. Baumann, K.H. Nelges, G. Hesbacher
ALKEM, Hanau (Federal Republic of Germany)

P. De Regge, L. Vandevelde, R. Boden, D. Huys
SCK/CEN, Mol (Belgium)

ABSTRACT

The JRC of the CEC has set up in its Ispra Establishment a Safeguards-oriented calibration and training laboratory called PERLA (PERformance LAboratory). Its scope is to help bridge the gap between laboratory development of instruments and techniques and their field use by Safeguards inspectors.

The laboratory already has many facilities operative and is equipped with Pu and U bearing standard samples, which were procured in such a way to resemble as closely as possible materials actually encountered in the fabrication plants. The characterization phase of the Pu PERLA standards has now almost finished and it is reported in this paper.

The following standard samples were produced for PERLA:
- PuO_2 samples, originating from three different batches (burn-ups) and containing g to kg quantities;
- MOX samples, originating from five different batches (with varying U/Pu ratios) in the form of powder, pellets and pin.

From the 8 above batches a total of 80 DA samples was taken following accurate procedures described in the paper and analyzed by three laboratories, namely IAEA-SAL, ALKEM and SCK/CEN.

The analytical schemes required the isotopic composition of Pu (and U for MOX samples), Pu and U elemental concentration, ^{241}Am and impurities.

The analytical results of the 3 laboratories were supplied to the JRC Ispra, together with the results of quality control measurements on available primary reference materials. The Pu and ^{241}Am data were decay corrected by the laboratories to an agreed upon reference date.

1. INTRODUCTION

PERLA (PERformance LAboratory) is a Safeguards training and calibration laboratory, set up by the Ispra Establishment of the Joint Research Centre (JRC) of the Commission of the European Communities (CEC) with the general aim of bridging the gap between the laboratory development and the application of Safeguards instruments and techniques in an industrial environment.

PERLA's main themes of concern are:
- assessment of the performances of instruments and methods in near field conditions;
- periodic calibrations under well defined conditions of instruments used routinely by inspectors and operators in industrial facilities;
- training of inspectors and operators;
- development of new methods according to needs.

The first absolute necessity of a facility which aims to act as a calibration and training laboratory in the field of NDA for Safeguards is to have available a large inventory of well characterized reference materials, representing to the largest possible extent samples that are most commonly encountered in the fuel cycle.

Identifying this inventory was, in fact, the first task of the PERLA team. A further important task was to acquire fissile materials and to characterize them at a high level.

The following standard samples were produced for PERLA:
- PuO_2 samples, originating from three different batches (burn-ups) and containing g to kg quantities;
- MOX samples, originating from five different batches (with varying U/Pu ratios) in the form of powder, pellets and pin.

A general description of the 8 above batches is given in Table 1.

From the 8 above batches a total of 80 DA samples was taken following accurate procedures and analyzed by three laboratories, namely IAEA-SAL, ALKEM and SCK/CEN.

TABLE 1 - Description of the sample batches

	Lot		
PuO_2	1	low burnup	∿71% Pu-239
	2	medium burnup	∿61% Pu-239
	3	high burnup	∿58% Pu-239
MOX	1	SNR C1 fuel	∿22% Pu, ∿66% U natural
	2	SNR C2 fuel	∿31% Pu, ∿57% U natural
	3	FDWR fuel	∿9.3% Pu, ∿79% U natural
	4	DWR fuel	∿4.2% Pu, ∿84% U natural
	5	KNK II fuel	∿22% Pu, ∿66% U enriched at ∿63%

ALKEM was also the supplier of the plutonium and prepared the PERLA samples, but it also acted as a third laboratory having produced new DA data with the agreed format, as well as the current information which it gave as producer.

Most of the PuO_2 samples, the kg-size included, were prepared by ALKEM at the JRC Transuranium Institute (TUI), Karlsruhe, with the cooperation of TUI staff.

The analytical schemes required the isotopic composition of Pu (and U for MOX samples), Pu and elemental concentration, ^{241}Am and impurities.

The analytical results of the three laboratories were reported to the JRC Ispra, together with the results of quality control measurements on available primary reference materials. The Pu and ^{241}Am data were decay corrected by the laboratories to an agreed upon reference date (1st November 1987).

The data presented in this paper are coded so that no reference can be made between results and the laboratory producing that result. Furthermore, the material batch numbers are also coded to avoid the possibility of tracing back the source batch.

The aim of this paper is to describe the procedures followed in the preparation and characterization of the plutonium bearing standards of PERLA, and to present and discuss the analytical results obtained.

2. GENERAL REQUIREMENTS, PROCUREMENT AND CHARACTERIZATION SCHEMES

2.1 Requirements

The first step of the procedure leading to the preparation of standards was to analyze the general requirements for the 8 batches. We established that the general requirements for PERLA standards were:

a) They must be representative of plant samples (e.g. PuO_2 cans, MOX industrial pins, etc.);
b) They should be prepared and characterized for specific NDA methods with defined "performance values" [1] or expected overall uncertainty values [2]. Therefore, overall random and systematic uncertainty must be "a priori" planned so that calibrations with these standards do not introduce an appreciable uncertainty component in the NDA measurements.
c) Most of them must belong to the same family, i.e. come from the same original production batch and thus have the same chemical and isotopic characteristics. In this way, for instance, the gamma spectrometrist can measure the same sample in the form of powder and pellets and pins excluding any influence from the above chemical and physical parameters.
d) Their characterization must be traceable back to primary standards.

2.2 Procurement and characterization schemes

These were then developed to ensure "a priori" fulfilment of the above requirements.

In establishing such schemes for PERLA standards we followed the general criteria established earlier very closely, when characterizing the so-called Plant Specific Reference Materials, for NDA, in an extensive exercise conducted jointly by IAEA, EURATOM and JRC-Ispra [3,4,5].

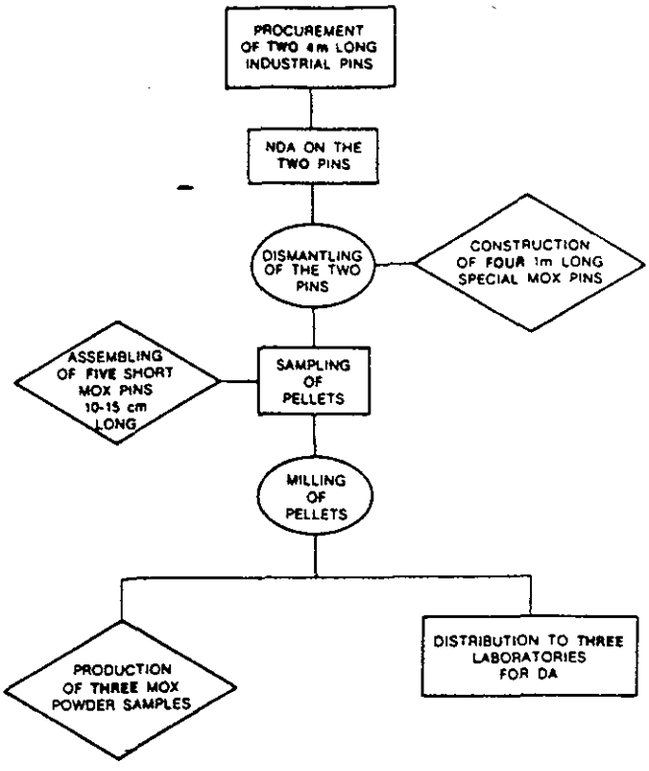

Figure 1. Procurement scenario for a reduced-size family concept (light-water reactor DWR, MOX Lot 4).

First the procurement scenarios for each "family" were established: in Figure 1 the scenario for the production of the family MOX Lot 4 (DWR-LWR reactor) is given.

Each family of Table 1 had, in principle, a different procurement scheme, having different origin and preparation procedures.

Having defined the preparation steps, the characterization procedures suitable for achieving the accuracy required were defined, namely:

a) error sources and error propagation schemes;
b) analytical schemes for DA laboratories;
c) statistical data evaluation procedures.

The characterization procedures are discussed in detail in Section 3 of this paper.

Finally, PERLA certificates and protocols schemes were outlined to describe the standards and the procedures followed fully, and to ensure and document traceability to primary standards.

3. CHARACTERIZATION FLOW SHEETS

As mentioned above the first important aspect to start with in the logical approach to procuring and characterizing the standards is to define "a priori" the required level of accuracy in connection with the NDA technique applied to those standards and with the "expected overall uncertainty values" [6] of that technique.

A list of required accuracies for Pu standards is given in Table 2 together with the so-called limiting factor, i.e. the technique and the parameter which imposes such a level.

The next step was to study the possibility of

TABLE 2 - Required overall uncertainty for PuO_2

Parameter	Uncertainty (%)	Limiting factor
Pu content	0.2	calorimetry
Pu-238 abundance	0.5	calorimetry
		γ-spectrometry
Pu-239 abundance	0.2	calorimetry
		γ-spectrometry
Pu-240	0.3	γ-spectrometry
Pu-241	0.3	γ-spectrometry
Am-241	0.5	calorimetry
		γ-spectrometry

reaching such a degree of characterization by DA which is the basis for the characterization. In Table 3 the typical expected DA accuracies are shown, as defined by the three laboratories taking part in the characterization, on the basis of attainable accuracies in DA [7,8].

An uncertainty build up model was then developed which propagates the following predicted error sources:

A) Sampling and DA

The sampling and analytical schemes account for sources of uncertainty from:

a) the single measurement (6 measurements/batch and laboratory);
b) the between dissolution (sample homogeneity: 2 dissolution/sample and laboratory);
c) variance between laboratories (3 laboratories).

"Summing" of those components and careful control in minimizing other experimental variables (humidity, weighing, etc.) gave an assurance that the quoted uncertainty was a good evaluation of the overall sample uncertainty.

The sampling flow sheet for PuO_2 Lot 1, which resulted from the above error analysis is shown in Figure 2; the analytical schemes are shown in Figure 3.

Very detailed procedures were discussed and agreed among the three laboratories ranging from the number of repetitions to the expected uncertainty from DA (Table 3), the nuclear data to be used, down to details such as the type of container to be used (Sovirel Erlenmayer flasks for PuO_2 and BC-4 canisters for MOX) in the transport of samples and in the chemical treatment.

B) Homogeneity

A definition of homogeneity was developed in [6] again for different limiting factors or techniques applied. In other words, calorimetry, for instance, is not influenced by an inhomogeneity inside a PuO_2 box while gamma spectrometry gives information on the internal homogeneity of a can.

Preliminary DA/NDA measurements were carried out on the original PuO_2 production batches ensuring that internal/external homogeneity was acceptable.

The sampling and DA schemes were worked out and implemented for homogeneity checks in order to have, as was said above, the sampling component of the uncertainty propagated to the final declared uncertainty.

C) Weighing

Careful sample weighing protocols were established both for DA and NDA samples. The laboratories were also required to establish carefully documented balance control based upon standard weights.

The results of the weight control activities concluded that the error component from that source was negligible, and it was excluded from the error propagation.

D) Humidity

One of the most important parameters which might affect NDA neutron measurements is humidity content. General H_2O content limits were imposed as was a strict check of the fabrication and sampling procedures, so as to ensure, on the one hand, a representative sampling and DA analysis,

TABLE 3 - Typical expected uncertainties for DA measurement methods

Parameter	Material	Laboratory A		Laboratory B		Laboratory C	
		Method	RSD(%)	Method	RSD(%)	Method	RSD(%)
Pu-conc.	PuO_2	AgO (gravim. 0.1%)	0.2	AgO or Mc.Don.	0.1	AgO	0.15
	MOX	AgO (LWR:0.3%; FBR:0.2%)	0.3/0.2	AgO or Mc.Don.	0.1	AgO (LWR:0.3%)	0.15
U-conc.	MOX	gravimetry (Pu by tit)	0.1	Davies & Gray	0.1	Davies & Gray	0.1
Pu-238	PuO_2	Mass spec (LB:1.0%)	0.5	Mass spec	1.0	Mass spec (LB:1.0%)	0.5
	MOX	α-spec	2.0	α-spec	2.0	α-spec	2.0
Pu-239	ALL	Mass spec	0.06	Mass spec	0.05	Mass spec	0.03
Pu-240	ALL	Mass spec	0.1	Mass spec	0.1	Mass spec	0.07
Pu-241	ALL	Mass spec	0.3	Mass spec	0.3	Mass spec	0.2
Pu-242	ALL	Mass spec	0.3	Mass spec	0.3	Mass spec	0.3
U-235	low	Mass spec	0.2	Mass spec	0.1	Mass spec	0.2
	high	Mass spec	0.1	Mass spec	0.03	Mass spec	0.1
Am-241	ALL	γ-spec	2.0	γ-spec	1.0	γ-spec	1.0
U-234	high	Mass spec	1.?	Mass spec	1.0	Mass spec	1.0
U-236	high	Mass spec	1.?	Mass spec	1.0	Mass spec	1.0
U-234	nat.	Mass spec	10?	Mass spec	10?	Mass spec	3-4
U-236	nat.	Mass spec	?	Mass spec	?	Mass spec	?

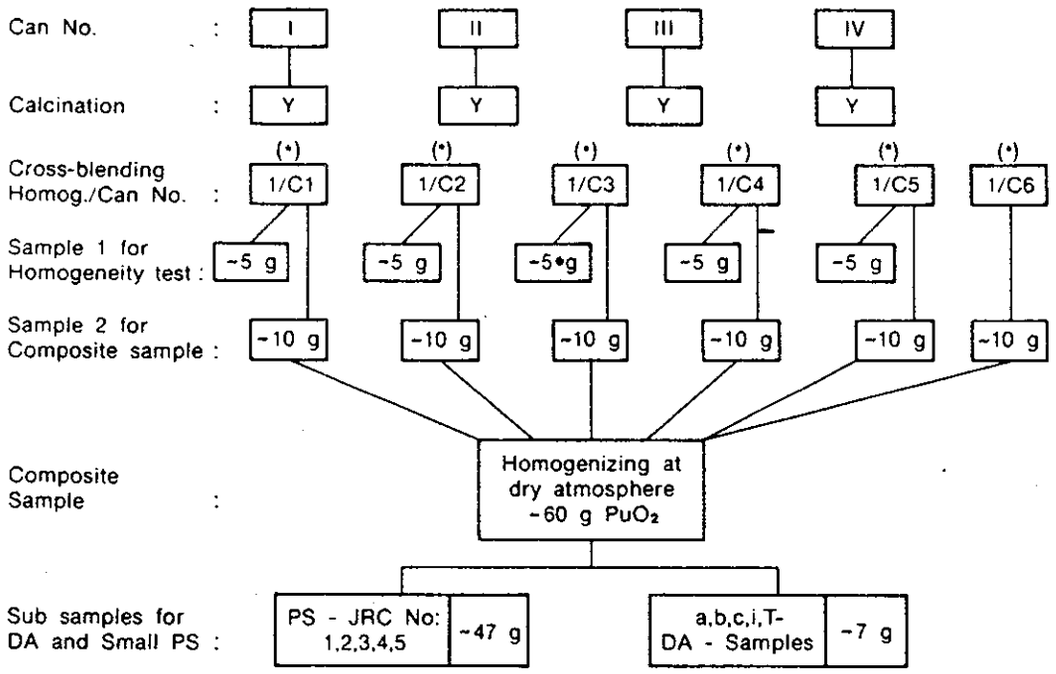

(*) ~1/6 mass from each can after calcination.

Figure 2. Sampling flow sheet for PuO_2 Lot 1.

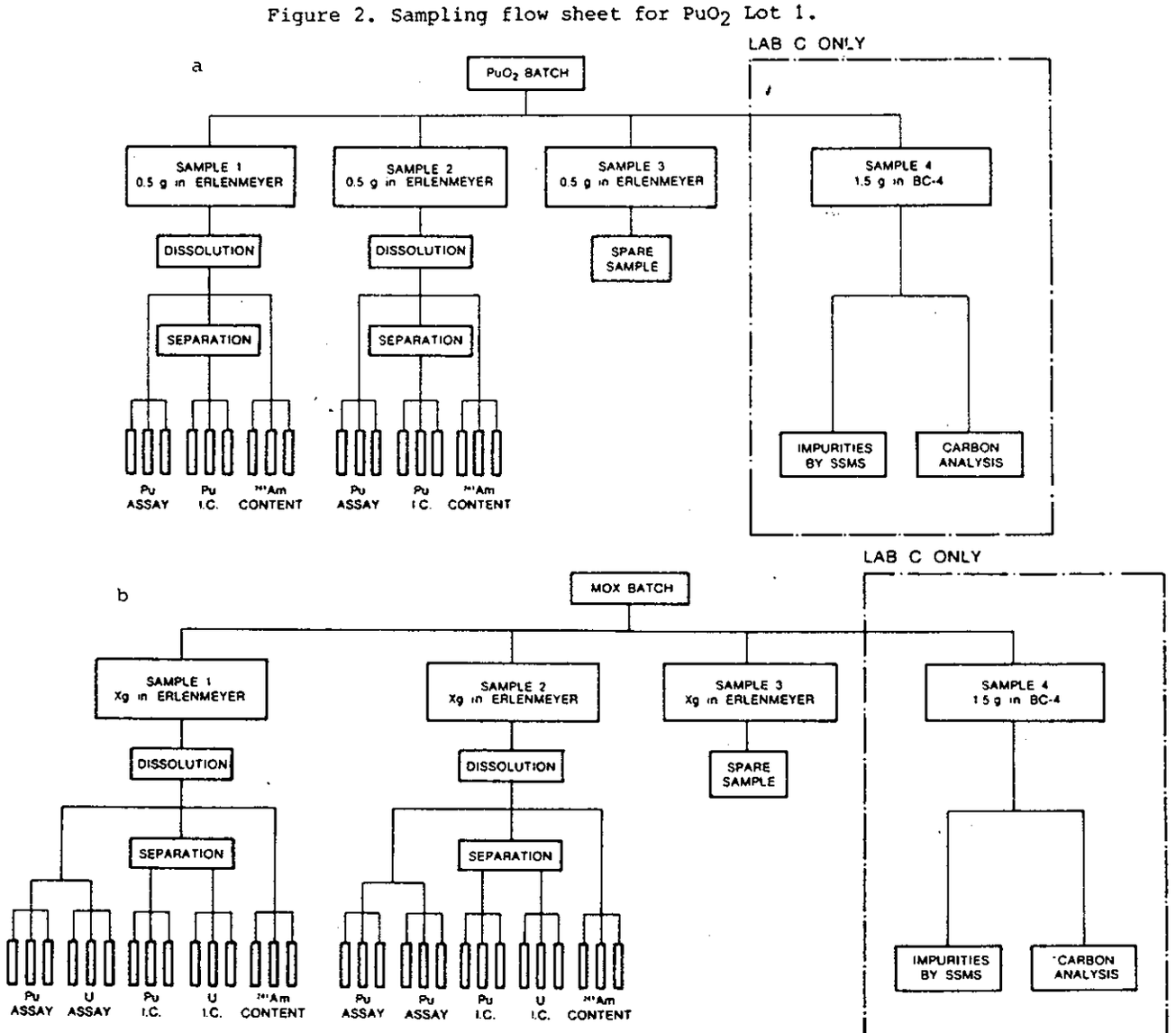

Figure 3. Analytical schemes for PuO_2 (a) and MOX (b). The same for laboratories A, B and C.

and on the other hand, that no further H_2O pick-up could occur after sampling. Actually, the whole preparation and sampling process was carried out in a dry nitrogen atmosphere.

4. ANALYTICAL METHODS

Dissolution

All the samples whatever the determination to be carried out, were dissolved in boiling HNO_3-HF (12 M - 0.05 M) for several hours depending on the type of material.

Pu concentration (PuO_2 and MOX samples)

The 3 laboratories have used the Pu potentiometric determination by the silver oxide method. Between 10 to 50 mg of Pu (depending on different laboratories) in an aliquot of 10 ml are oxidized to Pu(VI) by AgO and the AgO excess destroyed by sulphamic acid. Then Pu(VI) is reduced to Pu(IV) by Fe(II) in excess, the excess being titrated by potassium dichromate. Mo, Mn, V, W, Ce and Cr can interfere, but in this nuclear grade material their concentration is so small that their influence can be neglected.

U concentration (MOX samples)

Two laboratories used the Davis and Gray method as modified by Eberle and Lerner. U(VI) is reduced by Fe(II) to U(IV) in concentrated phosphoric acid solution. The excess iron is subsequently oxidized by HNO_3 in the presence of Mo and the U(IV) is determined by titration with $K_2Cr_2O_7$ to a potentiometric end point in the presence of V(IV). The vanadium increases the rate of equilibrium attainment and enhances the potential step at the equivalent point. In this case also the amount of potential interference is too small to influence the titration.

One laboratory used a thermogravimetric method for the oxygen to metal ratio and total metal determination. The U concentration is calculated by the difference between the total metal content and the concentration of the Pu-Am impurities.

U-Pu isotopic composition (PuO_2 and MOX samples)

The isotopic composition of all the samples was determined essentially by mass spectrometry after the separation of Pu from Am and U with the help of an ion exchanger such as Dowex Resin or Reversed-Phase-Chromatography. About 50 ng of Pu and 1 µg of U are loaded on the filaments for the thermal ionization. Only one laboratory used alpha spectrometry to determine ^{238}Pu.

^{241}Am concentration (PuO_2 and MOX samples)

In the 3 laboratories gamma spectrometry associated with Low Energy Photo detectors and multichannel analysers is the basic method for the ^{241}Am determination. However, each one uses the techniques in a different way. In one case the isotopic dilution method was preferred using ^{243}Am as a tracer. Mainly the 59 KeV line is used and ^{241}Am is calculated after correction of the influence of other radionuclides, of the dead time, etc.

Impurities

Only laboratory C received samples for the determination of the impurities; SSMS was used for all the elements with the exception of carbon, which was measured as CO_2 after combustion of the sample at a high temperature in a special furnace.

5. QUALITY CONTROL PROVISIONS

During the preparation of the destructive assay specimen of the Pu bearing PERLA standards (PuO_2 and MOX), a number of quality control measurements were carried out. The laboratories were, in fact, asked to perform and report sets of measurements employing certified reference materials, to be carried out during the analysis, in order to evaluate and correct systematic errors, if any, in their analytical techniques and, more generally, to allow the tracing back of elemental, isotopic, weight measurements to primary standards.

a) Preliminary homogeneity tests were performed on each original production PuO_2 lot before blending (as mentioned above), by taking samples from each can and measuring Pu concentrations and Pu isotopic compositions, according to the schemes already presented. The given specification for acceptance required a standard deviation of the single measurement on Pu concentration and ^{239}Pu lower than 0.1%, in order for it to be negligible with respect to the final error. The results obtained from these tests are presented in Table 4 and Figure 4, where the data obtained for Pu concentration and ^{239}Pu percentage are plotted. The standard deviations quoted confirm that the PuO_2 powders used for the preparation of the analytical samples and PERLA standards are homogeneous well within the 0.1% required.

b) The weighing of the PuO_2 and MOX powder DA samples was carried out according to special protocols which include the weighing of standard weights before and after each sampling.

The standard weights came from different sources: some of them were supplied by SCK/CEN, others came from the ALKEM factory and others came from the usual Sartorius balance kit.

It was possible to evaluate the difference between the average weight found ($\bar{x}_{exp}$) and the nominal weight (μ) for each scale and each standard weight by calculating:

$$t_{exp} = \frac{|\bar{x}_{exp} - \mu|}{\sigma_m} \quad \text{where } \sigma_m = \frac{s}{\sqrt{n}} \qquad (1)$$

(s is the standard deviation of the mean).

TABLE 4 - Relative standard deviation (%) of the single measurements evaluated in homogeneity tests of PuO_2 lots

PuO_2 lot	Number of cans	Pu-conc.	Pu-239
1	6	0.023	0.026
2	2	0.024	<0.01
3	6	0.064	0.009

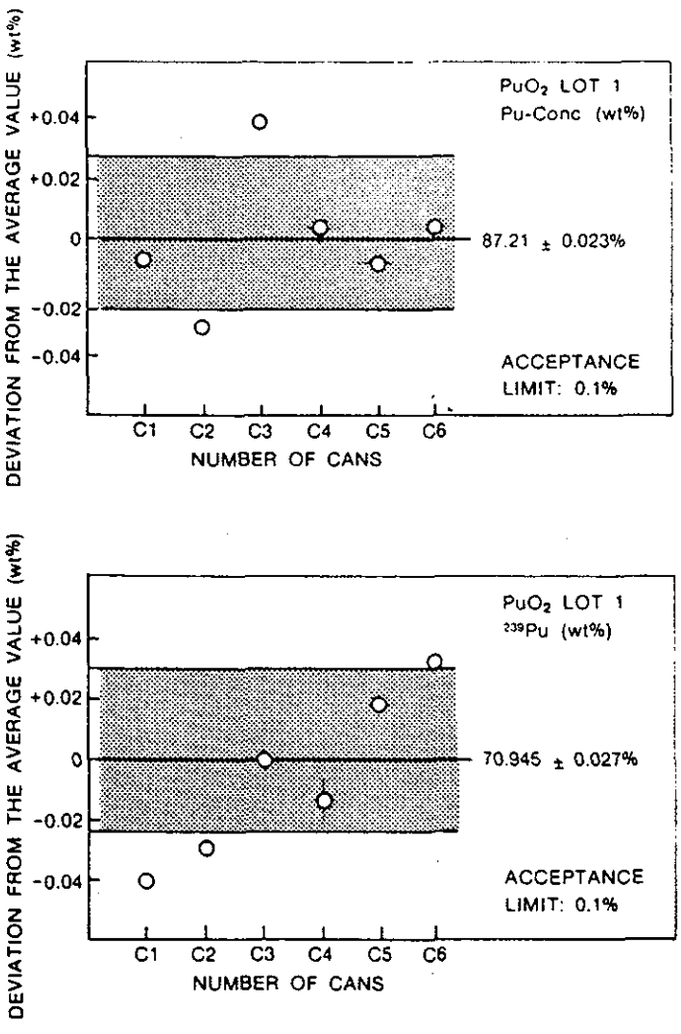

Figure 4. Plotting of homogeneity test results on PuO_2 Lot 1.

If t_{exp} is greater than t chosen from Fisher's table for a probability of P = 0.05 and for n-1 degrees of freedom, the deviation between $\bar{x}_{exp}$ and μ has statistical significance.

The standard weights and the balances used are shown in Table 5, where the experimental results are also reported. An example of data plot is given in Figure 5 with an indication of the period in which the preparation of the samples was carried out.

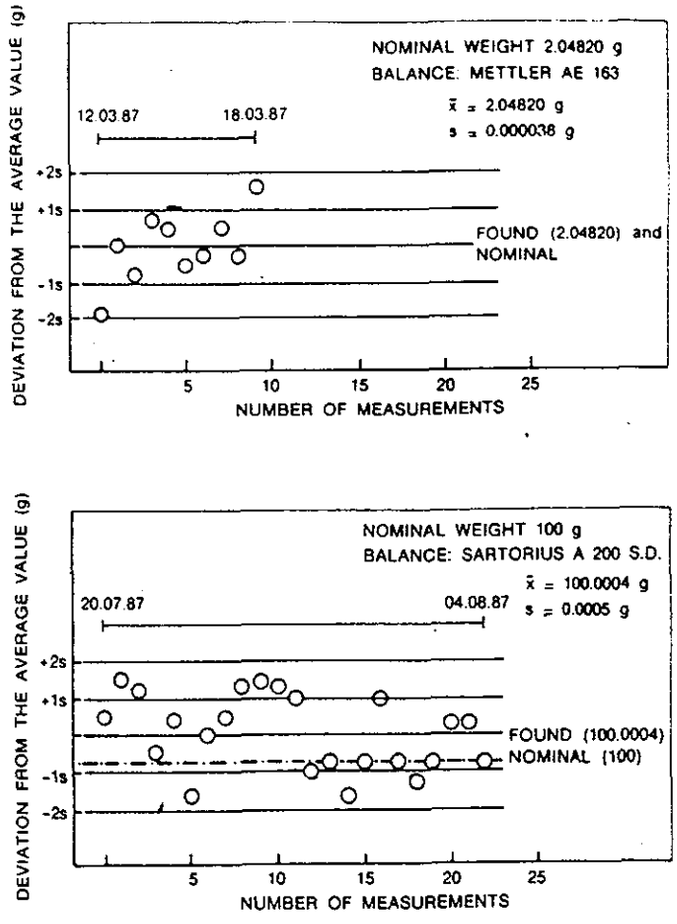

Figure 5. Plotting of scale test.

Discrepancies between the weights found and the nominal weights are in general of no statistical significance but, even when they are significant, the difference is practically negligible from the analytical point of view.

c) The results of analytical control checks are reported in the form of tables and graphs giving the percentage deviation of each measured parameter from the certified values. A summary of the results obtained in the three laboratories is given in Table 6.

The conclusion of this measurement is again that a few minor discrepancies with declared

TABLE 5 - Check of balances used during weighing of PuO_2 and MOX DA samples

Type of balance	Standard nominal weight (g) (μ)	Average found weight (g) ($\bar{x}_{EXP} \pm s$)	$\frac{\Delta x\%}{\mu}$ ($\frac{\bar{x}_{EXP}-\mu}{\mu}$)	Number of determinations
Sartorius A200 SD	0.43978	0.4397±0.0003	-0.02	16
"	1.04383	1.0438±0.00008	-0.003	20
"	2.04820	2.0482±0.00007	-	17
"	100.0	100.0004±0.0005	+0.0004	23
Mettler AE 163	0.43978	0.439785±0.000014	+0.001	10
"	1.04383	1.04883±0.000019	-	10
"	1.0	1.00002±0.000028	+0.002	9
"	2.04820	2.04820±0.000038	-	10
"	20.0	19.99997±0.000042	-0.00015	9

TABLE 6 - Quality control check on primary standards

Parameter measured	Standard used	Number of measurements	Percentage deviation from certified value
Laboratory A			
Pu-conc.	EC 201	14	-0.09
Pu-238	CBNM SMS6766	6	+0.92
Pu-238	NBS 947	2	-0.56
Pu-239	CBNM SMS6766	6	+0.014
Pu-239	NBS 947	2	+0.017
Pu-240	CBNM SMS6766	6	-0.046
Pu-240	NBS 947	2	-0.082
Pu-241	CBNM SMS6766	6	-0.02
Pu-241	NBS 947	2	+0.32
Pu-242	CBNM SMS6766	6	-0.15
Pu-242	NBS 947	2	-0.33
U-conc.	NBS 950a	N.I.	(1)
U-234	NBS U010	5	+1.30
U-234	NBS U500	2	+0.01
U-235	NBS U010	5	-0.06
U-235	NBS U500	2	-0.04
U-236	NBS U010	5	-0.59
U-236	NBS U500	2	+0.27
U-238	NBS U010	5	+0.001
U-238	NBS U500	2	+0.043
Am-241	N.I.		(2)
Laboratory B			
Pu-conc.	NBS 949f	N.I.	(3)
Pu-238	NBS 947	9	+0.96
Pu-239	NBS 947	9	-0.011
Pu-240	NBS 947	9	-0.014
Pu-241 (4)	NBS 947	9	+0.27
Pu-242	NBS 947	9	+0.03
U-conc.	NBS 960	7	(5)
U-234	NBS U010	11	-1.87
U-234	NBS U750	3	-0.13
U-235	NBS U010	11	+0.05
U-235	NBS U750	3	+0.03
U-236	NBS U010	11	+4.32
U-236	NBS U750	3	+0.22
U-238	NBS U010	11	-0.001
U-238	NBS U750	3	-0.091
Am-241	ORIS EL-4	2	(6)
Laboratory C			
Pu conc.	NBS 949f	14	-0.39
Pu-238	NBS 947	22	+0.06
Pu-239	NBS 947	22	+0.003
Pu-240	NBS 947	22	-0.003
Pu-241	NBS 947	22	-0.09
Pu-242	NBS 947	22	-0.07
U-conc.	ECNRM 110	6	+0.02
U-234	NBS U010	8	+0.21
U-234	NBS U500	6	+0.03
U-235	NBS U010	8	+0.06
U-235	NBS U500	6	+0.01
U-236	NBS U010	8	+0.61
U-236	NBS U500	6	+0.02
U-238	NBS U010	8	-0.001
U-238	NBS U500	6	-0.006
Am-241	CBNM ST-4	28	+0.32

(1) All measurements are within ±0.05% of the certified value.
(2) Relative determinations: each measurement is automatically corrected with the standard.
(3) All measurements are within ±0.07% of the certified value.
(4) 241/239 ratio is not used for calibration purposes.
(5) All measurements are within ±0.04% of the certified value.
(6) Both measurements are within ±0.2% of the certified value.
N.I.: not indicated.

values and expected uncertainties do not affect the required uncertainties of PERLA standards.

6. RESULTS AND EVALUATION

PuO_2 samples

The samples from the various batches were analyzed by the three laboratories mentioned according to the analytical schemes shown earlier in Figure 3. The analytical results reported for each measured parameter were then evaluated by Analysis of Variance (ANOVA):

- 1-way ANOVAs for the data from each laboratory to give a "laboratory mean" with its standard error, estimated by propagating variance components for the measurements (V_{REP}) and the errors between dissolution (V_{SAMP}) (subsample); the standard error of the "laboratory mean" is assumed as the overall uncertainty for a parameter for that laboratory, i.e.:

$$SE_1 = \sqrt{\frac{V_{REP}}{6} + \frac{V_{SAMP}}{2}} \qquad (2)$$

- 2-way ANOVAs for the data from all three laboratories to give a "grand mean" with its standard error estimated by propagating variance components for the measurements, the between dissolution (subsample) and the between laboratory (V_{LAB}) errors, i.e.:

$$SE_2 = \sqrt{\frac{V_{REP}}{18} + \frac{V_{SAMP}}{6} + \frac{V_{LAB}}{3}} \qquad (3)$$

Table 7 summarizes the results obtained for the

TABLE 7 - Summary of characterization measurements of PuO_2 lots. Reference date: 1st November 1987

Parameter measured	Lot	Laboratory mean (wt%) ± relative standard error (%) (2)			Grand mean (wt%) ± relative stand.error (%) (3)
		Lab. A	Lab. B	Lab. C	
Pu-conc.	1	87.07±0.06	86.93±0.05	87.05±0.07	87.02±0.06
	2	86.57±0.04	86.47±0.02	86.53±0.05	86.52±0.04
	3	86.87±0.04	86.55±0.06	86.75±0.11	86.72±0.11
Pu-238	1	0.2020±0.51	0.1979±0.12	0.1979±0.31	0.1993±0.65
	2	1.498 ±0.07	1.489 ±0.07	1.493 ±0.07	1.493 ±0.18
	3	1.728 ±0.23	1.717 ±0.29	1.717 ±0.06	1.721 ±0.23
Pu-239	1	70.956±0.003	70.961±0.007	70.949±0.007	70.955±0.004
	2	60.976±0.016	60.998±0.021	60.995±0.082	60.986±0.010
	3	58.102±0.007	58.061±0.009	58.124±0.005	58.096±0.030
Pu-240	1	24.579±0.008	24.577±0.016	24.592±0.016	24.583±0.019
	2	23.445±0.004	23.428±0.013	23.443±0.017	23.439±0.021
	3	24.768±0.008	24.771±0.008	24.765±0.008	24.768±0.008
Pu-241	1	3.289±0.06	3.290±0.06	3.285±0.03	3.288±0.06
	2	9.242±0.01	9.256±0.08	9.241±0.02	9.246±0.05
	3	9.762±0.02	9.790±0.04	9.760±0.02	9.771±0.05
Pu-242	1	0.9752±0.06	0.9743±0.07	0.9762±0.04	0.9752±0.06
	2	4.830 ±0.02	4.839 ±0.06	4.828 ±0.02	4.832 ±0.06
	3	5.640 ±0.02	5.661 ±0.04	5.633 ±0.04	5.645 ±0.15
Am-241 (µg/g Pu)	1	10120±0.20	10118±0.12	10369±0.44	10207±0.85
	2	13638±0.41	13475±0.10	13809±1.25	13636±0.75
	3	14240±0.83	14075±0.08	14408±1.15	14241±0.68

three PuO_2 lots; it displays the achieved level of measurement performance. The standard error of the "grand mean" is assumed to be the "overall uncertainty" of a parameter containing all the significant error components as discussed in previous sections.

A first general comment on Table 7 concerns the evaluated "standard error" of the grand mean which is always well below the required "overall uncertainty" as listed in Table 2. The only exception is ^{238}Pu of Lot 1 where an uncertainty of 0.7% is obtained against a required 0.5%. But, considering the low ^{238}Pu content (∿ 0.2%) the effect of 0.7% uncertainty on the effective power of the sample is negligible (less than 0.3% [9]). Then the samples of Lot 1 of laboratory B are perfectly acceptable from the NDA (calorimetry) point of view.

A second comment refers to the interlaboratory discrepancies; in all cases again with the exception of ^{238}Pu of PuO_2 Lot 1, the relative standard deviation between laboratories (Table 9) shows an excellent agreement with the expected DA uncertainties as quoted in Table 3, showing that all parameters of the characterization analyses, i.e. homogeneity, sampling, representativeness, differential humidity pick-up, sample preparation and conditioning, transport, chemical treatment, analytical measurements, etc., were under control, giving the proof of a good interlaboratory exercise as well as of an excellent characterization level.

A typical pattern of data is given in Figure 6 where the results of one parameter (Pu concentration) of the three laboratories are plotted, showing visually the conclusions just drawn. The ^{241}Am results showed slightly large interlaboratory differences: consequently, two laboratories rechecked the analyses using new reference standards, confirming essentially the previous average results.

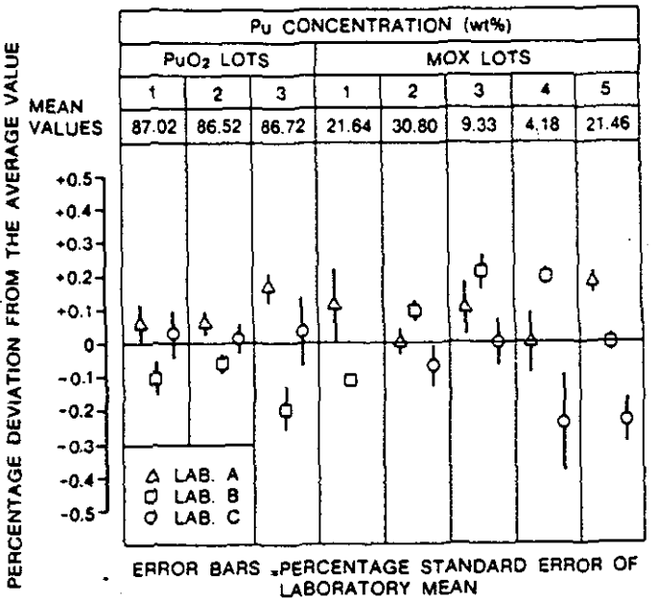

Figure 6. Pu concentration: plot of analytical results.

TABLE 8 - Summary of characterization measurements of MOX lots . Reference date: 1st November 1987

Parameter measured	Lot	Laboratory mean (wt%) ± relative standard error (%) (2)			Grand mean (wt%) ± relative stand.error (%) (3)
		Lab. A	Lab. B	Lab. C	
Pu-conc.	1	21.67±0.11	21.62±0.01	-	21.64±0.11
	2	30.80±0.04	30.83±0.03	30.78±0.06	30.80±0.04
	3	9.34±0.08	9.35±0.05	9.33±0.07	9.33±0.06
	4	4.18±0.09	4.19±0.02	4.17±0.20	4.18±0.12
	5	21.50±0.03	21.46±0.02	21.41±0.08	21.46±0.13
Pu-238	1	0.6890±2.90	0.6759±0.06	0.6759±0.37	0.6803±0.64
	2	0.3485±1.03	0.3488±0.11	0.3481±0.23	0.3485±0.06
	3	1.046 ±0.95	1.027 ±0.13	1.024 ±0.07	1.032 ±0.07
	4	1.415 ±0.71	1.412 ±0.12	1.412 ±0.13	1.413 ±0.08
	5	0.3643±1.07	0.3674±0.20	0.3648±0.27	0.3655±0.26
Pu-239	1	69.034±0.027	69.019±0.011	69.040±0.006	69.031±0.009
	2	71.204±0.003	71.186±0.015	71.189±0.019	71.193±0.008
	3	64.420±0.005	64.398±0.004	64.439±0.008	64.419±0.005
	4	59.536±0.015	59.495±0.010	59.516±0.004	59.516±0.020
	5	76.948±0.003	76.934±0.002	76.924±0.006	76.935±0.009
Pu-240	1	22.524±0.021	22.534±0.016	22.530±0.007	22.530±0.013
	2	23.033±0.007	23.041±0.017	23.041±0.024	23.038±0.011
	3	24.037±0.013	24.049±0.013	24.047±0.008	24.044±0.015
	4	24.725±0.008	24.731±0.010	24.733±0.016	24.730±0.010
	5	18.739±0.008	18.742±0.009	18.753±0.018	18.744±0.024
Pu-241	1	4.996±0.01	5.008±0.04	4.998±0.02	5.000±0.07
	2	3.807±0.03	3.815±0.08	3.809±0.24	3.810±0.06
	3	6.849±0.02	6.864±0.04	6.848±0.03	6.854±0.02
	4	9.428±0.04	9.449±0.03	9.439±0.01	9.439±0.06
	5	2.779±0.03	2.783±0.02	2.782±0.05	2.782±0.04
Pu-242	1	2.757±0.02	2.763±0.04	2.755±0.05	2.758±0.08
	2	1.607±0.04	1.610±0.07	1.613±0.04	1.610±0.12
	3	3.649±0.02	3.661±0.05	3.642±0.05	3.651±0.02
	4	4.897±0.05	4.912±0.04	4.900±0.02	4.903±0.09
	5	1.170±0.03	1.173±0.03	1.175±0.04	1.173±0.12
U-conc.	1	65.92±0.06	65.91±0.02	-	65.91±0.01
	2	56.87±0.03	56.79±0.05	56.75±0.09	56.80±0.06
	3	78.57±0.01	58.56±0.02	78.51±0.02	78.55±0.02
	4	84.04±0.01	83.90±0.01	84.04±0.03	83.99±0.05
	5	66.20±0.01	66.24±0.01	66.14±0.02	66.19±0.05
U-234	1	0.02440±0.4	0.02498±0.4	0.02497±0.4	0.02478±0.8
	2	0.01645±0.7	0.01697±0.4	0.01702± (*)	0.01681±1.0
	3	0.0096 ±1.04	0.0100 ±1.0	0.0102 ± (*)	0.0099 ±1.8
	4	0.0065 ±1.5	0.0068 ±4.4	0.0066 ± (*)	0.0066 ±1.5
	5	0.3936 ±0.01	0.3938 ±0.05	0.3932 ±0.15	0.3935 ±0.04
U-235	1	0.7282±0.05	0.7278±0.03	0.7294±0.04	0.7285±0.07
	2	0.7295±0.03	0.7303±0.04	0.7305±0.05	0.7301±0.04
	3	0.7390±0.12	0.7390±0.17	0.7415±0.04	0.7398±0.11
	4	0.7136±0.01	0.7142±0.04	0.7151±0.03	0.7143±0.06
	5	62.663±0.01	62.683±0.05	62.696±0.01	62.680±0.01
U-236	1	0.0083±1.2	0.0088±0.8	0.0087±1.1	0.0086±1.9
	2	0.0142±1.4	0.0148±0.7	0.0147±2.7	0.0146±1.2
	3	0.0023±1.7	0.0025±4.0	0.0023± (*)	0.0024±11.0
	4	0.00045±22.0	0.00099±15.1	0.00026± (*)	0.00057±40.0
	5	0.2597± (*)	0.2599±0.1	0.2594±0.1	0.2598±0.1
U-238	1	99.239±0.0010	99.239±0.0003	99.237±0.0004	99.238±0.0006
	2	99.240±0.0005	99.238±0.0003	99.238±0.0003	99.238±0.0002
	3	99.249±0.0004	99.248±0.0007	99.246±0.0002	99.248±0.0002
	4	99.279±0.0002	99.298±0.0003	99.278±0.0002	99.278±0.0005
	5	36.684±0.02	36.664±0.09	36.652±0.02	36.667±0.02
Am-241 (ug/g Pu)	1	35000±0.34	35333±0.07	36293±0.62	35542±1.05
	2	19793±0.77	19741±0.15	20031±0.35	19852±0.45
	3	19200±0.93	19180±0.06	19842±0.26	19407±1.10
	4	9050±1.83	9003±0.14	9369±1.17	9138±1.25
	5	25700±0.42	25235±0.05	25854±0.38	25596±0.75

(*) not yet evaluated.

MOX samples

Similar conclusions can be drawn from Tables 8 and 9 concerning the MOX samples. Again the standard error is practically always lower than the required "overall accuracy" and the interlaboratory standard deviation is always lower than or equal to the overall accuracy expected by the three laboratories.

7. CONCLUSIONS

Throughout the preparation and characterization of PERLA standards we tried to follow a simple logic:

- define needs;
- prepare accurate procedures for any process step to ensure the fulfilment of the needs.

The results obtained confirm that

a) the needs from the PERLA inventory characterization point of view were perfectly fulfilled, since the evaluated overall uncertainties are actually lower than the values required;
b) if we want to look at this exercise as an interlaboratory comparison we also fulfilled the goal of keeping uncertainty sources perfectly under control; the interlaboratory standard deviation is, in fact, always below, frequently well below, the assumed laboratory uncertainty.

8. ACKNOWLEDGEMENTS

Thanks are due to JRC-TUI, Karlsruhe staff who participated in the preparation of PERLA samples. Particularly, the collaboration of Messers. K. Richt J.F. Guegnon and J. Kalbusch is acknowledged.

TABLE 9 - Relative standard deviation (%) between the average results obtained by the three laboratories

Parameter measured	PuO_2 samples		MOX samples		Parameter measured	PuO_2 samples		MOX samples	
	Lot	RSD(%)	Lot	RSD(%)		Lot	RSD(%)	Lot	RSD(%)
Pu-conc.	1	0.09	1	0.16	U-conc.			1	0.01
	2	0.06	2	0.08				2	0.11
	3	0.19	3	0.11				3	0.04
			4	0.20				4	0.12
			5	0.21				5	0.08
Pu-238	1	1.19	1	1.11	U-234			1	1.3
	2	0.30	2	0.12				2	1.7
	3	0.37	3	1.15				3	3.1
			4	0.12				4	2.3
			5	0.45				5	0.08
Pu-239	1	0.01	1	0.01	U-235			1	0.11
	2	0.02	2	0.01				2	0.07
	3	0.06	3	0.03				3	0.19
			4	0.03				4	0.11
			5	0.04				5	0.03
Pu-240	1	0.03	1	0.02	U-236			1	3.1
	2	0.04	2	0.02				2	2.2
	3	0.01	3	0.03				3	4.9
			4	0.02				4	67.0
			5	0.04				5	0.1
Pu-241	1	0.08	1	0.12	U-238			1	0.001
	2	0.09	2	0.11				2	0.001
	3	0.17	3	0.13				3	0.001
			4	0.11				4	0.001
			5	0.08				5	0.044
Pu-242	1	0.10	1	0.15	Am-241	1	1.41	1	1.90
	2	0.11	2	0.19		2	1.22	2	0.78
	3	0.26	3	0.26		3	1.17	3	1.94
			4	0.16				4	2.18
			5	0.21				5	1.26

9. REFERENCES

1. Summary conclusions of ESARDA Working Group on non destructive assay, Proc. of 8th Ann. ESARDA Symp.; Consideration on NDA Instrument Performances, Copenhagen (DK), May 13-14, 1986.
2. A. Sandstroem, 3rd Adv. Group Meet. on Evaluation of Quality of Safeguards NDA Measurement data, IAEA, Vienna, 1983.
3. R. Abedin-Zadeh et al., Preparation of a plant specific standard for MOX pins, Proc. of 4th Ann. ESARDA Symp. Spec. Meet. on Harmonization and Standardization in Nuclear Safeguards, Petten (NL), 1982.
4. R. Abedin-Zadeh, T. Beetle, G. Busca, S. Guardini, E. Kuhn, D. Terrey, Preparation and characterization of plant specific reference materials: results and progress, 5th Ann. ESARDA Symp., Versailles (F), April 19-21, 1983.
5. G. Busca, M. Cuypers, S. Guardini, General criteria for the procurement of plant specific reference materials, Proc. of 4th Ann. ESARDA Symp. Spec. Meet. on Harmonization and Standardization in Nuclear Safeguards, Petten (NL), 1982.
6. Working Group "Definition of Procedures for the Preparation of PERLA Standards", Modified Procurement and Characterization Scheme for the Pu PERLA standards, JRC Special Activities Report No.I.07.C3.85.26, FMM/C-109, November 1985.
7. P. De Bièvre et al., How well can uranium and plutonium from irradiated fuel be assayed by the nuclear community? Final results of the IDA-80 Programme, Proc. of 7th ESARDA Symp., Liège (B), May 21-23, 1985, p.339.
8. W. Beyrich et al., The IDA-80 measurement evaluation Programme on mass spectrometric isotope dilution analysis of uranium and plutonium, Vol.1,2,3, EUR 7990 EN (1984); EUR 7991 EN (1984); EUR 7992 EN (1985).
9. R. Carchon, S. Guardini, Calorimetry for safeguards nuclear material management, ESARDA Bulletin, No.7, October 1984.

IAEA-SM-293/89
ORA 32.688

International Atomic Energy Agency
International Symposium
on
Recent Advances in Nuclear Material Safeguards
Vienna, Austria
10-14 November 1986

LATEST DEVELOPMENT AND IMPLEMENTATIONS OF INSTRUMENTS FOR URANIUM ASSAY BY DELAYED NEUTRON TECHNIQUES

* R. Adam, * P. Agostini, * L. Becker, * M. Bernede, * L. Caldon,
* G. Cordani, * F. Farese, ** R. Haas, * V. Vocino.

Commission of the European Communities,
* Joint Research Centre, Ispra Establishment, 21020 Ispra (VA)
** EURATOM Safeguards Directorate Luxemburg.

Abstract

The principle of delayed neutron technique is known for many years for Uranium assay. This paper shows the implementation of the technique for field instrumentation designed for safeguards inspections.

Two devices : SIGMA and DUCA have been studied and developed in the last years at JRC Ispra for the European Safeguards Directorate. With these devices, measurements can be made for the assay of Uranium 235 in Uranium- Thorium oxide contained in fuel pebbles (60mm diameter graphite spheres) (SIGMA) used in high temperature reactor and in Uranium oxide as powder or pellets contained in a cylindrical capsule with a diameter of 18mm and length of 83 mm (DUCA).

These instruments are constituted by:

- irradiation zone in which 4 Cf 252 sources supply a neutron flux for the active interrogation of the sample;

- a counting zone which houses the He3 detectors in a polyethylene block which measure the delayed neutron rate coming from the sample.
In the DUCA device the two functions (irradiation-counting) are obtained in the same zone; a bar carrying the 4 Cf 252 sources is moved in or out of the zone. (Shuffler principle)

Fig.1 and 2 show a schematic view of the SIGMA and DUCA devices.

SIGMA has been implemented more than 10 years ago but in the last years some improvements were made in order to obtain a device more inspector friendly to use, more reliable and able to improve the measurement accuracy to better then 0.3%. The improvements are summarized by:

- All the operations are made from the floor level;
- The possibility of automatic measurement repetition increases accuracy
- The use of a modern instrument control system to increase the reliability of the measurements;
- The self diagnosis system greatly facilitates instrument check out and maintainance.
- Computing of corrected mean values including statistical data
- The automatic measurement evaluation includes error propagation.

A fast neutron counting chain has been developed in order to reduce the counting losses above all in the first two seconds after the irradiation when the count rate is high. The dead time of the system is about 1 us.

The hardware of the control and data handling system consists of :

- a microcomputer (SIGMA: u MAC 5000 Analog Device - DUCA: Intel 8030) on which a dedicated software has been implemented
- an intelligent terminal (IRIS) linked to the microcomputer
- a neutron counting chain
- a synoptic panel
- a low voltage power supplier unit.

For DUCA a calibration formula has been developed in order to correlate the net total counts (I) with the content of Uranium 235 (U5) and Uranium 238 (U8). This formula takes into account the thermal flux depression in the matrix of the sample, the thermal fissions in U235, fast fissions in U235 and fast fissions in U238. The algorithm is :

$$I = a\,U_5^2 + bU_5 + c\,U_8 + d\,U_5U_8$$

where the calibration constants a, b, c and d have been optimized with a best fit method of linear regression for powders and pellets (with enrichment from natural to 6.5%). The agreements between declared and measured value was always better then 0.5% for pellets and 0.6% for powders using a simple measurement cycle. (It is planned to implement pellets and powder measurement, also on SIGMA).
The paper describes also laboratory tests, field tests and implementation exercise that have been done on these devices.

In conclusione we can say :

i) The system will give the minimum verification time and require minimum inspector effort at the plant

ii) The operating system provide automatic selfdiagnosis of the instrument

iii) New design for some subsystems in order to get maximum reproducibility, to improve the measurement accuracy

iv) The devices have two different fields of application:

- SIGMA, stationary at-HOBEG, has been dedicated to inspections on pebbles of AVR and THTR reactors
- DUCA, transportable, will be used for inspections on powder or pellets of Light Water Reactor with a sampling on bulk quantity.

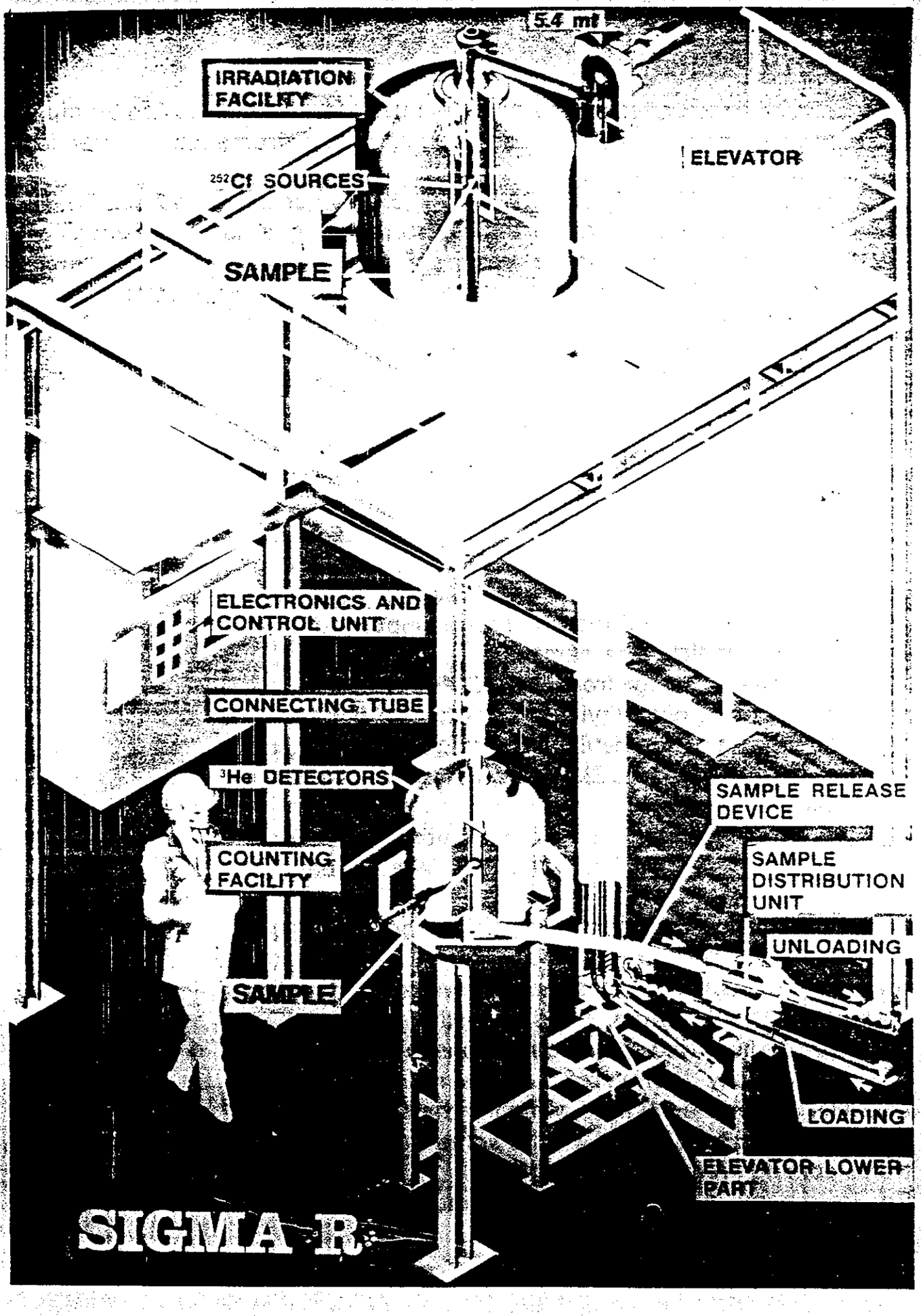
5.4 m
IRRADIATION FACILITY
ELEVATOR
^{252}Cf SOURCES
SAMPLE
ELECTRONICS AND CONTROL UNIT
CONNECTING TUBE
^{3}He DETECTORS
SAMPLE RELEASE DEVICE
COUNTING FACILITY
SAMPLE DISTRIBUTION UNIT
UNLOADING
SAMPLE
LOADING
ELEVATOR LOWER PART
SIGMA R

INTRODUCTION

The delayed neutron technique has been used for many years for Uranium assay: here the implementation of the technique on field instrumentation, used in routine inspections, is shown.

Two devices : SIGMA (2) and DUCA (4) (5) have been studied and developed in recent years at JRC Ispra for the Euratom Safeguards Directorate.

SIGMA was built more than 10 years ago (1) in order to make measurements for the assay of U235 on pebbles of the AVR and THTR reactors.

After some years of usage it was seen that certain modifications were required to simplify and achieve better reproducibility in instrument-operation, and to improve reliability. These modifications were carried out in order to improve the accuracy of SIGMA-R measurements.

Recently a request was made for a transportable instrument (the SIGMA instrument at HOBEG is stationary). So DUCA has been studied and developed in order to achieve this goal. DUCA has been designed in such a way that measurements can be made on sampled material from different kinds of reactor and in particular for Uranium oxide powder or pellets from Light Water Reactors.

Both these devices use four high flux Cf^{252} sources (neutron output 1.15 10^8 n/s) in order to supply a neutron flux to irradiate the sample.

The neutrons coming from the Cf^{252} sources are slowed down in a polyethylene block before penetrating the sample. The resulting thermal neutron flux induces fissions on the U235 and prompt and delayed neutrons are produced.

Delayed neutrons are counted by waiting 0.5 s for DUCA and 2.2 s for SIGMA-R to start taking measurements.

At this moment the sample will be in the counting zone in which, by means of a polyethylene moderator, the delayed neutrons are slowed down and are detected by He3 detectors, housed in the moderator.

The neutron flux used to induce fissions in the sample is not completly thermalized. Some neutrons have energies higher the 0.8 MeV, which is the threshold of fission for U238, so there will be some delayed neutrons coming from U238.

So, in general in the calibration formula, this effect has to be taken into account.

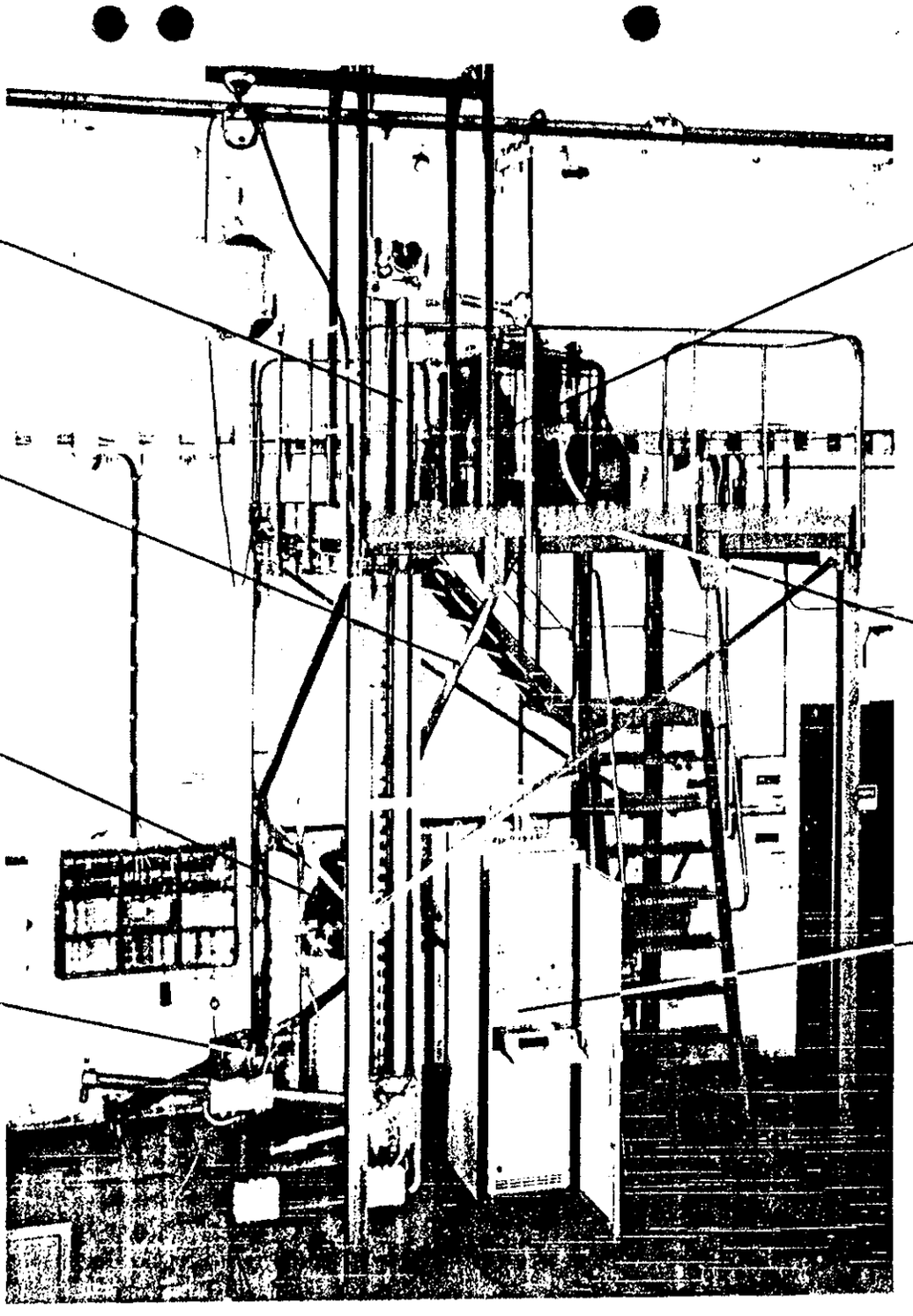
ELEVATOR
IRRADIATION FACILITY
CONNECTING TUBE
MAIN STRUCTURE
COUNTING FACILITY
CONTROL RACK
DISTRIBUTION UNIT

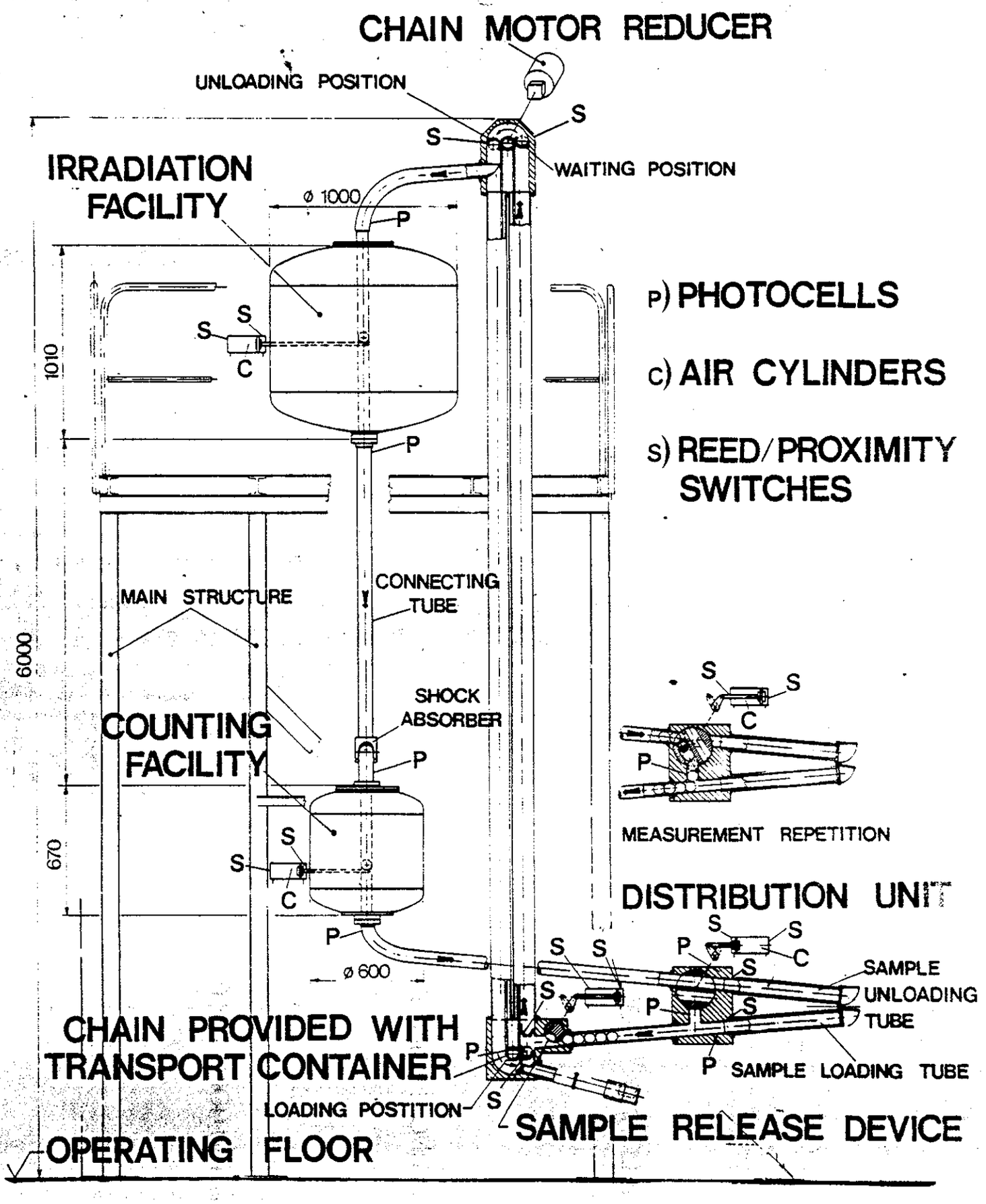
CHAIN MOTOR REDUCER
UNLOADING POSITION
S
S
WAITING POSITION
IRRADIATION FACILITY
ø 1000
P
P) PHOTOCELLS
C) AIR CYLINDERS
S) REED/PROXIMITY SWITCHES
1010
S
S
C
P
MAIN STRUCTURE
CONNECTING TUBE
6000
SHOCK ABSORBER
COUNTING FACILITY
P
670
S
S
C
P
ø 600
S
S
C
MEASUREMENT REPETITION
DISTRIBUTION UNIT
S
S
P
S
C
S
S
S
P
S
SAMPLE UNLOADING TUBE
P
P
SAMPLE LOADING TUBE
CHAIN PROVIDED WITH TRANSPORT CONTAINER
P
LOADING POSTITION
S
SAMPLE RELEASE DEVICE
OPERATING FLOOR

14320132

SPHERICAL FUEL ELEMENTS FOR THTR PEBBLE-BED REACTOR

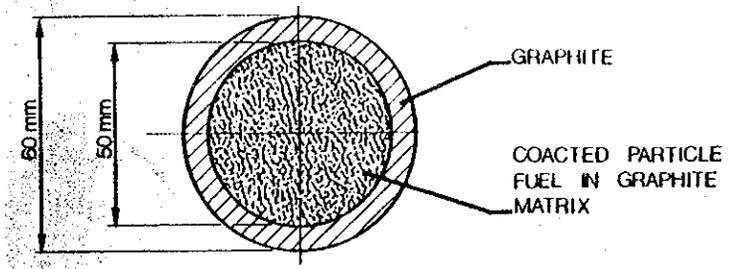

SIGMA-R SAMPLES

The central core contains a mixture of graphite and graphite-coated particles of (U, Th) oxides. (1)
The specification of the nuclear material content is as follows : each pebble contains

0.96 g (± 5%) of 93% enriched Uranium and
9.62 g (± 1%) of Thorium

CALIBRATION CURVE

The very narrow range of Uranium and Thorium weight per pebble allows the use of a straight line calibration curve. This model is sufficient good to forecast the U235 content of an unknown pebble with very high accuracy.
It is also planned to implement measurements on pellets and powders of low enriched uranium with this measurement system.
In this case a wider range of Uranium weights per sample, will be assayed and a new interpretation algorithm for the calibration curve will be needed.

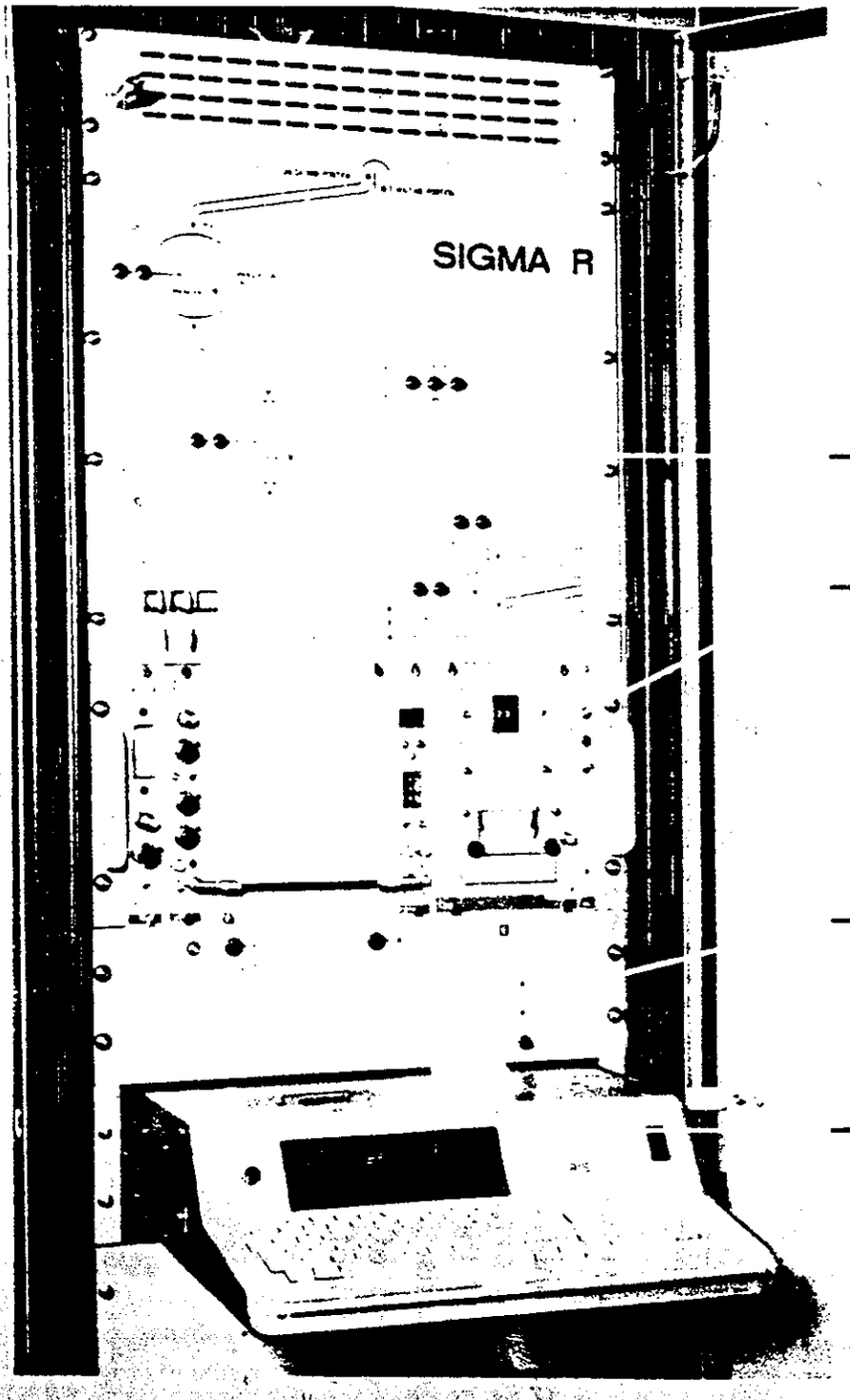

SIGMA CONTROL RACK

— Synoptic panel

— Pulse measuring chain
CAMBERRA:
- Power supply
- Amplifier discriminator
- Counter timer
- Printer

— Microprocessor
μMAC 5000 Analog Device
based on INTEL 8088

— IRIS Terminal :
Interface system-operator

BLOCK DIAGRAM OF SIGMA-R ELECTRONIQUE EQUIPMENT

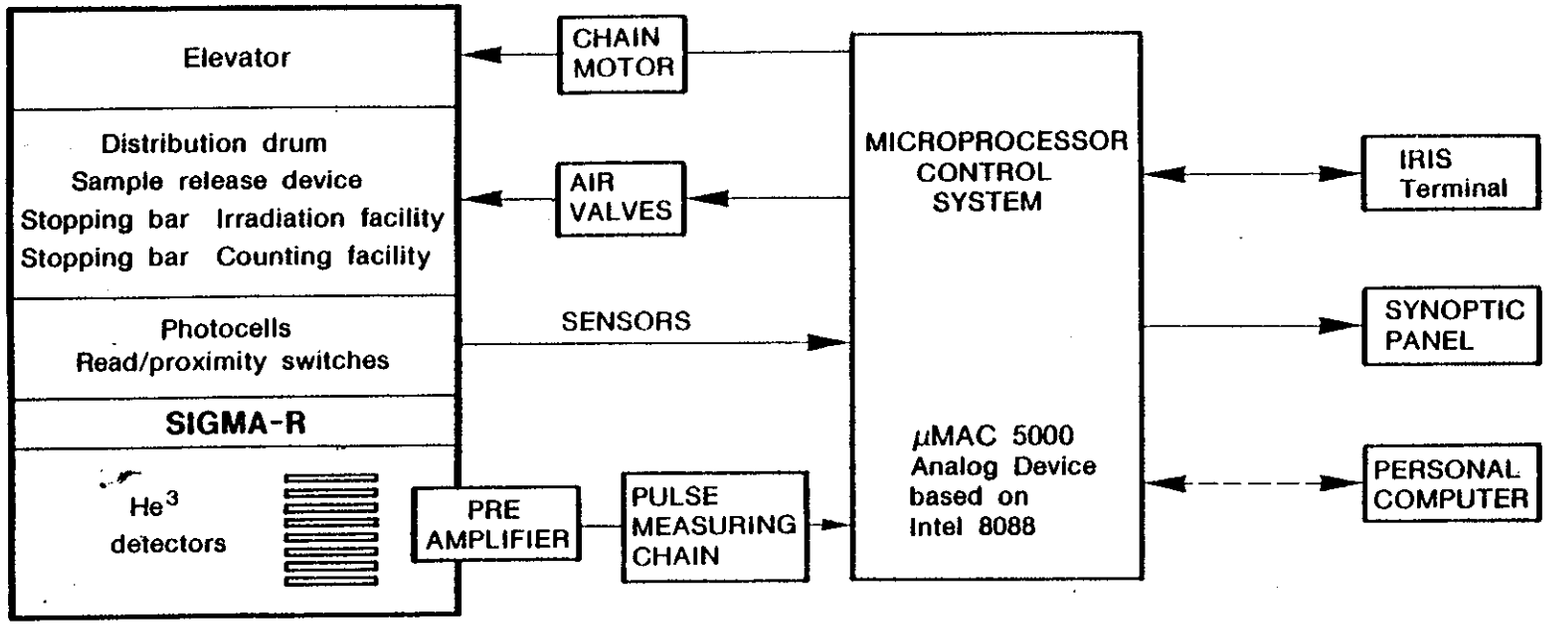

The inspectors do not need the personal computer, that has to be used only to change the software already implemented on the microprocessor.

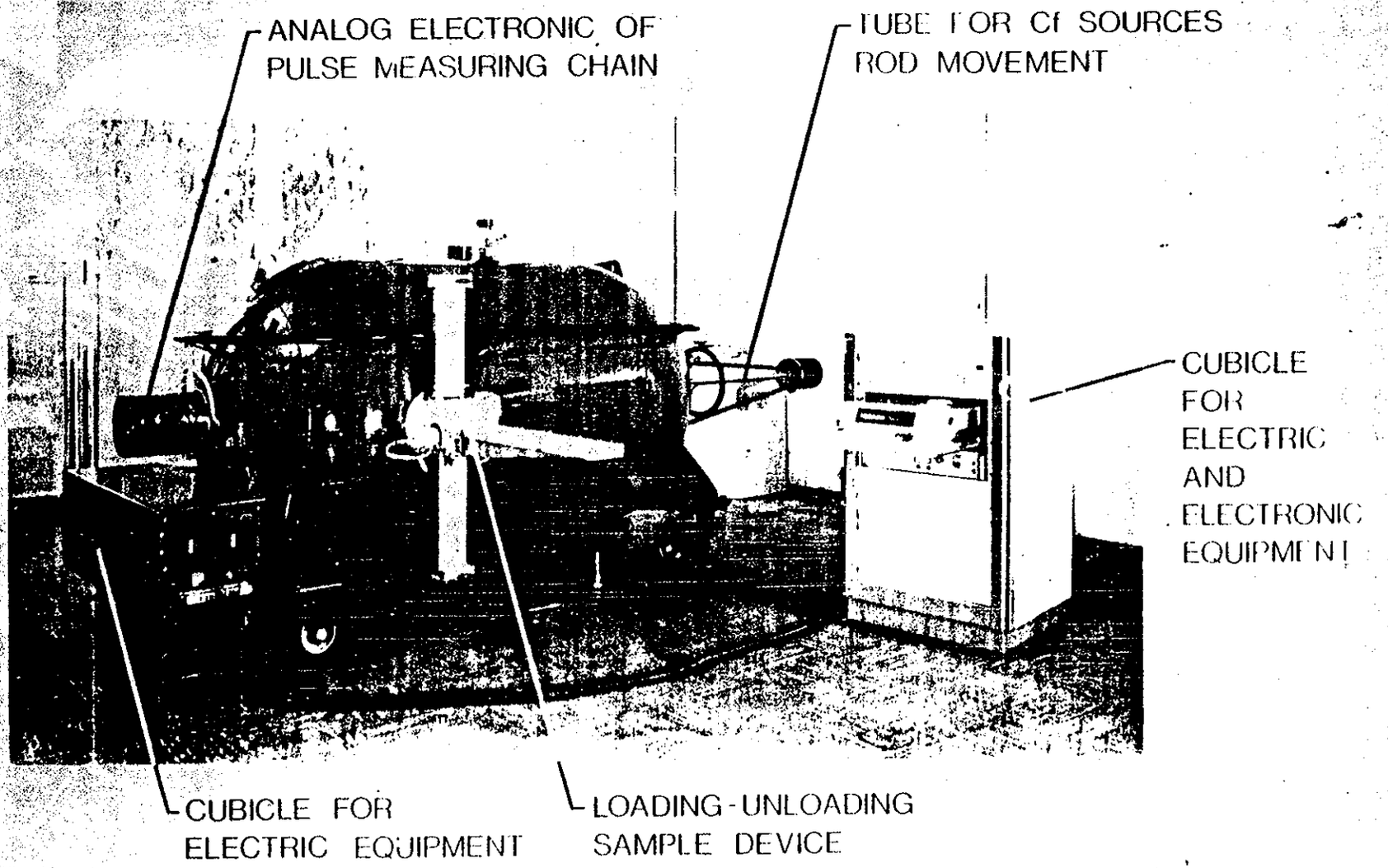
ANALOG ELECTRONIC OF
PULSE MEASURING CHAIN
TUBE FOR Cf SOURCES
ROD MOVEMENT
CUBICLE
FOR
ELECTRIC
AND
ELECTRONIC
EQUIPMENT
CUBICLE FOR
ELECTRIC EQUIPMENT
LOADING-UNLOADING
SAMPLE DEVICE

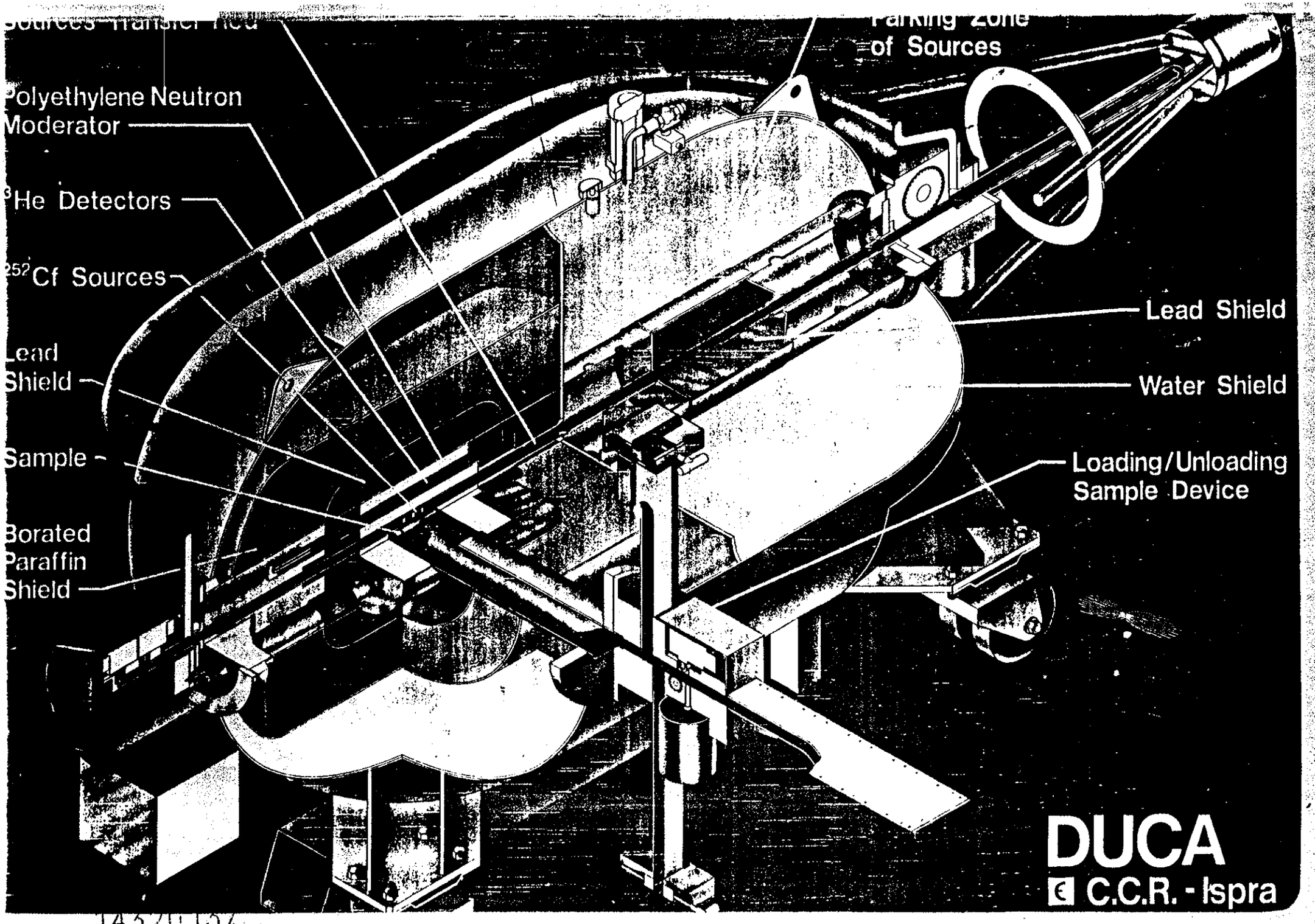
Sources Transfer Rod
Parking Zone of Sources
Polyethylene Neutron Moderator
^{3}He Detectors
^{252}Cf Sources
Lead Shield
Sample
Borated Paraffin Shield
Lead Shield
Water Shield
Loading/Unloading Sample Device
DUCA
C.C.R. - Ispra

1432157

ELECTRICAL EQUIPMENT

THE DRAWING SHOWS THE APPARATUS DURING THE SAMPLE IRRADIATION

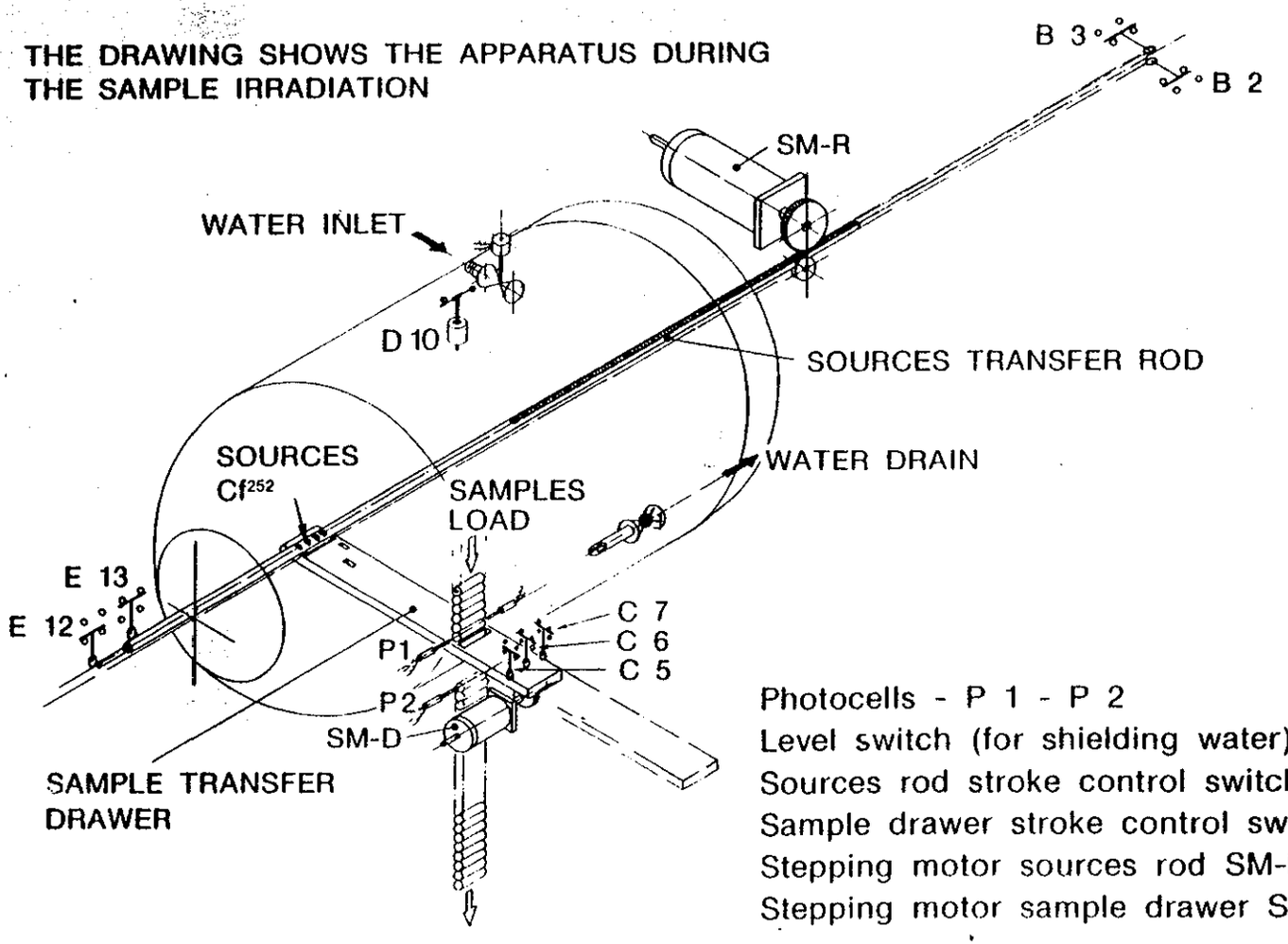

Photocells - P 1 - P 2
Level switch (for shielding water) - D 10
Sources rod stroke control switches - B 2, 3-E 12, 13
Sample drawer stroke control switches - C 5, 6, 7
Stepping motor sources rod SM-R
Stepping motor sample drawer SM-D

DUCA CONTROL RACK

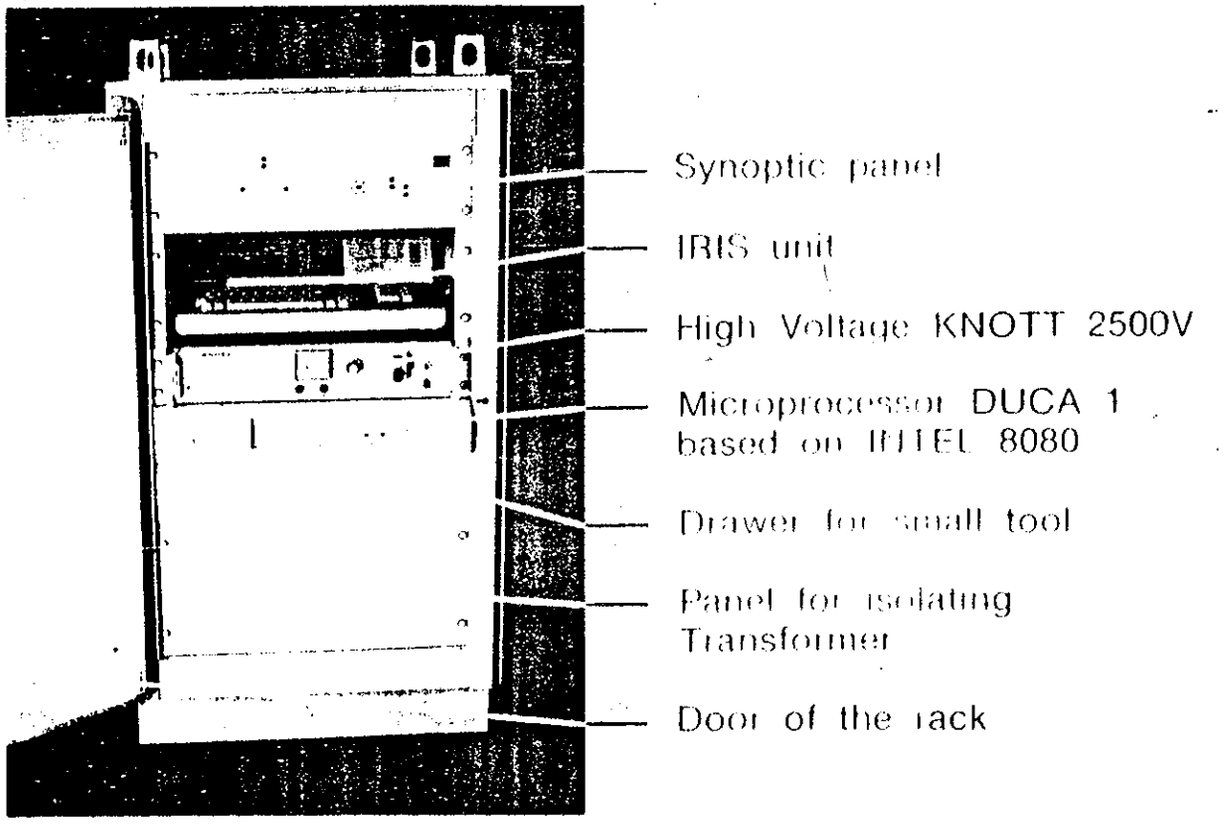

BLOCK DIAGRAM
OF DUCA ELECTRONIQUE EQUIPMENT

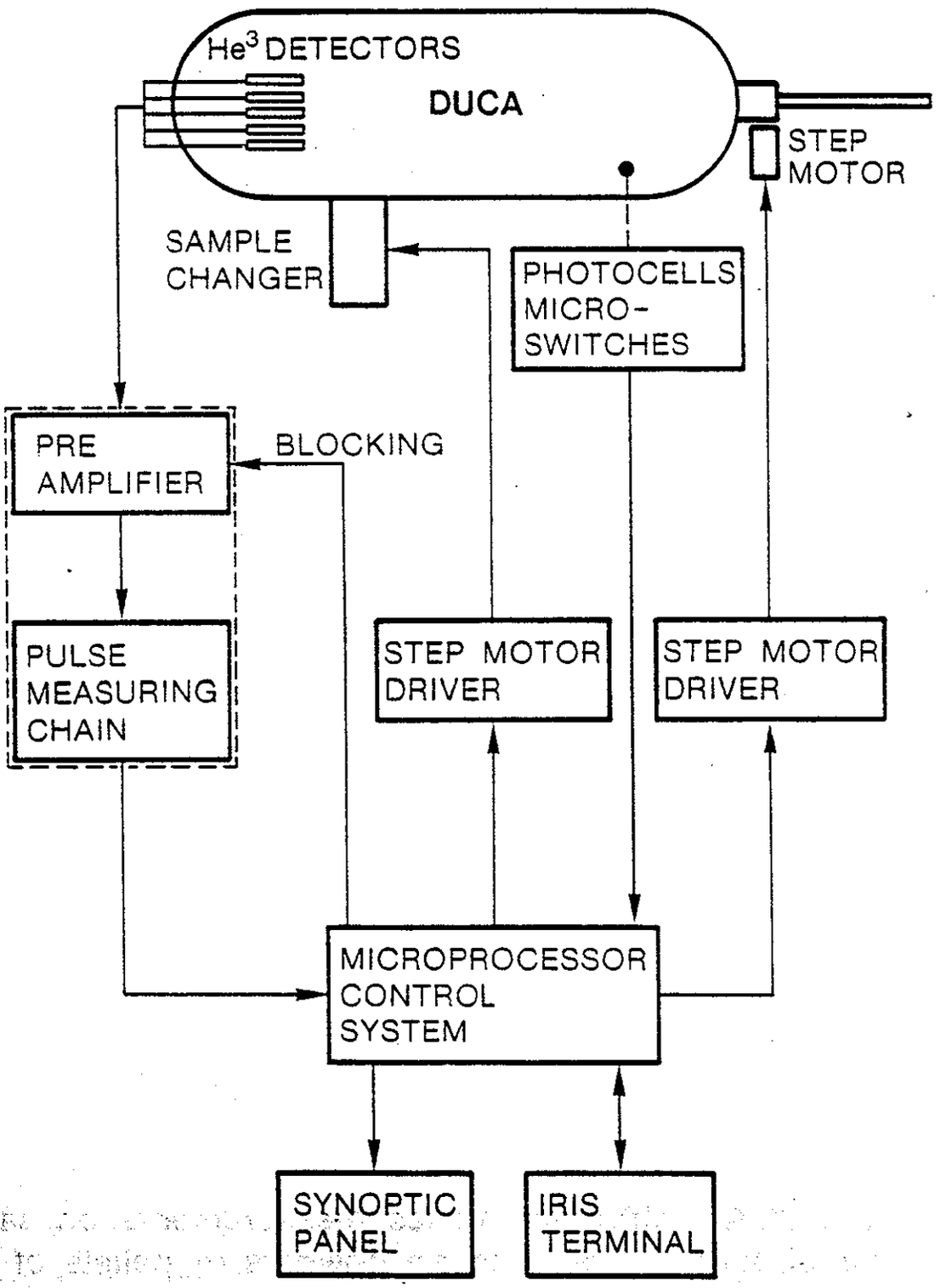

SAMPLE HOLDERS

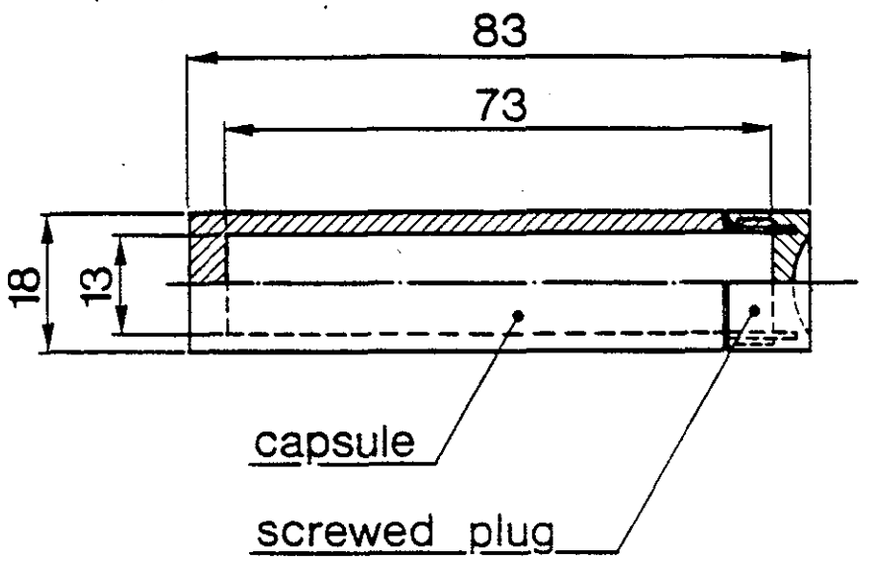

dimensions in mm

Inner volume = 9.7 cm^3

Material = polycarbonate

Weight of powders 25 ÷ 30 g of UO_2

Weight of pellets : from 25 up to 100 g of UO_2 (relating to the diameter of the pellets of the different kind of reactors)

The DUCA instrument makes measurements on sampling material such as for example powders or pellets of LWR's. But in general all kinds of fixile material can be measured in this device, provided of course the dimensions are compatible with the sample holder.

14320141

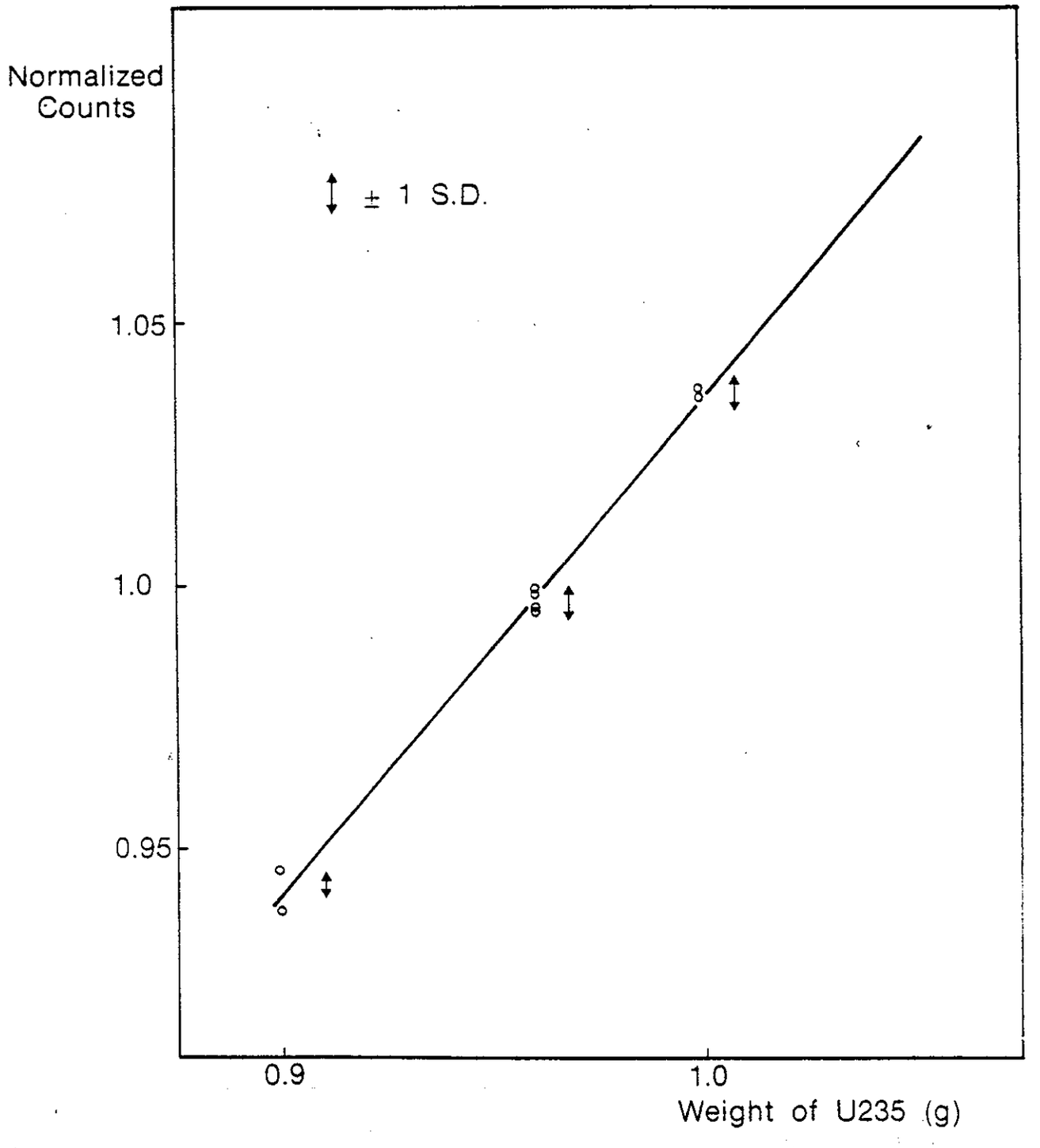

SIGMA-R CALIBRATION STRAIGHT-LINE

14320142

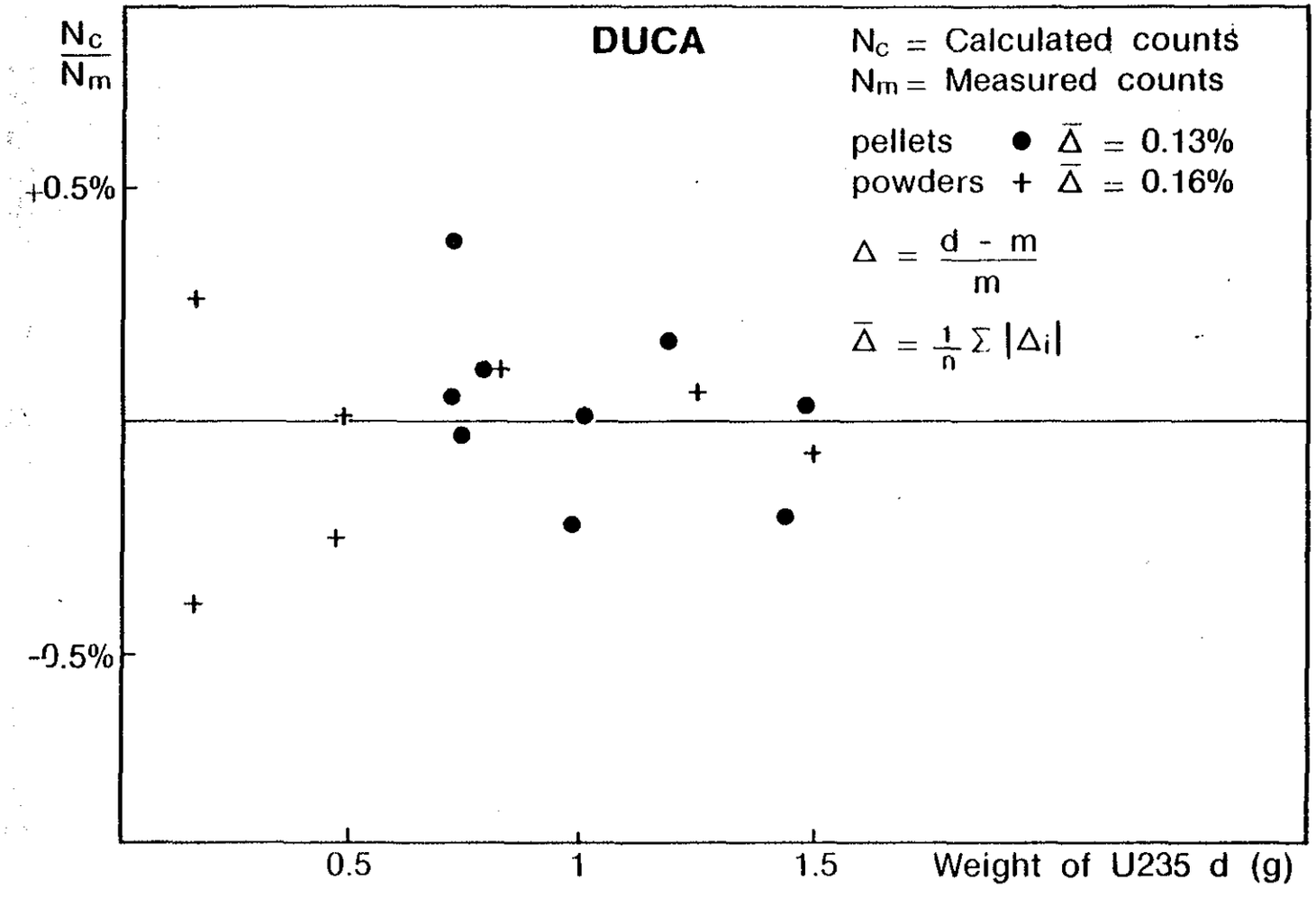
DUCA
N_c = Calculated counts
N_m = Measured counts
pellets ● $\bar{\Delta}$ = 0.13%
powders + $\bar{\Delta}$ = 0.16%
$\Delta = \frac{d - m}{m}$
$\bar{\Delta} = \frac{1}{n} \Sigma |\Delta_i|$
$\frac{N_c}{N_m}$
+0.5%
-0.5%
0.5
1
1.5
Weight of U235 d (g)

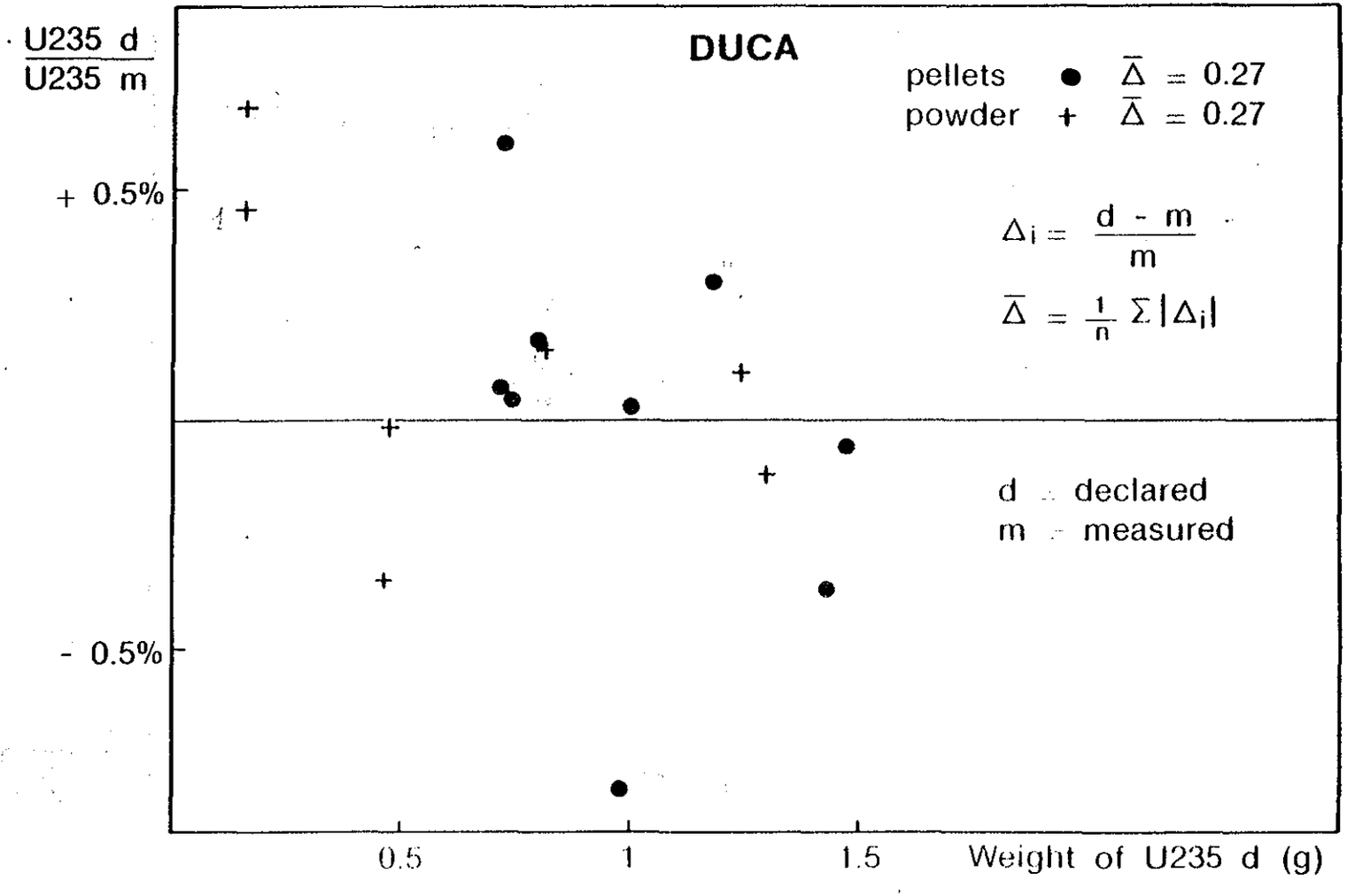
DUCA
pellets ● $\bar{\Delta}$ = 0.27
powder + $\bar{\Delta}$ = 0.27
$\Delta_i = \frac{d - m}{m}$
$\bar{\Delta} = \frac{1}{n} \Sigma |\Delta_i|$
d = declared
m = measured
U235 d / U235 m
+ 0.5%
- 0.5%
0.5
1
1.5
Weight of U235 d (g)

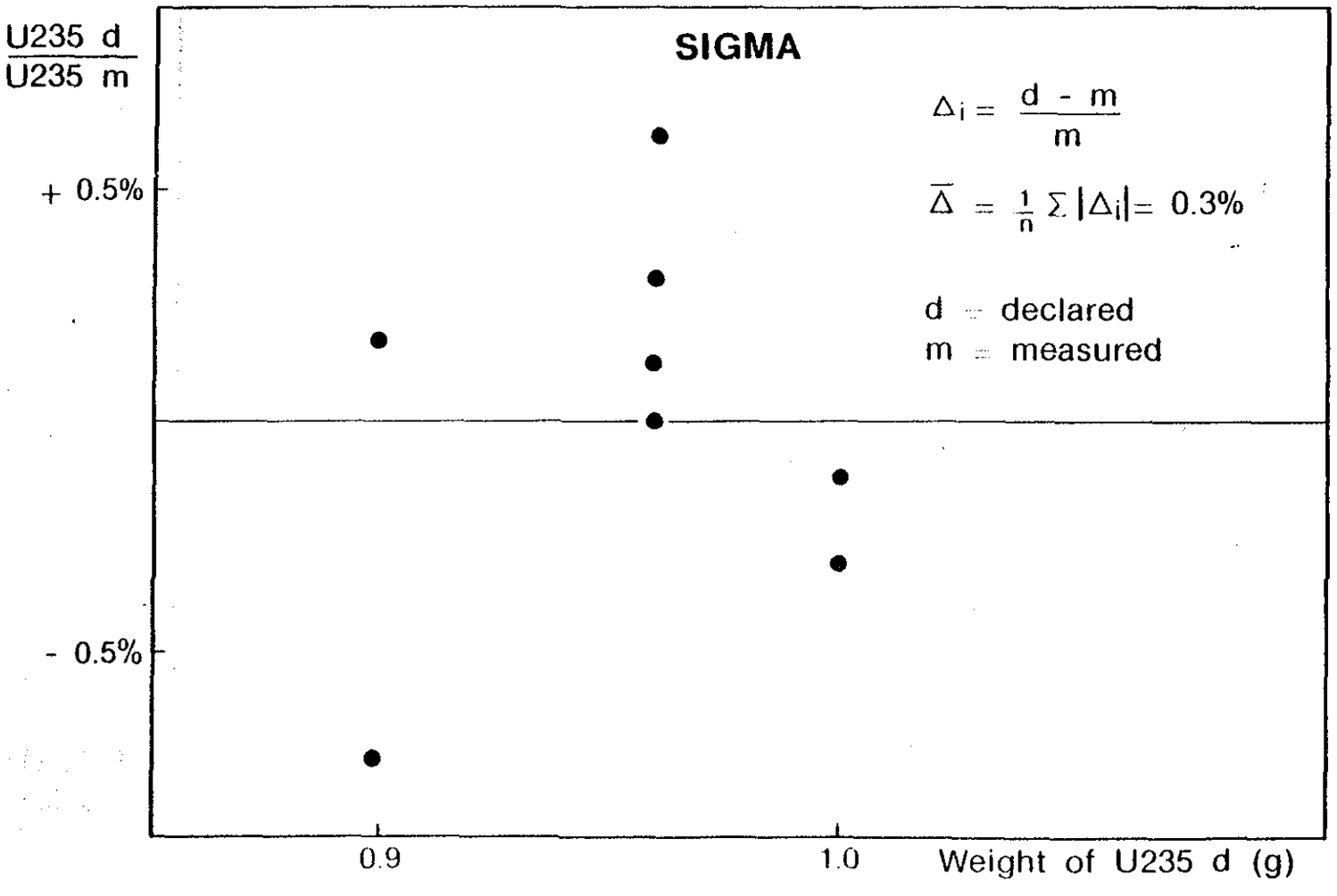
SIGMA
U235 d / U235 m
$\Delta_i = \frac{d - m}{m}$
$\bar{\Delta} = \frac{1}{n} \Sigma |\Delta_i| = 0.3\%$
d = declared
m = measured
+ 0.5%
- 0.5%
0.9
1.0
Weight of U235 d (g)

CONCLUSIONS

The SIGMA-R and DUCA instruments provide an automatic instrument control and data evaluation system, to simplify the inspector's in-field activity.
The following been achieved :

- higher reliability by means of the selection of high quality components and regular execution of automatic test sequences
- easier operation of the measurement system, used by the inspector, via an IRIS Terminal, guided step by step and with the aid of a symbolic panel
- for SIGMA-R the high quality components, together with the possibility of repetitive automatic measurement, increases accuracy (0.3%)
- for DUCA, the very fast system of movement of the Cf^{252} sources together with a very fast neutron counting chain (dead time about 1 μs) and a good calibration formula for Low Enriched Uranium provide the possibility of making very accurate measurements (0.3%)

The device have two different fields of application :

- SIGMA, <u>stationary</u> at HOBEG, has been dedicated to inspections on pebbles of AVR and THTR reactors (it is planned to implement pellets and powder measurement)
- DUCA, <u>transportable</u>, will be used for inspections on powder or pellets of Light Water Reactors after sampling on bulk quantities

REFERENCES

1 **M. Cuypers, E. Van Der Stricht, M. Boursier, M. Corbellini**
"Verification of the U235 flow at the output of the THTR fuel fabrication plant"
IAEA-SM-201/73

2 **L. Becker, G.F. Cordani**
"SIGMA-R - Main Specifications" 1.06.C3.84.123
September 1984

3 **R. Adam, B. Benoit, H. Meister**
"Etude pour la realisation de DUCA" FMM/N. 53 NDA

4 **P. Agostini, L. Caldon, G.F. Cordani**
"DUCA-TN N. ES 4.1300.A.003
June 1985"

5 **R. Adam, N. Farese, V. Vocino**
"Field Manual for DUCA"
NE.80.1571.A.001 May 1986

Additional Papers Distributed at the 31st NEACRP Meeting

- Summary of KFK 4461 : A. Mateeva; Qualifications of the JEF-1 Nuclear Data Library for Pressurized Water Reactor Burnup Analysis (distributed with National Report from F.R. Germany)

- Initial Report of the Special Committee on Reactor Risk Reference Document (NUREG - 1150) April 1988 - ANS (distributed with National Report from USA)

- The Measurement of Leakage Neutron Spectra from Various Sphere Piles with 14 MeV Neutrons.
  C. Ichihara, S.A. Hayashi, K. Kobayashi, I. Kimura, J. Yamamoto, M. Izumi, A. Takahashi.
  August 1988
  (distributed with National Report from Japan)

- Tritium Production-Rate Distributions in a Be-Sandwich Lithium Oxide Cylindrical Assembly.
  H. Maekawa, S. Yamaguchi, Y. Oyama, K. Kosako
  (ANS 8th Topical Meeting on Technology of Fusion Energy 9-13 October 1988, Salt Lake City)
  (distributed with National Report from Japan)

- Delayed Neutron Spectra by Decay Group for Fissioning Systems from Th-227 through Fm-255.
  T.R. England, M.C. Brady. 1988
  (B 2.4 Integral validation of recent delayed neutron data)

- Measurement of Delayed Neutron Energy Spectra for U-235, U-238, Pu-239.
  G.P. Couchell, P.R. Bennett, M.H. Haghighi, E.S. Jacobs D.J. Pullen, W.A. Schier, Q. Sharfuddin, R.S. Tanczyn, M.F. Villani. 1988
  (B 2.4 Integral validation of recent delayed neutron data)

KERNFORSCHUNGSZENTRUM KARLSRUHE

Institut für Neutronenphysik und Reaktortechnik
Projekt Wiederaufarbeitung und Abfallbehandlung

KfK 4461

Qualification of the JEF-1 Nuclear Data Library for Pressurized Water Reactor Burnup Analysis

A. Mateeva *

* Delegated from the Institute for Nuclear Research and Nuclear Energy, Sofia, Bulgaria

Kernforschungszentrum Karlsruhe GmbH, Karlsruhe

Qualification of the JEF-1 Nuclear Data Library for Pressurized Water Reactor Burnup Analysis

Abstract

The Joint Evaluated File JEF-1 is used as a basis to generate group constants for fuel cycle analyses of PWRs. This group constant set is applied to the NEACRP-benchmark on "Recycling of Reprossed Uranium" and to postirradiation experiments in the KWO/PWR. The results in k_∞ for the NEACRP-benchmark almost coincide with the average of the solutions submitted to the benchmark. The calculated end-of-life nuclide concentrations are in good agreement with experimental results obtained for a KWO/PWR configuration with the exception of the EOL concentration of Cm242; a careful check shows that very probably the experimental values are too low; this conclusion is consistent with the overall findings.

As another example, JEF-1 nuclear data are used to analyse a tight lattice configuration of advanced PWRs. This APWR is being investigated in a joint cooperation between the Karlsruhe Nuclear Research Center, SIEMENS/KRAFTWERKUNION, and the Paul Scherrer Institute PSI at Würenlingen, Switzerland. A special aspect is addressed in this paper, i.e. the reliable determination of the reactivity change upon voiding a tight lattice. It is shown that the use of consistent weighting spectra for the normal (water-in) and the voided (water-out) configuration drastically reduces the void reactivity change compared to that case, when the same weighting spectrum (e.g. that of the water-in configuration) for both the normal and the voided state of an APWR is used.

Content

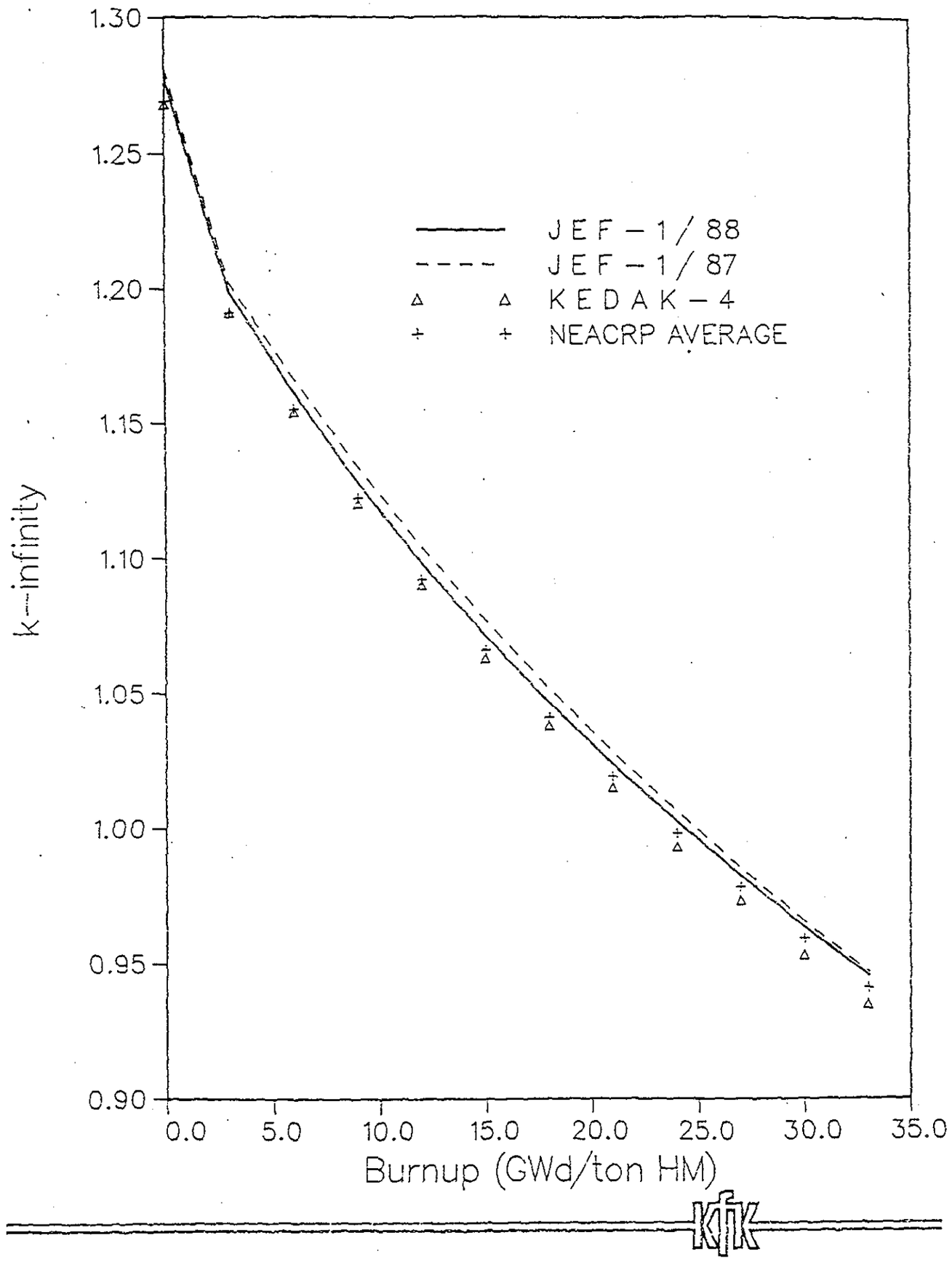

Fig. 1: Burnup Dependence of k_∞ for the NEACRP-Benchmark on "Recycling of Reprocessed Uranium" (Exercise 1a)

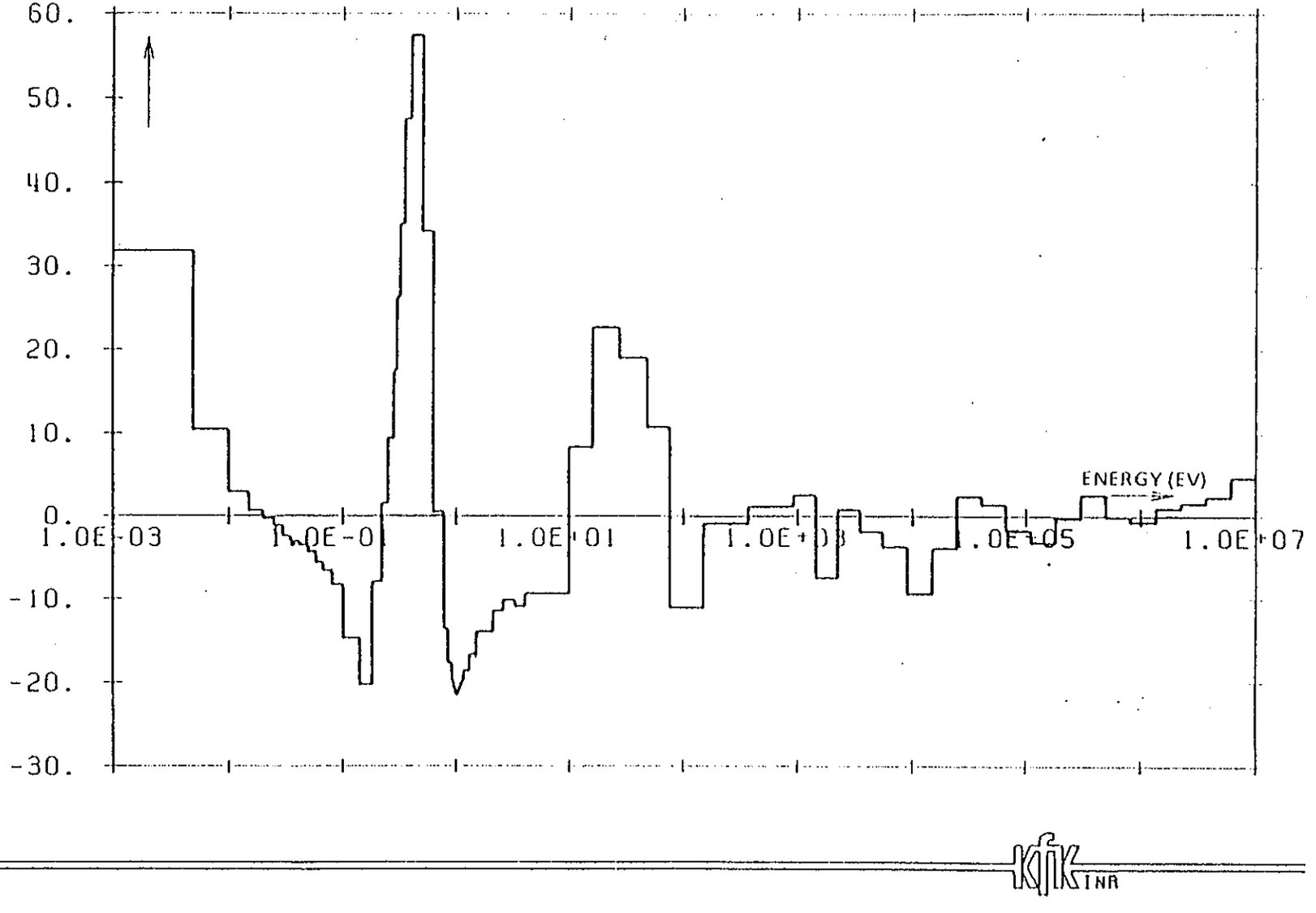

Fig. 2: Difference in % for the Fission Cross Section of Pu241

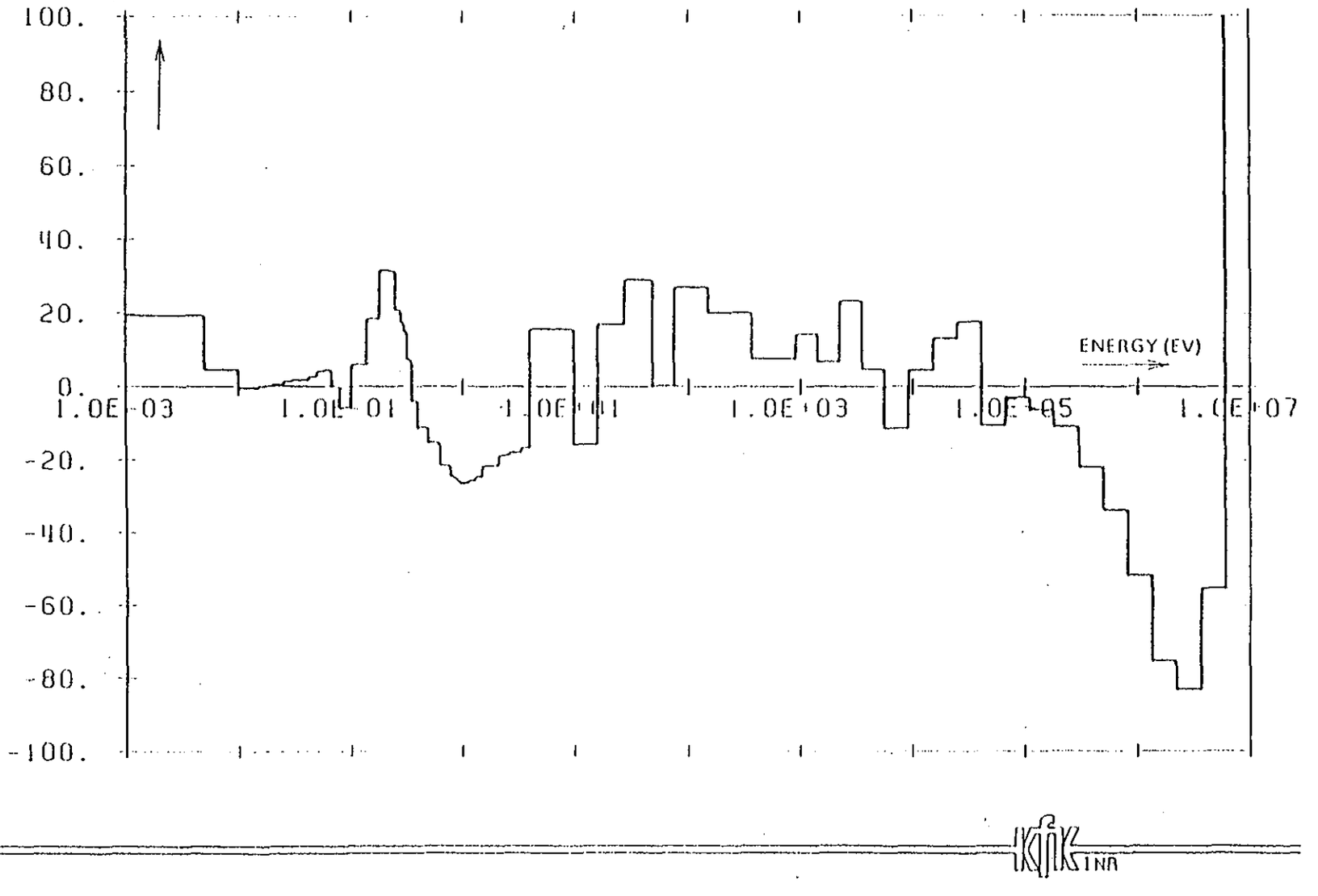

Fig. 3: Difference in % for the Capture Cross Section of Pu241

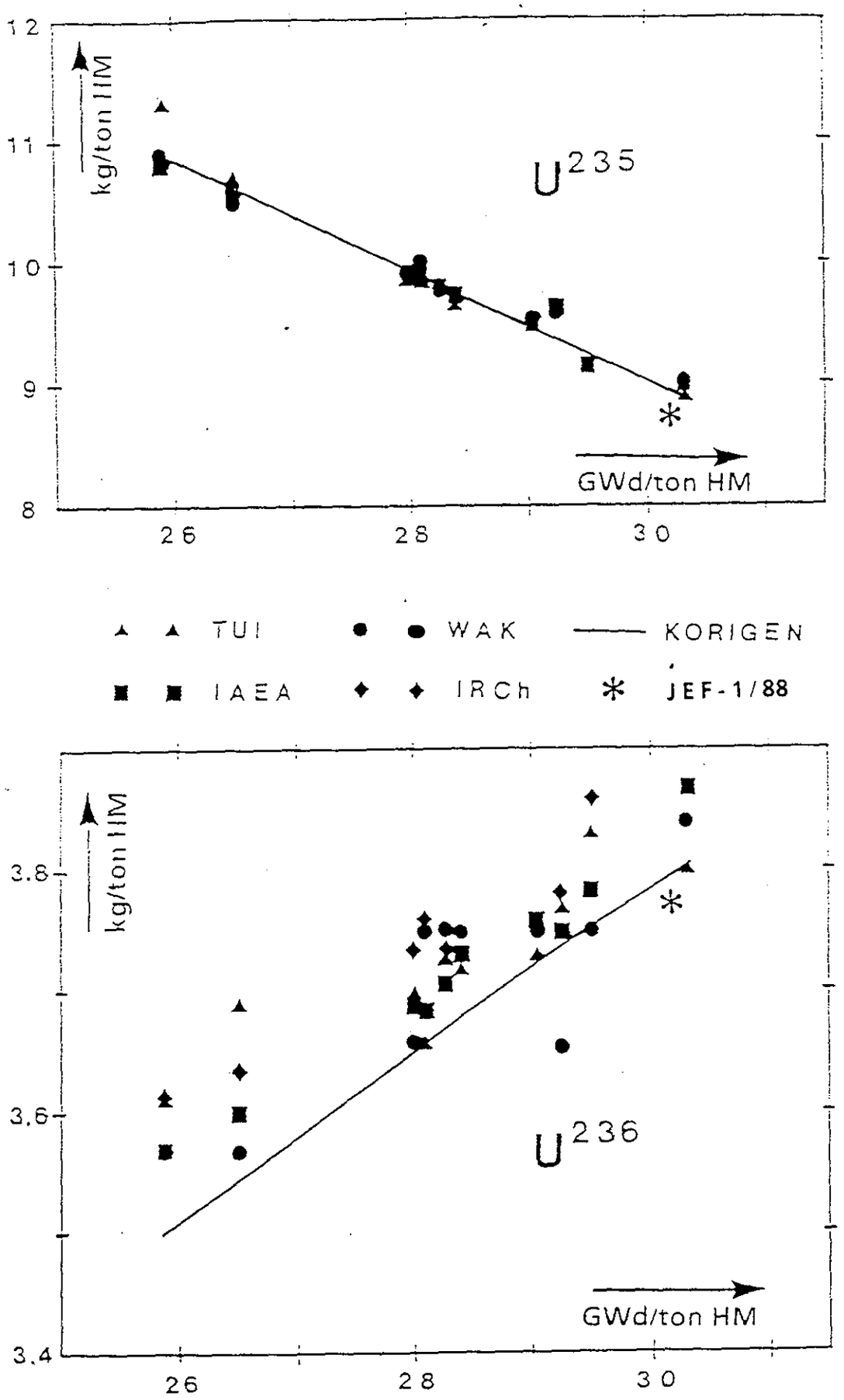

Fig. 4: Burnup Dependent Isotopic Concentrations for U235 and U236

14320155

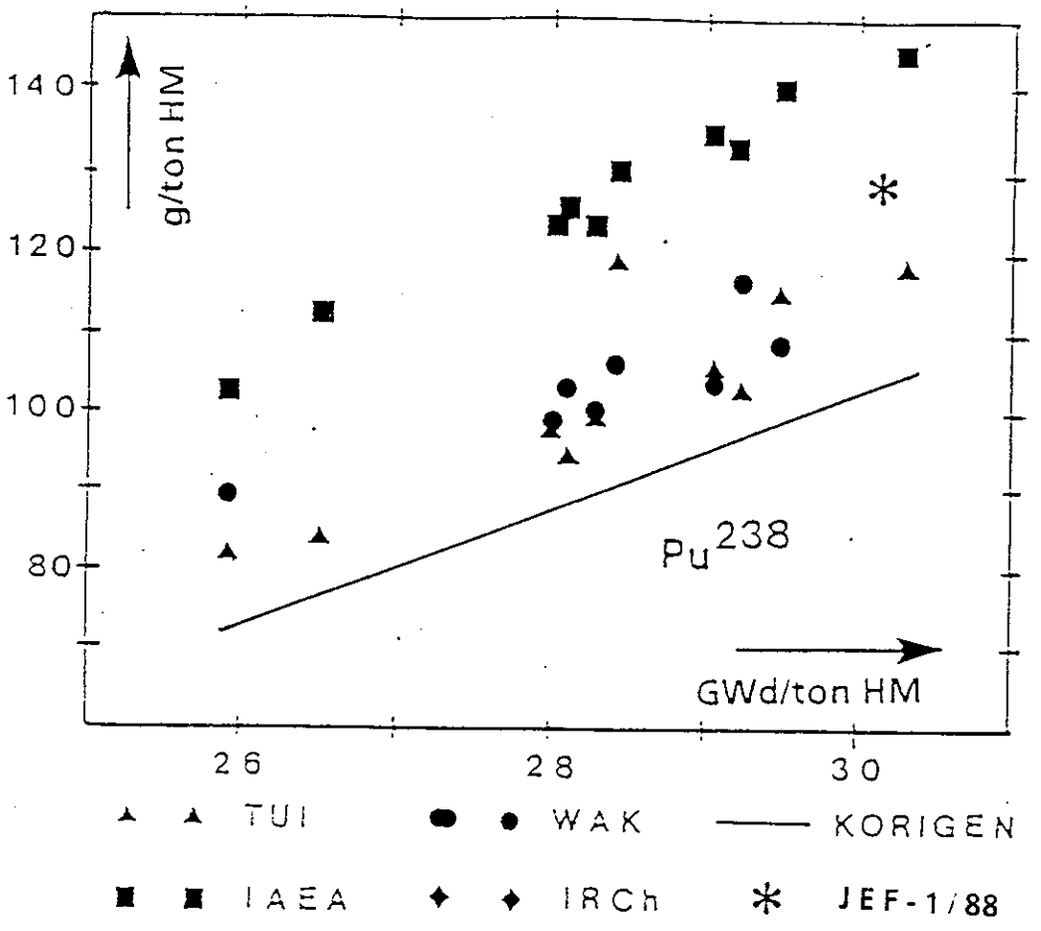

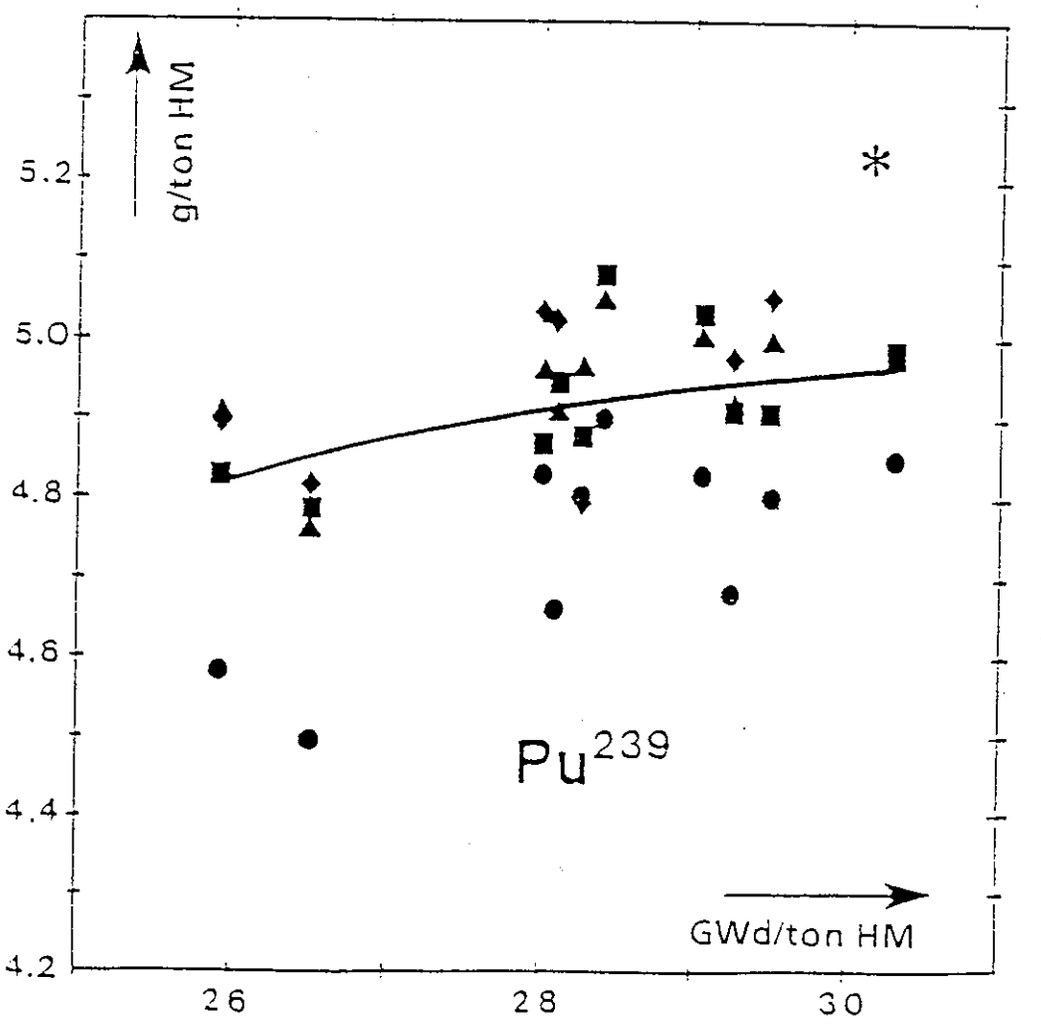

Fig. 5: Burnup Dependent Isotopic Concentrations for Pu238 and Pu239

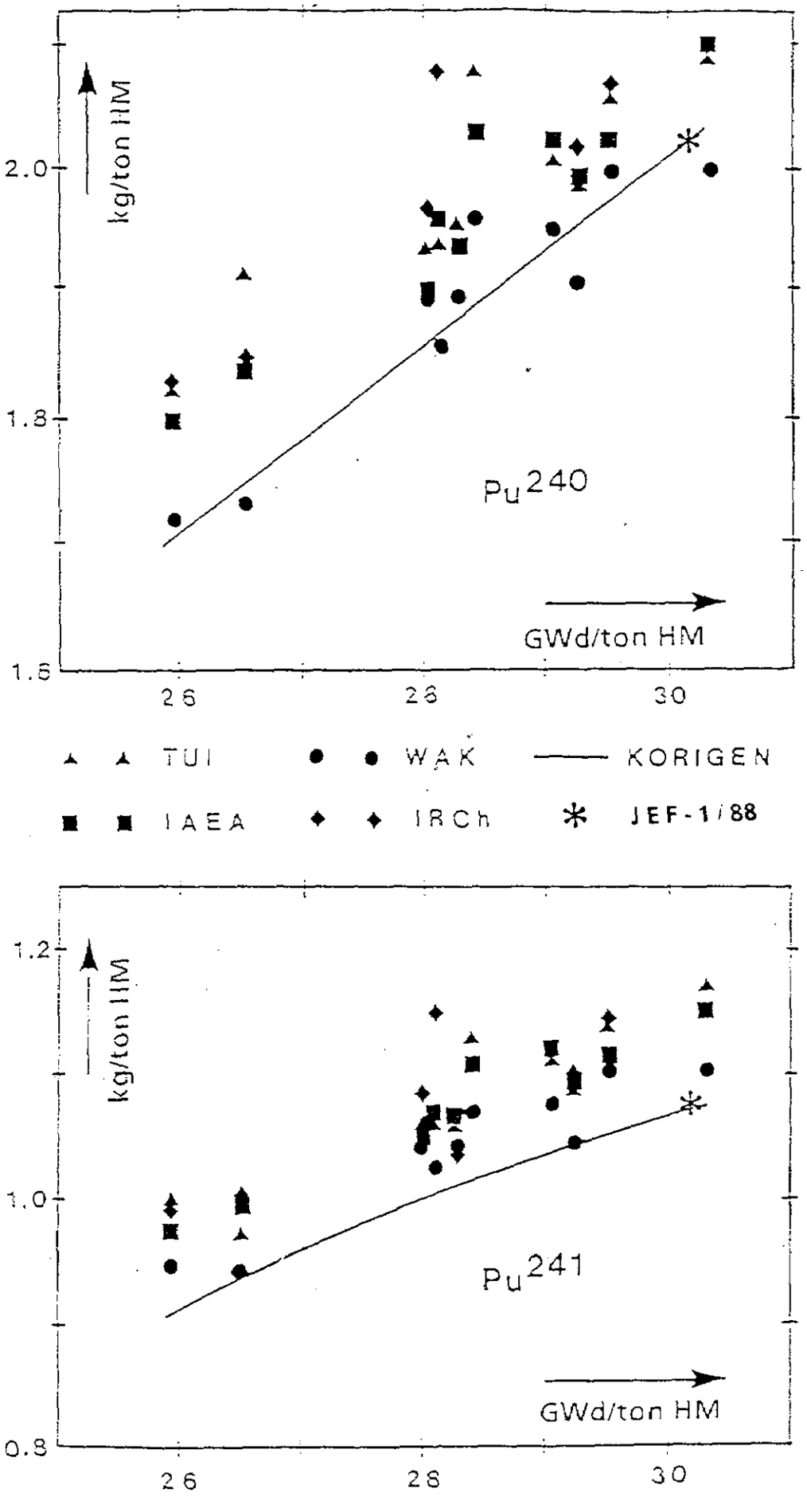

Fig. 6: Burnup Dependent Isotopic Concentrations for Pu240 and Pu241

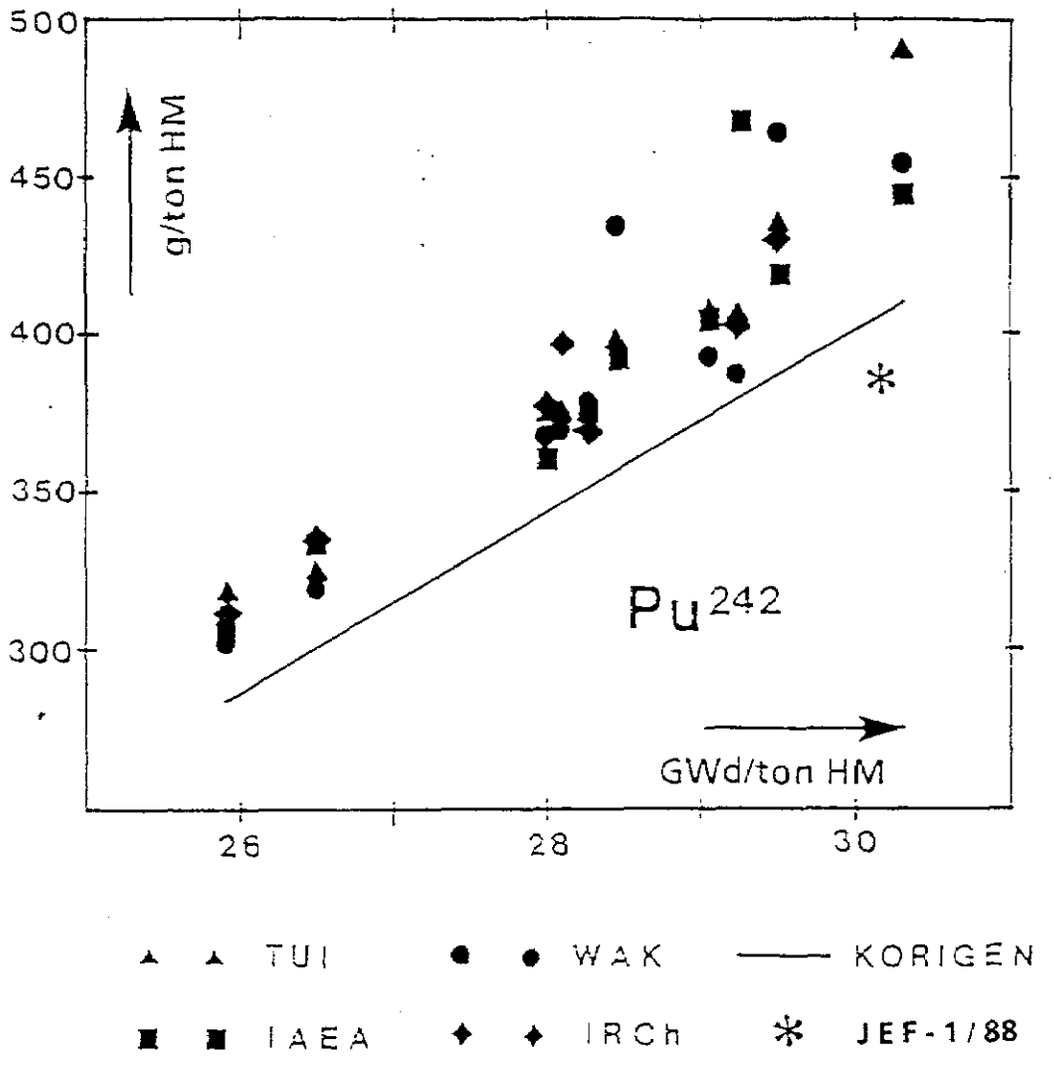

Fig. 7: Burnup Dependent Isotopic Concentration for Pu242

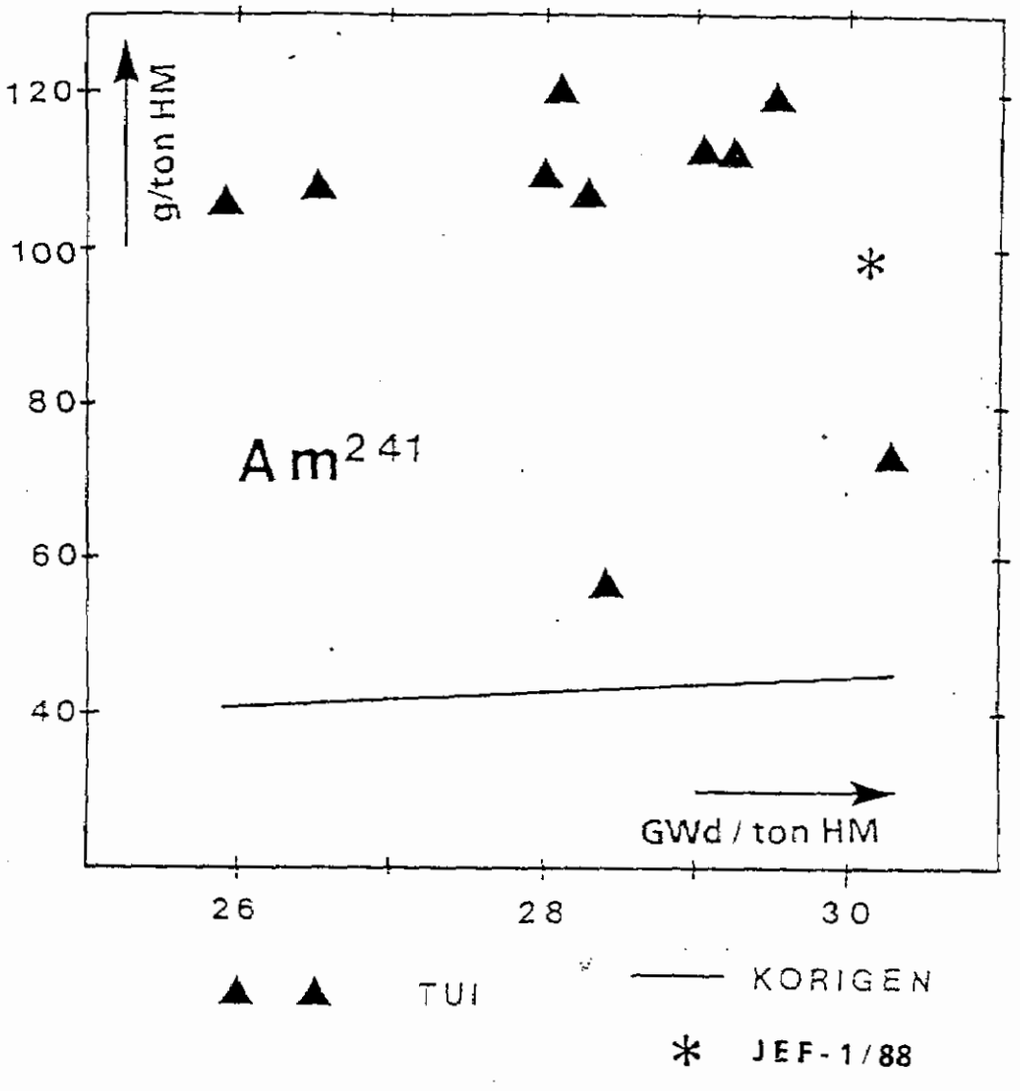

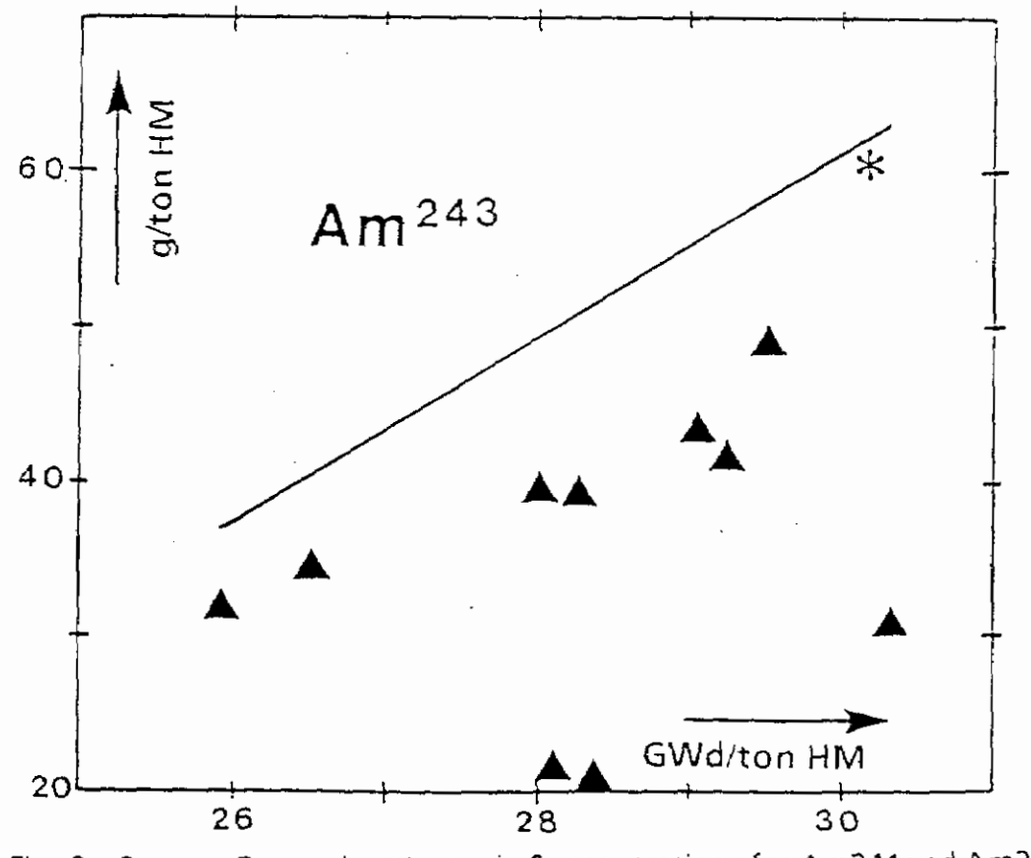

Fig. 8: Burnup Dependent Isotopic Concentrations for Am241and Am243

14320159

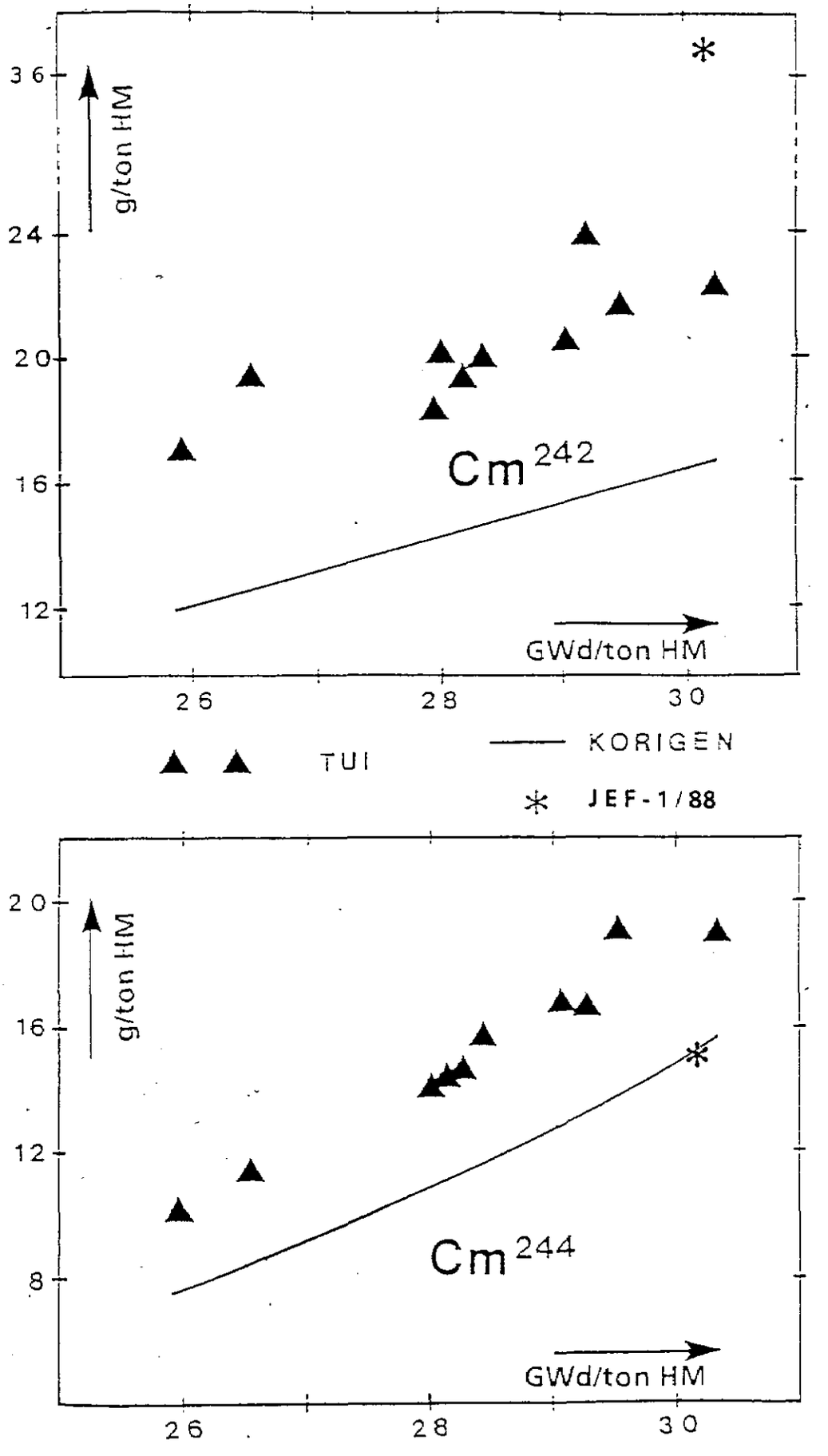

Fig. 9: Burnup Dependent Isotopic Concentrations for Cm242 and Cm244

AMERICAN NUCLEAR SOCIETY

INITIAL REPORT

of the

SPECIAL COMMITTEE

ON

REACTOR RISK REFERENCE DOCUMENT

(NUREG - 1150)

A P R I L 1 9 8 8

American Nuclear Society
555 North Kensington Avenue
La Grange Park, Illinois 60525

Published by the

AMERICAN NUCLEAR SOCIETY
555 NORTH KENSINGTON AVENUE
LA GRANGE PARK, IL 60525

Printed in USA

TABLE OF CONTENTS

I. Introduction

In February 1987 the U.S. Nuclear Regulatory Commission (NRC) issued, in "draft-for-comment" form, a report entitled REACTOR RISK REFERENCE DOCUMENT, NUREG-1150. The opening paragraph of the Executive Summary States:

> "The Reactor Risk Reference Document, NUREG-1150, provides the results of major risk analyses for five different U.S. light-water reactors (Surry, Zion, Sequoyah, Peach Bottom, and Grand Gulf) using state-of-the-art methods. The broad base of probabilistic risk information contained in this document is intended to provide a data base and insights to be used in a number of regulatory applications. It is anticipated that these regulatory actions will include (1) implementation of the NRC Severe Accident Policy Statement, (2) implementation of NRC safety goal policy, (3) consideration of the NRC Backfit Rule, (4) evaluation and possible revision of regulations or regulatory requirements for emergency preparedness, plant siting, and equipment qualification, and (5) establishment of risk-oriented priorities for allocating agency resources. This report has been published in draft form. Since estimates of severe accident likelihoods, consequences, and risk and their use in regulation are important subjects, public comment is sought on the quality and format of the information and how best to present it for use in the regulatory process."

The report was widely distributed and comments actively solicited, with October 1, 1987 set as the close of the public comment period. During that period the NRC received a large number of responses to their invitation to comment from institutions and individuals within the United States and from abroad. Most of these responses were lengthy and reflected a serious consideration of the document. Following the close of the public comment period, the NRC began the process of modifying NUREG-1150 with an initial goal of publishing the final report in the summer of 1988. Based on the comments received by the NRC, it is obvious that (a) the final version of the NUREG-1150 will be significantly different from the draft and definitely improved, and (b) the final report will not be ready before the end of 1988.

Many members of the American Nuclear Society (ANS) felt that the Society should express its views regarding a document that has the potential of influencing the perception of accident risk associated with nuclear power plants and having an impact on the regulatory process. For this reason, in the fall of 1987, the President of the ANS appointed a Special Committee to follow and comment upon the progress of NUREG-1150. The Committee includes members from the United States and abroad.*

This report summarizes the Committee's initial findings and recommendations based upon: (1) a review of the Draft for Comment issued February 1987, and portions of the major supporting documents; (2) a

*See Attachment 1 for a list of the Committee Membership and Attachment 2 for the Committee's Assignment.

review of the extensive comments received during the public comment period; (3) briefings of the Committee by the NRC staff and others; and (4) visits to Sandia National Laboratories by the Chair and Vice Chair to observe the expert review panel process and to discuss the ongoing major effort to substantially revise the document.

The objectives of this document are to report to the ANS membership on the initial findings and recommendations of the Committee, and to provide the NRC with the benefit of our views. It is the Committee's hope that our comments will help the NRC during this revision process and thus, contribute to an improved final report.

Most reviews of complex technical documents tend to emphasize shortcomings and areas of substantial technical concern. This review is no different, in that regard. However, the Committee believes that constructive criticism is the most important contribution that it can make in this initial report. In keeping with the assignment from the Society's President, the Committee also devoted some effort to identifying broader technical items directed at helping to frame the national discussion and review of this important study. In a number of instances, comments are directed at problems in the draft NUREG-1150 which have been recognized by the NRC. We have indicated several areas where we understand the problems are being addressed.

This initial report is not intended as an exhaustive commentary on NUREG-1150. Rather, it addresses aspects of NUREG-1150 that we believe deserve early attention as part of the on-going revision effort. We have not included specific comments on the level 1 (accident sequence development) and level 3 (off site consequence) analysis in this initial report, nor have we presented an overall assessment of NUREG-1150 at this time. The Committee plans to continue to follow the activities of the NUREG-1150 Project in order to contribute to improvements in the process and the final document.

II. FINDINGS AND OBSERVATIONS

1. Advancement in Reactor Risk Technology

The NUREG-1150 undertaking includes several advancements in reactor risk assessment technology, some of which are commented on below:

- It presents a comprehensive statistical treatment of modeling and phenomenological uncertainties, whereas the treatments of uncertainty in prior probabilistic risk assessments (PRAs) have primarily addressed data uncertainties - mostly in the "front end" analyses.

- It includes far more detail in the area of containment event trees than previous PRAs, and places added attention on the containment function.

- It makes visible the need for and use of expert judgment. All probabilistic risk assessments use expert judgment. NUREG-1150 formalizes and goes a significant way towards resolving the issues concerning its use. (However, the Committee is concerned about the degree of reliance on expert judgment in NUREG-1150, as discussed later in this report.)

- It reflects many of the important advancements in severe accident analysis made in the years since publication of the Reactor Safety Study (WASH-1400) in 1975.

Taken together, this attempt at quantification of uncertainty and the blending of the statistical treatments with deterministic analyses and expert opinion is an advancement in the technology, which the Committee applauds. However, as with most technological developments, a large amount of effort will be required in order to work out the problems encountered. Even in the areas of technological advancement noted above, the Committee has suggestions for improvement, which are discussed in the following paragraphs.

The Committee believes that NUREG-1150 can represent an important step in the convergence of technical opinion on reactor risk. However, it should not be implemented as a reference document until the issues and problems have been thoroughly reviewed and a reasonable degree of consensus has been achieved among the nuclear safety community.

2. Objectives and Scope

While NUREG-1150 constitutes a worthwhile update of the state-of-the-art in PRA in support of the assessment of potential severe accident conditions from internal initiators, it also highlights uncertainties in their assessment. It is limited to the analysis of five specific plants from which few specific results can be generically extrapolated to other plants; however, problem issues can be rated according to their significance for overall nuclear power plant safety. This raises questions as to what is the most appropriate objective and use for a revised NUREG-1150. It would seem that its most useful purpose would be as a guide: a) in defining regulatory issues that can be considered as resolved or as being of marginal importance in the severe accident areas, and b) in providing ranking of priorities for resources to be dedicated by the US NRC and industry to the resolution of subsisting problems that are significant enough to further reduce the risks.

The scope of NUREG-1150 has so far excluded external initiators and has included to only a limited extent the impact which emergency operating procedures and accident management can have in accident sequences, especially with regard to prevention of extensive core damage and the maintenance of containment performance. These are both important items that merit inclusion with regard to a useful purpose of NUREG-1150, as suggested above. However, it may be more practical to deal with these issues in accompanying or subsequent documents. The NRC has indicated that external events will be treated in a follow-on study.

3. Risk vs. Uncertainty in Risk

The Lewis Commission criticized the Reactor Safety Study (WASH-1400) for emphasizing best estimates of risk and not providing adequate emphasis on the uncertainties involved in risk estimates. The pendulum has swung too far in the opposite direction in the draft version of NUREG-1150 in that it emphasizes the quantification of uncertainty over the quantification of risk. For some of the results in NUREG-1150 only the range of possible results is presented (as a solid bar on a figure) with no information on the possible distribution of results within the range of uncertainty. The Committee believes that the best estimate of the risk and the range of uncertainty in the risk are equally important. We understand that there are plans to place more emphasis on the calculation and presentation of best estimates, possibly by presenting the probability distribution functions, in the modified NUREG-1150 report.

The Committee is also concerned that the key ground rules or assumptions upon which the risk estimates are based are not consistent throughout the study. In particular, is this a best estimate of risk and the uncertainty in the risk or is this study a conservative estimate? The Committee finds evidence that both approaches are used in different parts of the study. Because of this situation, it is difficult to know the degree of conservatism in the NUREG-1150 results.

4. Expert Opinion

The area of greatest concern expressed by reviewers of the Draft Report is that of expert opinion, its elicitation and use. The NRC and its contractors have been very responsive to the constructive criticisms raised in that regard and have completely restructured the expert opinion polling process. They have improved the process and expanded the breadth of expertise to include experts from industry, the national laboratories and academe. The expert review panels have met and received training by decision theorists, experienced in the process of eliciting expert opinion. Expert panels have been formed in the following areas:

- Accident Analysis (front end)
- Containment Loading
- Core Concrete Interaction
- Containment Response (Structural)
- In-Vessel Phenomena
- Source Terms

Elicitations of quantitative weighting factors for the various issues assigned to the expert groups are scheduled to be completed shortly, with approximately two months between the initial meetings of the expert panels and the elicitation of their opinions.

Despite the improvements in the process, such as including a broader base of expertise and following a more formal approach, several substantive concerns remain, including:

- Reliance on Expert Opinion - While the use of expert opinion appears to be necessary, the Committee is concerned by the extent to which the risk results in NUREG-1150 are dependent on it, and we encourage the substitution of analysis for expert opinion whenever possible. There is more reliance on expert opinion in the ongoing revision of NUREG-1150 than there was in the Draft Report. Having expanded the pool of expertise and improved the process of expert opinion polling, the NUREG-1150 Project has also increased both the percentage and absolute magnitude of the effort which is based on opinions of experts.

  The Committee is also concerned about the large number of estimates that the expert review panels have been asked to generate in the effort to revise NUREG-1150. For instance, it was estimated that the Containment Loading Panel was initially asked to determine more than 9,000 individual numbers. This number has subsequently been substantially reduced; however, many thousands of numbers are still required from the various expert panels in the current version of NUREG-1150. The Committee believes that this situation has the potential for producing inconsistent and erroneous results.

- Interrelationships Between Expert Panels - The expert panels have been established as independent groups and have been provided with only an initial briefing and a subsequent brief update on the issues addressed by the other panels. Each expert panel has been requested to produce its input to the report during approximately the same time frame. Under this structure, the Committee believes that there is little opportunity for one panel to interact with or even understand the interrelationships with the other panels, possibly resulting in a disjointed analysis. The Project staff is attempting to address the interface problem; however, the basic compartmentalized structure of the expert panels still exists. Thus, there still remains the danger that analysis interdependencies will be overlooked and data transfer may be incomplete.

- Issue Selection and Definition - In the NUREG-1150 process the issues are pre-selected by the Project and presented to the expert panels. The panels are told that they can add, delete, or change the issues, and it is our understanding that the panels have made some modifications to the issues. As a practical matter, however, considering the time constraints of the current schedule and the heavy workload on the panels, the ability of the panels to make major changes in the issues is very limited. The expert opinion process is a complex activity involving: (a) issue selection and definition by the Project; (b) some modifications of the issues by the expert panels as a result of the presentations to them; (c) decomposition of the issues based on their internal discussions; and (d) elicitation of the opinions of the panels. It is important that the key roles of both the Project and the panels in determining the outcome of the expert opinion process be conveyed to the reader of the report.

5. Interrelationships and Synergisms

The fact that the expert review panels work independently is only one aspect of the concern the Committee has in this area. There are inconsistencies in the Draft Report which seem to result from the process whereby independent analyses are linked together to form the complete analysis. Two examples of problems with interrelationships and synergisms are cited below:

> The output of the expert panels is in the form of numerical weights for various "levels" of each issue, e.g., containment opening size due to postulated rapid overpressure. In the Draft Report, there was a disconnect between the output from the containment panel and the subsequent treatment of source terms for an early overpressure failure. All early containment overpressure failures were assumed to result in a 7 ft^2 (3 ft diameter) opening in PWRs and a 10 ft^2 opening in BWRs even though most containment experts assigned zero weight to such opening sizes at the containment pressures used in the source term analysis.
>
> With respect to postulated containment loading from hydrogen burns, serious questions exist with regard to how much of the zirconium was used up in generating hydrogen prior to vessel meltthrough and how much participated in subsequent core-concrete interactions. It appears to the Committee that in some sections of the analyses zirconium mass is not conserved and more is burned and used up in other ways than is available in the core.

The Committee has been told by the Project that some of the inconsistencies in the initial draft were recognized from the start but were allowed to remain due to the draft nature of the report and the pressing need to get the document out for comment. Nevertheless, the Committee is concerned that the potential for similar discrepancies still exists in the modified NUREG-1150, and recommends a thorough consistency review of the final document, to identify and correct such problems prior to publication.

6. Early Containment Overpressure Failure

Accurate quantification of the probability and releases associated with early containment failure is very important. If the containment does not fail early in an accident, the risks are substantially reduced. It is essential that careful consideration be given to quantification of the time dependent loads on the containment and the corresponding containment response. The roles played by hydrogen burns and direct containment heating must be presented in an unambiguous fashion, with supporting analyses. This was not done in the Draft Report, resulting in considerable confusion as evidenced by the comments received. Without going into examples of inconsistencies and other questions of the treatments of the probability of occurrence and the associated releases from early containment failures in the Draft Report, the Committee underscores the great importance of correctly performing those portions of the analysis and providing a rigorous documentation in the final report.

It is essential that the expert review panels know in detail how their data are going to be used, particularly in conjunction with postulated early containment failure. The Containment Response Panel should be aware of the importance of the low end of the curves depicting containment failure probability as a function of pressure, since most of the early containment failure probability comes from the overlap between the low pressure end of this curve and the high pressure end of the curve giving containment loading pressure versus probability. They should meet and exchange data directly with the Containment Loading and Source Term Panels to assure that all concerned understand what specific numbers mean, and what boundary conditions might be imposed on any set of numbers utilized.

Another area not treated well in the Draft Report is the size of containment opening, given the postulated early overpressure failure of containment. Containment opening size is a crucial parameter affecting source terms. The Committee understands that the reanalysis effort is centered on large and small opening sizes of 7 ft^2 and 0.7 ft^2, respectively. We recommend that an opening size of 0.1 ft^2 be analyzed and have directed the NUREG-1150 Project's attention to the parametric study of the effect of opening size included in the report of the ANS Special Committee on Source Terms published in 1984. That report showed source terms for a PWR high pressure sequence, TMLB', with a 7 ft^2 (3 ft diameter) opening are essentially the same as for a 1 ft^2 (13 in. diameter) opening, but that they are reduced by roughly an order of magnitude with a 0.1 ft^2 opening (approximately 4 in. diameter). Thus, we would not expect to see much difference between the 7 ft^2 and 0.7 ft^2 cases currently being studied in the NUREG-1150 reanalysis, but would expect a large difference for the 0.1 ft^2 case.

We understand that the NUREG-1150 Project is undertaking analyses of a 0.1 ft^2 opening with the CONTAIN program, in response to the Committee's suggestion that smaller opening sizes be investigated.

7. Parametric Source Term Models

Among the major analytical methodologies used for the first time in reactor risk assessment in NUREG-1150 are the parametric source term models, XSOR and RELTRAC. They have been the subject of many of the comments received on the Draft Report, where they were simply presented and used without any appreciable discussion of their foundation or applicability. The XSOR models were used for all plants studied, except Peach Bottom, which was studied with the RELTRAC model.

The parametric nature of the NUREG-1150 undertaking results in the need to characterize source terms, i.e., the releases of radioactive material to the environment, for a large number of cases associated with the plant damage states and containment end states considered. The number of individual source terms is made even larger when the variations in the source term phenomenological issues are included, e.g., twelve issues in the case of the Surry analysis. As a result, very simplified methods, i.e., the parametric source term models, were adopted for the study since calculating thousands of source terms with detailed computer programs, such as the NRC's Source Term Code Package (STCP), would not have been

practical. This approach also permitted the inclusion of the quantification of phenomena not modeled in the STCP, such as revaporization of volatile fission products from the reactor coolant system following meltthrough of the reactor pressure vessel bottom - a phenomenon which has been demonstrated to be important in other analyses.

It must be recognized, however, that because of the simplicity which allows them to quickly calculate large numbers of source terms, these parametric models do not reflect the details present in state-of-the-art source term analyses. Simplified representations of complex phenomena and interactions are, at once, the strengths and the weaknesses of these models, in the sense that they are very useful for parametric studies but are not of the same quality as more detailed analyses.

XSOR models are essentially mass balance equations, which employ factors used to describe the fraction of the mass of a given fission product group located in the reactor core, the reactor coolant system, etc., in the analysis of a specific accident scenario. In the NUREG-1150 process, numerical values of these factors are obtained from the expert opinion polling process.

Unfortunately, very complex and interrelated phenomena have to be reduced to numerical values for each of the factors, e.g., FVES, FCONV, etc., which are treated as independent variables in the simple mass balance equations. The ability to replace more detailed analyses with these models essentially depends on the ability to adequately represent the more detailed analyses with the respective mass balance fractions. In some instances this may not be a major concern, e.g., if values of the fractions have been determined from a detailed analysis of an accident scenario which is not greatly different the accident scenario for which the XSOR code is being applied. In other instances, the applicability of the XSOR codes raises several concerns.

One of the major concerns stems from the fact that the XSOR codes do not include time as a variable. The only way that temporal effects can be incorporated is to utilize integral values of the factors which are derived from more detailed analyses in which temporal effects have been included. The problem with that approach is that if applicable detailed analyses do not exist, where does the quantification of the time dependencies and other effects come from?

Another major concern relates to the heavy reliance on assumptions, For instance, in the Draft Report applications of these models, post-vessel meltthrough revaporization was assumed to result in a linear increase in the release from the reactor coolant system in direct proportion to the fraction revaporized. However, analyses of revaporization for high pressure sequences in PWRs, with methodologies other than the STCP, illustrate that even though revaporization may occur, it results in migration of fission products elsewhere in the reactor coolant system rather than release from it. In this example, an assumption which was the basis for the input to XSOR is not in agreement with the results of detailed analyses of the phenomena involved.

Essentially all of the sophistication in the source term analyses in NUREG-1150 has to be embodied in the simple numerical factors input to the parametric source term models, since there is no sophistication in the models themselves. Most of the inputs to the XSOR codes are being provided by the expert panels; however, the level of skill and availability of data needed in order to provide the correct input almost requires the detailed solution of the problem being simplified.

Because of the limitations inherent in the simplified models, and because these models are new and form a major cornerstone of the risk estimates, the Committee is concerned that there was little attempt in the Draft Report to address their limitations, applicability or validation. Comparison with more detailed calculations is essential, with emphasis on those scenarios and combinations of input parameters that contribute significantly to risk.

8. Information and Data Not Used

The Committee recognizes that a cut-off date for incorporating new information and data must be established in any study. However, in light of the fact that a major revision of this study is underway, the opportunity exists to incorporate into the final report important data and information not previously used, or not available when the Draft Report was prepared.

There are a number of examples of important experimental data that should be utilized in NUREG-1150. These include: TREAT-STEP and LOFT-FP-2 on release and early transport and agglomeration of fission products; Marviken and LACE on downstream transport and agglomeration of fission products; DEMONA and LACE on fission product retention in containment, including steam condensation on aerosols and the effect of hygroscopicity; pool scrubbing tests on fission product retention with saturated fluid conditions; definitive investigations on formation, transport and retention of iodine compounds; and hydrogen burning. Many of these investigations were co-sponsored by the NRC.

9. Accident Management

The increased use of PRA has concurrently led to improved predictability of the probability of severe accidents and of the conditions associated with those scenarios. There has been an incentive to develop accident management strategies to cope with such potential exceptional situations, both from the viewpoint of protection of the plant itself and for the purpose of on-site and off-site emergency preparedness.

The analyses of predicted accident scenarios that could lead to extensive core damage and breach of the successive barriers constituted by the reactor coolant system pressure boundary and the containment provide excellent opportunities to develop insights. Such insights should be used to address operational improvements which could be made and operator intervention which could stop a predicted severe accident sequence progression, especially for the risk dominant sequences. For example, emphasis placed on avoiding severe core damage and possible melt ejection

at high pressure and avoiding rapid loss of the containment performance are particularly relevant.

The influence of emergency operating procedures and accident management on risk reduction from severe accident conditions is of prime importance. This implies a recognized need for special attention on how utilization of plant systems and planned operator intervention can affect the plant behavior and the physical phenomena predicted in the NUREG-1150 analyses of severe accident conditions.

Accident management has been included only to a very limited extent in the front end portion of NUREG-1150. Depending on the objectives and scope of the NUREG-1150 exercise it is recommended that accident management be given more attention and be examined in the final report or in an accompanying or subsequent document.

10. Readability

NUREG-1150 is a very difficult report to read and understand. This is due to both the very complicated process developed for the NUREG-1150 analysis and to the inadequate and often very incomplete descriptions in the Draft Report.

To begin with, NUREG-1150 is not a stand alone report. To understand it, one has to read back through several additional massive supporting reports. Even if one does this, it appears that there is still information, important to the NUREG-1150 conclusions, that is not reported anywhere in the NUREG-1150 documentation package.

Another difficulty in understanding the NUREG-1150 analysis is the decision to collapse or aggregate the results at various steps in the analysis. For example, there were very many end point conditions at the conclusion of all the core damage calculations. These conditions were sorted (aggregated) into groups with similar physical characteristics, in order to have a reasonable number of starting points for the following containment analysis. Similar aggregation of results was done in containment and source term parts of the analysis. This aggregation of results has the effect of making it nearly impossible to trace the calculation of a given scenario from beginning to end.

11. Presentation of Results

From the NRC's response to the volume of critical comments on the box-and-whisker format used in the Draft Report to display results we understand that the final version of NUREG-1150 will adopt some other method of presentation. Alternatively, a probability distribution function format would provide a visual impression of the range of uncertainty and allow a reader to appreciate the central tendency of the distribution. We also note that the solid bar format used to present uncertainty ranges at some places in the report is even worse than the box-and-whisker method, for it gives no information on the distribution of uncertainty, and focuses the reader's attention directly at the upper end of the range. The pie-chart representation of individual contributors to core damage is a very effective way of presenting the

relative results. However, some indication of the absolute frequency values should be included there.

The relationships between the NUREG-1150 results and the earlier WASH-1400 results are not described in any meaningful way in the Draft Report. WASH-1400 is an important historical document and comparison of its results with those of NUREG-1150 would provide insight and highlight advances that have occurred since 1975. To a large extent, the Draft Report's concentration on the quantification of uncertainty to the exclusion of best estimates of risk has obscured the progress since WASH-1400. We understand that planned changes for the final report will address this concern.

III. RECOMMENDATIONS

The Committee has the following recommendations on NUREG-1150.

1. The dependence of the risk estimates on expert opinion and not on analytical or experimental results should be limited. Expert review panels should be asked to generate values of certain parameters and their uncertainties only if one of the following conditions are met:

   (1) the results of reviewable analyses are not available in a reasonable time; or

   (2) the panel has reason to believe the available analytical results are inapplicable or incomplete.

2. The continuity of the effort would be improved by bringing together the expert panels, perhaps in a workshop format, as early as practicable. The individual experts could then see how their output is to be used, with emphasis on group-to-group transfer of information and data. Such an exercise would help smooth out discontinuities at the interfaces and provide a feedback during the analysis effort. It is particularly important that the expert panels on containment loading and containment response meet together and also with the source term panel.

3. The results of the parametric source term models should be confirmed by performing detailed analyses of source terms for selected cases, particularly those that result in the highest estimated risks for each plant studied.

4. We recommend the performance of a thorough final review of the most important results. The review should focus on:

   (1) Insuring consistency of results, especially across the interfaces between expert panels.
   (2) Insuring that important interrelationships and synergisms are properly included. Check especially the results from the parametric source term models.
   (3) Checking for any non-physical scenarios or mutually exclusive assumptions.

5. A concerted effort should be made to improve the readability of NUREG-1150. We suggest that there be included a tutorial section (or attached appendix) in which the reader is guided through the entire multistage process, by representative examples, including at least one complete example from start to finish with emphasis on actual numbers passed from one stage to the next.

   We suggest that the final report be organized and edited by someone skilled in written technical communication.

6. The reference status of NUREG-1150 should be de-emphasized. The Committee suggests that the present title, Reactor Risk Reference Document, be changed to be more descriptive of the analysis of risk uncertainty which is presented. The study should be presented as a snapshot of risk assessment technology at this time and be promoted for the methodological innovations it has employed.

7. A discussion of the experimental and analytical data upon which the analyses and conclusions of NUREG-1150 are based should be included. The discussion should include the rationale for including or excluding the results of various experimental and analytical programs. A matrix format may be a useful part of such a discussion.

8. The report should indicate which inputs and assumptions represent conservative values and which ones are best estimates. Some overall discussion of the degree of conservatism in the document would be appropriate.

9. In some accident sequences, especially those where considerable time is available to react, accident management can have a major impact on the course of the accident and the resultant risks. The Committee recognizes that including the effects of accident management this late in the study may be a major problem. Nonetheless, because of its importance, we recommend that treatment of accident management be reported either in the final report or in a supplementary report. This is particularly important for accident sequences which are identified to be substantial contributors to risk and/or which allow (even for highly unlikely sequences) that timely measures can be taken to protect the containment and mitigate the off-site consequences.

   NUREG-1150 should make more explicit the timing for high pressure and low pressure accident scenarios with regard to the resulting loads on the containment and to the definition of emergency operating procedures. In particular, the assessment of direct containment heating and other loads of importance for the containment response should be clarified. Containment performance and potential failure-times and modes merit a greater in-depth treatment than was the case in the Draft Report.

10. In the presentation of results:

    (1) Abandon the box-and-whisker format and the solid bar presentations. We suggest that probability distributions be presented instead.

    (2) Give approximately equal weight to presentation of the best estimate of risk and the uncertainty in the risk.

    (3) Present the key results in such a way that the reader can easily identify which portions of the analyses introduce uncertainty.

    (4) Compare directly the best estimates from NUREG-1150 with the comparable results from WASH-1400 and discuss reasons for changes since WASH-1400.

The Committee has taken into consideration the status of the ongoing NUREG-1150 modification process in the above recommendations. We recognize that some of the recommendations will require substantial effort to be implemented. However, we have tried not to make recommendations that are clearly impossible to accommodate at this late date. Our recommendations would probably have been somewhat different if they had been made before the modification process had begun. Further, the Committee is aware that the issues included in many of the above recommendations are currently being addressed by the NUREG-1150 Project. We are encouraged by the response of the Project to the issues that have been raised by members of the nuclear safety community.

ANS SPECIAL COMMITTEE ON

REACTOR RISK REFERENCE DOCUMENT (NUREG-1150)

Chair

Dr. Leo LeSage
Director, Applied Physics Div.
Argonne National Laboratory
Argonne, IL

Vice Chair

Mr. Edward A. Warman
Sr. Consulting Engineer
Stone & Webster Engineering Corp.
Boston, MA

Members

Mr. Richard C. Anoba
Project Engr., Corp. Nuclear Safety
Carolina Power & Light Co.
Raleigh, NC

Mr. Ronald K. Bayer
Virginia Power
Glenn Allen, VA

Dr. R. Allan Brown
Mgr., Nuclear Systems & Safety Dept.
Ontario Hydro
Toronto, Ontario

Mr. James C. Carter, III
IDCOR Program Manager
International Technology Corp.
Oak Ridge, TN

Dr. J. Peter Hosemann
Head, Dept of Safety & Environment
Paul Sherrer Institut
Wurenligen, Switzerland

Dr. W. Reed Johnson
Dept. of Nuclear Engineering
University of Virginia
Charlottesville, VA

Dr. Walter B. Loewenstein
Dep. Director, Nuclear Power Div.
Palo Alto, CA

Dr. Nicholas Tsoulfanidis
Nuclear Engineering Dept.
University of Missouri-Rolla
Rolla, MO

Mr. Willem F. Vinck
Consultant
Brussels, Belgium

Administrative Secretary
Mrs. Marianne Mnichowski
American Nuclear Society
LaGrange Park, IL

ASSIGNMENT
TO THE
ANS SPECIAL COMMITTEE ON REACTOR RISK REFERENCE STUDY (NUREG-1150)

This ANS Special Committee comprised of U.S. and International membership is appointed by the President of the American Nuclear Society to provide Society insight on the recently published NRC report entitled "Reactor Risk Reference Document - Draft for Comment" - NUREG-1150, its major supporting documents, and any subsequent revisions of NUREG-1150.

The objectives of the Committee are as follows:

(1) To provide an opportunity for ANS members, experts in addressing major technical issues and knowledgeable in the subject area, to contribute to a coordinated understanding of this important study which addresses the risks of the nuclear power option.

(2) To provide a centralized Society summary representing a wide range of technical expertise which gives the ANS the opportunity to play an important role in providing constructive technical comments to the NRC.

(3) To provide the basis for a Society perspective on whether NUREG-1150 is representative of the state of reactor risk knowledge.

Four key elements of the Committee's activities are:

(1) Providing general and focused detailed technical inputs to the NRC and the ad hoc advisory committee constituted by the NRC to review this current risk study.

(2) Identifying a technical basis for broader technically pertinent observations by the Society directed at helping to frame the national discussion and review of this important study.

(3) Soliciting Society member input.

(4) Helping develop technical consensus on this important document.

The results of the Committee efforts will be reported to the Society membership as a timely contribution to improving the knowledge and understanding of nuclear power plant safety.

Addendum to National Report from US

Comments on NUREG-1150 (Leo Lesage)

- NUREG-1150 is intended by the NRC to be a replacement for WASH-1400. It is a detailed evaluation of the severe accident risk associated with 5 LWRs. They are :
  Surry* (PWR)
  Sequoyah (PWR)
  Zion (PWR, large dry containment)
  Peach Bottom* (BWR, Mark I containment)
  Grand Gulf (BWR, Mark III containment)

- NUREG-1150 was intended to include all the improvements in methodology & data since WASH-1400. It also placed major emphasis on the calculation of the uncertainties in the risk estimates. WASH-1400 was critisized for not treating the uncertainties in the risk estimates.

- In reality, the front end (core damage frequency) PRA studies were improved over WASH-1400 but not markedly so. The back end (containment & source term) were greatly changed. Many more scenarios were evaluated, orders of magnitude more containment event tree (CET) paths were considered. Because so many paths were considered, it was far too expensive to do full deterministic calculation for each. There fore, a set of very simplified parametric equations was developed to interpolate between the more detailed deterministic calculations. These equations were one source of controversy.

- For many input parameters (especially in the back end analysis) there in no adequate model or code. In other cases different models & codes predicted widely different values for the parameters. The use of formalized "expert opinion" was used to select the parameter values & these variation (uncertainty range) for these parameters. Teams of experts were selected, trained and polled. Experts in the use of "expert opinion" were employed to run the process.

---

* Analyzed in WASH-1400

14320179

- A draft version of NUREG-1150 was issued "for comment" in February 1987. Many comments were received from the US and world wide. Comments were received on all parts of the report but the most frequent comments were on :
  - The expert opinion process
  - The emphasis on uncertainty ranges at the expense of best estimate values
  - Accurate & up-to-date representations of the 5 LWR plants
  - Over complicated method of presenting results
  - Readability. The calculations are incredably complicated, the editing was awful.

- Three peer review Committees were established for NUREG-1150 :
  - A committee under Herb Kouts (BNL) functioned briefly in the spring of 1987 to review the methodology of NUREG-1150. A report was issued. Suggestions on improving the "expert opinion" process were made.
  - A formal NRC review committee was set up with prof. Bill Kastenberg of UCLA as chairman. A very detailed, broad and long report was issued in the spring of 1988. The Committee was then disbanded.
  - The American Nuclear Society (ANS) formed a committee in Oct 1987. Leo LeSage was chairman. An interim report was issued in April 1988. This committee is still functioning. It will issue a final report after the final NUREG-1150 is issued.

- Major modifications are currently being made in NUREG-1150 in response to the many comments. A major part of the work is being performed at Sandia National Lab. The expert opinion process has been significantly upgraded & completely repeated. Many additional calculations are being done, and many repeated. The method of presenting the results is being completely changed, and the report will (apparently) be completely "reedited".

- The members of the ANS Committee felt the draft report had many severe problems. The Committee is, however, greatly encouraged by the changes that are being incorporated into the final report, but the final product is still uncertain.

- NUREG-1150 is important because it is supposed to be the most definitive statement available on the risk of severe accidents in LMRs (in the US). To be useful, or a first step, it must attract a degree of consensus in the technical community. The draft document could not attract these consensus, but (I feel) the revised document has a chance.

- How have the risk values changed since WASH-1400?. The final values are not yet available. In the draft the front end (core damage frequencies) were lower by factors of 2 to 5 but the uncertainties in the new values more than included the old values. The back end comparison was not done in draft NUREG-1150 (it is not straight-forward) but there was a good perception that there was no improvement between WASH-1400 and NUREG-1150. I feel that the new back end analysis will likely show a significant decrease in risk from WASH-1400. Some excessive conservatisms are being removed.

- A third major part of NUREG-1150 included the dispersion, dose & risk calculations using the source terms calculated in the 2nd part. The ANS Committee did not address this part of the report. Based on these results the NRC is seriously considering propsing a reduction in the evacuation zones around LWRs. (from a 10 mile radius to possibly 2 miles).

The Measurement of Leakage Neutron Spectra from Various Sphere Piles with 14 MeV Neutrons

Chihiro Ichihara, Shu A. Hayashi, Katsuhei Kobayashi
Research Reactor Institute, Kyoto University
Kumatori-cho, Sennan-gun, Osaka 590-04, Japan

Itsuro Kimura
Dept. Nuclear Engineering, Kyoto University
Yoshida, Sakyo-ku, Kyoto, Kyoto 606, Japan

Junji Yamamoto, Mikio Izumi, Akito Takahashi
Dept. Nuclear Engineering., Fac. Engineering., Osaka university
2-1 Yamada-oka, Suita, Osaka 565, Japan

August 19, 1988

Abstract

In order to check the existing nuclear data files such as ENDF/B-IV, JENDL-3 etc., neutron leakage spectra from various kinds of sphere piles have been measured using the intense pulsed neutron source at OKTAVIAN and time-of-flight techniques. Measured piles include LiF, TEFLON:$(CF_2)n$, Si, Cr, Mn, Co, Cu, Nb, Mo and W. The thicknesses of the piles were 0.4 to 4.7 mean free paths for 14MeV neutrons. The obtained data were compared with the theoretical calculation using three kinds of transport codes, ANISN, NITRAN and MCNP and the evaluated nuclear data files, ENDF/B-IV, JENDL-3T and ENDL-73. ENDF/B-IV and ENDL- 73 data contain several problems resulting as considerably large disagreement in the spectra for most of the piles, while JENDL-3T data gave preferable calculated spectra to the other data did. Judging from the intercomparison between the measured and the predicted with JENDL-3T, it can be seen (1)satisfactory for Cu in whole energy range, (2)good for Si and Cr above 1 MeV and (3)good for Mn below 5 MeV but considerably large underprediction above this energy.

1 Introduction

An integral experiment is useful for the evaluation of the existing data files and calculational method. We have measured the angular flux in the fission reactor candidate materials using time-of-flight techniques and photo-neutrons from the electron linac at Kyoto University Research Reactor Institute. The results were analyzed using one-dimensional Sn codes, mainly ANISN and multi-group constants mainly derived from JENDL–2 or ENDF/B–IV nuclear data [1] to [6]. The design study of fusion reactors or fusion -fission hybrid reactors needs the evaluation of the data at higher energy region.

A new data file JENDL–3 is expected to correspond these requirements, and the temporary version of this file, JENDL–3T was provided prior to the publication. In the present work, leakage neutron spectra from several candidate materials for fusion or fusion-fission hybrid reactors were measured and compared with the theoretical prediction using JENDL–3T data (Si, Cr, Mn and Cu), ENDF/B–IV data (LiF, TEFLON, Si, Cr, Mn, Co, Cu and Nb), ENDL (Mo,W).

2 Experiment

2.1 Sample Piles

Sample piles were formed as spherical so as to place the tritium target at their centers. The samples include lithium fluoride, TEFLON:$(CF_2)_n$, silicon, chromium, manganese, cobalt, copper, niobium, molybdenum and tungsten. Those samples were packed into spherical shells made of stainless steel or normal steel. Table-1 shows the list of the measured sample piles, where pile diameter and sample thickness (in unit of cm and in mean free paths for 14MeV neutrons) of each pile are given. The geometries of the piles are shown in Fig.1.

2.2 Experimental Set up

The experiment has been performed by the time-of-flight(TOF) technique using the intense 14MeV neutron source facility OKTAVIAN [7] of Osaka University. The experimental arrangement in the OKTAVIAN facility is shown in Fig.2. A tritium target is placed at the center of each pile. The energy of the incident deuterons was about 250keV. A cylindrical liquid scintillator NE-213 (5in-diam. × 2in-long) was used as a neutron detector. The detector was located at the angle of 55deg with respect to the incident deuteron beam. Neutron flight path was about 11 m from the center of the tritium target to the surface of the detector. A pre-collimator system made of polyethylene-iron multi-layers was set between the pile and the detector to reduce neutron background. The aperture size of this collimator was determined so that the whole surface of the piles facing to the detector could be viewed.

3 Data Processing

The detector efficiency was determined by combining the O5S calculation and the relative efficiency derived from the TOF measurements of ^{252}Cf spontaneous fission spectrum and the leakage spectrum from a graphite 30 cm in diameter.

The activation foils (aluminum, niobium and zirconium) were irradiated to monitor the source neutron strength during the measurements. By using these monitor values and measured source neutron spectra, the neutron leakage current spectra from the sample surface were determined by the method stated elsewhere [8].

4 Calculation

4.1 Group constant from JENDL-3T and ENDF/B–IV

A 125-group library(P5S16), FSX125G/J3-T [9] was used for the ANISN [10] calculation. This library was processed from JENDL–3T data using the process code, PROF.GROUCH–G/B [11]. A 135-group library(P5S16), GICXFNS processed from ENDF/B–IV was also used for the ANISN calculation. By using both libraries, leakage neutron spectra were calculated for the piles of silicon, chromium, manganese and copper.

4.2 DDX library for the NITRAN calculation

A double-differential cross section library with 135-group energy bins and 19 angular bins was prepared for the NITRAN [12] calculation of the cobalt pile.

4.3 MCNP calculation

For the calculation of the spectra for lithium fluoride, TEFLON, niobium, molybdenum and tungsten piles, a point Monte Carlo transport code MCNP [13] was used. The standard continuous energy cross section file BMCCS1(mostly from END/B–IV) was used for this code. The surface current tally from the outer surface of the piles was employed for this calculation.

5 Result

The measured and predicted spectra are shown in Figs. 3-a through 3-j together with the ratio of the calculated and measured values(C/E). In Table-1, listed are the calculation methods and the cross section libraries used.

5.1 Lithium fluoride and TEFLON

The predicted spectra for both LiF and TEFLON show considerable underestimation in the range 2 MeV< E_n <10 MeV(Fig.3-a, 3-b), which suggests too small value in the inelastic level scattering cross sections.

5.2 Silicon

Fig.3-c shows the experimental and calculated leakage spectrum from the silicon pile. Both calculations show similar spectra and good agreement between calculation and experiment is seen in general. Slightly better prediction is obtained by JENDL– 3T. However, there still exist some amount of discrepancies in the energy region 0.2 MeV< E_n <2 MeV. This implies both nuclear data have problems in the cross section data, possibly inelastic continuum-level scattering.

5.3 Chromium

Quite different result from the experiment was obtained by the calculation using ENDF/B–IV data (Fig.3-d). It seems that the inelastic level scattering cross section in ENDF/B–IV is too large for chromium. JENDL-3T data give much better prediction as to this problem. However, for the energy region 0.2 MeV< E_n <2 MeV, both data file give a little overestimation similar to the silicon result.

5.4 Manganese

The ENDF/B–IV prediction gives quite erroneous spectrum for the energy region 1 MeV< E_n <14 MeV (Fig.3-e). The JENDL–3T data are much improved, but there still exists a little discrepancy above 5 MeV probably due to the inelastic continuum-level scattering and/or (n,2n) cross sections.

5.5 Cobalt

The calculated spectrum shows large underestimation to the experiment almost uniformly (Fig.3-f). The cause of this underestimation is not clear from the present analysis.

5.6 Copper

The ENDF/B–IV calculation considerably underestimates the spectrum around 10 MeV (Fig.3-g). However, other part of the calculation seems good. The calculation using JENDL-3T data predicts the experiment very well. It can be concluded that JENDL-3T data are satisfactory for copper.

5.7 Niobium

Though the calculation using ENDF/B–IV data predicts the elastic scattering peak well, the shape of the spectrum under 10 MeV differs from the experiment (Fig.3-h). There might be a problem about the (n,2n) and inelastic continuum level scattering cross section, which are dominant reactions at this energy range.

5.8 Molybdenum

From this rather old evaluation data (ENDL–73), considerable underestimation below elastic scattering peak is observed probably caused by the underestimation of the inelastic level scattering cross sections (Fig 3-i). There also exists the overestimation in the energy range 0.7 MeV$< E_n <$4 MeV, which implies the problem as to the inelastic continuum level scattering cross sections.

5.9 Tungsten

The prediction using the data from ENDL-73 gives a quite different spectrum from the experiment(Fig.3-j). As the discrepancy is observed over almost all energy region, complete re-evaluation of the tungsten data should be required.

Acknowledgment

Part of this work has been supported by a Grant-in-Aid for Scientific Research of the Ministry of Education, Science and Culture, Japan, and undertaken with the framework of the co- operative research program of the OKTAVIAN facility. We are grateful to Prof. K. Sumita of Osaka university for his continuous support to this work.

References

[1] I. Kimura, et al.: *NBS Sp. Publ. 425*, Vol.1, 184(1977)

[2] I. Kimura, et al.: *Nucl. Data for Sci. and Tech.*, 98(1983)

[3] T. Mori, et al.: *J. Nucl. Sci. Technol.*, 20[12], 991(1983)

[4] T. Mori, et al.: *ibid.*, 22[9], 708(1986)

[5] S. A. Hayashi, et al.: *Ann. Nucl. Energy*, 13[3], 131(1986)

[6] S. A. Hayashi, et al.: *J. Nucl. Sci. Technol.*,24[9], 702(1987)

[7] K. Sumita, et al.: *Proc. 12-th SOFT*, vol.1, 687(1982), Juelich

[8] A. Takahashi, et al.: *OKTAVIAN Report*, C-83- 02(1983).

[9] K. Kosako, et al.: *JAERI-M (in preparation).*

[10] W. W. Engle, Jr.: *K-1693*, (1967).

[11] A. Hasegawa: *to be published in JAERI report.*

[12] A. Takahashi and D. Rusch: *KfK-2822/1*, (1979).

[13] J. F. Briesmeister ed.: *MCNP-A General Monte Carlo Code for Neutron and Photon Transport, LA-7396-M*, Rev.2, (1986)

Table-1 Characteristic parameters of the piles, calculation codes and nuclear data files used

Pile	Dia. (cm)	Sample Thickness (cm)	(MFPs)	Calc. Code	Cross-section Libraries
LiF	61.0	27.5	3.5	MCNP	BMCCS1 ^{6}Li:LASL(101) ^{7}Li:ENDF/B-IV(1272) F:ENDF/B-IV(1277)
TEFLON	40.4	10.0	0.7	MCNP	BMCCS1 C:LASL(102) F:ENDF/B-IV(1277)
Si	61.0	20.0	0.4	ANISN	FSX125/J3T-1 and GICXFNS
Cr	40.4	10.0	0.7	ANISN	FSX125/J3T-1 and GICXFNS
Mn	61.0	27.5	3.4	ANISN	FSX125/J3T-1 and GICXFNS
Co	40.4	10.0	0.5	NITRAN	DDX Library from ENDF/B-IV
Cu	61.0	27.5	4.7	ANISN	FSX125/J3T-1 and GICXFNS
Nb	28.6	11.2	1.1	MCNP	BMCCS1 ENDF/B-IV(1191)
Mo	61.0	27.5	1.5	MCNP	BMCCS1 ENDL-73(533)
W	40.4	10.0	0.8	MCNP	BMCCS1 ENDL-73(540)

FSX125/J3T-1: 125-group library processed from JENDL-3T with PROF.GRAUCH/G-B code

GICXFNS: 135-group library processed from ENDF/B-IV with NJOY

Fig.1 The geometries of the sample piles.

(a) 28 cm diameter shell for use with Nb pile.

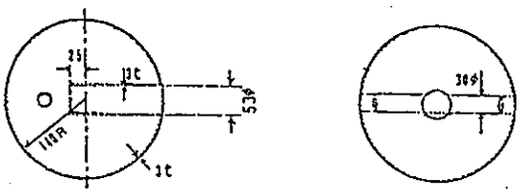

(b) 40 cm diameter shell for use with TEFLON, Cr, Co and W pile.

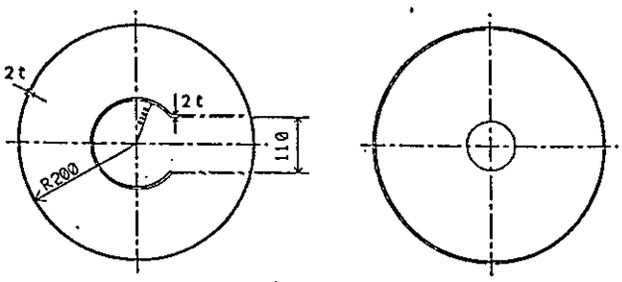

(c) 60 cm diameter shell for use with Si pile.

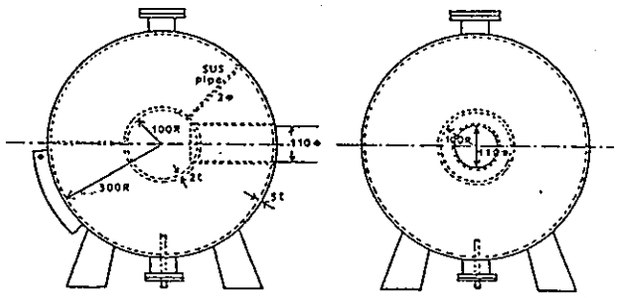

(d) 60 cm diameter shell for use with LiF, Mn, Cu and Mo pile.

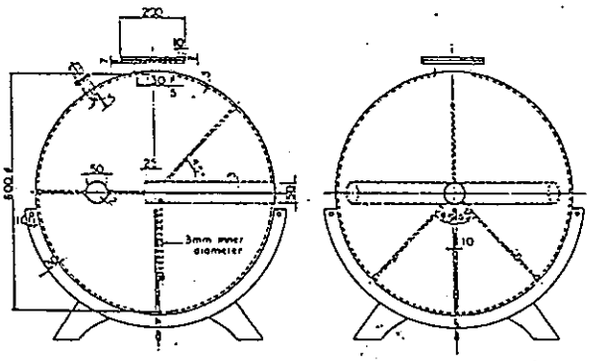

Fig.2 Experimental arrangement in OKTAVIAN facility.

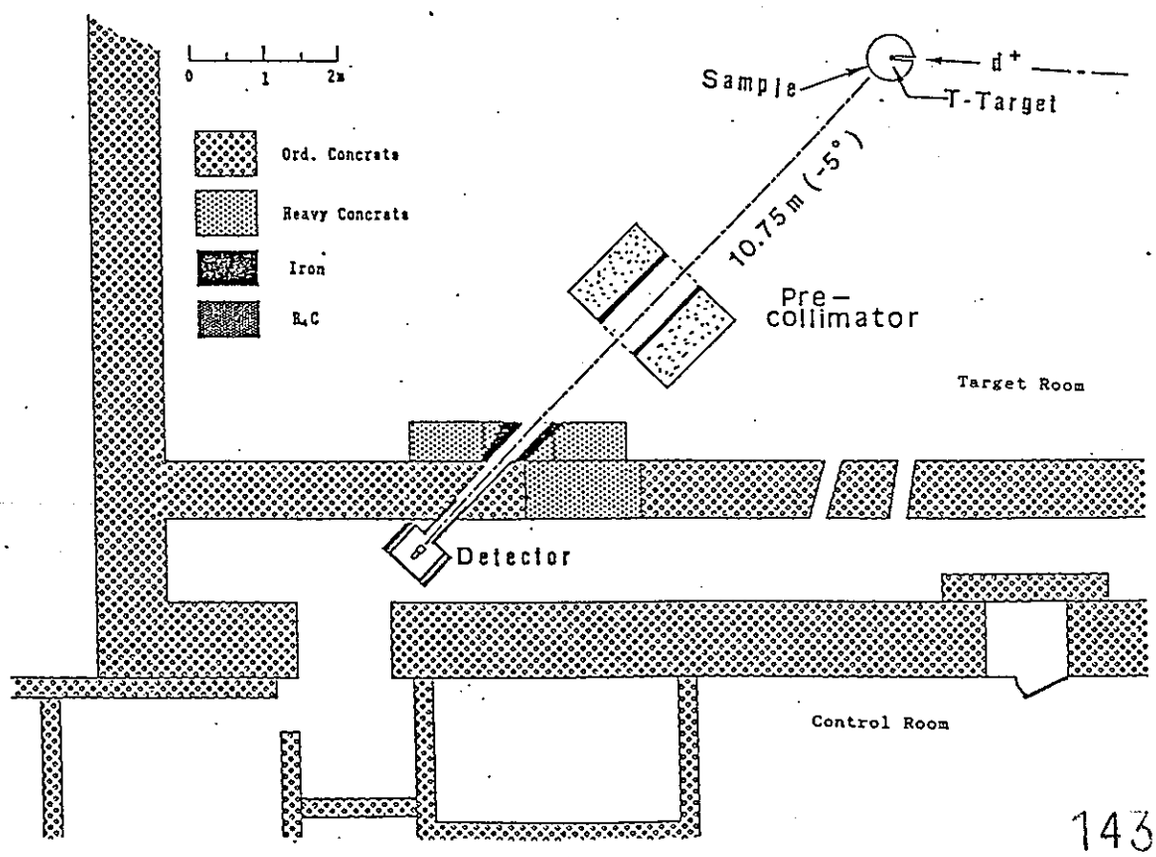

Fig.3 Experimental and calculated spectra

(a) Lithium Fluoride 60 cm Sphere

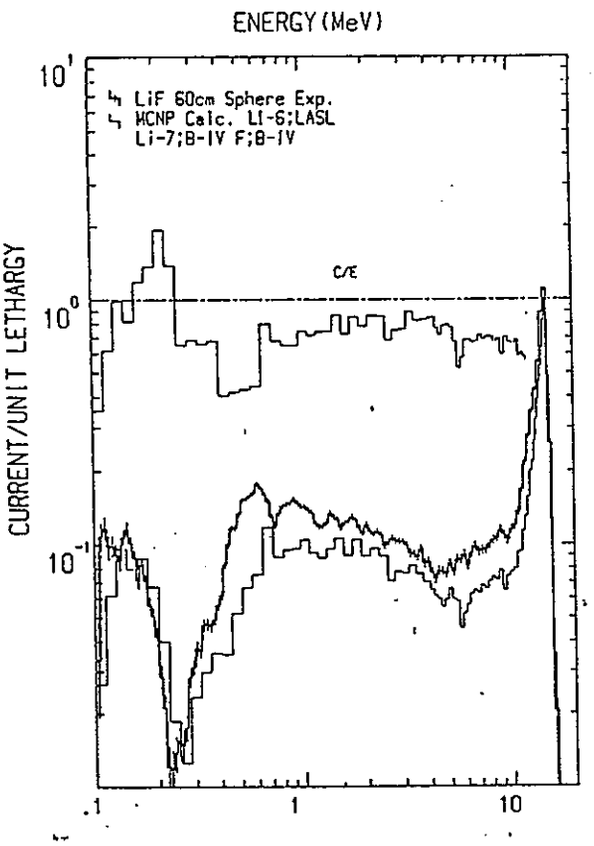

(b) TEFLON: $(CF_2)_n$ 40 cm Sphere

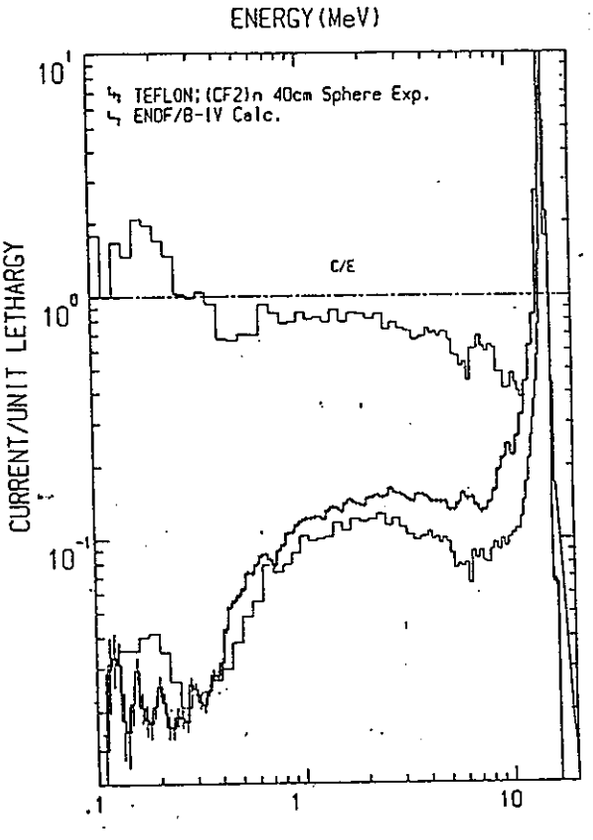

(c) Silicon 60 cm Sphere

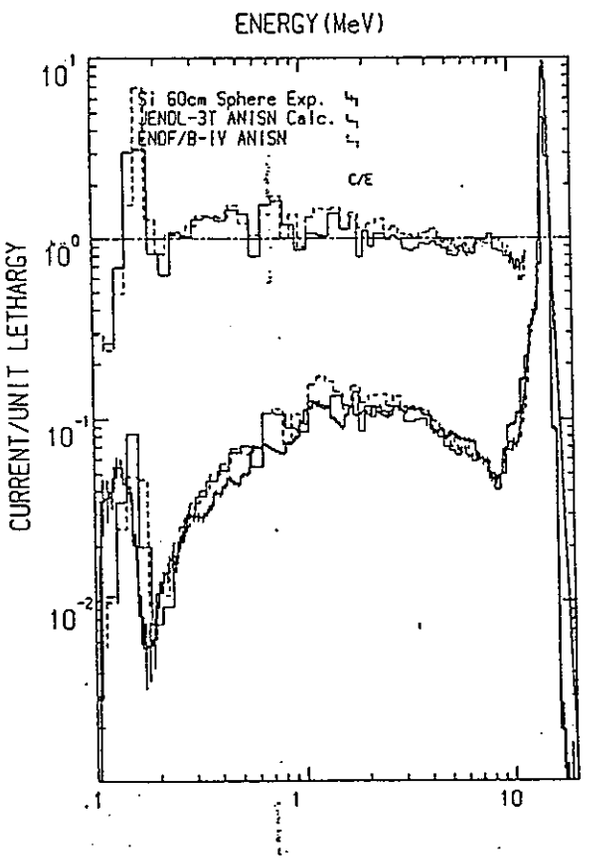

(d) Chromium 40 cm Sphere

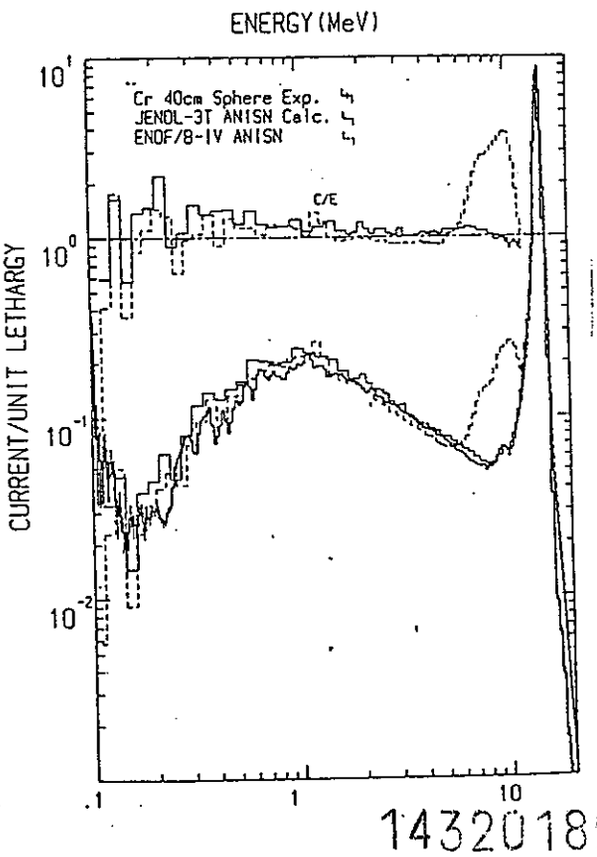

(e) Manganese 60 cm Sphere

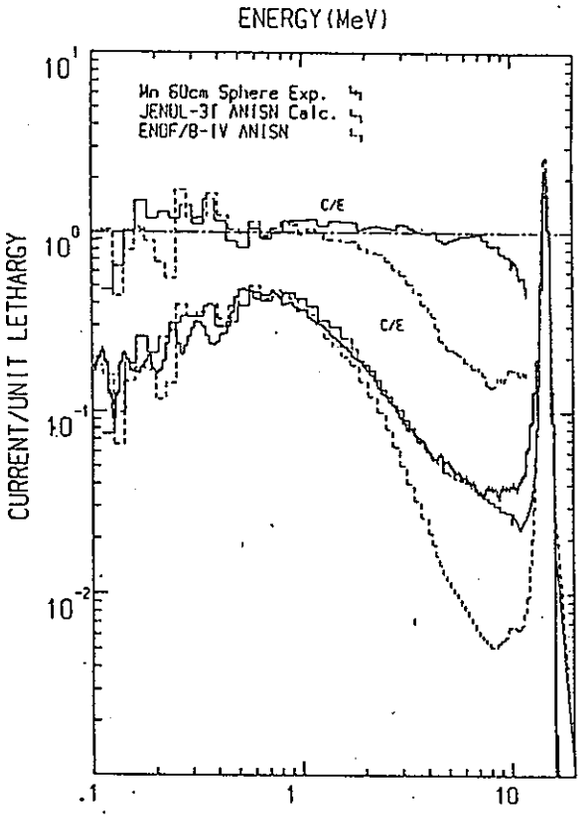

(f) Cobalt 40 cm Sphere

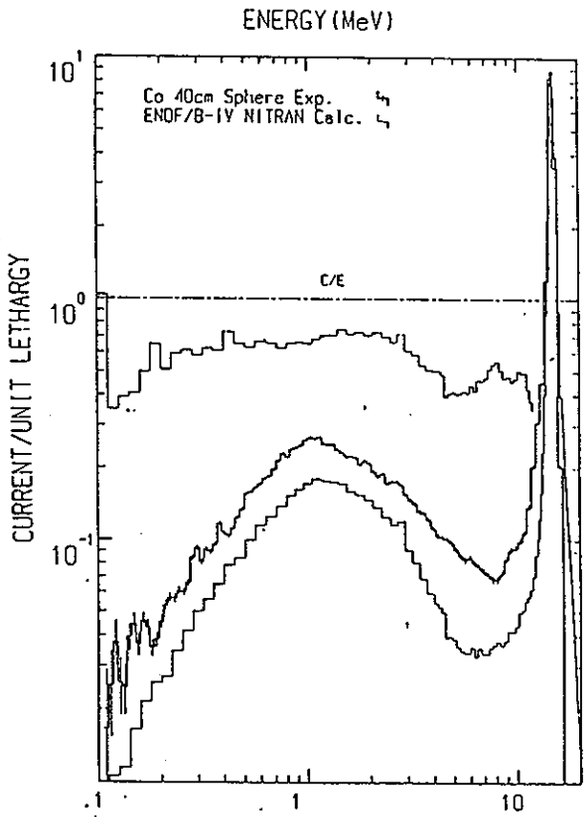

(g) Copper 60 cm Sphere

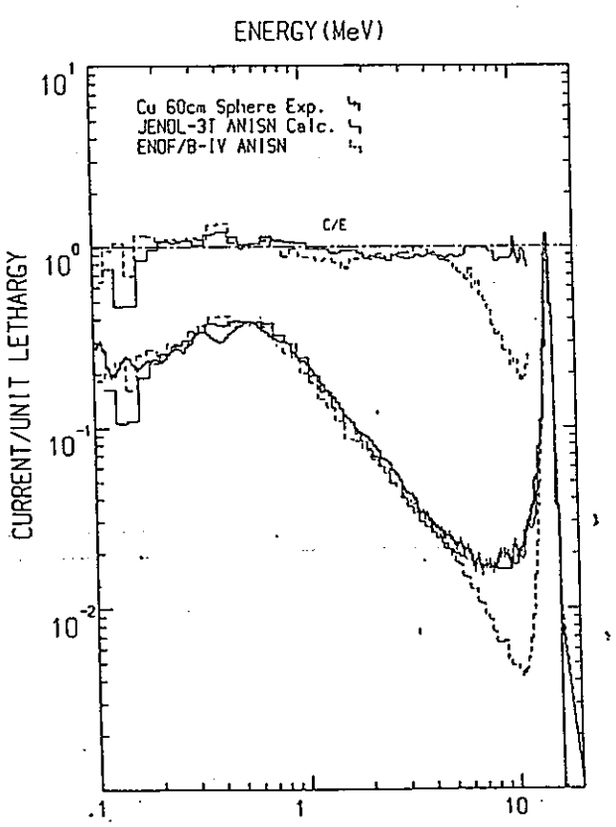

(h) Niobium 28 cm Sphere

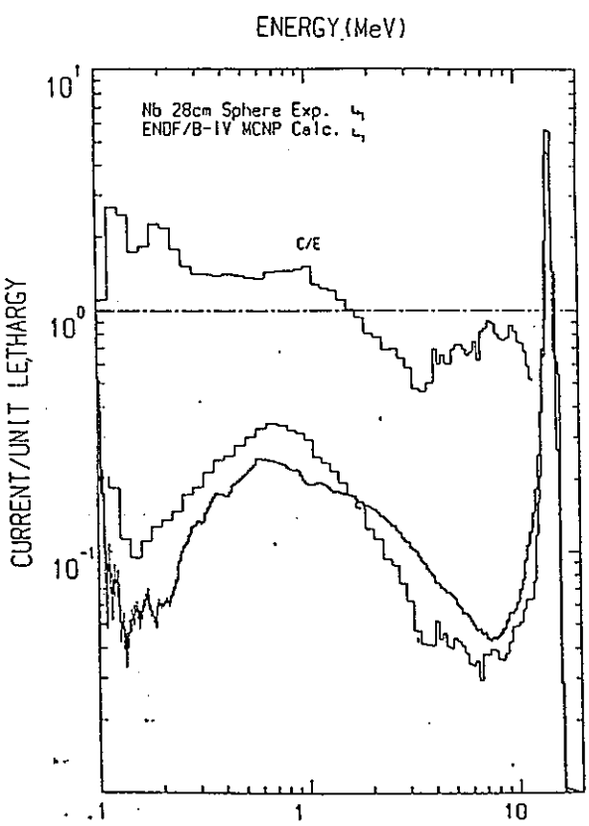

14320190

(i) Molybdenum 60 cm Sphere

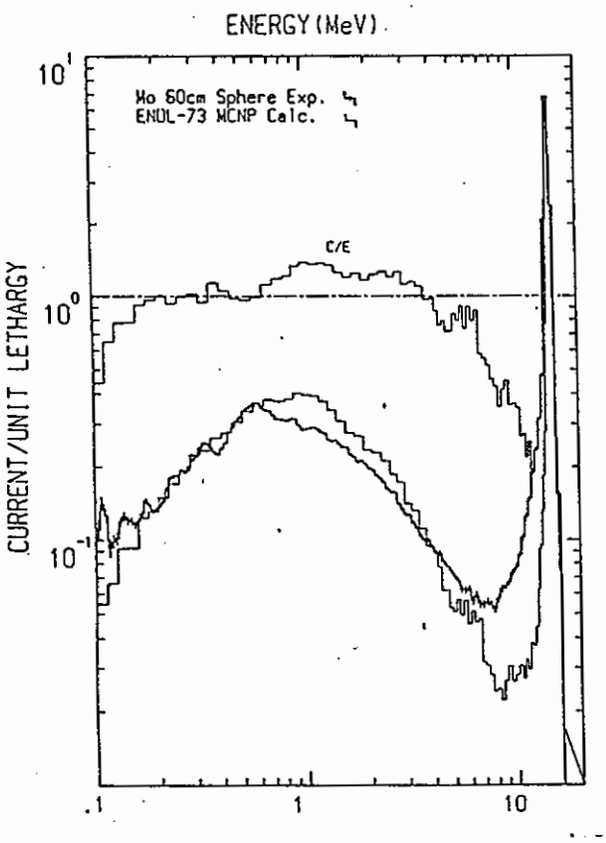

(j) Tungsten 40 cm Sphere

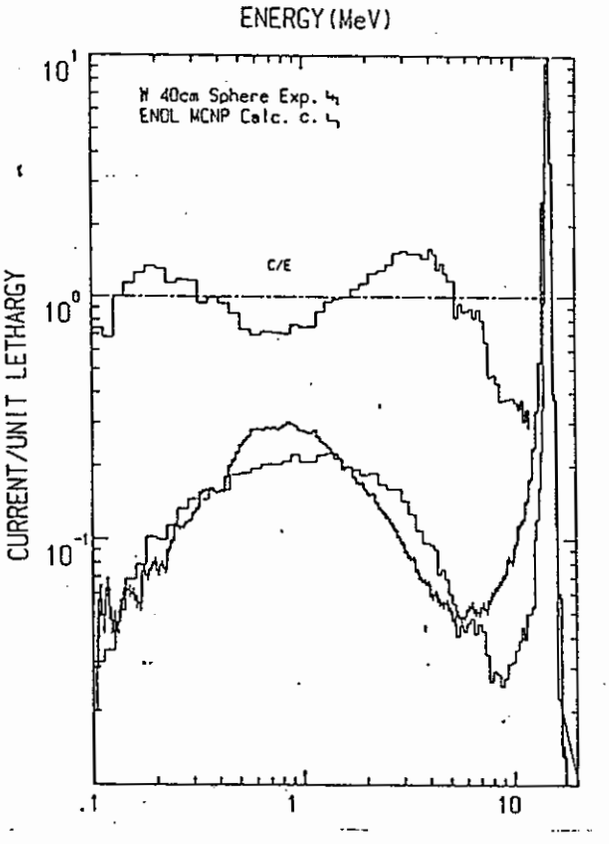

This paper is to be submitted to the ANS 8th Topical Meeting
on Technology of Fusion Energy,Oct. 9-13, 1988, Salt Lake City.

TRITIUM PRODUCTION-RATE DISTRIBUTIONS IN A Be-SANDWICH LITHIUM-OXIDE CYLINDRICAL ASSEMBLY

H. Maekawa, S. Yamaguchi, Y.Oyama and K. Kosako
Department of Reactor Engineering, Japan Atomic Energy Research Institute
Tokai-mura, Naka-gun, Ibaraki-ken, 319-11 Japan
(292) 82-6015

ABSTRACT

Tritium production-rate (TPR) distributions of ^{6}Li, ^{7}Li and ^{N}Li were measured in a simple-geometrical assembly, i.e., Be-sandwich Li_2O assembly. The Be-region of 50.8 mm-thick was sandwiched by 50.6 and 506 mm-thick Li_2O regions. Tritium production rates along the central axis were measured by four techniques, i.e., liquid scintillation method with Li_2O pellets, self-irradiation method with LiF TLDs, Li-glass scintillators and a small sphere NE213 detector. The TPRs measured by the four methods agreed well each other within the experimental errors. The calculation was performed by DOT3.5 with the nuclear data files of JENDL-3T and ENDF/B-IV. A agreement is observed between the calculated and measured TPRs within the experimental errors except near the Be region.

INTRODUCTION

Tritium production rate (TPR) is one of most important items in fusion neutronics experiments. The TPR distribution was measured in a Li_2O cylindrical assembly by the use of the FNS facility.[1] The calculated TPRs based on JENDL-3PR1 and -3PR2 agreed well with measured ones.[2] As beryllium is the most promising neutron multiplier in the fusion blanket, benchmark experiments have been carried out using assemblies of Li_2O and Be as the JAERI/USDOE collaborative program on fusion blanket neutronics. A large discrepancy was, however, observed between calculated and measured TPRs in the cases of assemblies having Be-region.[3] The discrepancy was also pointed out in the neutron spectra leaking from Be slabs.[4]

In order to provide the benchmark data for the examination of these discrepancies, TPR distributions of ^{6}Li, ^{7}Li and ^{N}Li, denoted as T_6, T_7 and T_N respectively, were measured in a simple-geometrical assembly, i.e., Be-sandwich Li_2O assembly. It is easy to make a calculational model accurately.

Tritium production rates along the central axis were measured by four techniques to confirm the observed TPRs experimentally. They were liquid scintillation counting method with $^{6}Li_2O$, $^{7}Li_2O$ and $^{N}Li_2O$ pellets, self-irradiation method[5] with TLD-600, TLD-700 and TLD-100, Li-glass scintillators method (only for T_6),[6] and indirect method using a small sphere NE213 spectrometer[7] (only for T_7). Measured TPRs were compared with each other and with calculated ones based on the nuclear data files of JENDL-3T* and ENDF/B-IV.

EXPERIMENTAL

Assembly and Arrangement

The Be-sandwich Li_2O assembly was formed by loading Li_2O and Be blocks in a framework consisting of thin-walled aluminum square tubes. The loading method and experimental arrangement were similar to the previous experiment[1]. A sketch of the experimental arrangement is shown in Fig. 1. The Be-region of 50.8 mm-thick was sandwiched by 50.6 and 506 mm-thick Li_2O regions. The effective radius was 315 mm. The distance between the D-T neutron source and the surface of assembly was 200 mm. Deuteron beam energy was 330 keV. Absolute neutron yield was determined by the associated α-particle method[8].

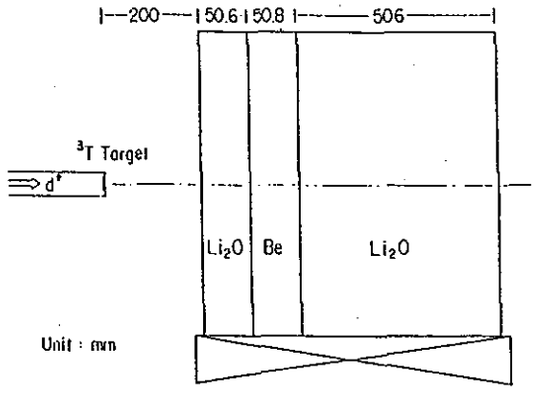

Fig. 1 Experimental arrangement.

* JENDL-3T is a temporary file for testing the evaluated data for JENDL-3. The data in JENDL-3T will be partly revised in JENDL-3.

Liquid Scintillation Method with Li_2O Pellets

Three types of sintered Li_2O pellets, i.e., $^6Li_2O$ (^{6}Li:95.446 atom %), $^7Li_2O$ (^{7}Li:99.952 atom %) and $^NLi_2O$ (natural abundance), were used to measure the TPRs of ^{6}Li, ^{7}Li and ^{N}Li (T_6, T_7 and T_N) separately. The size and density of pellets were 12 mm dia. × 2 mm and about 83 % of theoretical density, respectively. The pellets were sealed in a 0.2 mm-thick aluminum capsule to avoid the tritium contamination from the humidity in the circumstances air. They were placed in the 2.5 mm deep cavities between welding rims of the special-sized Li_2O blocks arranged along the central axis. Average beam current and total irradiation time were 2 mA and 10 hours, respectively. Total neutron yield during the irradiation was 9.80×10^{15} at the target.

The irradiated Li_2O pellets were resolved in 8 ml water; complete solution required about 2 days. The solution was distilled with the apparatus used in the previous experiment[1]. About 7 ml of the collected water was pipetted into a vial; then, 14 ml of liquid scintillation cocktail (Clear Sol, manufactured by Nakarai Chemicals Ltd.) was added. The tritium activity in the sample was measured by a special-designed liquid scintillation counting system, LSC-7100 (Ouyou-Kouken Industrials Ltd.). After the correction for escaped tritium during the irradiation, T_6 and T_7 were obtained by making use of the atomic ratios of pellets.

Self-Irradiation Method with LiF TLDs

The LiF powder of TLD-600 (^{6}Li: 95.62 atom %), TLD-700 (^{7}Li: 99.993 atom %) and TLD-100 (natural abundance) purchased from Harshaw Chemical Co. Ltd. was sealed in 2 mm dia. × 12 mm Pyrex glass ampoules. Five TLDs of each type were placed in the same cavities mentioned above. Total neutron yield during the irradiation was 9.86×10^{15} at the target. For 25 days after the neutron irradiation to wait the full decay of activated nuclei except for tritium, the TLDs were annealed in the condition of 400°C and 2 hours. After this process, they were stored in a low background storage for 3264 hours (about 4.5 months). The thermoluminescence caused by the self-irradiation of β-rays from tritium during the keeping period were measured by a TLD reader (National UD-502B).

Lithium-Glass Scintillators Method

The scintillators used were small disk (10 mm dia. × 0.3 mm) of NS15 ^{6}Li-glass and BS15 ^{7}Li-glass scintillators manufactured by Nikon Co. The scintillators were coupled to a 13 mm dia. photomultiplier tube (Hamamatsu R647-04) using a quartz light guide. The ^{6}Li content in the NS15 scintillator was 1.59×10^{22} [atom/cm^3]. Measuring procedures and data processing method were just the same as those described in Ref. 6.

Indirect Method Using NE213 Spectrometer

Neutron spectra along the central axis were measured by a small sphere NE213 spectrometer.[7] The structure of detector assembly was similar to that of the Li-glass detector. Measured pulse-height spectrum was unfolded to the neutron spectrum. The T_7 value was calculated from the measured neutron spectrum with the $^7Li(n,n't)^4He$ cross section of JENDL-3T.

ANALYSIS

The neutron fluxes in the assembly were calculated by the two-dimensional transport code DOT3.5[9] with P_5-S_{16} approximation. The 125-group cross section set, FSX125/J3T based on JENDL-3T was used as well as the ENDGIX[10] based on ENDF/B-IV. The nuclide density used in the calculation is shown in Table 1. The result of a Monte Carlo calculation was adopted as the input source neutron spectrum. This spectrum was confirmed by the result of a time-of-flight experiment. The calculational model was similar to that used in the previous analyses[1,2].

Table 1 Homogenized nuclide density used in the calculation.

Region	Li_2O	Be
Nuclide		
^{6}Li	4.2211-3*	
^{7}Li	5.2774-2	
Be		1.2152-1
C		7.7109-5
O	2.8498-2	4.9813-4
Al		2.9013-5
Cr	1.4333-4	
Fe	5.2773-4	2.4678-5
Ni	6.2963-5	

*Read as 4.2211×10^{-3} [10^{24}atoms/cm^3].

RESULTS AND DISCUSSION

Figure 2 shows tritium production-rate distributions measured by the four methods. The T_6 values of pellet and Li-glass are corrected for self-shielding effect. The error due to the self-shielding correction is not included in its error. As the TPR distributions of TLD were not measured absolutely at the present, the data of T_6 at 224 mm in the figure are normalized to 1.80×10^{-28} (arbitrary value) and the other TLD data are shifted relatively. Although those data were measured independently by quite different methods, a good agreement is observed within their experimental errors. This fact suggests that the measured data are consistent among each other.

The C/E value (calculated to experimental values ratio) distributions of are shown in Figs.

3 ∿ 6. The data of JENDL-3T were used for the cross sections of $^{6}Li(n,t)^{4}He$ and $^{7}Li(n,n't)^{4}He$ in the TPR calculations after the flux calculations based on both JENDL-3T and ENDF/B-IV by DOT3.5. The bands in Figs 4 ∿ 6 mean the range of experimental error.

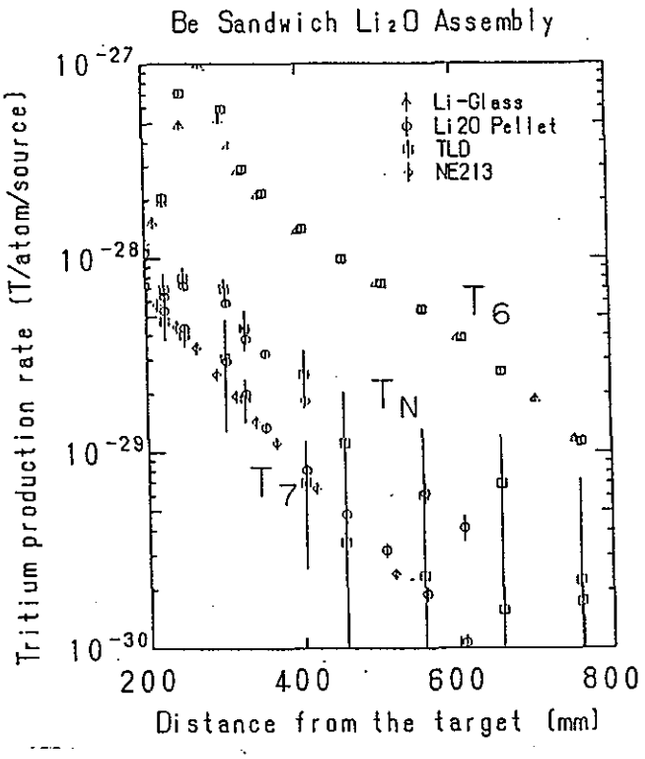

Fig. 2 Tritium production-rate distributions in Be-sandwich Li_2O assembly.

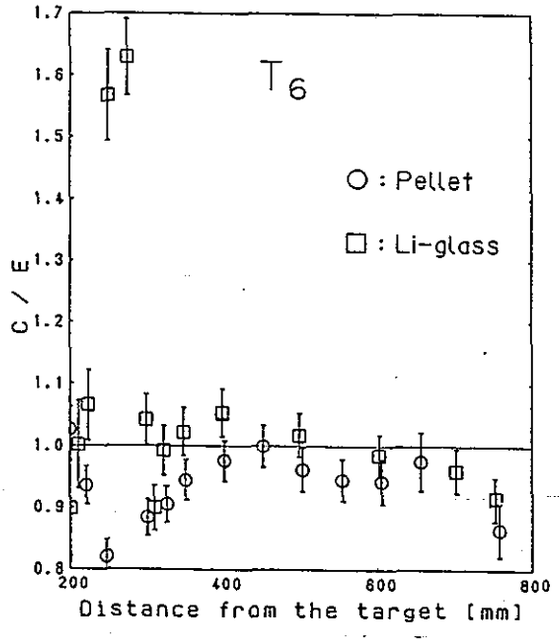

Fig. 3 Comparison of C/E values for T_6. The calculation is based on JENDL-3T.

The T_6 in Fig. 3 is measured by pellets. The self-shielding correction factor is about 0.5 for the T_6 data of pellet near the Be-region. On the other hand, that is about 0.99 for those of Li-glass except in the Be-region where it is about 0.8. The T_6 data inside of Be-region mean one of spectrum indices. There is no correction for the effect of room-returned neutrons. This effect may appear in the data of T_6 near the back-surface. It can be seen from Figs. 3 and 4 that the T_6 calculations based on both JENDL-3T and ENDF/B-IV agree well with the measured ones except near and inside of Be-region. Especially a large discrepancy is observed inside of Be-region considering the experimental error (about 4 %) and the self- shielding correction (about 20 %). This fact suggest that the accuracy of Be nuclear data in JENDL-3T and ENDF/B-IV are insufficient.

The T_7 data in Fig. 5 are measured by pellets. There are some differences in the calculated T_7 data between JENDL-3T and ENDF/B-IV. This fact suggest that the difference of Be nuclear data affect on the calculated T_7. We can not, however, conclude which nuclear data file is better.

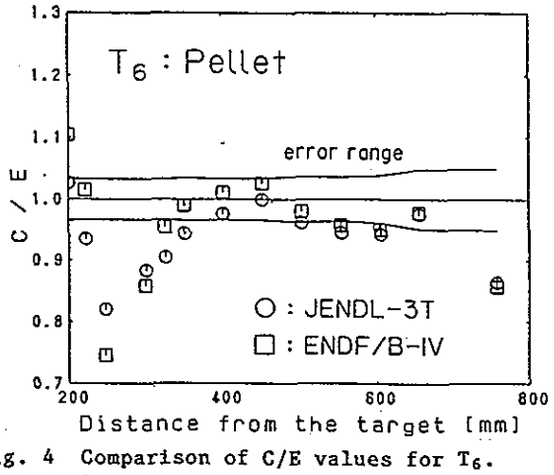

Fig. 4 Comparison of C/E values for T_6. The experimental data are measured by pellets.

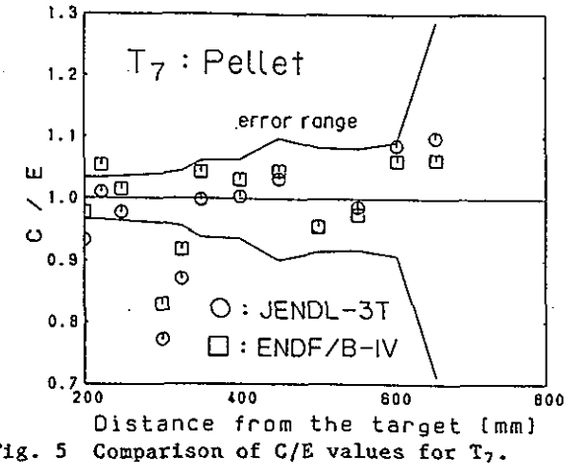

Fig. 5 Comparison of C/E values for T_7. The experimental data are measured by pellets.

The C/E of T_N is useful practically for the evaluation of tritium breeding capability. It can be seen from Fig. 6 that the agreement is not so bad between the calculations and measurement except near the Be-region. If the nuclear data of Be are improved, the TPR can be estimated within about 5 %.

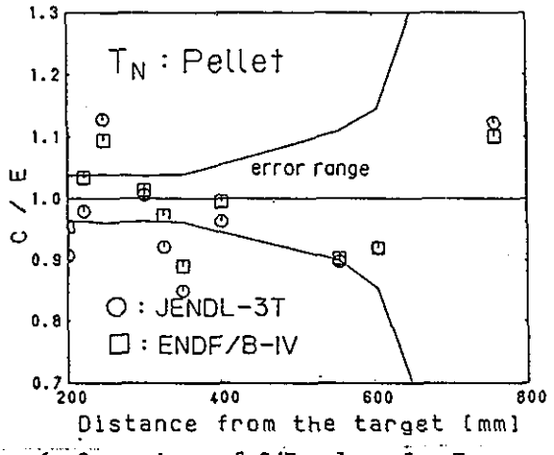

Fig. 6 Comparison of C/E values for T_N. The experimental data are measure by pellets.

SUMMARY

The tritium production-rate (TPR) distributions were measured in a Be-sandwich Li_2O assembly by four methods independently. They agreed well with each other within the experimental errors. A good agreement is observed between the measured and calculated TPRs except near the Be-region. This fact suggests that the accuracy of Be nuclear data is insufficient for the evaluation of tritium breeding ratio in a blanket having Be neutron multiplier.

ACKNOWLEDGEMENT

This work is an activity associated with the JAERI/USDOE collaborative program on fusion blanket neutronics. The authors would like to thank Drs. T. Nakamura and M. A. Abdou for their support of this work. They also grateful to Messrs. J. Kusano, C. Kutsukake, S. Tanaka and Y. Abe for their operation of the FNS accelerator, and to Mr. T. Takahashi for his preparation of Li_2O pellets.

REFERENCES

1. H. MAEKAWA, et al., "Fusion Blanket Benchmark Experiments on a 60 cm-thick Lithium-Oxide Cylindrical Assembly," *JAERI-M 86-182*, Japan Atomic Energy Research Institute (1986).

2. H. MAEKAWA, et al., "Integral Test of JENDL-3PR1 Through Benchmark Experiments on Li_2O Slab Assemblies," *Proc. Int. Conf. on Nuclear Data for Basic and Applied Science, May 13-17, 1985, Santa Fe, New Mexico, U.S.A., Vol. 1* pp101-106.

3. M. Z. YOUSSEF, et al., "Analysis for Phase II Experiments of the JAERI/US Collaborative Program on Fusion Blanket Neutronics, Part II: Tritium Production and In-System Spectrum," *Int'l Symp. on Fusion Nuclear Technology, MO-02, Apr. 10-15, 1988, Tokyo, Japan*.

4. Y. OYAMA, H. MAEKAWA,"Measurement and Analysis of an Angular Neutron Flux on a Beryllium Slab Irradiated with Deuterium -Tritium Neutrons," *Nucl. Sci. Eng. 97*, 220 (1987).

5. H. MAEKAWA, "A Method for Obtaining the Tritium Production Rate Distribution with a LiF Thermoluminescence Dosimeter," *JAERI-M 6055*, Japan Atomic Energy Research Institute (1975) (In Japanese); *UCRL-TRANS-11196*, Univ. of Carifornia (1979).

6. S. YAMAGUCHI, et al., "An On-line Method for Tritium Production Measurement with a pair of Lithium-Glass Scintillators," *Nucl. Instr. Method A254*, 413 (1987).

7. Y. OYAMA, et al., "A Small Spherical NE213 Scintillation Detector for use in In-Assembly Fast Neutron Spectrum Measurements," *ibid., A256*, 333 (1987).

8. H. MAEKAWA, et al., "Neutron Yield Monitors for the Fusion Neutronics Source (FNS) -- For 80° Beam Line --," *JAERI-M 83-219*, Japan Atomic Energy Research Institute (1983).

9. W. A. RHOADES, F. R. MYNATT, "The DOT III Two-Dimensional Discrete Ordinates Transport Code," *ORNL/TM-4280*, Oak Ridge National Laboratory (1979).

10. K. KOSAKO, et al., "Neutron Cross Section Libraries for Analysis of Fusion Neutronics Experiments," *JAERI-M 88-076*, Japan Atomic Energy Research Institute (1988) (In Japanese).

B.2.4
for information

DELAYED NEUTRON SPECTRA BY DECAY GROUP FOR FISSIONING SYSTEMS FROM ^{227}Th THROUGH ^{255}Fm

T. R. England and M. C. Brady*

Los Alamos National Laboratory
Los Alamos, New Mexico, USA

ABSTRACT

The quality and quantity of delayed neutron precursor data has greatly improved over the past approximately 15 years. Supplementation of the data with model calculations and the use of models to extend the number of precursors to 271 is now practical. These data, along with improved fission-product parameters, permit direct calculations of aggregate behavior for many fissioning nuclides. The results can even by approximated using a few (usually six) temporal groups. This paper summarizes an extensive four-year effort to provide a complete set of evaluated data and emphasizes its use to generate the temporal approximations; precursor data and group values are intended for inclusion in ENDF/B-VI.

INTRODUCTION

Most applications of delayed neutrons use an approximate temporal group representation of measured aggregate data.[1] Such data have been limited to the few fissioning nuclides that have aggregate measurements, and even these have inadequate or no spectral measurements.

Improvements in the experimental techniques of isotope separation and neutron spectroscopy have made the study of delayed neutron emission from individual precursor nuclides more practical and productive over the past fifteen or so years. The quantity and quality of the delayed neutron emission probabilities and particularly the neutron emission spectra for the individual nuclides have been greatly improved. Such data are still inadequate for use in calculations of aggregate behavior from individual precursors. We have evaluated the measured data, supplemented it with model spectra for completeness, and added model values for probable unmeasured precursors. The resulting extensive data base will be incorporated into ENDF/B-VI.

This paper can only briefly describe the data base. We will concentrate on its use to produce aggregate delayed neutron yields, halflives, and spectra in the classical six-group representation for 43 fissioning systems from ^{227}Th to ^{255}Fm. Group data are also required in ENDF/B-VI. Comments and observations made concerning the use of more than six time groups are included. The application of the data in both its explicit and reduced (six temporal group representation) forms in the point reactor kinetics equations are also discussed. Results from beta-effective calculations in a simple Godiva-type system are presented, but this paper will concentrate on the precursor data base and emhasize the temporal group representations.

---

* M. C. Brady, presently with Nuclear Engineering Applications Dept., Oak Ridge National Laboratory.

PRECURSOR DATA BASE

Based on energetics, approximately 271 fission products should be delayed neutron precursors. Only a brief description of the types and sources of data for precursors, including fission-product yields, can be given here, along with a summary of the relative importance of the experimental data *vs* that provided by various model calculations.

Fission-product yields are based on a preliminary evaluation for ENDF/B-VI.[2] This comprises data at one or more neutron incident energies [denoted as thermal (T), fast (F), and high (H) and for spontaneous fission (S)] for 34 fissioning nuclides. Forty-three cases are included in this paper for 28 fissioning nuclides. Most of the yields are based on models.

Emission probabilities (Pn values) for 85 precursors have ben measured[3] and evaluated.[4] The evaluation also provides a fit to the parameters in the systematic Herrmann-Kratz equation[5] used to predict the unmeasured Pn's.

Spectra for 34 precursors have been measured.[6-8] Thirty of these were found to be inadequate in the measured energy range and had to be supplemented with nuclear models.[9,10] The same models were used to estimate the spectra for the remaining 237 precursors. Two models were used. The BETA code[10] was used to extend 30 measured spectra. Otherwise we used a modified evaporation model, described in Ref. 11, because it has the virtue of producing the shape of typical spectra without the need to know, as does the BETA code, energy levels, spins, and parities of precursors and daughters; such data are unknown for most short-leved nuclides. Figure 1 shows a comparison of measured and model results.

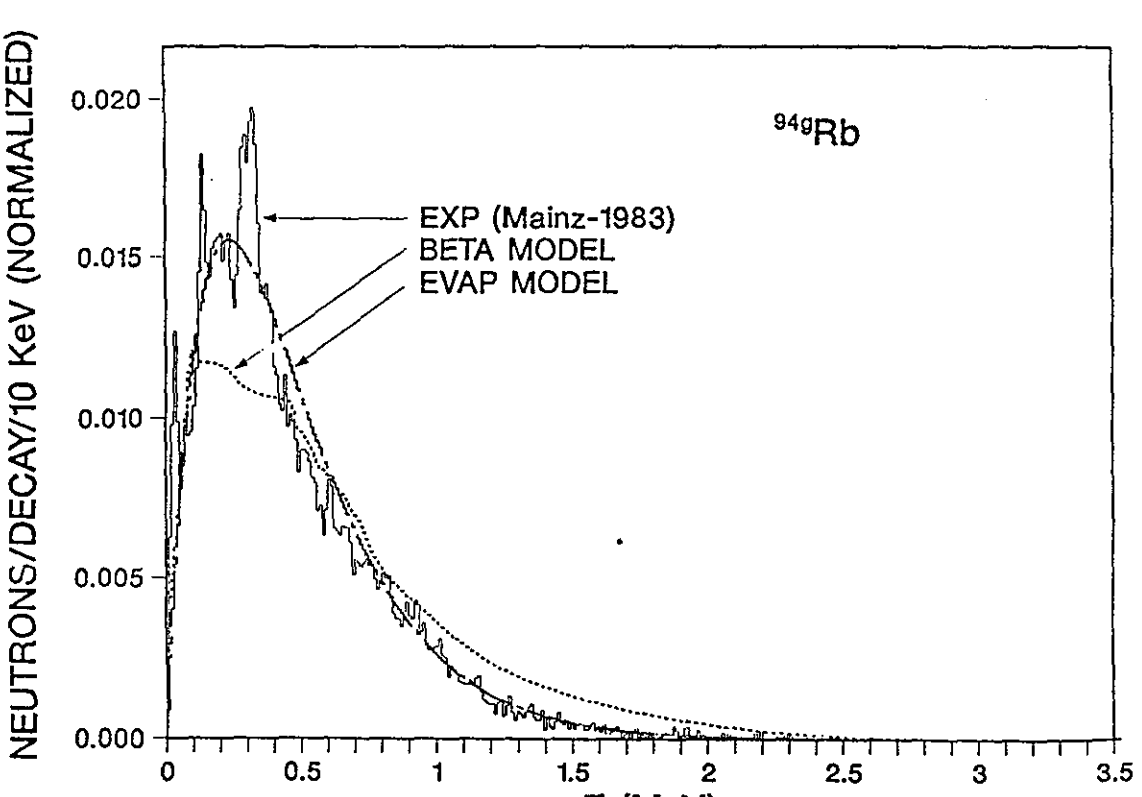

Fig. 1. Delayed neutron spectra for nuclide ^{94g}Rb.

The simple count of nuclides having measured data is misleading. The 85 having measured Pn values account for 80% or more of the total emission rate and the 34 having measured spectra account for 67% or more of the total. These contributions at reactor shutdown depend on the fissioning nuclide; e.g., for ^{235}U thermal fission, the respective contributions are 96% and 84%.

The largest effort in the evaluation was directed at model estimates of unmeasured spectra and the expansion of the incomplete measured spectra. This effort and the models are summarized in Refs. 9 and 11; it will be described in complete detail when Ref. 12 is published.

REDUCTION OF DATA INTO DECAY AND SPECTRA GROUPS

The use of a few temporal groups to represent the behavior of a large, unknown number of precursors started with aggregate experiments. It is still a convenient approximation for use in applications and can be duplicated from aggregate calculations of the individual precursors.

The fission product depletion code, CINDER-10, was used to calculate the activities of all precursor nuclides for various cooling times (to 300 seconds) following a prompt irradiation in each of the fissioning systems. These nuclide activities were folded in with the evaluated emission probabilities to produce aggregate delayed neutron emission values. The delayed neutron activity curves, as illustrated in Fig. 2, can be approximated mathematically as a sum of N exponenetials representing N-time-groups:

$$n_d(t) = \sum_{i=1}^{N} A_i e^{-\lambda_i t}. \qquad (1)$$

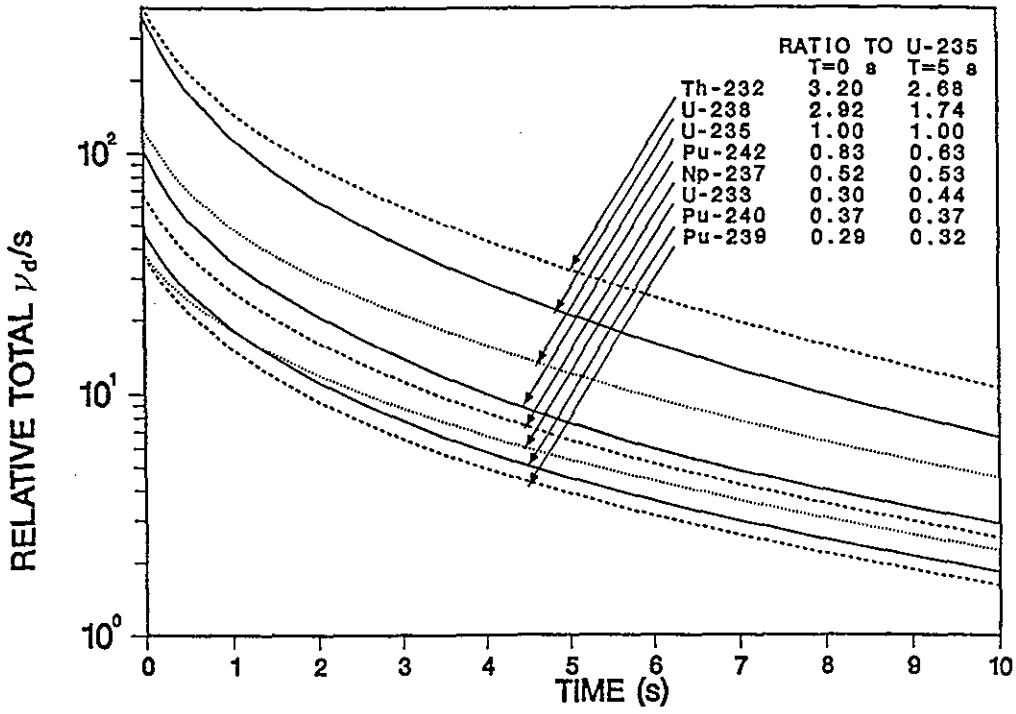

Fig. 2. Total ν_d/s for eight fuels vs time (pulse).

The parameters A_i and λ_i in Eq. (1) are determined using a nonlinear, least-squares fitting code. The data represents a pulse irradiation, implying that A_i is the product of the group decay constant, λ_i, and the group yield per fission, a_i.

Initial calculations for $^{235}U(F)$, $^{238}U(F)$, and $^{239}Pu(F)$ were performed using three, six, nine, and twelve groups. Increasing the number of groups from six to nine resulted in a significant improvement in the fit; however, the results from point kinetics calculations using both the six- and nine-group fits for prompt changes in reactivity did not reveal any significant differences. [12,13]

Based on these results and the general acceptance of a six-group representation, the fits for the remaining 40 fissioning systems were performed only for six-groups. Table I presents the normalized group abundances and decay constants for all 43 fissioning sytems.

TABLE I

Delayed Neutron Six-Group Parameters

Fission Nuclide		Group 1	2	3	4	5	6
Th227T	alpha	0.1027	0.2182	0.1304	0.3555	0.1647	0.0284
	lambda	0.0128	0.0354	0.1098	0.2677	0.5022	2.0956
Th229T	alpha	0.0867	0.1907	0.1297	0.3887	0.1729	0.0312
	lambda	0.0128	0.0350	0.1123	0.2760	0.4950	2.0456
Th232F	alpha	0.0364	0.1259	0.1501	0.4406	0.1663	0.0808
	lambda	0.0131	0.0350	0.1272	0.3287	0.9100	2.8203
Th232H	alpha	0.0326	0.0997	0.1431	0.5062	0.1336	0.0848
	lambda	0.0130	0.0350	0.1307	0.3274	0.9638	3.1667
Pa231F	alpha	0.0826	0.2230	0.1608	0.3885	0.1050	0.0401
	lambda	0.0129	0.0347	0.1150	0.2856	0.6706	2.3111
U232T	alpha	0.1360	0.2745	0.1509	0.3052	0.1007	0.0326
	lambda	0.0128	0.0350	0.1073	0.2557	0.6626	2.0254
U233T	alpha	0.0674	0.1927	0.1383	0.2798	0.1128	0.2091
	lambda	0.0129	0.0333	0.1163	0.2933	0.7943	2.3751
U233F	alpha	0.0859	0.2292	0.1781	0.3516	0.1142	0.0409
	lambda	0.0129	0.0347	0.1193	0.2862	0.7877	2.4417
U233H	alpha	0.0900	0.2007	0.1912	0.3684	0.1090	0.0405
	lambda	0.0128	0.0378	0.1271	0.2981	0.8543	2.5314
U234F	alpha	0.0550	0.1964	0.1803	0.3877	0.1324	0.0482
	lambda	0.0131	0.0337	0.1210	0.2952	0.8136	2.5721
U234H	alpha	0.0808	0.1880	0.1791	0.3888	0.1212	0.0420
	lambda	0.0128	0.0364	0.1256	0.2981	0.8475	2.5696
U235T	alpha	0.0380	0.1918	0.1638	0.3431	0.1744	0.0890
	lambda	0.0133	0.0325	0.1219	0.3169	0.9886	2.9544
U235F	alpha	0.0350	0.1807	0.1725	0.3868	0.1586	0.0664
	lambda	0.0133	0.0327	0.1208	0.3028	0.8495	2.8530
U235H	alpha	0.0458	0.1688	0.1769	0.4079	0.1411	0.0595
	lambda	0.0131	0.0356	0.1246	0.2962	0.8260	2.6575
U236F	alpha	0.0302	0.1722	0.1619	0.3841	0.1775	0.0741
	lambda	0.0134	0.0322	0.1202	0.3113	0.8794	2.8405
U236H	alpha	0.0438	0.1540	0.1719	0.4018	0.1578	0.0707
	lambda	0.0131	0.0333	0.1252	0.3030	0.8802	2.8167
U237F	alpha	0.0178	0.1477	0.1445	0.3864	0.2095	0.0941
	lambda	0.0138	0.0316	0.1211	0.3162	0.9073	3.0368

TABLE I (Cont.)

U238F	alpha	0.0139	0.1128	0.1310	0.3851	0.2540	0.1031
	lambda	0.0136	0.0313	0.1233	0.3237	0.9060	3.0487
U238H	alpha	0.0195	0.1184	0.1490	0.3978	0.2081	0.1072
	lambda	0.0135	0.0320	0.1214	0.3142	0.9109	3.0196
Np237F	alpha	0.0400	0.2162	0.1558	0.3633	0.1659	0.0589
	lambda	0.0133	0.0316	0.1168	0.3006	0.8667	2.7600
Np237H	alpha	0.0326	0.1571	0.1589	0.3929	0.1789	0.0796
	lambda	0.0133	0.0322	0.1211	0.2933	0.8841	2.7922
Np238F	alpha	0.0216	0.1845	0.1519	0.3760	0.1861	0.0798
	lambda	0.0136	0.0308	0.1189	0.3077	0.8988	2.9676
Pu238F	alpha	0.0377	0.2390	0.1577	0.3562	0.1590	0.0504
	lambda	0.0133	0.0312	0.1162	0.2888	0.8561	2.7138
Pu239T	alpha	0.0306	0.2623	0.1828	0.3283	0.1482	0.0479
	lambda	0.0133	0.0301	0.1135	0.2953	0.8537	2.6224
Pu239F	alpha	0.0363	0.2364	0.1789	0.3267	0.1702	0.0515
	lambda	0.0133	0.0309	0.1134	0.2925	0.8575	2.7297
Pu239H	alpha	0.0678	0.1847	0.1553	0.3685	0.1750	0.0487
	lambda	0.0129	0.0353	0.1215	0.2885	0.8486	2.5587
Pu240F	alpha	0.0320	0.2529	0.1508	0.3301	0.1795	0.0547
	lambda	0.0133	0.0305	0.1152	0.2974	0.8477	2.8796
Pu240H	alpha	0.0534	0.1812	0.1533	0.3715	0.1849	0.0558
	lambda	0.0130	0.0329	0.1191	0.2918	0.8462	2.7080
Pu241T	alpha	0.0167	0.2404	0.1474	0.3430	0.1898	0.0627
	lambda	0.0137	0.0299	0.1136	0.3078	0.8569	3.0800
Pu241F	alpha	0.0180	0.2243	0.1426	0.3493	0.1976	0.0682
	lambda	0.0136	0.0300	0.1167	0.3069	0.8701	3.0028
Pu242F	alpha	0.0196	0.2314	0.1256	0.3262	0.2255	0.0716
	lambda	0.0136	0.0302	0.1154	0.3042	0.8272	3.1372
Am241T	alpha	0.0305	0.2760	0.1531	0.3122	0.1825	0.0457
	lambda	0.0133	0.0300	0.1145	0.2949	0.8818	2.6879
Am241F	alpha	0.0355	0.2540	0.1563	0.3364	0.1724	0.0454
	lambda	0.0133	0.0308	0.1130	0.2868	0.8654	2.6430
Am241H	alpha	0.0740	0.1757	0.1754	0.3589	0.1783	0.0377
	lambda	0.0129	0.0346	0.1267	0.3051	0.9536	3.3205
Am242mT	alpha	0.0247	0.2659	0.1512	0.3337	0.1756	0.0489
	lambda	0.0135	0.0301	0.1152	0.2994	0.8646	2.8107
Am243F	alpha	0.0234	0.2945	0.1537	0.3148	0.1656	0.0480
	lambda	0.0135	0.0298	0.1138	0.2986	0.8820	2.8111
Cm242F	alpha	0.0763	0.2847	0.1419	0.2833	0.1763	0.0375
	lambda	0.0130	0.0312	0.1129	0.2783	0.8710	2.1969
Cm245T	alpha	0.0222	0.1788	0.1672	0.3706	0.2054	0.0559
	lambda	0.0134	0.0307	0.1130	0.3001	0.8340	2.7686
Cf249T	alpha	0.0246	0.3919	0.1349	0.2598	0.1614	0.0273
	lambda	0.0135	0.0294	0.1053	0.2930	0.8475	2.4698
Cf251T	alpha	0.0055	0.3587	0.1736	0.2693	0.1688	0.0242
	lambda	0.0157	0.0288	0.1077	0.3246	0.8837	2.6314
Cf252S	alpha	0.0124	0.3052	0.1813	0.2992	0.1729	0.0290
	lambda	0.0136	0.0291	0.1068	0.3024	0.8173	2.6159
Es254T	alpha	0.0073	0.3148	0.1547	0.2788	0.2010	0.0435
	lambda	0.0194	0.0289	0.1048	0.3185	0.8332	2.7238
Fm255T	alpha	0.0060	0.4856	0.1766	0.1940	0.1160	0.0218
	lambda	0.0149	0.0287	0.1027	0.3130	0.8072	2.5768

In this table T, F, and H, refer to fission neutron incident energies of thermal, fast, and high energy and S refers to spontaneous fission.

Having determined the six-group parameters for each fissioning nuclide, the next logical step was to calculate a consistent set of six-group spectra.

Equation (1) is the mathematical representation of delayed neutron activity following a fission pulse. The physical representation using the individual fission-product precursor data is (ignoring coupling)

$$n_d(t) = \sum_{j=1}^{271} \lambda_j \, Pn_j \, YI_j \, e^{-\lambda_j t} , \qquad (2)$$

where YI_j is the direct fission yield of nuclide j and Pn_j is its emission probability.

Both Eqs. (1) and (2) describe the delayed neutron activity per fission following a pulse and should be equivalent. In the present evaluation, it is required that

$$A_i e^{-\lambda_i t} = \sum_k f_{k,i} \, \lambda_k \, Pn_k \, YI_k \, e^{-\lambda_k t} , \qquad (3)$$

where the subscript i represents mathematical group i, the summation is over all precursors contributing to group i, and $f_{k,i}$ is the fraction of delayed neutrons produced by precursor k that contribute to group i. It is assumed that the fission-product precursor may contribute to either or both of the adjacent mathematical groups determined by the decay constants. [Previous analyses of individual precursor data, with respect to its reduction to the six-group representation, simply assigned each precursor to a particular group based on either halflife or λ bounds.[6,14]] The sum of $f_{k,i}$ for any k must be unity. These fractions were determined by requiring the least-squares error

$$\int_0^\infty \left\{ \lambda_k e^{-\lambda_k t} - \left[f_{k,i} \, \lambda_i \, e^{-\lambda_i t} + (1 - f_{k,i}) \, \lambda_{i+1} \, e^{-\lambda_{i+1} t} \right] \right\}^2 dt \qquad (4)$$

to be a minimum.[13,15] A modification of Newton's method was used to return the minimum of Eq. (4). The equilibrium group spectra were then found as

$$\Phi_i(E) = \sum_k f_{k,i} \, YC_k \, Pn_k \, \phi_k(E) , \qquad (5)$$

where $\phi_k(E)$ is the normalized delayed neutron spectrum of precursor k and YC_k is the cumulative yield from fission for precursor k. The normalized six-group spectra for ^{235}U fast and thermal fission are given in Figs. 3-8 over a 1-MeV energy range in comparison with the six-group spectra taken from ENDF/B-V for ^{235}U. Differences between our thermal and fast spectra are much less than those with the ENDF/B-V evaluation. All spectra are normalized such that the integral over 1 MeV is unity in these comparisons.

Using the method outlined above, the group-one spectrum shown in Fig. 3, has three contributing precursor nuclides. The precursor ^{87}Br contributes 100% of its delayed neutrons to group one, as is expected; however, two additional precursors, ^{137}I and ^{141}Cs contribute about 20% of their delayed neutrons to group one. This result allows the group one spectrum to change for different fissioning systems, as suggested by ENDF/B-V data.

Precursor and group spectra are in energy bins of 10 keV for up to 300 groups. In some applications[11] we have used the same bin structure to > 8.5 Mev, but these calculations did not use temporal groups.

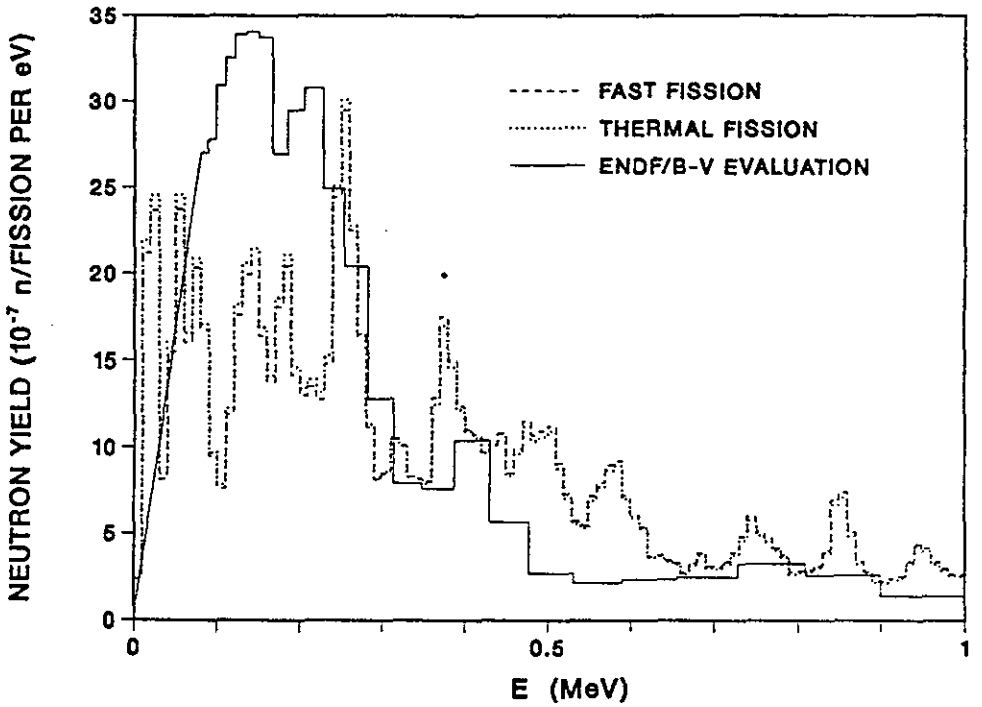

Fig. 3. Group 1 normalized ν_d spectra ^{235}U.

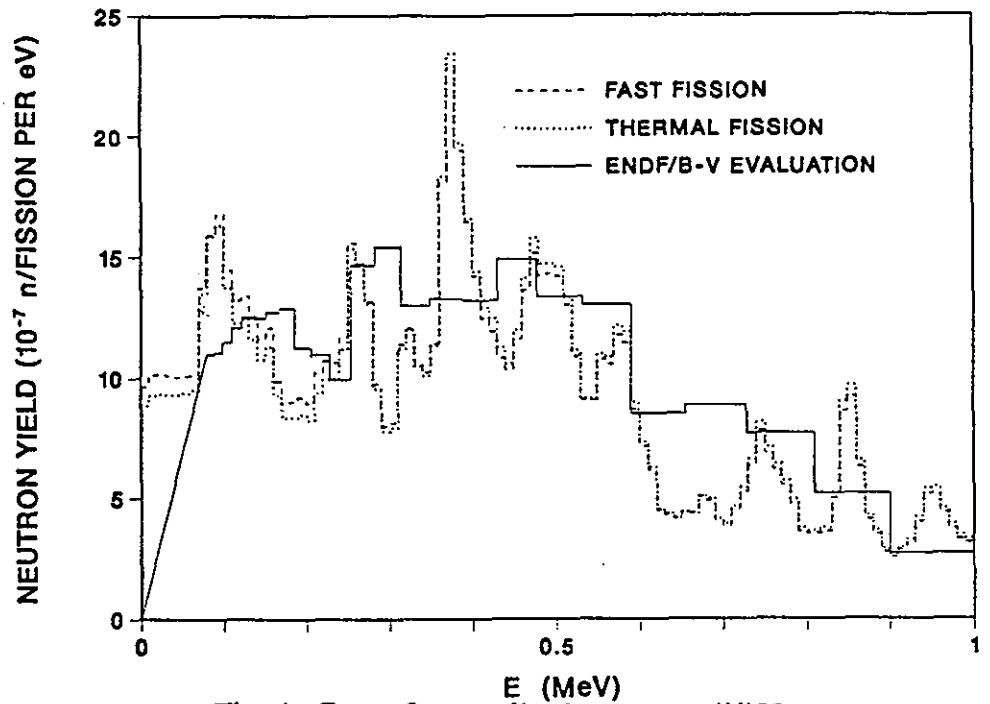

Fig. 4. Group 2 normalized ν_d spectra ^{235}U.

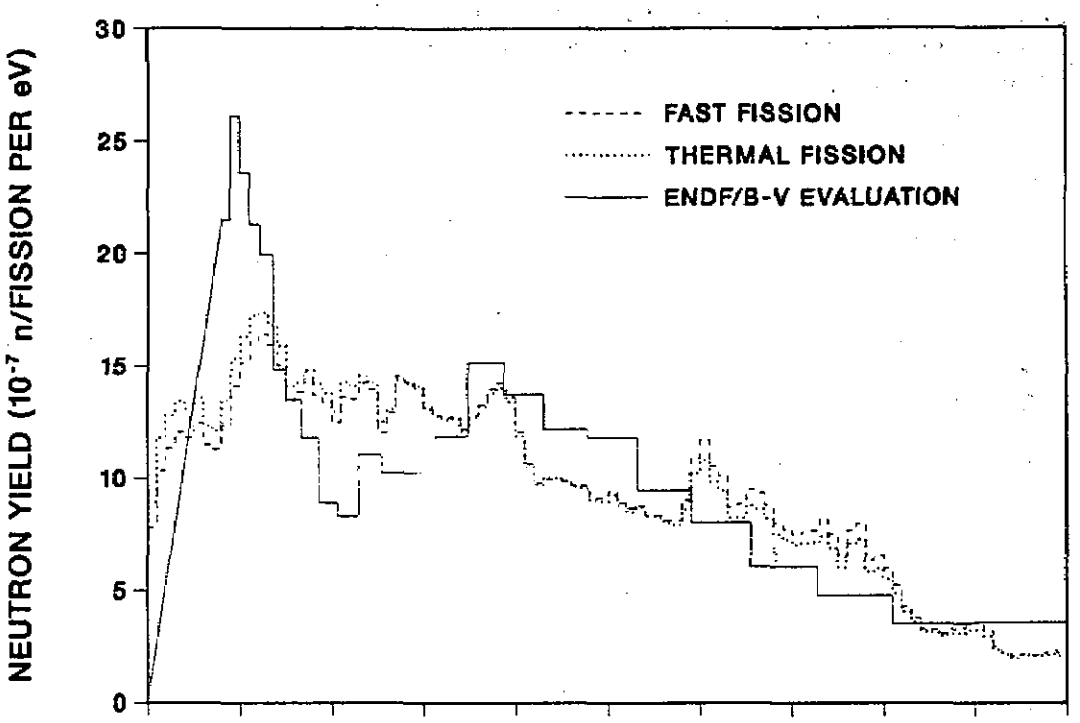

Fig. 5. Group 3 normalized ν_d spectra ^{235}U.

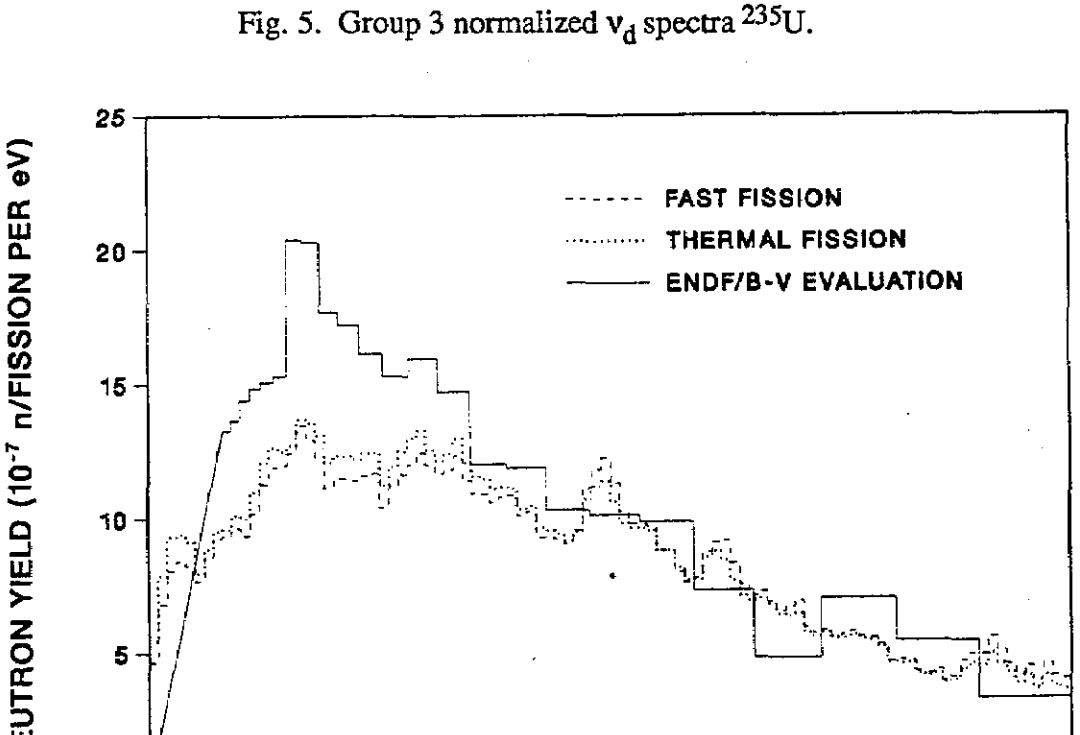

Fig. 6 Group 4 normalized ν_d spectra ^{235}U.

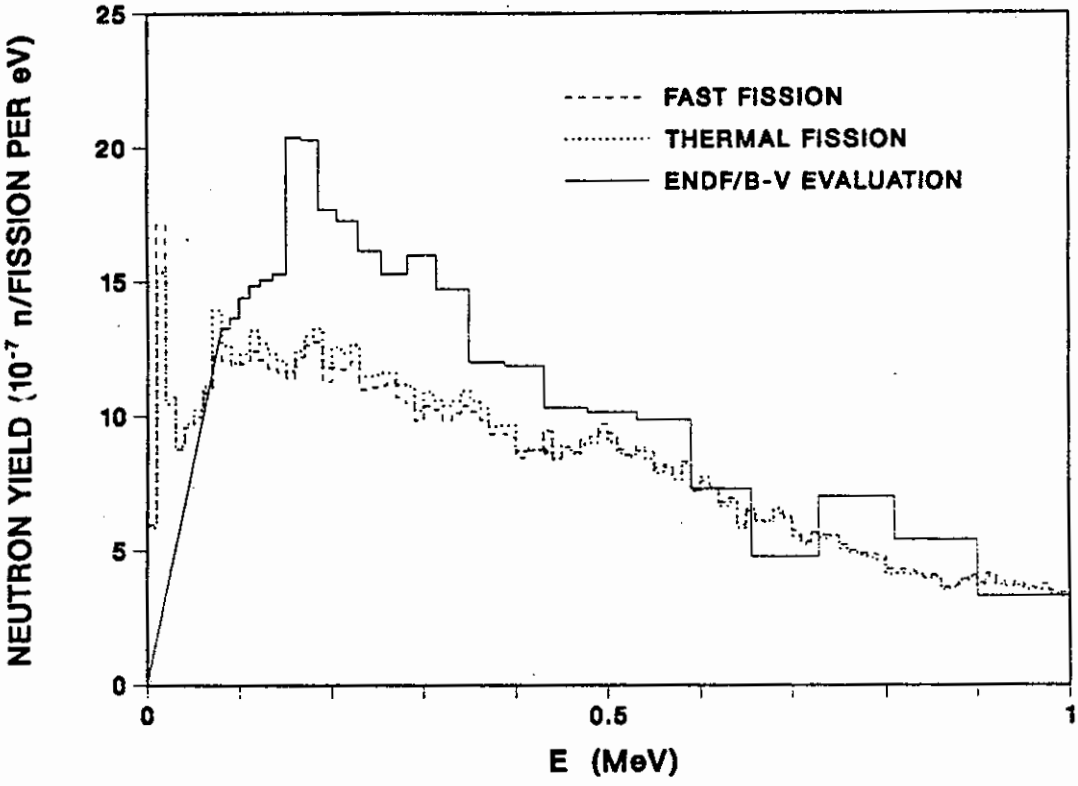

Fig. 7. Group 5 normalized ν_d spectra ^{235}U.

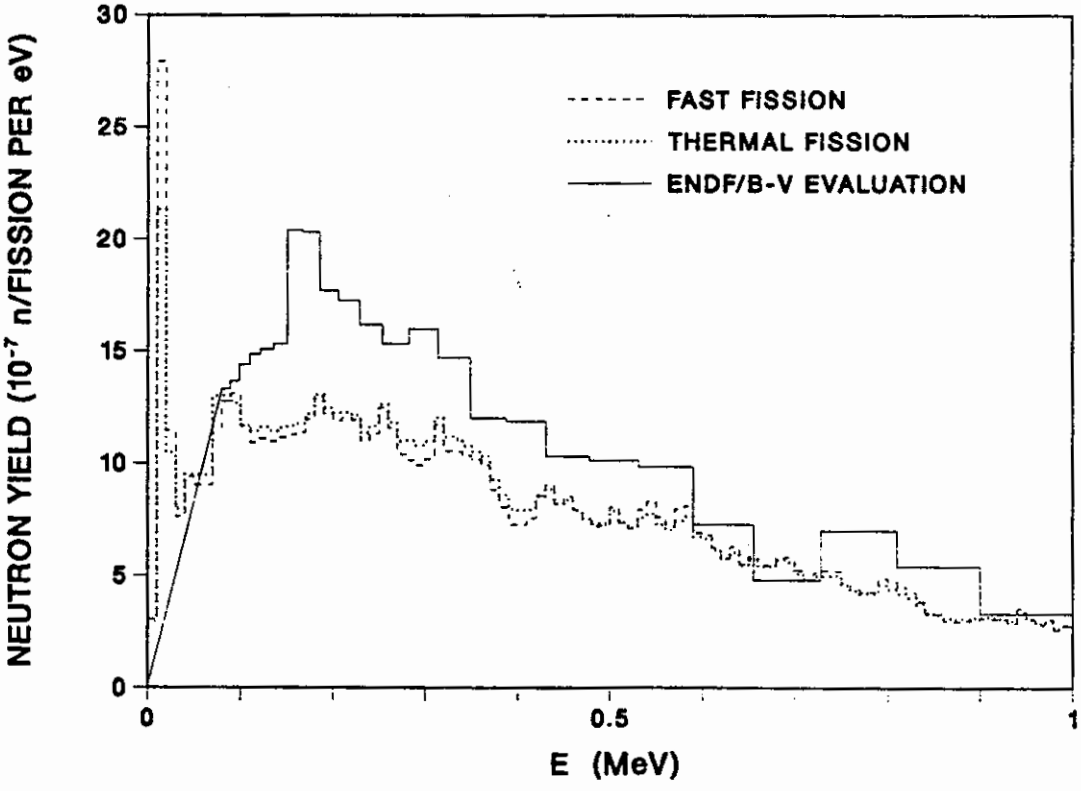

Fig. 8. Group 6 normalized ν_d spectra ^{235}U.

APPLICATIONS OF THE GROUP DATA

The accuracy of the six-group parameters is difficult to quantify as it is influenced by not only the uncertainties included in the basic data that was used in calculating the delayed neutron activity curves (i.e., the direct fission yields, halflives, and emission probabilities) but also by the uncertainty introduced by the least-squares fit to that data. Likewise, the calculation of the uncertainties for the group spectra is not straightforward because of the method used to calculate the fractional contribution from each precursor to the various groups.

A reasonable check on the group abundances and decay constants would be to use them in a point kinetics calcuation. These calculations were performed for step changes in reactivitiy in a $^{235}U(F)$ system and the results are given in Fig 9. The point kinetics equations were modified[13,16] for the calculation using the explicit precursor data. A total of 386 nuclides were required in that calcuation to include the 271 percursors and their parents. Agreement of the fitted six-groups with the explicit calculations is very good. The results using the ENDF/B-V six-group parameters is also given for comparison; the number of delayed neutrons produced is constant for all cases.

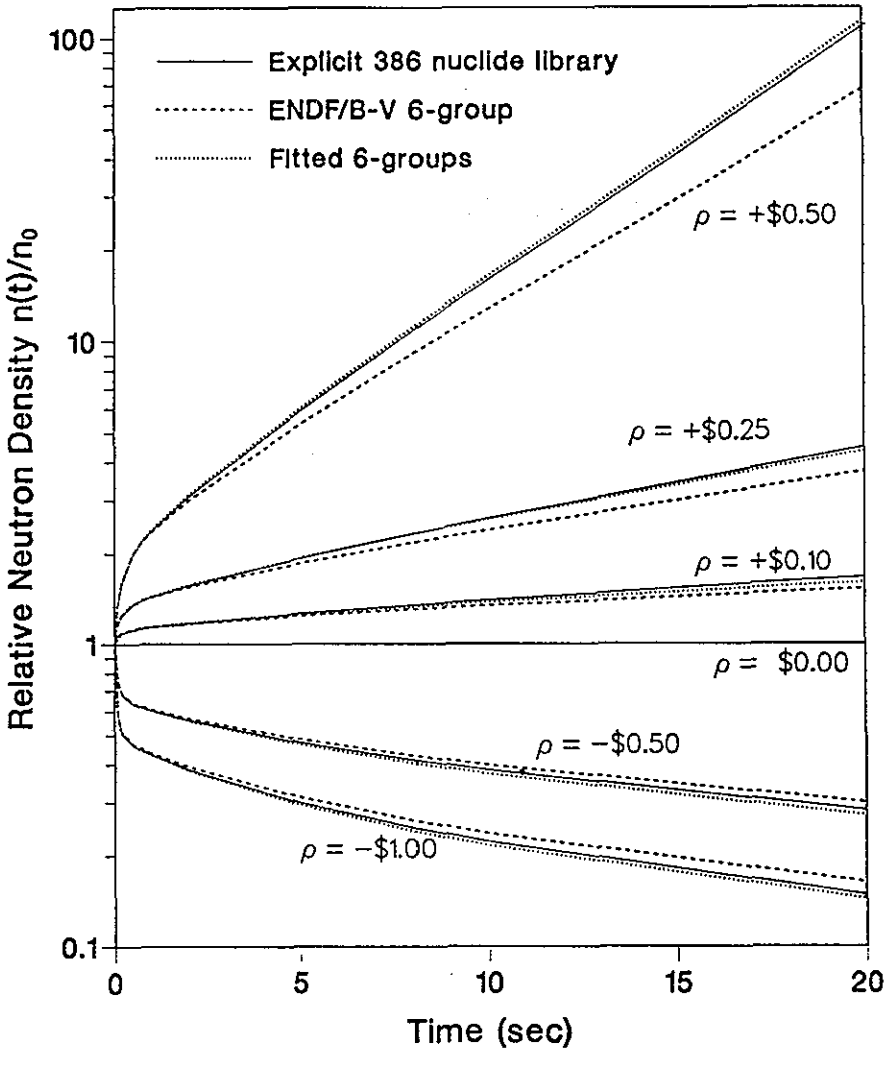

Fig. 9. Calculated neutron density following step reactivity (ρ) inputs for ^{235}U fast fission.

14320205

Rossi-alpha (β_{eff}/generation time) calculations were performed to insure that the group spectra produce results which are consistent with those using the aggregate spectra derived from the individual precursor data. The one-dimensional transport theory code, ONEDANT[18] was used to model a Godiva reactor (a bare sphere of enriched ^{235}U metal) and to calculate the fluxes and adjoint fluxes needed for the perturbation calculation. This was accomplished with a modified version of the PERT-V code[19] which uses first order perturbation theory based on the multigroup diffusion model and calculates the effective delayed neutron fraction, β_{eff}, and the mean generation time. The PERT-V code allows the user to input either a single delayed neutron spectrum or individual group spectra, the results for Rossi-alpha, α_{DC}, calculated using each of these options are given below:

Aggregate Spectrum	-1.1185×10^6 s^{-1}
Six-Group Spectra	-1.1123×10^6 s^{-1}.

The perturbation calculations were performed using the six-group decay constants and fractional abundances for $^{235}U(F)$ from Table I, and a total delayed neutron yield of 0.0167 neutrons per fission, which is the value recommended in ENDF/B-V.

The measured value of α_{DC} noted in the Cross Section Evaluation Working Group Benchmard Specifications (BNL 19302), Fast Reactor Benchmark No. 5 is $-(1.11 \pm 0.02) \times 10^6$ s^{-1}. The ratio of the six-group result to the experiment is 1.0020 and that using the aggregate spectrum is 1.0076. These results are in excellent agreement and provide an adequate support of the methods used to derive the six-group spectra.

SUMMARY

An evaluated library for 271 delayed neutron precursors has been completed. Six-group parameters and spectra have been calculated for 43 fissioning systems that are consistent with the explicit precursor results. Although some disagreement with the ENDF/B-V is observed, the major improvement has been in the delayed neutron group spectra and in data produced for unmeasured systems. ENDF/B-V contains six group spectra for only seven fissioning nuclides and these are in a very coarse bin structure that extends only to about 1.2 MeV, whereas the present group spectra cover 28 fissioning nuclides in a fine 10 -keV energy bin structure and extend to 3.0 MeV (the maximum range of the experimental data for any precursor). The normalized spectra, and the group constants to a lesser degree, appear to be nearly independent of the incident neutron energy and therefore the $\bar{\nu}_d$ data recommended for inclusion in ENDF/B-VI contain only one set of group constants and spectra (usually that of the fast system) for each of the 28 fissioning nuclides. The delayed neutron yields are a function of incident neutron energy, especially for high energy (14-MeV) fission and are given as they were in ENDF/B-V. The actual values for $\bar{\nu}_d$ recommended for ENDF/B-VI, but not the abundances or spectra, are those taken from the previous ENDF/B-V evaluation[17] or newly evaluated measurements. Nuclides with no reported measurement of $\bar{\nu}_d$ in the literature were assigned the calculated values. We have presented some results related to β_{eff} and point kinetics; these were primarily used to check the validity of the precursor and group data.

ACKNOWLEDGMENTS

We greatly appreciate the direct assistance and communications with F. M. Mann, R. E. Schenter, C. W. Maynard, W. B. Wilson, R. T. Perry, T. Parish, R. J. LaBauve, E. D. Arthur, D. C. George, G. Rudstam, and K. -L. Kratz.

REFERENCES

1. G. R. KEEPIN, *Physics of Nuclear Kinetics*, Addison-Wesley Publishing Co. (1956).

2. T. R. ENGLAND and B. F. RIDER, "Status of Fission Yield Evaluations," R. E. Chrien and T. W. Burrows, Eds., Proc. NEANDC Specialists' Meet. on Yields and Decay Data for Fission Product Nuclides, Brookhaven National Laboratory, Upton, N.Y., October 24-27, 1983 (Brookhaven National Laboratory report BNL 51778). [These data have recently been updated through 1987 for ENDF/B-VI by B. F. Rider and T. R. England.

3. P. L. REEDER, R. A. WARNER, R. GILL, and A. PIOTROWSKI, "Pn Measurements at TRISTAN by a Beta-N Coincidence Technique," Proc. Specialists' Meet. on Delayed Neutrons, Univ. of Birmingham, Birmingham, England, September 15-19, 1986.

4. F. M. MANN, M. SCHREIBER, R. E. SCHENTER, and T. R. ENGLAND, "Evaluation of Delayed-Neutron Emission Probabilities," *Nucl. Sci. Eng.* **87**, 418 (1984); also see update by F. M. Mann in Proc. of Specialists' Meet. on Delayed Neutrons, Univ. of Birmingham, England, September 15-19, 1986.

5. K. -L. KRATZ and G. HERRMANN, "Systematics of Neutron Emission Probabilities from Delayed Neutron Precursors," *Z. Physik* **263,** 435 (1973).

6. G. RUDSTAM, "Six-Group Representations of the Energy Spectra of Delayed Neutrons from Fission," *Nucl. Sci. Eng. 80*, 238 (1982) (Private communication of spectra, 1981).

7. K. -L. KRATZ, "Review of Delayed Neutron Energy Spectra," Proc. Consultants Meet. on Delayed Neutron Properties, Vienna, Austria, March 26-30, 1979 (International Atomic Energy Agency report INDCNDS-107/G+Special (1979). (Private communication of spectra, 1983).

8. R. C. GREENWOOD and A. J. CAFFREY, "Delayed-Neutron Energy Spectra of $^{93\text{-}97}$Rb and $^{143\text{-}145}$Cs," *Nucl. Sci. Eng.* **91**, 305 (1985).

9. T. R. ENGLAND, M. C. BRADY, E. D. ARTHUR, and R. J. LABAUVE, "Status of Evaluated Precursor and Aggregate Spectra," Presented at Specialists' Meet. on Delayed Neutrons, Birmingham, England, September 15-19, 1986 (see also Los Alamos informal document LA-UR-86-1983).

10. F. M. MANN, C. DUNN, and R. E. SCHENTER, "Beta Decay Properties Using a Statistical Model," *Phys. Rev. C* **25**, 1524 (1982).

11. T. R. ENGLAND, E. D. ARTHUR, M. C. BRADY, and R. J. LABAUVE, "Background Radiation from Fission Pulses," Los Alamos National Laboratory report LA-11151-MS (February 1988) [Data summary in Trans. Am. Nucl. Soc. *54*, 349 (1987)].

12. M. C. BRADY, "Evaluation and Application of Delayed Neutron Precursor Data," doctoral dissertation, Texas A & M University (August 1988) [to be published as a Los Alamos report (thesis series)].

14320207

13. M. C. BRADY and T. R. ENGLAND, "Few-Group Representation of the Energy Spectra of Delayed Neutrons," *Trans. Am. Nucl. Soc.* **54**, 341 (1987).

14. T. R. ENGLAND, W. B. WILSON, R. E. SCHENTER, and F. M. MANN, "Aggregate Delayed Neutron Intensities and Spectra Using Augmented ENDF/B-V Precursor Data," *Nucl. Sci. Eng.* **85**, 139 (1983).

15. D. SAPHIER, D. ILBEY, S. SHALEV, and S. YIFTAH, "Evaluated Delayed Neutron Spectra and their Importance in Reactor Calculations," *Nucl. Sci. Eng.* **62**, 660 (1977).

16. M. C. BRADY, T. R. ENGLAND, and W. B. WILSON, "Few Group Analysis of Current Delayed Neutron Data," *Trans. Am. Nucl. Soc.* **53**, 469 (1986).

17. SAMSON A. COX, "Delayed Neutron Data-Review and Evaluation, Argonne National Laboratory report ANL/NDM-5 (April 1974). [For ENDF/B-V, these data were updated, but unpublished, by R. E. Kaiser and S. G. Carpenter, Argonne Nat. Lab.-West.]

18. R. DOUGLAS O'DELL, F. W. BRINKLEY, JR., DUANE R. MARR, "User's Manual for ONEDANT; A Code Package for One-Dimensional, Diffusion-Accelerated, Neutral-Particle Transport," Los Alamos National Laboratory manual LA-9184-M (Feb. 1982).

19. D. C. GEORGE and R. J. LABAUVE, "PERTV-A Standard File Version of the PERT-V Code," Los Alamos National Laboratory report LA-11206-MS (Feb. 1988). [Original report prepared by R. W. Hardie and W. W. Little, Jr., BNWL-1162 (Sept. 1969)].

B.2.4
for information

MEASUREMENTS OF DELAYED NEUTRON ENERGY SPECTRA FOR ^{235}U, ^{238}U AND ^{239}Pu

G.P. Couchell, P.R. Bennett, M.H. Haghighi, E.S. Jacobs, D.J. Pullen, W.A. Schier, Q. Sharfuddin, R.S. Tanczyn and M.F. Villani

Department of Physics and Applied Physics
University of Lowell, Lowell, Massachussetts 01854

ABSTRACT

Delayed neutron (DN) energy spectra have been measured as a function of delay time after fission for ^{235}U, ^{238}U and ^{239}Pu using a helium jet transfer system for fission product transfer. DN equilibrium spectra were also measured for all three nuclides. Beta-neutron correlations were used for background suppression and for energy determination by the neutron time-of-flight method. Each spectrum spans a DN range of 0.01 - 4.00 MeV. The ^{235}U and ^{239}Pu spectra show marked similarity, while those from the fast fission of ^{238}U are considerably more energetic. DN six-group spectra for ^{235}U and ^{239}Pu have been deduced from these measurements using a constrained least-squares iterative method.

INTRODUCTION

Composite (aggregate) delayed neutron (DN) energy spectra have been measured as a function of delay time following thermal fission of ^{235}U and ^{239}Pu and fast fission of ^{238}U. In separate measurements, DN equilibrium spectra were also determined for the same three nuclides. A major objective of this program was to contribute to the DN data base used to calculate neutron effectiveness in reactor kinetics and control analysis, particularly for fast breeder and space reactor systems.[1-3]

Two approaches are commonly used in DN spectral studies. One involves measurements of DN spectra from individual precursors, while the other is the direct measurement of composite DN spectra containing contributions from all precursors decaying within specific time intervals after fission. Although energy spectra from most major DN contributors have now been measured, the spectra of 65% of the 105 identified precursors[4] have yet to be studied. In terms of the Keepin six DN groups,[5] the measured precursors account for practically all the yield of groups 1-3. However, unmeasured precursors are significant for groups 4-6, particularily for group 5 where less than half the DN yield is accounted for by precursors having measured spectra.[6]

The direct measurement of composite DN spectra avoids the uncertainties associated with combining many individual precursor spectra to produce DN spectra useful for reactor studies. Previous composite measurements,[7-10] however, have not included delay time intervals less than 1s and so have not been very sensitive to DN groups 5 and 6. Because composite measurements offer the most immediate

possibility of determining DN spectra useful for reactor analysis, we designed a system incorporating a helium jet for rapid transport of fission fragments which allows measurement of composite DN spectra for delay times ranging from less than 0.2s (0.1s for equilibrium measurements) to well over a minute.

For reactor kinetics calculations it is useful to approximate the time evolution of the measured spectra using the Keepin six-group approach. To deduce six-group energy spectra from the measurements, we have developed a constrained least-squares iterative analysis procedure that results in solutions that are well behaved and essentially unique.

EXPERIMENTAL TECHNIQUE

The University of Lowell DN system[11] combines a helium-jet and tape transport system with an isolated neutron time-of-flight (TOF) spectrometer. Fission products are sprayed onto a continuously moving tape which transports them to the spectrometer for determining the flight time of each neutron and thus its energy. The possible emission of a neutron is signaled by the detection of a beta particle which must always precede it. Since the spectrometer is activated by neutron-beta coincidences, the delay time after fission is controlled by passing the tape bearing the fission products in front of two well collimated beta detectors. The delay-time intervals are determined by the selected tape speed, the distance between each beta detector and the position on the tape of the helium-jet spray-on point. Fission products are produced continuously using either our 5.5 MeV Van de Graaff accelerator or 1-MW swimming pool reactor as a neutron source.

A schematic diagram of the experimental arrangement for accelerator measurements is shown in Fig. 1. With this helium-jet/ tape-transport arrangement we have been able to make aggregate DN spectral measurements for a delay-time interval 0.17 - 0.37s for each of the fissionable nuclides investigated. The short initial time of the interval is indicative of the fast transfer time of about 0.12s of the helium jet. The 0.2-s width of the interval represents a convolution of the fission-chamber flush time with the time required for the tape to traverse the 2.3-cm width of the first beta detector. Following the first beta detector the tape passes before the second beta detector, 6.9 cm in width. This allows a second delay time interval, 0.41 - 0.85s, to be measured simultaneously with the 0.17 - 0.37s interval. In this fashion aggregate DN measurements can be made in nearly successive delay time intervals over the time range 0.17 - 85s, which includes >90% of all delayed neutrons emitted.

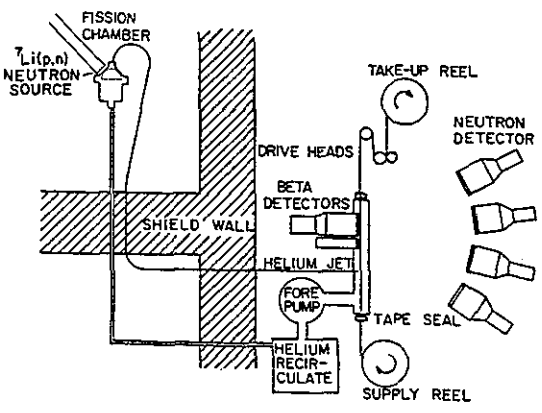

Fig. 1. Schematic of the experimental arrangement.

To span a broad energy range, 0.01 - 4.00 MeV, each DN spectrum was constructed from two separate measurements. Li-6 loaded glass scintillators were used to determine the spectrum in the region 0.01 - 0.30 MeV. The 0.15 - 4.00 MeV region of

the ^{235}U spectrum was measured with BC 501 liquid scintillators (some early spectra were measured with Pilot U plastic scintillators and spanned the region 0.15 - 2.00 MeV). Pulse-shape analysis was used for gamma-ray suppression with both Li-6 and BC 501 scintillators.

Typical DN neutron TOF spectra with BC 501 scintillators are shown in Fig. 2. Improved time (energy) resolution is achieved by dividing the spectrum into two parts, according to the pulse amplitude of the neutron detector signal. Each TOF spectrum is analyzed by 1) subtracting the random background and gamma peak, 2) subtracting the neutron detector

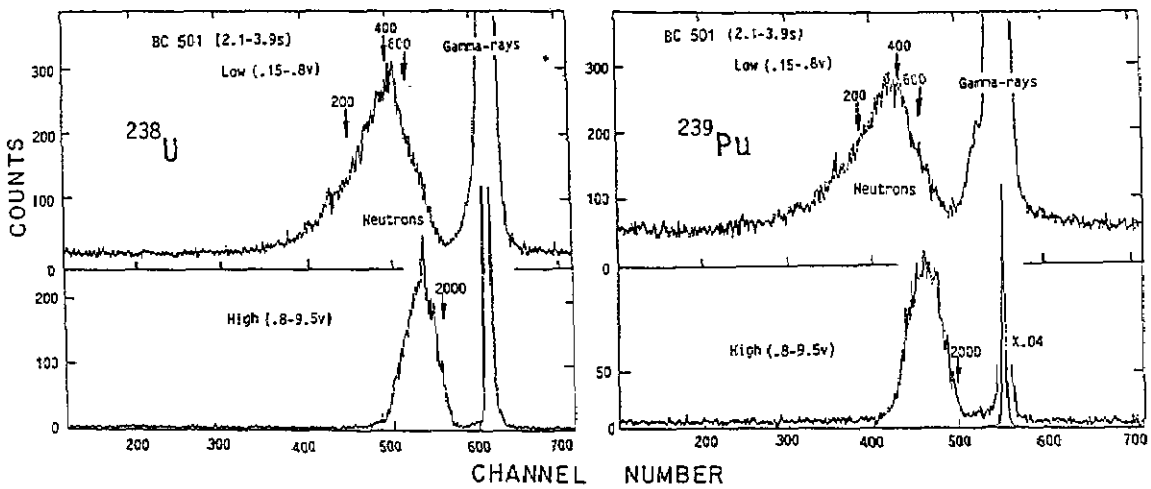

Fig. 2. Delayed neutron TOF spectrum measured in the 2.1 - 3.9s delay time interval for ^{238}U and ^{239}Pu. Each spectrum is divided into two pulse height ranges, 0.15 - 0.80 and 0.8 - 9.5 volts.

time-response tails, and 3) converting the result into an efficiency-corrected energy spectrum.[12] For each delay-time interval the BC 501 and Li-6 glass spectra are normalized to give the same area in the 150 - 400 keV region and then combined using linear-ramp weighting functions over the 150 - 250 keV energy region.

For the direct measurement of DN equilibrium spectra the tape and beta detector assembly were modified so as to exclude the tape transport delay. The modified arrangement is shown in Fig. 3. The fission products are transferred by the helium jet directly onto a slowly moving, thin KAPTAN tape at a position immediately in front of a 5-cm long beta scintillator. The

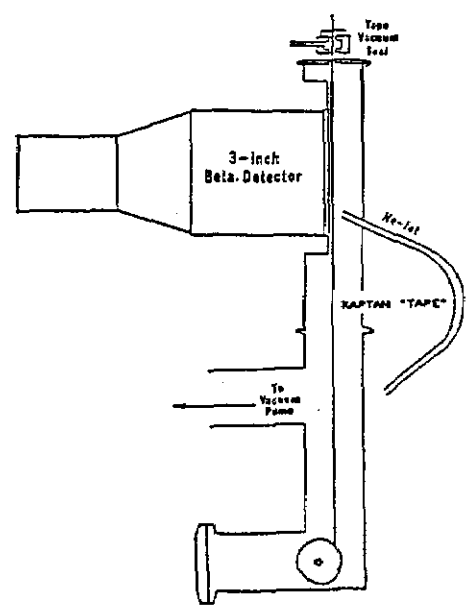

Fig. 3. Modified arrangement for transferring fission products in DN equilibrium spectrum measurements.

14320211

transfer time is now determined by the helium jet system alone and the tape speed can be adjusted to provide dwell times of up to 200s in front of the beta detector.

Whereas in our standard geometry the beta particles do not have to penetrate the tape to be detected, they do so in this modified geometry and KAPTAN was chosen to provide high transmission of the beta spectra. In a test study using the low-energy betas from a ^{14}C source, for example, 65% of its beta spectrum was detected after transmission though the tape, the effective beta cut-off energy being about 20 keV. Since most betas emitted are much more energetic than this the presence of the tape introduces negligible distortion to the equilibrium DN spectrum.

COMPOSITE DELAYED NEUTRON SPECTRA

The delay time intervals chosen for the measurements are given in Table I, which also shows the contributions of the six DN groups to each interval in the case of ^{239}Pu thermal fission. The ^{235}U and ^{238}U 6-group contributions are very similar. Composite DN energy spectra have been measured for delay time intervals 1 - 8 for ^{235}U, 1 - 7 for ^{239}Pu and 1-6 for ^{238}U. Equilibrium spectra have also been constructed for all three nuclides from these measurements. In addition, equilibrium spectra were directly measured using the modified experimental arrangement shown in Fig. 3.

Results of our study of DN spectra following thermal fission of ^{235}U have been previously reported.[13] The ^{235}U measurements were repeated for fission induced by fast neutrons. No significant differences were observed in the ^{235}U DN spectra resulting from thermal and fast fission.[14] We now present final results of our investigation of DN spectra from the thermal fission of ^{239}Pu and report on preliminary measurements from fast fission of ^{238}U.

TABLE I

Contributions (%) of six groups to delay-time intervals for ^{239}Pu thermal fission.*

Delay Interval (s)	Group					
	1	2	3	4	5	6
	$T_{1/2}$ (s)					
	52.1	23.0	6.11	2.35	0.81	0.26
1. 0.17 - 0.37	0.1	2.8	7.2	31.9	35.8	22.3
2. 0.41 - 0.85	0.2	3.7	9.3	38.8	35.8	12.3
3. 0.79 - 1.25	0.3	4.8	11.5	44.6	33.1	5.7
4. 1.2 - 1.9	0.3	6.1	14.1	49.8	27.7	2.0
5. 2.1 - 3.9	0.5	9.8	20.1	54.9	14.6	0.2
6. 4.7 - 10.2	1.3	22.4	32.1	42.5	1.7	0.0
7. 12.5 - 29.0	4.2	58.2	30.9	6.7	0.0	0.0
8. 35.8 - 85.5	11.3	84.9	3.8	0.0	0.0	0.0

* Based on group parameters of Ref. 18.

Thermal Fission of ^{235}U and ^{239}Pu

The spectra from ^{239}Pu are compared with our earlier measurements for ^{235}U in Fig. 4. The total counts in each spectrum have been normalized to 10^4. The two sets are remarkably similar, as has also been noted by Kratz and Gabelmann[15] in their composite measurements of these nuclides. The spectra have higher average energies than those derived from the ENDF/B-V six-group spectra,[16] with the largest discrepancy being about 80 keV for a delay time of about 1 second. Our results are in much better agreement with the composite spectra average energies measured by Kratz and Gabelmann.

Fast Fission of ^{238}U

Spectra have been obtained with BC 501 detectors (0.25 - 4.00 MeV) following fast fission of ^{238}U. Measurement with ^{6}Li-glass detectors (0.01 - 0.25 MeV) are currently in progress, with intervals 3 and 4 (Table I) so far completed. In Fig. 5 the two completed spectra for ^{238}U are compared with the corresponding ones for ^{239}Pu. Although some of the same structure persists in the two sets, the ^{238}U spectra are notably more energetic.

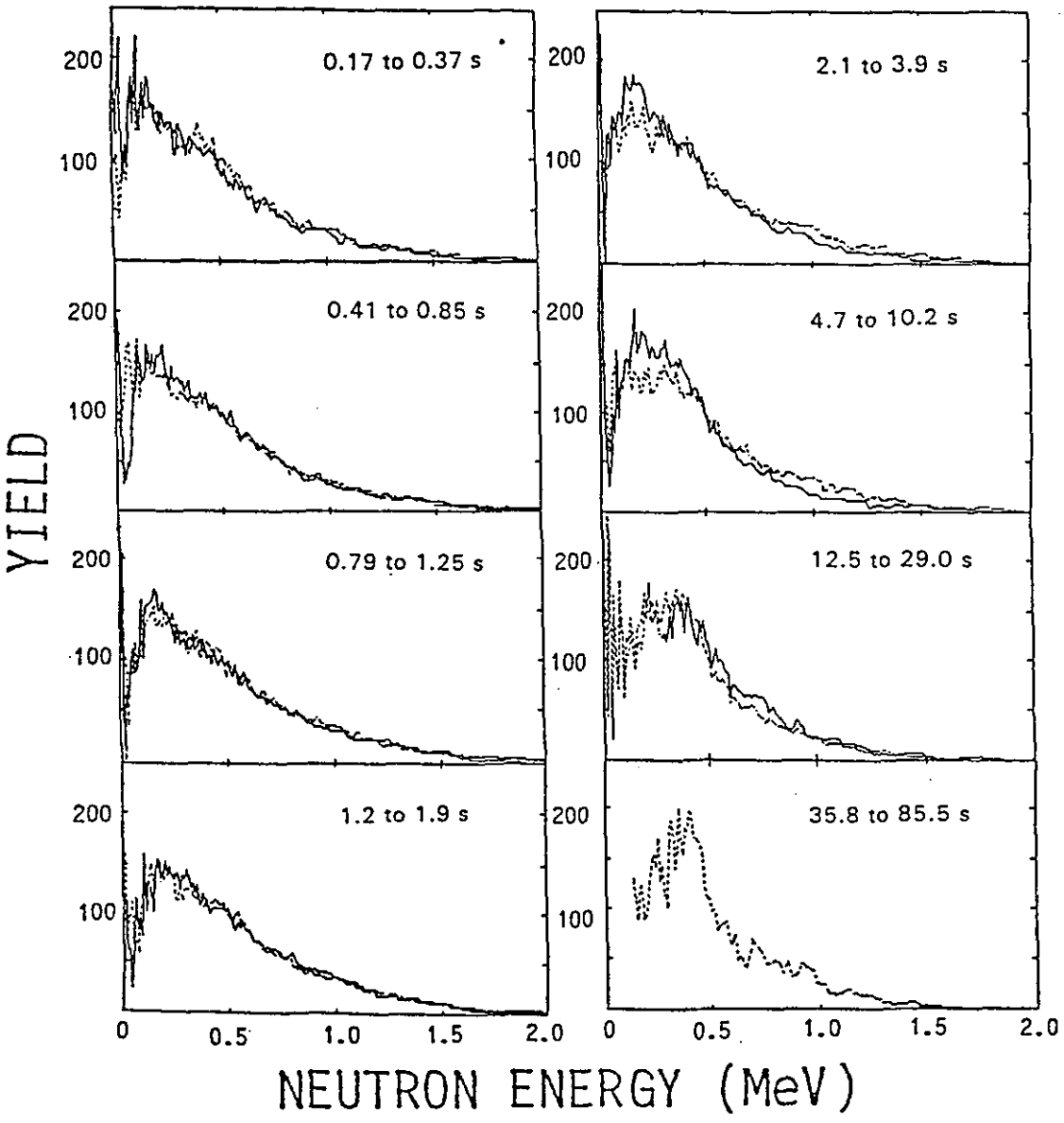

Fig. 4. Composite DN energy spectra from the thermal fission of ^{239}Pu (solid curves) compared with those from ^{235}U.

14320213

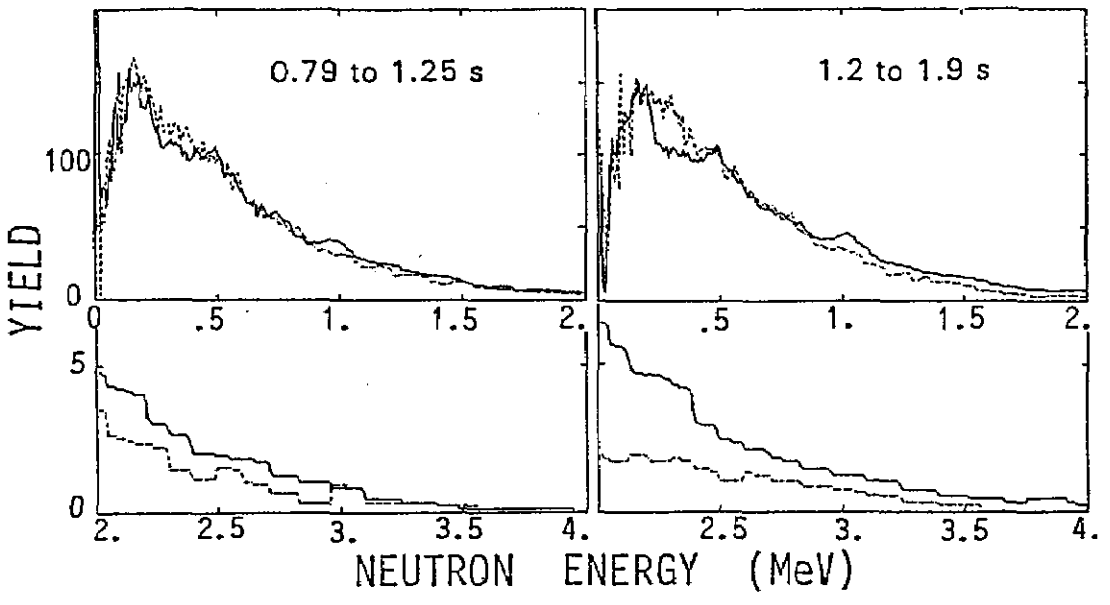

Fig. 5. Composite DN energy spectra from fast fission of ^{238}U (solid curves) compared with those from thermal fission of ^{239}Pu.

DN Equilibrium Spectra

The measured DN equilibrium spectra resulting from ^{235}U, ^{238}U and ^{239}Pu fission are shown for the energy range 0.01 - 4 MeV in Fig. 6. For comparison purposes the spectra are all normalized to the same (10^4) total yield. All three spectra display rather similar structures, although the ^{238}U spectrum is seen to be somewhat harder than that for either ^{235}U or ^{239}Pu. The average energy for the measured ^{238}U spectrum is some 70 keV higher than for ^{235}U and 125 keV higher than for ^{239}Pu.

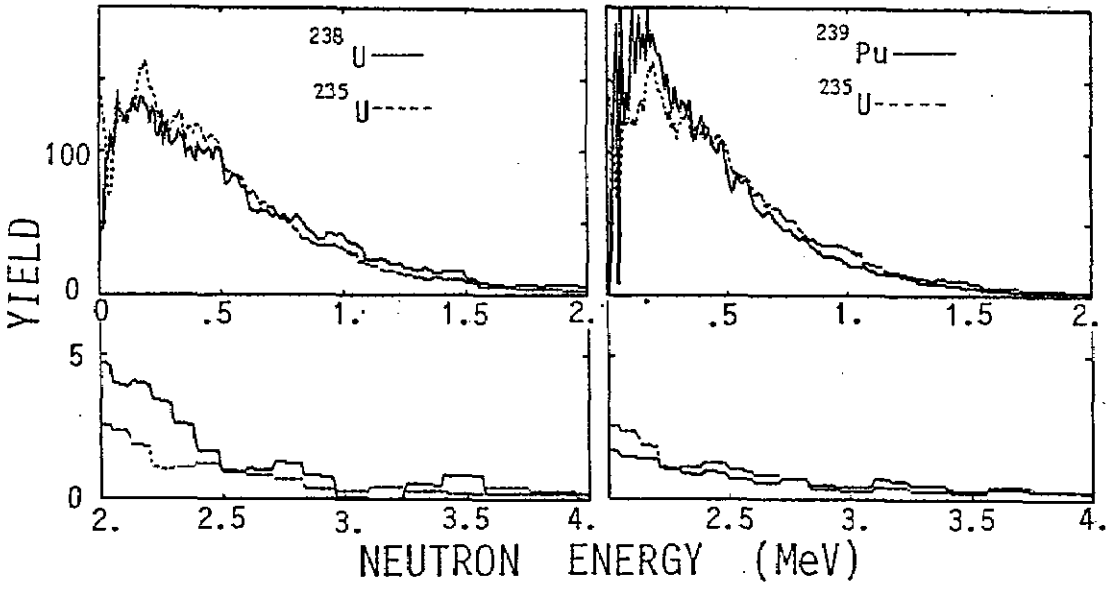

Fig. 6. Measured equilibrium DN energy spectra for ^{235}U ($\bar{E}_n$ = 520 keV), ^{238}U ($\bar{E}_n$ = 590 keV) and ^{239}Pu ($\bar{E}_n$ = 465 keV).

14320214

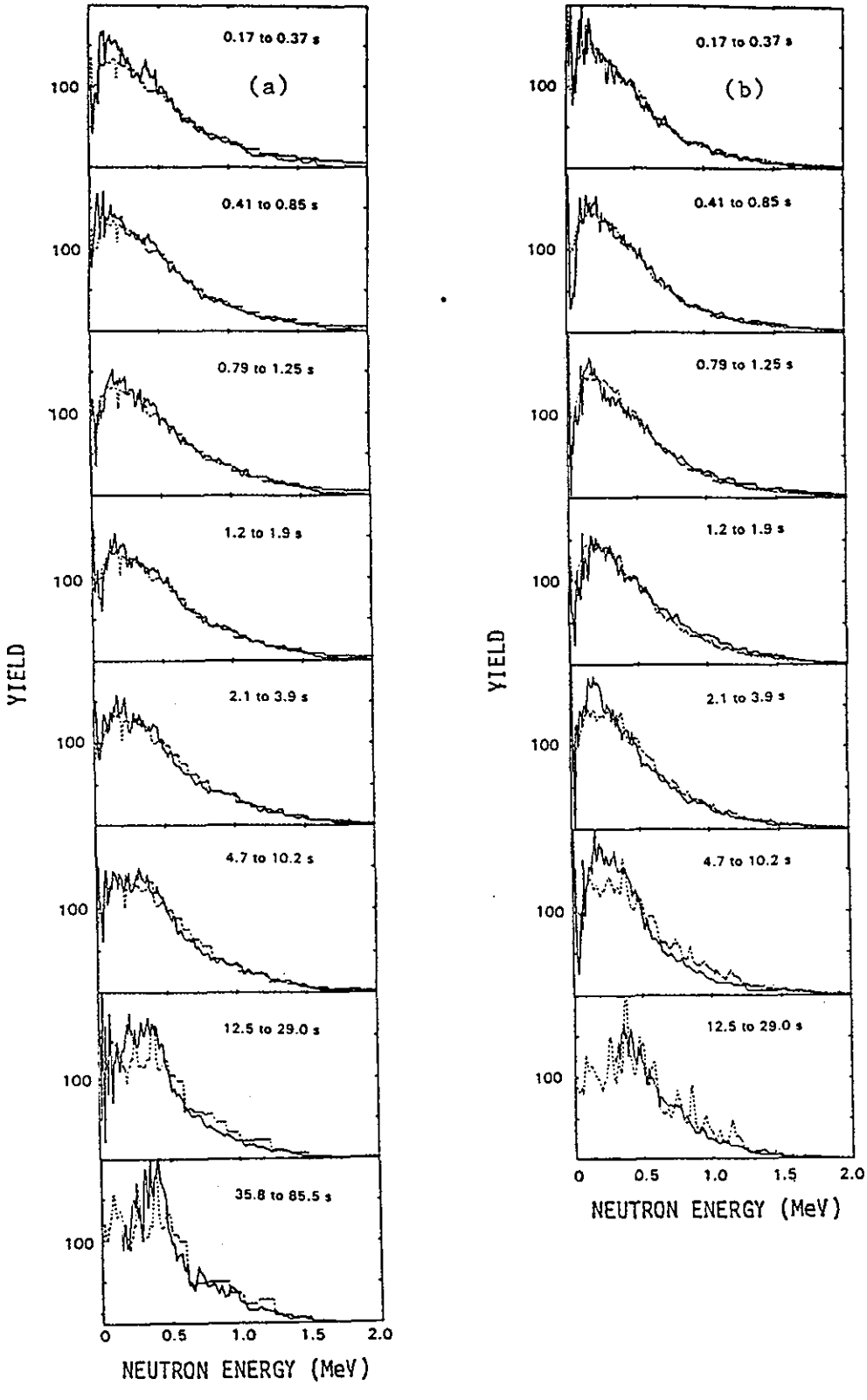

Fig. 7. Comparison of measured DN composite spectra (solid curves) with those deduced from individual precursor 6-group data (Ref. 18) for a) ^{235}U and b) ^{239}Pu.

14320215

We have also calculated equilibrium spectra from our aggregate time-dependent delayed neutron measurements.[17] The overall agreement between the directly measured and deduced equilibrium spectra is found to be very satisfactory for all three cases.

ANALYSIS AND DISCUSSION

It is interesting to compare composite DN spectra with those generated by summing the DN spectra from individual precursors. Individual precursor data, supplemented by theoretically calculated spectra for unmeasured precursors, were summed in a weighted fashion to generate 6-group DN spectra in a compilation provided to us by T.R. England.[18] The precursor 6-group spectra were then appropriately combined for comparison with our measured spectra. Such comparisons for ^{235}U and ^{239}Pu DN spectra are shown in Fig. 7 and for the measured equilibrium DN spectra in Fig. 8. The overall agreement is seen to be very good. Individual precursor data for ^{238}U were not available to us for making a similar comparison.

We have also deduced 6-group DN energy spectra from our measurements. Stable six-group solutions were obtained by applying a constrained least-squares fitting method[17] to composite DN spectra measured at six or more of the delay-time intervals shown in Table 1. The group spectra deduced for ^{235}U and ^{239}Pu are all physically reasonable and give excellent fits to the measured spectra. Because the sensitivity of the measurements is low for the delay group 1 (see Table I), its spectrum was treated as known[18] and the spectra for groups 2 - 6 were determined using our computer code SIXGD.

Spectra for groups 2 - 6 deduced for the thermal fission of ^{235}U and ^{239}Pu are compared with corresponding group spectra from the compilation of T.R. England[18] in Fig. 9. There is considerable similarity in the two sets with the exception of the ^{239}Pu group 2. However, the group 2 ^{239}Pu spectrum is subject to particularly large uncertainties. Six-group spectra for ^{238}U will follow after completion of the low energy composite measurements.

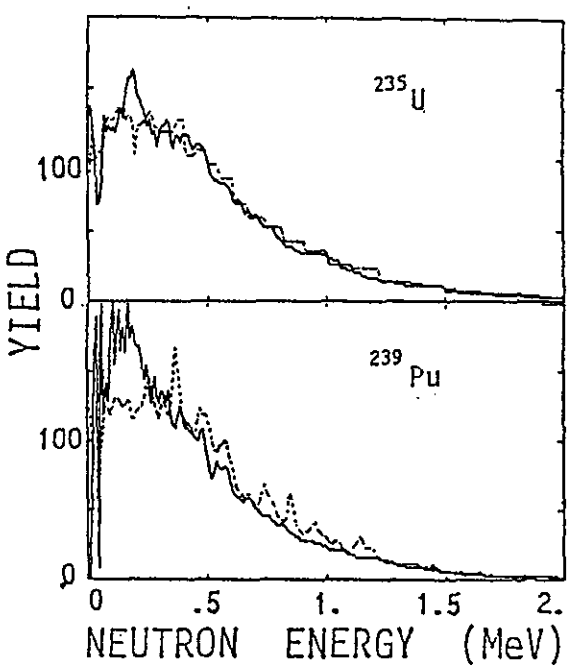

Fig. 8. Comparison of measured DN equilibrium spectra (solid curves) with those deduced from 6-group data (Ref. 18).

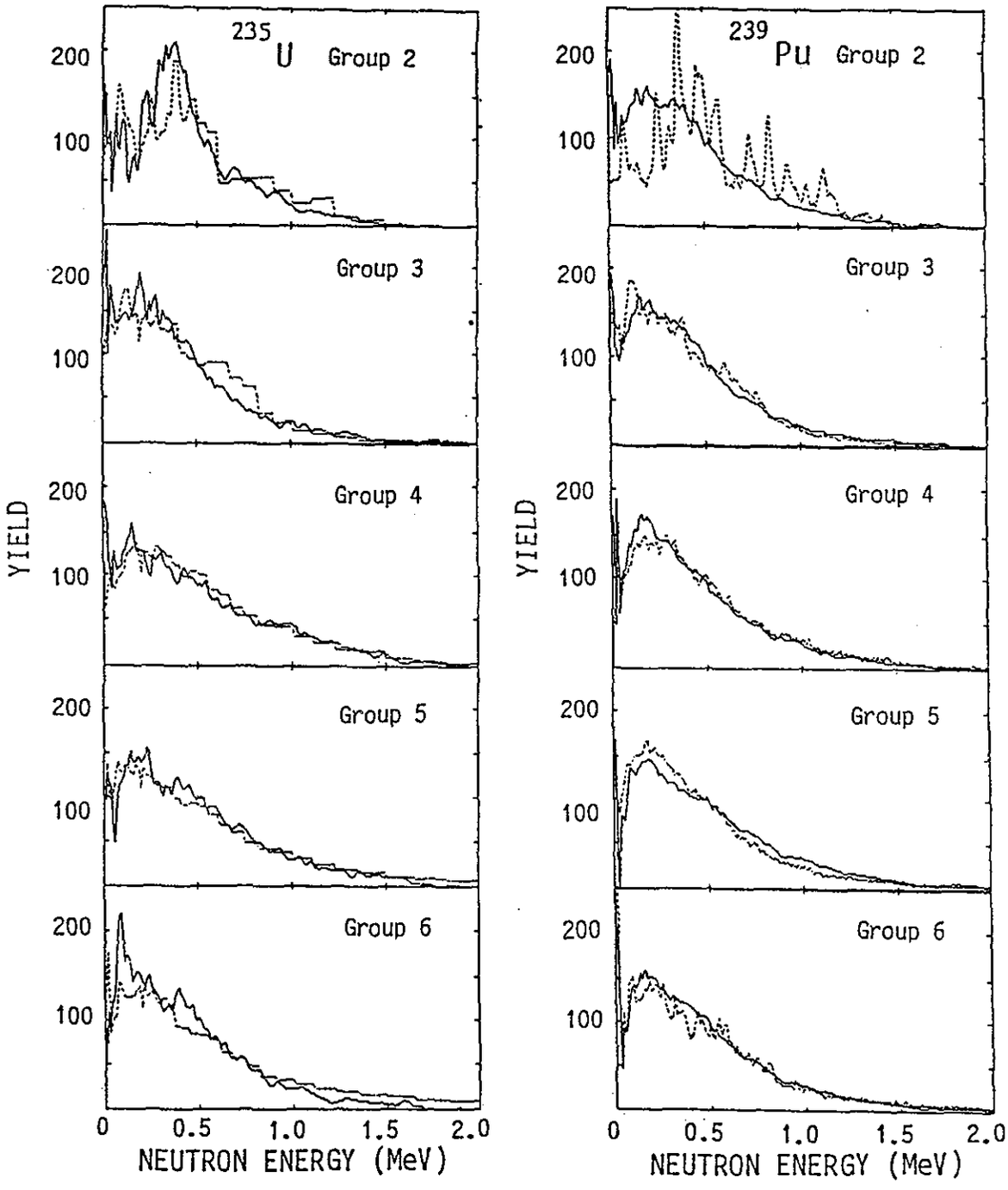

Fig. 9. Comparison of 6-group spectra deduced from present study (solid curves) with corresponding spectra from the compilation of T.R. England (Ref. 18) for ^{235}U and ^{239}Pu.

In conclusion, to emphasize the importance of the ^{238}U and ^{239}Pu studies, Table II is presented which shows these two isotopes contribute nearly 80% of the delayed neutrons in the prototype breeder reactor.

TABLE II

Contributions to Fission and DN Production in Core of 1000 Mwe Fast Reactor at End of Cycle.

Isotope	% of Core Fissions (Ref. 2)	ν_d(DN/Fission) (Ref. 19)	% of DN
U-235	0.6	0.0167	0.86
U-238	10.6	0.0439	40.0
Pu-239	70.2	0.0063	38.0
Pu-240	5.4	0.0095	4.4
Pu-241	12.1	0.0152	15.8
Pu-242	0.5	0.0221	0.95

ACKNOWLEDGEMENTS

This work is presently supported by the U.S. Department of Energy. Development of the experimental system and preliminary measurements were performed under a grant from the National Science Foundation.

REFERENCES

1. D. SAPHIER, D. ILBERG, S. SHALEV and S. YIFTAH, "Evaluated Delayed Neutron Spectra and their Importance in Reactor Calculations," Nucl. Sci. Eng.,62, 660 (1977).

2. A.E. WALTAR and A.B. REYNOLDS, Fast Breeder Reactors, Pergamon Press, New York (1981).

3. M.S. EL-GENK and M.D. HOOVER, ed., Trans. of the Third Symp. on Space Nucl. Power Systems, Alberquerque, NM, (1986).

4. T.R. ENGLAND, W.B. WILSON, R.E. SCHENTER and F.M. MANN, "Aggregate Delayed Neutron Intensities and Spectra Using Augmented ENDF/B-V Precursor Data," Nucl. Sci. Eng., 85, 139 (1983).

5. G.R. KEEPIN, Physics of Nuclear Kinetics, Addison-Wesley, Reading, Massachusetts (1965).

6. G. RUDSTAM, "Six-Group Representation of the Energy Spectra of Delayed Neutrons from Fission," Nucl. Sci. Eng., 80, 238 (1982).

7. R. BATCHELOR and H.R. McK.HYDER, "The Energy of Delayed Neutrons from Fission," J. Nucl. Energy, 3, 7 (1956).

8. G. FIEG, "Measurements of Delayed Fission Neutron Spectra of U-235, U-238 and Pu-239 with Proton Recoil Proportional Counters," J. Nucl. Energy, 26, 585 (1972).

9. S. SHALEV and J. CUTTLER, "The Energy Distribution of Delayed Fission Neutrons," Nucl. Sci. Eng., 51, 52 (1973).

10. W.R. SLOAN and G.L. WOODRUFF, "Spectrum of Delayed Neutrons from the Thermal-Neutron Fission of Uranium-235," Nucl. Sci. Eng., 55, 28 (1974).

11. W.A. SCHIER, G.P. COUCHELL, D.J. PULLEN, N.M. SAMPAS, C.A. CIARCIA, M.H. HAGHIGHI, Q. SHARFUDDIN and R.S. TANCZYN, "New Experimental System for Measuring Composite Delayed-Neutron Spectra Following Fission," Nucl. Instr. Meth. in Phys. Res., 227, 549 (1984).

12. C.A. CIARCIA, W.A. SCHIER, G.P. COUCHELL, D.J. PULLEN, R.S. TANCZYN, M.H. HAGHIGHI, and Q. SHARFUDDIN, Comp. Phys. Comm., 39, 238 (1986).

13. R.S. TANCZYN, Q.SHARFUDDIN, W.A. SCHIER, D.J. PULLEN, M.H. HAGHIGHI, L. FISTEAG and G.P. COUCHELL, "Composite Delayed Neutron Energy Spectra for Thermal Fission of ^{235}U," Nucl. Sci. Eng., 94, 353 (1986).

14. Q. SHARFUDDIN, W.A. SCHIER, G.P. COUCHELL, L.V. FISTEAG, M.H. HAGHIGHI, D.J. PULLEN and R.S. TANCZYN, "Search for an Energy Dependence in ^{235}U Delayed Neutron Spectra," Nucl. Sci. Eng. 98, 341 (1988).

15. K.-L. KRATZ and GABELMANN, "Beta-Delayed Neutron Spectra for Applications in Reactor Technology, Nuclear Physics and Astrophysics," in Proc. Int. Conf. on Nucl. Data for Basic and Applied Science, Santa Fe, New Mexico, 1985; publ. Gordon and Breach, (1986), p.661.

16. R.E. KAISER and S.G. CARPENTER, "Evaluation of ^{235}U and ^{239}Pu Delayed-Neutron Spectra," in Fission-Product Decay Library of the Evaluated Data File (ENDF/B-V), National Nuclear Data Center, Brookhaven National Laboratory (1978).

17. G.P. COUCHELL, W.A. SCHIER, D.J. PULLEN, L. FISTEAG, M.H. HAGHIGHI, Q. SHARFUDDIN and R.S. TANCZYN, in Proc. Specialists' Meeting on Delayed Neutron Properties, Birmingham, U.K., 1986; publ. Univ. Birmingham Press (1987), p.215.

18. T.R. ENGLAND, private communication (1988).

19. R.J. TUTTLE, "Delayed Neutron Yields in Nuclear Fission," in Proc. Consultants Mtg. on Delayed Neutron Properties, Vienna, 1979; INDC(NDS)-107/G.